

Subcomponent Synthesis via Mechanochemistry

By

Prasit Kumar Sahoo

CHEM11201104005

**National Institute of Science Education and Research
Bhubaneswar, Odisha – 752050**

*A thesis submitted to the
Board of Studies in Chemical Sciences
In partial fulfillment of requirements
for the Degree of*

DOCTOR OF PHILOSOPHY

of

HOMI BHABHA NATIONAL INSTITUTE

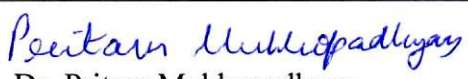
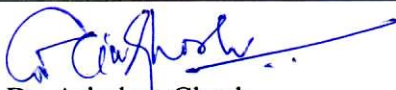


June, 2016

Homi Bhabha National Institute¹

Recommendations of the Viva Voce Committee

As members of the Viva Voce Committee, we certify that we have read the dissertation prepared by **Prasit Kumar Sahoo** entitled “**Subcomponent Synthesis via Mechanochemistry**” and recommend that it may be accepted as fulfilling the thesis requirement for the award of Degree of Doctor of Philosophy.

Chairman –		Date: 12.12.16
	Prof. A. Srinivasan	
Guide / Convener –		Date: 12.12.16
	Dr. Prasenjit Mal	
Examiner –		Date: 12/12/16
	Dr. Pritam Mukhopadhyay	
Member 1 –		Date: 12/12/16
	Dr. Sudip Barman	
Member 2 –		Date: 12/12/16
	Dr. Arindam Ghosh	

Final approval and acceptance of this thesis is contingent upon the candidate's submission of the final copies of the thesis to HBNI.

I/We hereby certify that I/we have read this thesis prepared under my/our direction and recommend that it may be accepted as fulfilling the thesis requirement.

Date: 12/12/2016

Place: Bhubaneswar


12.12.16

(Dr. Prasenjit Mal)

Guide

¹ This page is to be included only for final submission after successful completion of viva voce.

STATEMENT BY AUTHOR

This dissertation has been submitted in partial fulfillment of requirements for an advanced degree at Homi Bhabha National Institute (HBNI) and is deposited in the Library to be made available to borrowers under rules of the HBNI.

Brief quotations from this dissertation are allowable without special permission, provided that accurate acknowledgement of source is made. Requests for permission for extended quotation from or reproduction of this manuscript in whole or in part may be granted by the Competent Authority of HBNI when in his or her judgment the proposed use of the material is in the interests of scholarship. In all other instances, however, permission must be obtained from the author.

Prasit Kumar Sahoo

DECLARATION

I, hereby declare that the investigation presented in the thesis has been carried out by me. The work is original and has not been submitted earlier as a whole or in part for a degree / diploma at this or any other Institution / University.

Prasit Kumar Sahoo

List of Publications arising from the thesis

Journal Published

- 1.[#] **P. K. Sahoo**, A. Bose; P. Mal, Solvent-Free Ball-Milling Biginelli Reaction by Subcomponent Synthesis. *Eur. J. Org. Chem.* **2015**, 32, 6994
- 2.[#] C. Giri,* **P. K. Sahoo**,* R. Puttreddy, K. Rissanen, P. Mal, Solvent-Free Ball-Milling Subcomponent Synthesis of Metallosupramolecular Complexes. *Chem. Eur. J.*, **2015**, 21, 6390 (*contributed equally)
- 3.[#] **P. K. Sahoo**, C. Giri, T. S. Haldar, R. Puttreddy, K. Rissanen and P. Mal, Mechanochemical Synthesis, Photophysical Properties, and X-ray Structures of N-Heteroacenes. *Eur. J. Org. Chem.* **2016**, 7, 1283
4. B. N. Ghosh, F. Topić, **P. K. Sahoo**, P. Mal, J. Linnera, E. Kalenius, H. M. Tuononen, K. Rissanen, Synthesis, structure and photophysical properties of a highly luminescent terpyridine-diphenylacetylene hybrid fluorophore and its metal complexes. *Dalton Trans.*, **2015**, 44, 254
- 5.[#] C. Giri*, **P. K. Sahoo***, K. Rissanen, P. Mal; Capturing Hydrophobic Trifluoroiodomethane in Water into an M4L6 Cage. *Eur. J. Inorg. Chem.* **2016**, 31, 4964 (*contributed equally)

Communicated

- 6.[#] S. Maity, **P. K. Sahoo**, B.M. Pratheek, S. Chattopadhyay, P. Mal; Mechanochemical Synthesis of Oxo-Monastrol Derivatives and their Concomitant Anticancer and Antioxidant Activities.
- 7.[#] T. K. Achar*, **P. K. Sahoo***, P. Mal, Soft Force Relay in C-CN Activation of 1,2-dicyano pyrazines via SNAr ipso Substitution. (*contributed equally)

Under Preparation

8. # **P. K. Sahoo**, P. Mal, Electron Deficient *N*-Heteroacenes under Mechano-Mechano-milling.

Pertaining to thesis

Conferences and Presentation

1. **Oral Presentation:** X J-NOST Conference for Research Scholar, 2015 at NISER, Bhubaneswar on 14th – 17th December, 2015
2. **Poster Presentation:** 10th Mid-year CRSI Symposium in Chemistry (CRSI Mid), 2015 at NIT Trichy during 23rd – 25th July, 2015
3. **Poster Presentation:** Indo French Symposium On Functional Metal-Organics: Applications in Materials and Catalysis at NISER, Bhubaneswar on 24th – 26th February, 2014
4. Science Academies' Lecture Workshop on "Organic and Inorganic Assembly", February 21 – 22, 2015 at Department of Chemistry, Kalinga Institute of Industrial Technology (KIIT), Bhubaneswar, India
5. Indo-European Symposium on Frontiers of Chemistry, November 10 - 12, 2011 at NISER, Bhubaneswar

Prasit Kumar Sahoo

To my Parents

ACKNOWLEDGEMENTS

This work might not have been possible without the copious contributions from others. First, I would like to thank my research advisor, Dr. Prasenjit Mal for his valuable guidance, continuous support, helpful discussions and providing space for free thinking throughout the last four and half years.

I am thankful to Prof. T. K. Chandrashekar, founder Director-NISER and Prof. V. Chandrashekhar, Director-NISER for the laboratory facilities and obviously University Grant Commission (UGC) for financial support.

I would like to recognize my thesis monitoring committee (TMC) members Prof. Alagar Srinivasan, Dr. Sudip Barman and Dr. Arindam Ghosh, chairperson-SCS, Dr. Moloy Sarkar and all other faculty members in SCS for their support and useful suggestions.

I remember Prof. K. Rissanen and his group members for their prompt support in crystallography study.

I am extremely fortunate to have lab mates like Tapas, Saikat, Anima, Khokan, Toufique, Ankita, Tuhin and Sunny. Their cheerful accompany, traceless discussion, generous cooperation have provided a thought-provoking and friendly environment which helps this journey smooth. Also, I do remember wonderful and memorable stay with my ex-lab mate Nitesh Kumar.

I thank all of my NISER friends for the memorable moments.

Most importantly, I would like to thank my parents, sister, friends and family who were a witness to every step of the way and provided me support and confidence whenever I needed it the most. Thank you all so much for your unconditional love and unwavering support.



Homi Bhabha National Institute

PhD PROGRAMME

-
- | | | |
|---|---|--|
| 1. Name of the Student | : | Prasit Kumar Sahoo |
| 2. Name of the Constituent Institution | : | National Institute of Science Education and Research (NISER) |
| 3. Enrolment No | : | CHEM11201104005 |
| 4. Title of the Thesis | : | Subcomponent Synthesis via Mechanochemistry |
| 5. Board of Studies | : | Chemical Science |
-

Introduction

Recently, mechanochemistry^{1,2} (solvent-free ball-milling) has gained substantial interest due to its advantages over traditional solution-based methods. Mechanochemical Synthesis are generally time saving, environmental friendly and economical. However, the subcomponent self-assembly approach under system chemistry, is a method in which ligands of metallo-supramolecular complexes are produced in situ from their subcomponents. With rising public concern over alternative energy and global warming, it is important to decrease the usage of chemicals in routine chemical synthesis. Essentially, developing recyclable methodology and eliminating waste are important parts of chemical reactions. Therefore organic synthesis using subcomponent technique under mechano-milling is a useful tool for doing chemical reaction in a greener fashion.

Scope and Organization of the Present Thesis

Recently, ball-milling is used for synthetic transformations due to its benefits over solution based methods. Many advantages are associated during synthesis by mechanochemistry. This method has huge importance for green processes due to time efficiency, environmentally friendliness and inexpensive synthesis. In this thesis, attempts have been made to show that day by day use of ball-milling become superior tool over solution based conventional method. The present thesis has been organized in five chapters and the contents of each chapter have been summarized as follows:

CHAPTER 1: Subcomponent Synthesis and Use of Mechanomilling in Organic Synthesis

This chapter mainly focuses on brief introduction of subcomponent synthesis and use of mechano-chemistry in the organic and metalo-supramoleculer synthesis. This Chapter consists mostly the efficiency of different non-conventional energy sources³ in organic synthesis. Apart from this, how subcomponent technique use for the synthesis of high-purity metal complexes with a minimum number of steps has also been discussed. We have summarized some important outcomes on chemical reactions using ball-milling as an energy sources. Finally this chapter finishes with discussing the objective of present thesis.

CHAPTER 2: Subcomponent Approach towards the Synthesis of Dihydropyrimidones via Mechano-Milling and its Biological Application

(Ref: 1. P. K. Sahoo; A. Bose; P. Mal, *Eur. J. Org. Chem.* **2015**, 32, 6994

2. S. Maity, P. K. Sahoo, B.M. Pratheek, S. Chattopadhyay, P. Mal; Mechanochemical Synthesis of Oxo-Monastrol Derivatives and their Concomitant Anticancer and Antioxidant Activities. (*Communicated*)

In this chapter we have discussed about the system chemistry⁴ on small molecules through covalent mechanochemistry. The multicomponent Biginelli reaction was considered as a model system to use the subcomponent technique in organic synthesis. All the reactions were performed under solvent-free, mechanochemical (ball milling) condition at ambient temperature. Br⁺-catalyzed oxidation⁵ of benzyl alcohols led to the component benzaldehydes and byproduct H⁺ which was principally act as a catalyst for a cascade transformation to dihydropyrimidones (DHPM) within the same reaction pot. Remarkably, in solution phase the reaction system could not work at room temperature even after 24 h.

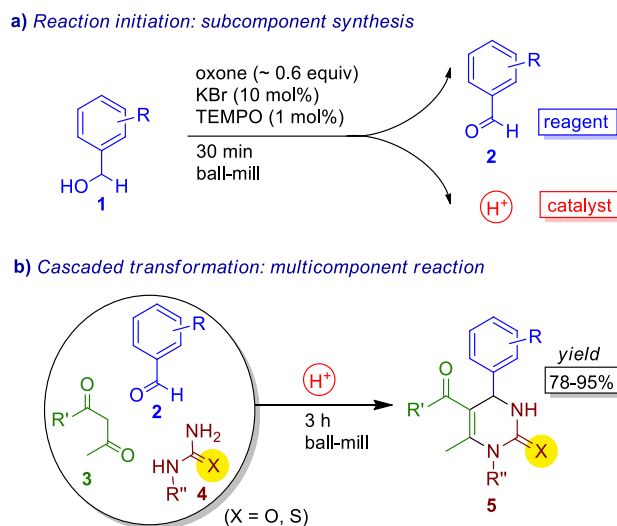


Figure 1. Subcomponent Synthesis followed by Multicomponent Transformation

Monastrol⁶ is one of the DHPM derivatives is a well-known anticancer drug. Herein, we have synthesized several oxo-Monastrol derivatives (DHPMs) having one or more hydroxyl groups. Antioxidant activity was investigated by free radical (DPPH, hydroxyl, nitric oxide and superoxide) scavenging potency of these compounds.

CHAPTER 3: Mechanochemical Self-Sorting and Subcomponent Substitutions in Metallosupramolecular Complexes and its Application in CF3I Encapsulation

(Ref: 1. C. Giri*, P. K. Sahoo*, R. Puttreddy, K. Rissanen, P. Mal, *Chem. Eur. J.* **2015**, *21*, 6390

2. C. Giri*, P. K. Sahoo*, K. Rissanen, P. Mal, *Eur. J. Inorg. Chem.* **2016**, *31*, 4964

(*contributed equally)

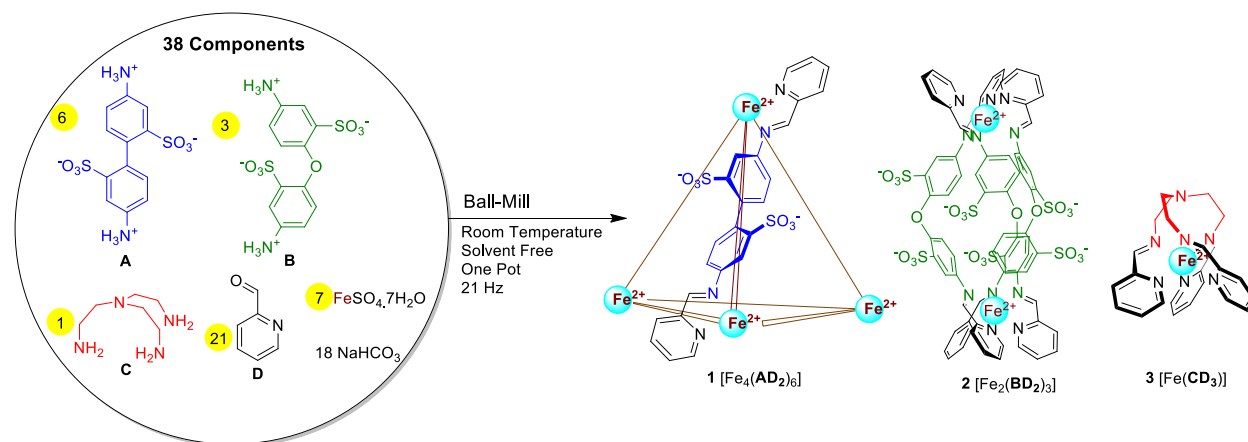


Figure 2. Self Sorting of Supramolecular Assemblies

Subcomponent self-assembly^{7,8} from components A, B, C, D, and Fe²⁺ under solvent-free conditions by selfsorting has been demonstrate in this chapter. Three structurally different metallosupramolecular iron(II) complexes were synthesized under mechanochemical condition. Under the same conditions, three distinct structures tetranuclear [Fe₄(AD₂)₆]⁴⁺ 22-component cage 1, dinuclear [Fe₂(BD₂)₃]²⁻ 11-component helicate 2, and 5-component mononuclear [Fe(CD₃)]²⁺ complex 3 were prepared simultaneously in a one-pot reaction from 38 components.

However through subcomponent substitution reaction, these complexes were transformed to their smaller and more stable counterparts.

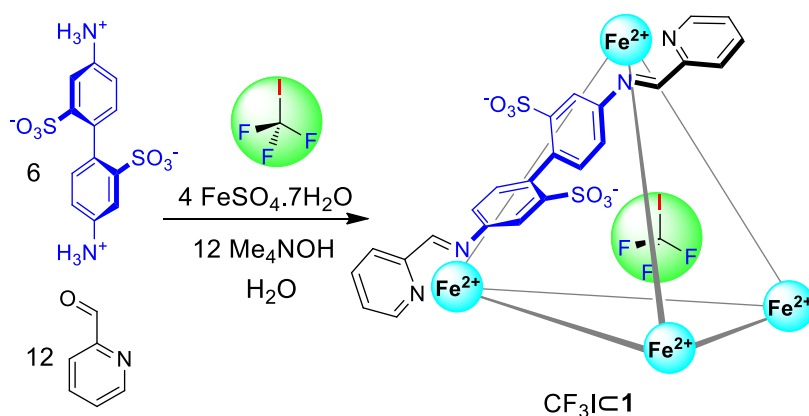


Figure 3. Quantitative Encapsulation of CF_3I by an Anionic M_4L_6 Cage

At ambient condition, near quantitative encapsulation of hydrophobic, gaseous substrate trifluoroiodomethane (CF_3I) was observed by a metallo-organic supramolecular anionic cage in water. The binding constant were calculated by relative comparison with benzene encapsulation.

CHAPTER 4. Mechanochemical Synthesis, Photophysical Properties, and X-ray Structures of N-Heteroacenes

(Ref: **1. P. K. Sahoo**, C. Giri, T. S. Haldar, R. Puttreddy, K. Rissanen and P. Mal, *Eur. J. Org. Chem.* **2016**, 7, 1283

2. P. K. Sahoo, P. Mal, Electron Withdrawing N-Heteroacenes under Mechano-milling. (*Manuscript under Preparation*)

In this chapter we have discussed about the syntheses of pyrazaacenes^{9,10} which are achieved under solvent-free ball-milling conditions. The method is easy, high yielding, time-efficient, and environmentally benign. Whereas the solution-based methods are tedious, poor yielding, and difficult to isolate the product. We are able to synthesized upto octacene analogues containing pyrene as a building blocks. Product could be purified simply without any Column

chromatographic purifications. The UV/Vis absorption spectra of the pyrazaacenes show intense absorption bands in the near-IR region. The method is equally efficient for the synthesis of electron deficient N-heteroacenes. The single-crystal X-ray analyses of selected pyrazaacene derivatives showed pairwise π - π interactions and some C-H \cdots π interactions, which may result in conductivity properties in the solid state.

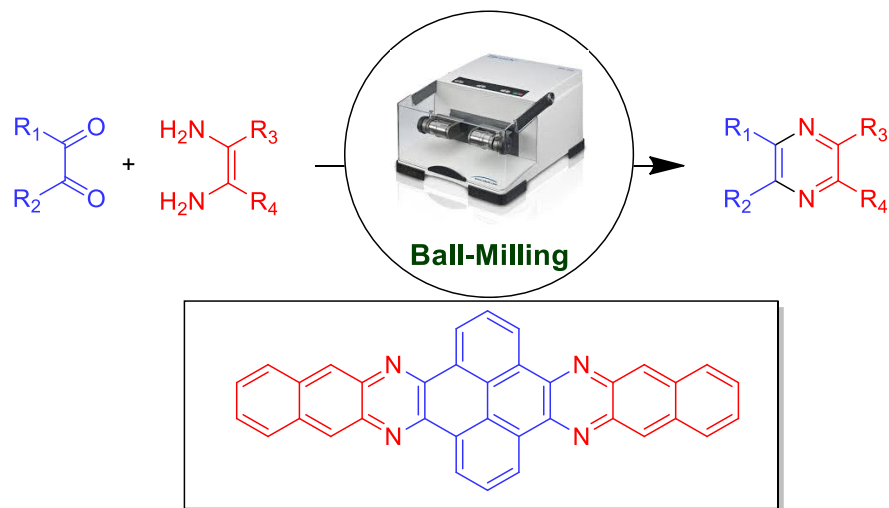


Figure 4. Synthesis of N-Acenes under Mechanomilling

CHAPTER 5. Cation- π Induced C-C Activation on N-acenes

T. K. Achar*, **P. K. Sahoo***, P. Mal, Soft Force Relay in C-CN Activation of 1,2-dicyano pyrazines via SNA_r ipso Substitution. (*Communicated*) (*contributed equally)

Cation- π interaction¹¹ is one of the important tool in molecular recognition and catalysis. In this chapter we have discussed about a C-C bond activation induced by a noncovalent interaction. Pyrazene is one the important heterocyclic core of several natural products. Aiming to introduce environmentally benign transition metal free C-CN bond activation,¹² herein we report a decyanation of pyrazne using tetrabutyl ammonium hydroxide (TBAH) at ambient temperature in a very short reaction time period. The reagent used here TBAH plays a dual role, it act as a

base to abstract proton from alcohol as well as the tetrabutyl ammonium cation interact with the pyrazene moiety through cation- π interaction which activate the C-CN bond. But during the course of the reaction we have isolated exclusively monosubstituted product, it was probable may be after one substitution the electron deficiency of the pyrazene ring was highly decreased which disfavor the next one.

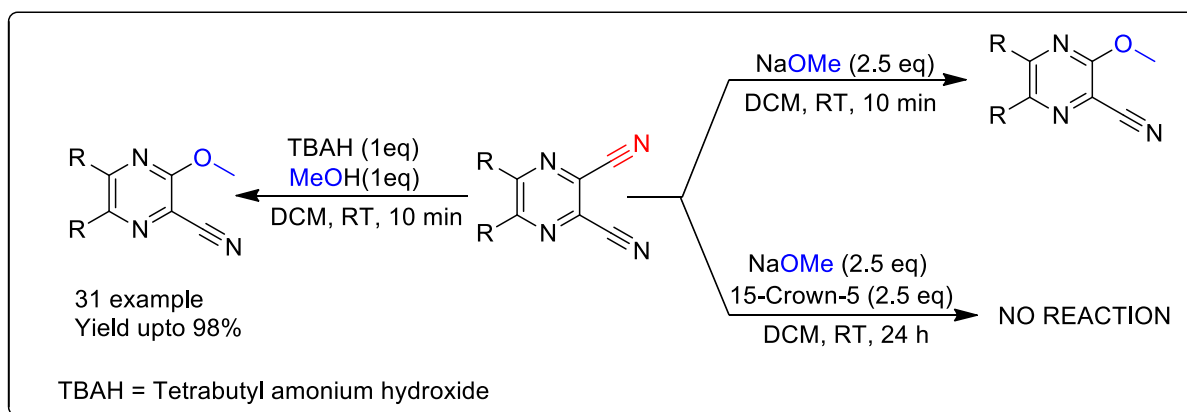


Figure 5. Cation- π induced C-C Activation on N-acenes

NOTES AND REFERENCES

- (1) Wang, G.-W. *Chem. Soc. Rev.* **2013**, *42*, 7668.
- (2) Achar, T. K.; Maiti, S.; Mal, P. *RSC Adv.* **2014**, *4*, 12834.
- (3) Baig, R. B. N.; Varma, R. S. *Chem. Soc. Rev.* **2012**, *41*, 1559.
- (4) Giuseppone, N. *Acc. Chem. Res.* **2012**, *45*, 2178.
- (5) Hussain, H.; Green, I. R.; Ahmed, I. *Chem. Rev.* **2013**, *113*, 3329.
- (6) Mayer, T. U.; Kapoor, T. M.; Haggarty, S. J.; King, R. W.; Schreiber, S. L.; Mitchison, T. J. *Science* **1999**, *286*, 971.
- (7) Nitschke, J. R. *Acc. Chem. Res.* **2007**, *40*, 103.
- (8) Castilla, A. M.; Ramsay, W. J.; Nitschke, J. R. *Acc. Chem. Res.* **2014**, *47*, 2063.
- (9) Mateo-Alonso, A.; Kulisic, N.; Valenti, G.; Marcaccio, M.; Paolucci, F.; Prato, M. *Chem. Asian J.* **2010**, *5*, 482.
- (10) Kulisic, N.; More, S.; Mateo-Alonso, A. *Chem. Commun.* **2011**, *47*, 514.
- (11) Mahadevi, A. S.; Sastry, G. N. *Chem. Rev.* **2013**, *113*, 2100.
- (12) Wen, Q.; Lu, P.; Wang, Y. *RSC Adv.* **2014**, *4*, 47806.

List of Abbreviations Used

Å	Angstrom
AcOH	Acetic Acid
Anal.	Analytically
Anhyd	Anhydrous
aq	Aqueous
BM	Ball Milling
bp	Boiling Point
BPO	Benzoyl Peroxide
br	Broad
°C	Degree Celcius
Calcd	Calculated
cm	Centimeter
Conc	Concentrated
conv	Conversion
d	Doublet, Days
DCE	Dichloroethane
DCM	Dichloromethane
dd	Doublet of a Doublet
DIBALH	Diisobutylaluminium Hydride
dil	Dilute
DMF	<i>N,N</i> -Dimethyl Formamide
DMSO	Dimethyl Sulfoxide
eq	Equation
equiv	Equivalent
Et	Ethyl
EtOAc	Ethyl Acetate
FAB	Fast Atom Bombardment
g	Grams
h	Hours

HRMS	High-resolution Mass Spectrometry
$h\nu$	Irradiation, Photochemical Reaction
<i>i</i>	Iso
ITC	Isothermal Titration Calorimetry
IR	Infrared
K	Kelvin
kcal	Kilo calories
lit	Liter
m	Multiplet
M	Molar
MeCN	Acetonitrile
mp	Melting point
Me	Methyl
MHz	Mega Hertz
Min	Minutes
mL	Milliliter
mM	Millimolar
mmol	Millimole
mol	Mole
MS	Mass Spectra
N	Normal
NBS	<i>N</i> -Bromosuccinimide
NCS	<i>N</i> -Chlorosuccinimide
nm	Nanometer
NMR	Nuclear Magnetic Resonance
ns	Nanosecond
pet.ether	Petroleum ether
PM	Planetary Milling
ppm	Parts per Million
rt	Room Temperature
s	Singlet, Seconds

TFE	Trifluoroethanol
TLC	Thin Layer Chromatography
tw	Twisted
TFA	Trifluoroacetic acid
US	Ultrasound
UV	Ultraviolet
Vis	Visible
vs	Versus
XRD	X-Ray Diffraction

Table of Contents

Synopsis	Subcomponent Synthesis via Mechanochemistry
Chapter 1	Subcomponent Synthesis and use of Mechanomilling in Organic Synthesis
1.1	Abstract
1.2	Introduction
1.3	Multicomponent to Subcomponent Self-Assembly
1.3.1	Principles of Self-Assembly
1.3.2	Selection of Metals
1.3.3	Topological Architecture using Subcomponent Self-Assembl
1.4	Ball Milling Mechanochemistry in Supramolecular Chemistry
1.5	Ball Milling in Organic Synthesis
1.6	Conclusions
1.7	Notes and References
Chapter 2	Subcomponent Approach towards the Synthesis of Dihydropyrimidones via Mechano-Milling and its Biological Application
2.1	Abstract
2.2	Introduction
2.3	Results and discussions
2.4	Conclusions
2.5	Experimental Section
2.6	Notes and References
	¹ H and ¹³ C NMR spectra

**Chapter 3 Mechanochemical Self-Sorting and Subcomponent Substitutions in
Metallosupramolecular Complexes and its Application in CF₃I
Encapsulation**

- 3.1 Abstract
- 3.2 Introduction
- 3.3 Results and discussions
- 3.4 Conclusions
- 3.5 Experimental Section
- 3.6 Notes and References
 ¹H and ¹³C NMR spectra

**Chapter 4 Mechanochemical Synthesis, Photophysical Properties, and X-ray Structures
of N-Heteroacenes**

- 4.1 Abstract
- 4.2 Introduction
- 4.3 Results and discussions
- 4.4 Conclusions
- 4.5 Experimental Section
- 4.6 Notes and References
 ¹H and ¹³C NMR spectra

Chapter 5 Cation- π Induced C-C Activation on N-Acenes

- 5.1 Abstract
- 5.2 Introduction
- 5.3 Results and discussions
- 5.4 Conclusions
- 5.5 Experimental Section
- 5.6 Notes and References
 ¹H and ¹³C NMR spec

CHAPTER 1

Subcomponent Synthesis and use of Mechanomilling in Organic Synthesis

1.1 ABSTRACT

In recent times, chemists have put sincere efforts to develop methods to use alternative energy as a source of energy-input for chemical transformations. The solution based traditional synthesis is extremely useful, however they are associated with certain disadvantages. For example, generation of waste by-products due to overheating, uses of large quantity of solvents which causes environmental hazard. So, developing recyclable methodology and eliminating waste are important parts of chemical reactions. Synthesis by mechanochemistry are generally time saving, environmental friendly and economical. However, the subcomponent self-assembly approach under system chemistry, is a method in which ligands of metallo-supramolecular complexes are created in situ from their respective subcomponents. Therefore organic synthesis via subcomponent synthesis under mechano-milling might be considered as a useful tool for doing chemical reaction in a greener fashion. This chapter mainly focuses on brief introduction on subcomponent synthesis and application of mechano-chemistry in the organic and metallo-supramolecular synthesis.

1.2 INTRODUCTION

An essential aspect of living systems is the ability of their bio-molecular mechanism to build a very complex set of functional structures from relatively simpler units. Although the same building blocks are utilized across large number of structures and the linkages that join them are in several cases formed reversibly, under thermodynamic control. The biological structures towards living systems have evolved from a spontaneous self-assembly process with high degree of compartmentalization. However, the small molecules are synthesized using kinetically controlled reactions through covalent process. Thus products created are the results of strong irreversible covalent bonds. In these sorts of reactions, the conditions are optimized and components are chosen carefully in order to obtain the desired product. Practically, chemists have been able to efficiently synthesize a wide range of both natural and unnatural products.

The unique relationship between science and art has been discovered around 1860 by French scientist MarcellinBerthelot when he wrote ‘Chemistry creates its own object. This creative quality, resembling that of art itself, distinguishes it essentially from natural and historical sciences.’ Which brings the difference between chemistry with other sciences. However, the beauty of art has direct relationship with the common people and somehow suppresses the beauty of chemistry. The beauty of chemistry lies in the molecules themselves. Joachim Schummer has written about the beauty of chemistry ‘Modern chemistry is exactly the art that provides creative access to what Plato considered the realm of the most beautiful bodies. Therefore, it is no surprise that chemists put their creative activity also in the service of beauty.’¹ The discovery of molecular nanotechnology and modern material science demand new novel objects.

Supramolecular chemistry quenches the thirst of those fields. Supramolecular chemistry is one of major research field in modern chemistry. Chemistry beyond our imagination; Lehn defines supramolecular chemistry “*chemistry beyond molecule*”. A more precise definition is given by the *International Pure and Applied Chemistry (IUPAC)*: “*A field of chemistry related to species of greater complexity than molecules that are held together and organized by means of intermolecular interactions. The objects of supramolecular chemistry are supermolecules and other polymolecular entities that result from the spontaneous association of a large number of components into a specific phase (membranes, vesicles, micelles, solid state structures, etc.)*.” The main attraction with supramolecular chemistry over the last few decades has led to build more functional and Nano sized structures. It gives limitless opportunities for cross boundary research in the field of chemistry, physics and biology. The modern material sciences are looking for new novel materials with unusual properties day by day. Supramolecular chemistry provides enough possibilities to synthesize these materials.

The beginning of supramolecular chemistry lies in the introduction of *coordination theory* in 1893 by Alfred Werner and followed the *lock-and-key* concept in 1894 by Emil Fischer. The neglected non covalent interactions such as coordinative bond, ion-dipole, dipole-dipole, hydrogen bonding, π - π and van der Waals etc. are vastly used in the early 1960s by Lehn, Cram and Pederson to build definite supramolecular structures. From the *coordination theory*⁹ Werner proposes the coordination number (CN) had the oxidation number of the metal atom in a molecular system. Werner could suggest the correct geometry with structures of the coordination compounds by assigning the numbers and nature of the isomers obtained. However, very soon it was conceived as an independent

research field of chemical research. Mostly, the *CN* varies with size of the metal (-ion) and coordinating ligands. Also, in case of bonding between metal ion and ligands the *thermodynamic trans effect* and *kinetic trans effect* also play an important role. With time, the coordination chemistry has become an integral part of supramolecular chemistry. However, applying the new techniques in supramolecular chemistry concerning the economic point of views are the most challenging for the researchers in recent years. One of the most recent developments in supramolecular chemistry has been sub component self-assembly, wherein the ligands of the metallo-supramolecular complexes are formed *in situ* from their subcomponents. The other way it is called as system chemistry. This emerging field allows to design complex networks, and might even give knowledge to understand the origin of life. In most cases, imine bonds were formed and the ligands as well as the corresponding complexes were achieved simultaneously.

Table 1.1: Several interactions and their typical bond energies are shown¹⁴

Interactions	bond energies in KJ / mol
Covalent CC bond	160-500
Coordinative bond	40-340
ion-ion interactions	40-370
ion-dipole interaction	40-210
hydrogen bond	4-65
dipole-dipole interaction	4-40
cation- π interaction	4-80
π - π interaction	4-20
<i>van-der-Waals</i> interaction	<4-20

Small molecules, cations or anions can be self-assembled by utilizing these non-covalent interactions to form large supramolecules having different physicochemical properties compare to those starting building blocks. Self-assembly process is kinetically reversible; in fact, it has a huge advantage over traditional stepwise synthesis concerning about large molecules. We know that nature assemble the simple precursors into extremely complex biomolecules by using of these non-covalent interactions; from where life starts.

1.3 Multicomponent to Subcomponent Self-Assembly

Nature manifests myriad beautiful creations^{1, 2} which involve complex self-assembled architectures made from simple building blocks with the effective use of weak non-covalent interactions.^{3, 4} Due to this, supramolecular science⁵ and systems chemistry^{6, 7} have been among the most rapidly developing areas of chemical research over the last decade.^{8, 9} Systems chemistry aims to provide detailed understanding of the organizational principles of complex molecular systems with functions different from conventional materials.^{10, 11} This approach can offer an easy access to new materials simply by changing the inputs of a multicomponent system. Thus the self-sorting systems,^{12, 13} including subcomponent self-assembly approach,¹⁴⁻¹⁶ are now a well-adopted methodology in supramolecular chemistry to create the complex systems with topological diversity by exploiting imine bonds as one of the key building blocks.

The subcomponent self-assembly¹⁷⁻²¹ is an integral part of self-sorting reactions^{12, 13, 22, 23} in which ligands of the metallo-supramolecular complexes are formed *in situ* from their subcomponents. This concept has proved to offer a promising method for synthesis of

high-purity products from complex mixtures of starting materials.^{3, 24} The metal-ion assisted subcomponent self-assembly of a rigid aromatic linear bis-amine, pyridine-2-carboxaldehyde and iron(II) resulting in tetrahedral M_4L_6 cage in water reported by Nitschke and us opened a new page on supramolecular tetrahedral complexes.²⁵ Recently, by exploiting the same dynamic imine chemistry,^{26, 27} we have used this concept to prepare the smallest possible tetrahedral M_4L_6 cage complex²⁸ and for the anion-controlled formation of an aminated-(bis)imine Fe(II)-complex.²⁹ In all the above mentioned cases the dynamic behavior of the imine bond is the key factor to control the self-assembly process.^{30, 31}

In order to create useful molecular machines, control over molecular topology must be exercised.^{32, 33} The subcomponents of molecular-scale devices must be threaded together with the same precision as the yarns of a textile or the shafts and gears of a macroscopic machine; the complex topologies of biochemical machinery bear witness to the necessity of correct form for function.^{34, 35} The new methods of controlling molecular topology that we propose to develop here thus serve as an essential enabling technology for the creation of molecule-scale devices within the domain of chemical nanotechnology, a field on the cutting edge of modern chemistry.³⁶⁻³⁸

1.3.1 Principles of Self-Assembly

An essential aspect of living systems is the ability of their bio-molecular mechanism to build a very complex set of functional structures from relatively simpler units. Although the same building blocks are utilized across large number of structures and the linkages that join them are in several cases formed reversibly, under thermodynamic control.³⁹⁻⁴¹

The biological structures towards living systems have evolved from a spontaneous self-assembly process with high degree of compartmentalization. However, the small molecules are synthesized using kinetically controlled reactions through covalent process.⁴² Thus products created are the results of strong irreversible covalent bonds. In these sorts of reactions, the conditions are optimized and components are chosen carefully in order to obtain the desired product. Practically, chemists have been able to efficiently synthesize a wide range of both natural and unnatural products.^{1, 43, 44}

However, the new means of creating complex molecular structures and materials using self-assembly methodology from simple building blocks *via* the simultaneous reversible formation of covalent and coordinative bonds is demonstrated. Firstly, the fundamental questions about how structural complexity, including topological complexity, may be constructed will be asked and following the functions would be incorporated in the structure to mimic the biological processes.^{45, 46} The research on molecular self-assembly thus branches out from the core discipline of synthetic chemistry into the areas of topology, materials science, and nanotechnology and will have a multidisciplinary impact that reaches beyond the chemical sciences.

1.3.2 Selection of Metals

In metal driven self-assembly processes, the coordination number and the coordination geometry across the metal ion has an important to build a self-assembled architecture. Therefore, selection of appropriate metals and ligand is very crucial, as witnessed in large number of literature reports. In 1960s Busch first introduced the concept of *template effect* by selecting an appropriate metal ion for a self-assembly process.^{47, 48} The template generally organizes the atoms around it in a distinct arrangement in order to favour the formation of a single product from the multiple products possible and also to promote attractive interactions between the building blocks ordered around it.

The geometry of the coordinated metal ion and nature of ligands should provide the construction manual for any self-assembly process. So, the selection of appropriate metal ion(s) and ligand(s) is very important, as observed in various literature.^{13, 49-53} Herein, a generalized overview on nanoscale architectures built from monodentate (pyridine), bidentate (bipyridine, phenanthroline, catechol) and tridentate (terpyridines) ligands shown in Fig. 1.1. As depicted in a simplified way in Fig. 1.1, most literature-known self-assemblies are constructed on Pd^{II} or Pt^{II} ions for square planar arrangement using monodentate ligands, at Cu^{I} or Ag^{I} ions for bidentate ligands, and at Co^{II} / Cu^{II} / Fe^{II} / Zn^{II} / Hg^{II} etc., octahedral grouping using terpyridine chelating motifs.⁵⁴

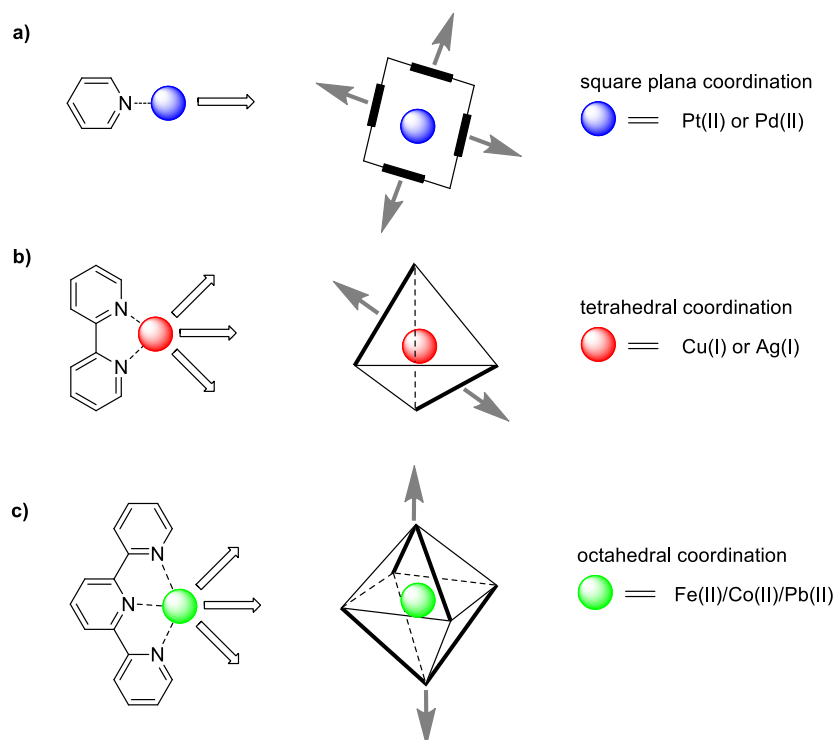


Figure 1.1. A generalized overview on co-ordination driven self-assembly.

The very first example of a metal induced creation of supramolecular architecture was shown by Busch and co-workers (Fig. 1.2). Mixture of 2-aminoethanethiol and diacetyl led to an equilibrium mixture of products including **1**. However, the square-planar nickel(II) ion in Fig. 1.2 induces a tetradentate ligand into a cyclic product **2** which was further substituted with α,α' -dibromo-*o*-xylene to nickel(II) complex **3**.⁵⁵

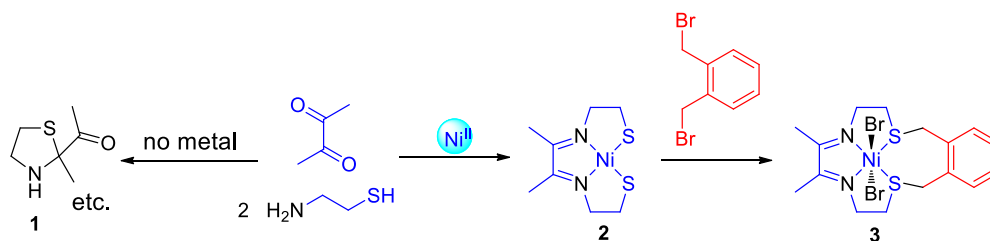


Figure 1.2. Nickel(II) as a macrocyclization template.

In aqueous solution, copper(I) is known to disproportionate to copper(II) and copper(0) metal. Also, due to reversible in nature, imines are generally minor product, when amines and aldehydes are mixed in water. Whereas, this stability pattern inverted by mixing of either imines or amines, aldehydes and copper(I) in aqueous solution. Imines are excellent ligands for copper(I) and stabilize the metal in this oxidation state, and consecutively the metal coordination can protect imines from hydrolyzing. Exploiting the mutual stabilization of copper(I) and imines in aqueous solution, Nitschke and co-workers demonstrated the preparation of complex **4** from the precursors shown in Fig. 1.3.^{15, 56}

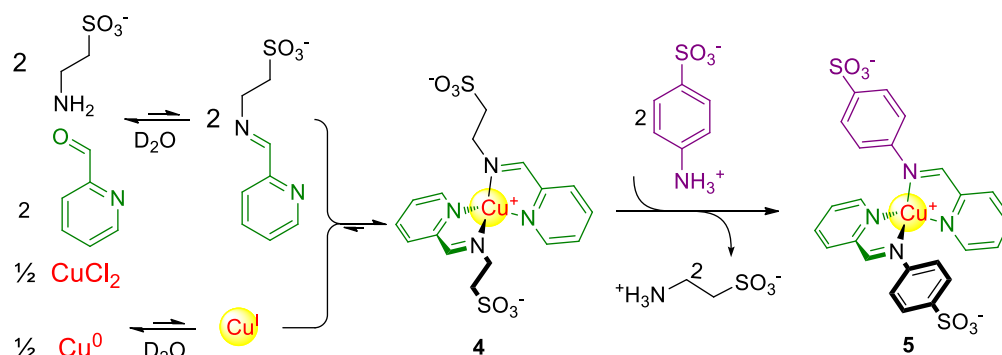


Figure. 1.3.Stabilization of copper(I) and imines and followed by substitution.

Furthermore, reported by Nitschke and co-workers, by mixing of 2-formyl pyridine (3.0 equivalents), 6-methyl-2-formyl pyridine (3.0 equivalents), tris(2-aminoethyl)-amine (1.0 equivalent) and ethanolamine (3.0 equivalents) in aqueous solution yielded a dynamic library of imines which were further self-sorted into two distinct complexes (**6** and **7**, Fig. 1.4) upon addition of Cu(I) tetrafluoroborate (1.5 equivalents) and Fe(II) sulfate (1.0 equivalent) as shown in Fig. 1.4.⁵⁷

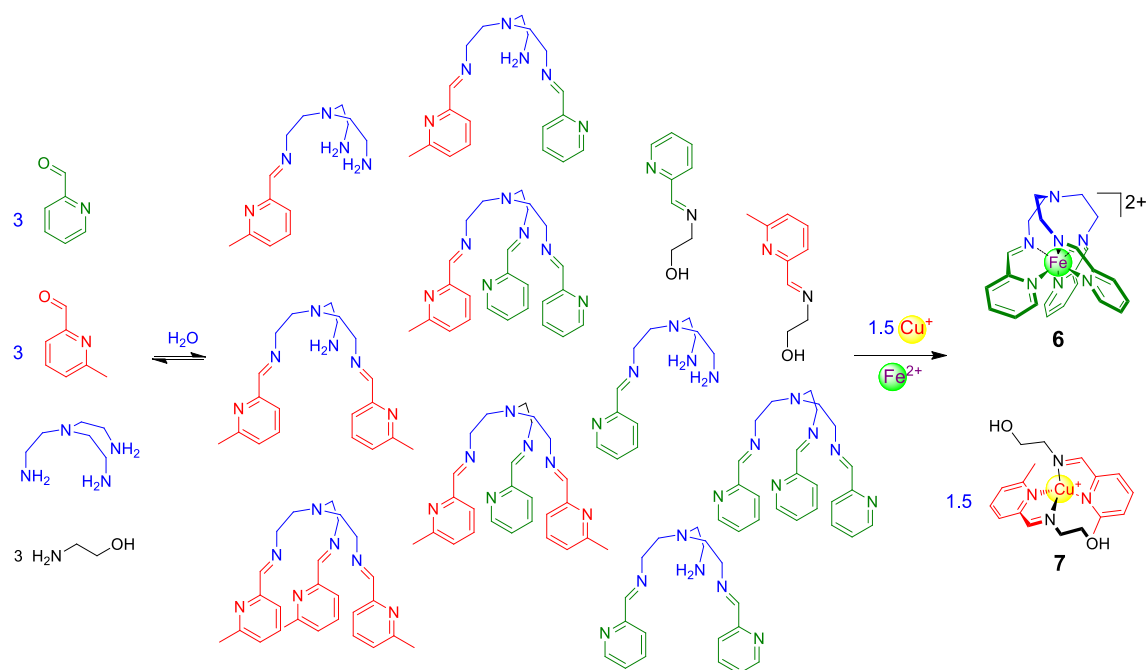


Figure 1.4. Self-sorted to two distinct products from a dynamic combinatorial library.^{32, 33, 52, 58}

Selective guest binding by molecular cages are well explored, contrastingly, in the solid state close packing of the molecules often inhibits guest entry, and thus led to the cages inactive.⁵⁹ Fujita and co-workers have demonstrated networked molecular cages as crystalline sponges for fullerenes and other guests (Fig. 1.5).⁶⁰ Additionally, the concept has been extended to bind proteins and other molecules as guest, in metallosupramolecular cages.^{61, 62}

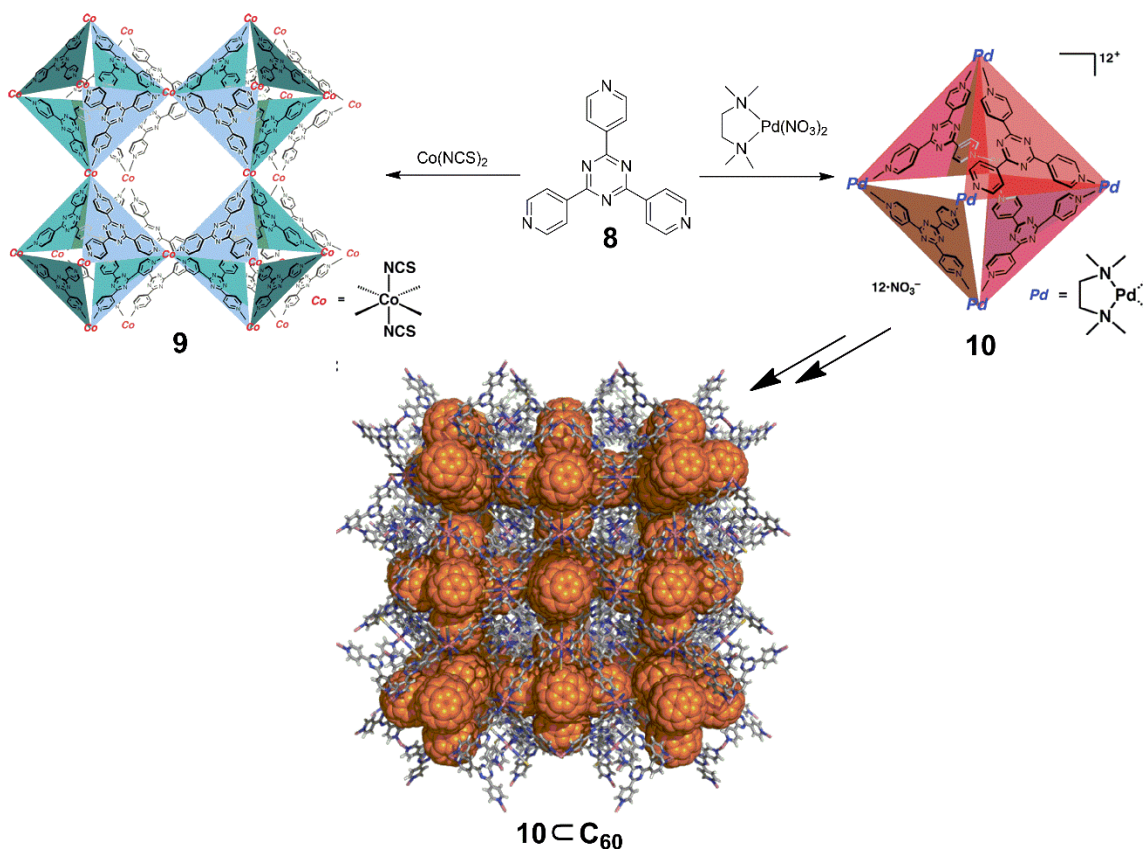


Figure 1.5. Networked molecular cages as for fullerenes guests.

Construction of porphyrin-based discrete assemblies of designed self-assembly to create discrete nanoscopic architectures of Pd^{II}/Pt^{II} has been developed by Mukherjee and co-workers. They have established that a tetratopic unit was the right choice for designing an unprecedented hexagonal open box system (Fig. 1.6). Thus, nanoscopic Pt₁₂Fe₁₂ heterometallic molecular box with six porphyrin walls is demonstrated.⁶³ In a recent review, they have covered the literature on template-free multicomponent coordination-driven Pd(II)/Pt(II) molecular cages and use of these systems in catalysis/host-guest chemistry.²³

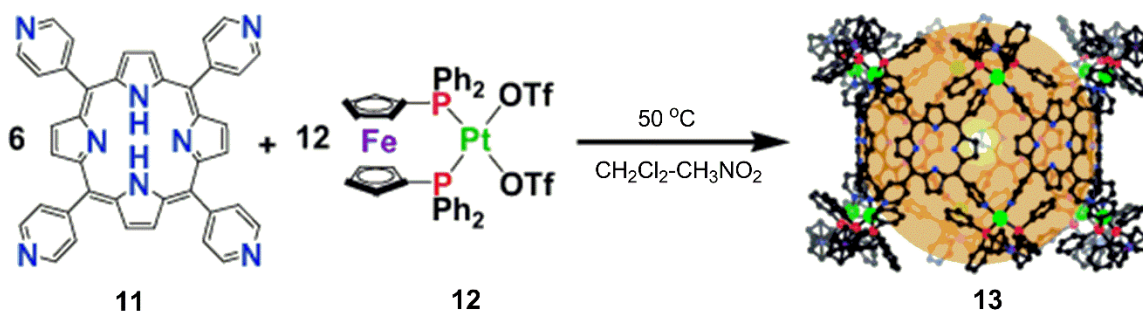


Figure 1.6. Hexagonal open box system using porphyrin wall.

Seth M. Cohen⁶⁴ and R. W. Boyle⁶⁵ used the concept of heteroleptic copper and zincdipyrromethene complexes for the synthesis and structural characterisation of different metallo-supramolecular architecture as shown in Fig. 1.7.

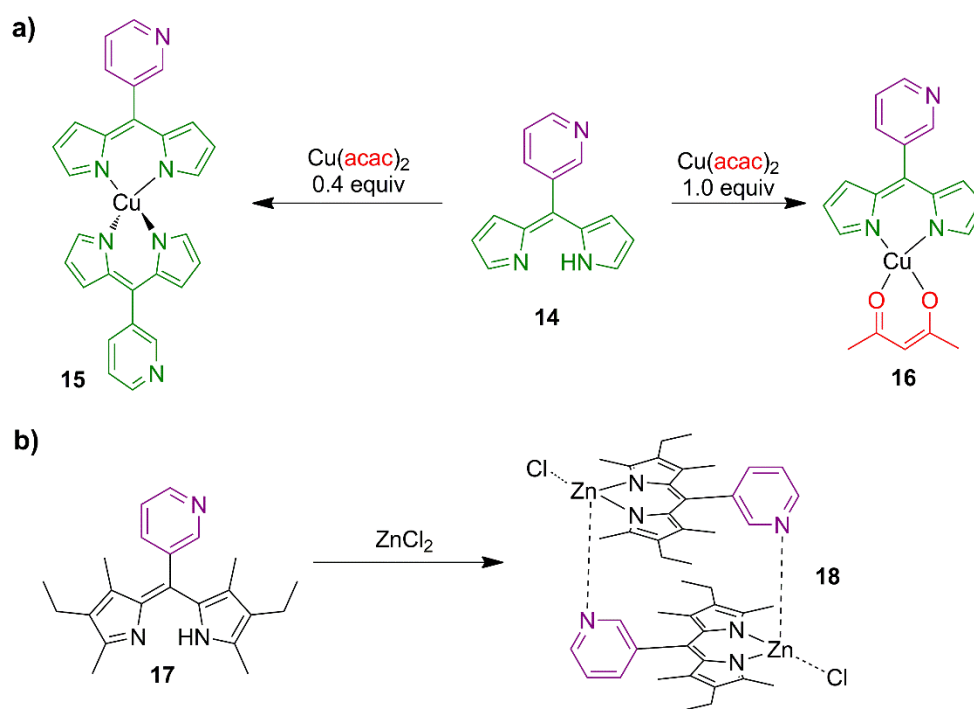


Figure. 1.7. Heteroleptic copper and zinc dipyrromethene complexes.

The future development of discrete functional supramolecules will be based on potent strategies to create divers multicomponent designed architectures. The structural

heteroleptic diversity is therefore important, not only in terms of applications towards functional materials, but also to acquire knowledge on understanding of multicomponent self-assembly. As shown in Fig. 1.8, Schmittel's group utilizes the **heteroleptic phenanthroline** (HETPHEN)⁶⁶ and **heteroleptic terpyridine and phenanthroline** (HETTAP)⁶⁷ complexation approach⁵⁴ used to prepare a whole range of heteroleptic nanoboxes, nanogrids,⁶⁸ nanoracks⁶⁹, supramolecular basket,⁷⁰ Dumbbells,⁶⁷ Clips, Nanotubular Structures with Large Void,⁷¹ Dynamic Ladders, Prisms,⁷² Technomimetic Molecular Wheels,⁷³ etc.

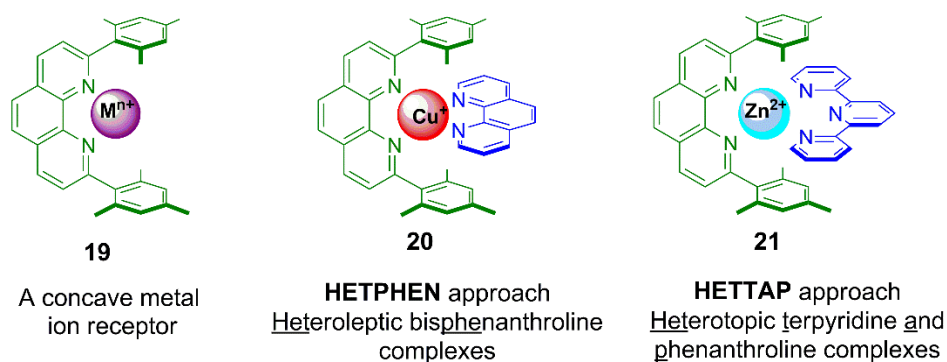


Figure 1.8. Schmittel's approach for construction of self-assembled system.

1.3.3 Topological Architecture using Subcomponent Self-Assembly

Pioneering work of Sauvage's catenane (Fig. 1.9) led to the development of a research area in which complex topological architectures were created by several groups like Stoddart (Borromean ring and Solomon link, Fig. 1.11),⁷⁴⁻⁷⁶ Cooper (Interlocked cages, Fig. 1.12),^{3, 77, 78} Rissanen and Leigh (Pentafoil Knot),⁷⁹ Sanders (Organic trefoil knot),⁹ Nitschke (Tetrahedral iron(II) cage),^{25, 80} etc.

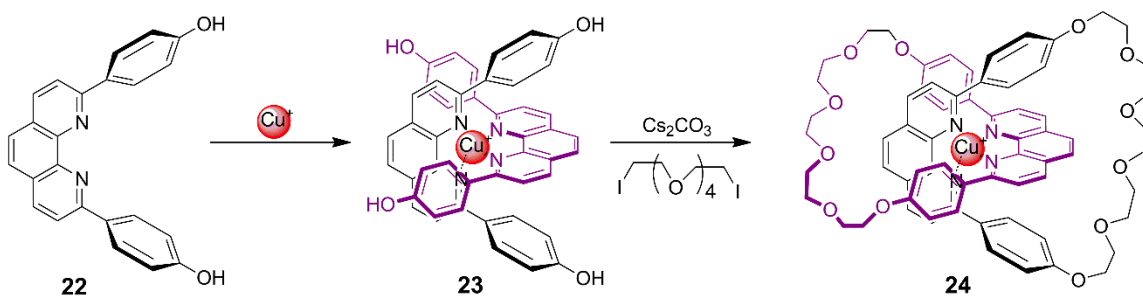


Figure 1.9. Sauvage's [2]catenane system.

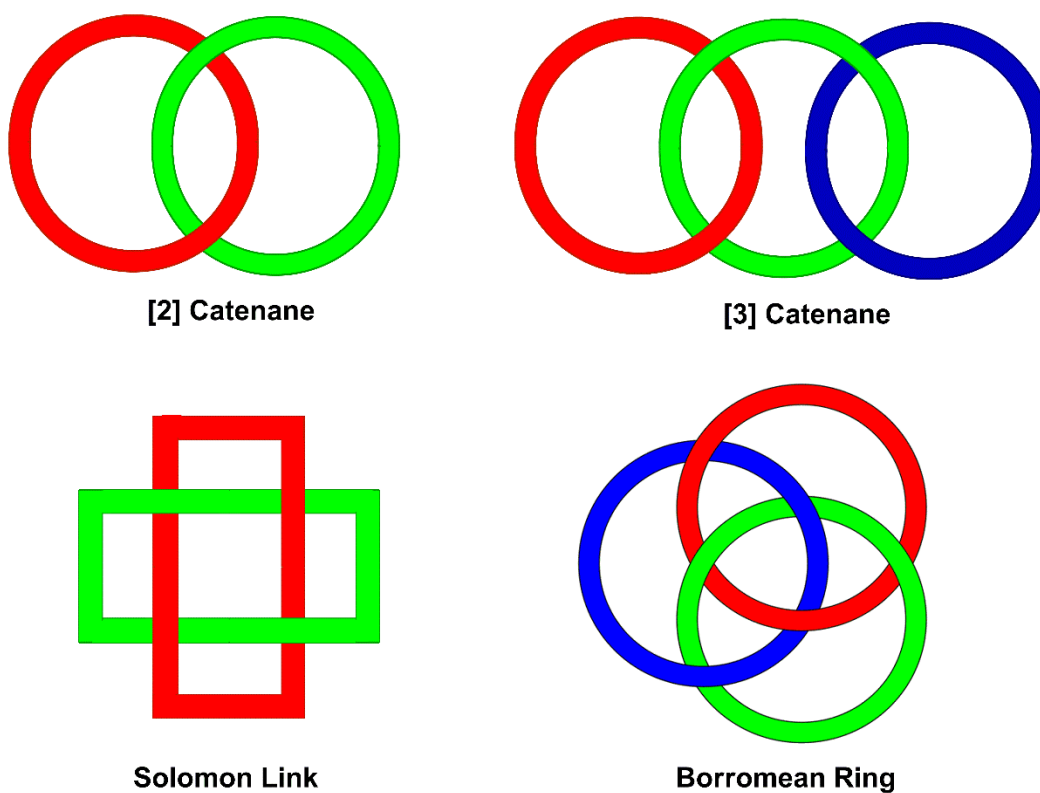


Figure 1.10. Examples of topological architectures.

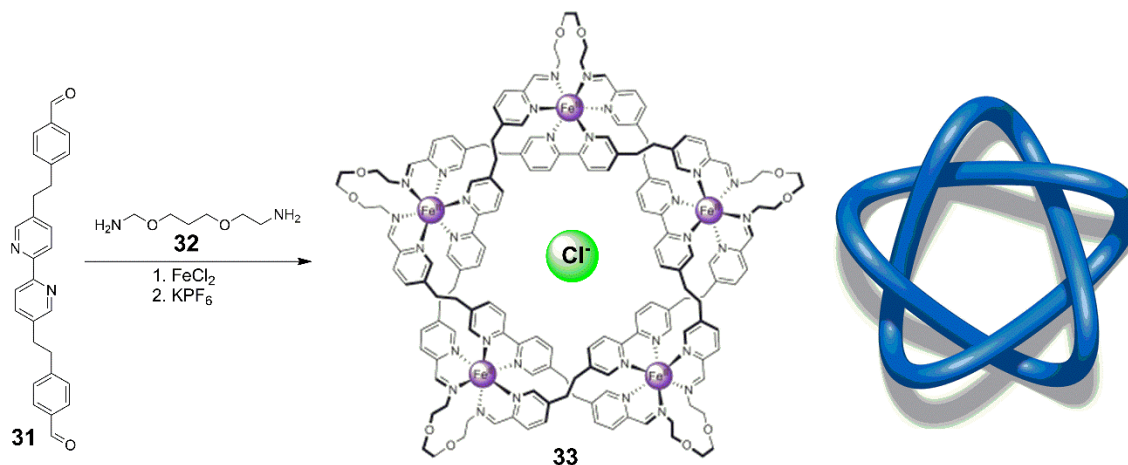


Figure 1.13. Pentafoil knot by Rissanen and Leigh.⁷⁹

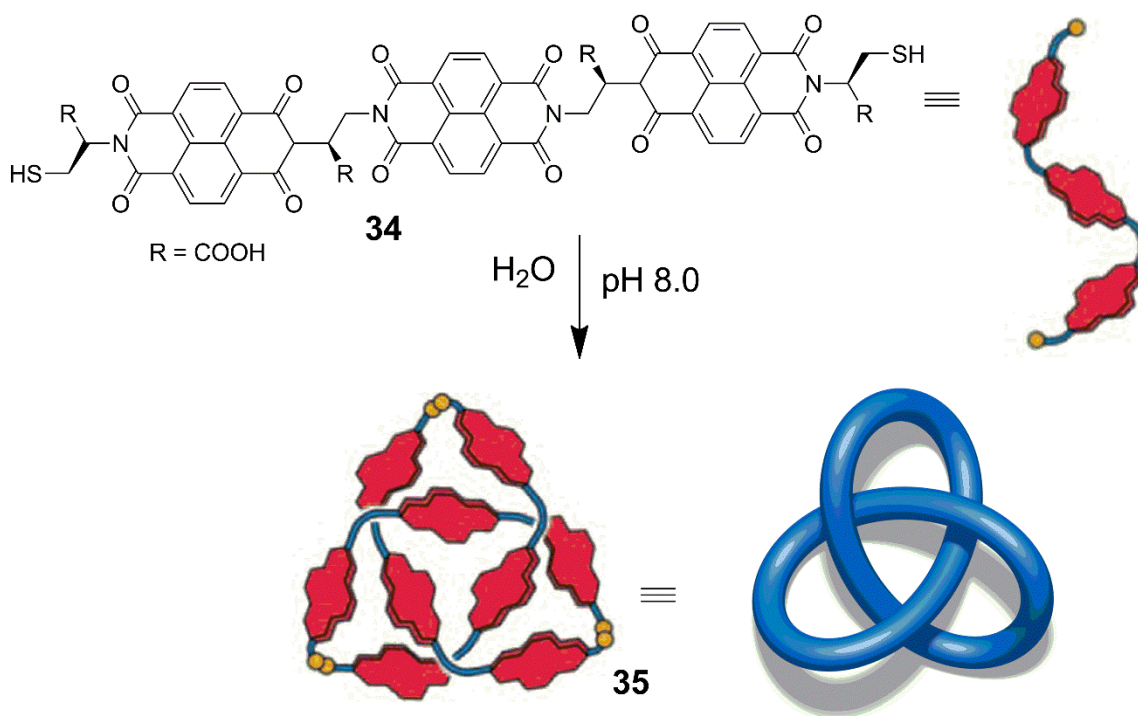


Figure 1.14. Organic Trefoil knot by Sanders.⁹

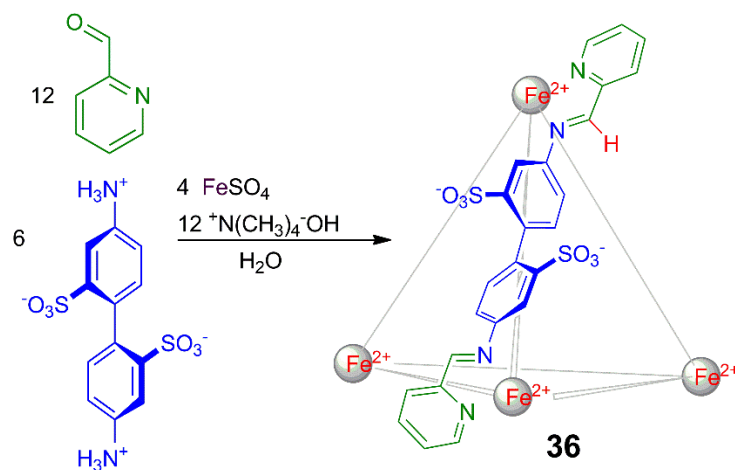


Figure 1.15. Nitschke's Tetrahedral Iron(II) Cage.^{25, 80}

1.4 Ball Milling Mechanochemistry in Supramolecular Chemistry

Recent surge of interest on nonconventional energy sources like microwave, visible light mechanochemical mixing, and ultrasound are gaining popularity to the chemist as an alternative energy sources which can be used to replace conventional laboratory techniques. By imposing these alternative means of activation, innumerable chemical transformations have been achieved and thereby developing many existing protocols with superior results. In few years mechanochemical synthesis⁸¹⁻⁸⁴ has drawn a great interest due to its advantage compare to traditional solution-based method.⁸⁵ The core benefit of this process is solvent free condition which does not require any traditional workup.^{86, 87} In addition, this process has high impact on ecology, economy and time saving.⁸⁸ Quantitative conversion, less by products and no purification bring extra importance to this procedure.^{89, 90} Synthesis of classical organic molecules is well explored, including multi step synthesis by this process.⁹¹ However, synthesizing metallo-organic complexes

by exploring this technique is relatively little known.^{92, 93} Recently, James and his co-workers synthesized mononuclear complexes by mechanochemical synthesis.⁹⁴

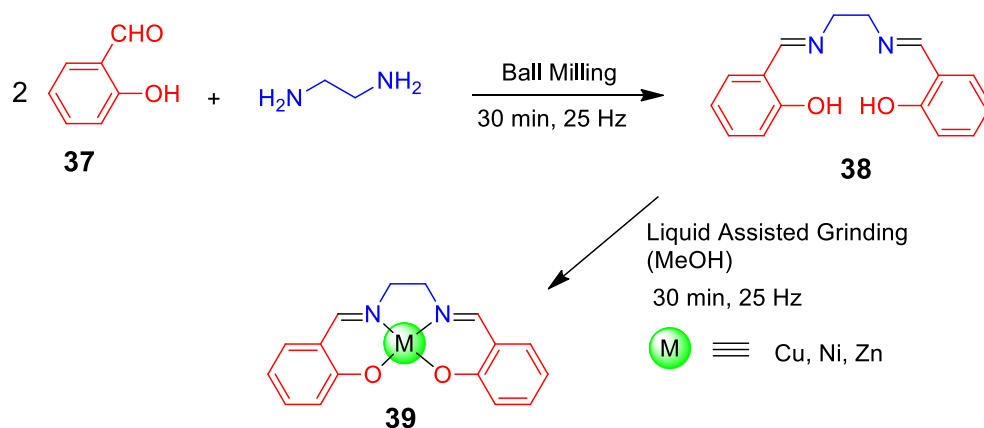


Fig. 1.16. Synthesis of mononuclear metal complexes by James and co-workers.⁹⁴

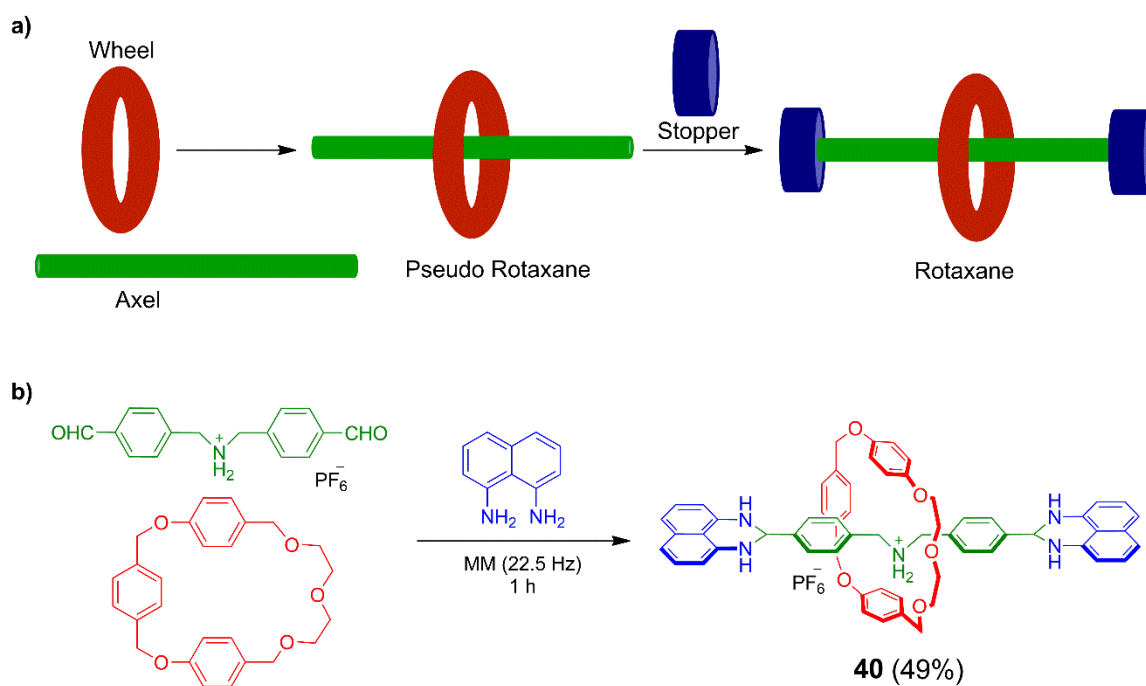


Figure 1.17. Mechanochemical synthesis of [2]rotaxanes. a) A generalized approach for construction of [2]rotaxane. b) Chiu's ball milling approach.

Chiu and co-workers reported a mechanochemical synthesis of both [2]- and [4]rotaxanes in high yields under solvent-free conditions at frequency of 22.5 Hz (Fig 1.17).⁹⁵ In solid-state formation of imine through the dehydration of amine and aldehyde could be achieved by ball milling, they used 1,8-diaminonaphthalene to prepare interlock molecules such as [2]- and [4]rotaxanes through the condensation with aldehyde unit of pseudorotaxane resulting dihydropyrimidine stopper units. In addition, they have also demonstrate for the synthesis of smallest [2]rotaxane.⁹⁶

Severin and co-workers reported the synthesis of sphere like nanostructure using ball mill. Condensation of 4-formylphenylboronic acid with pentaerythritol and 1,3,5-trisaminomethyl-2,4,6-triethylbenzene for 1 h at 20 Hz, afforded 94% of the cage compound (Fig. 1.18).⁹²

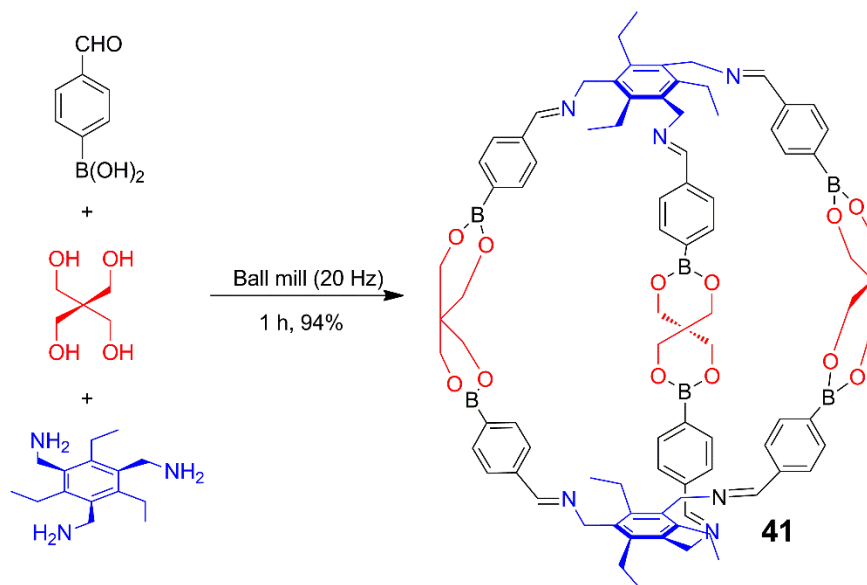


Figure 1.18. Mechanochemical synthesis of molecular sphere like nanostructure.⁹²

Sanders and co-workers demonstrated the reversibility and thermodynamic control in mechanochemical covalent synthesis, towards base catalyzed metathesis of aromatic

disulfides as a model reaction.⁹⁷ This methodology is an example under the research area of dynamic combinatorial system of ‘system chemistry’.^{41,98}

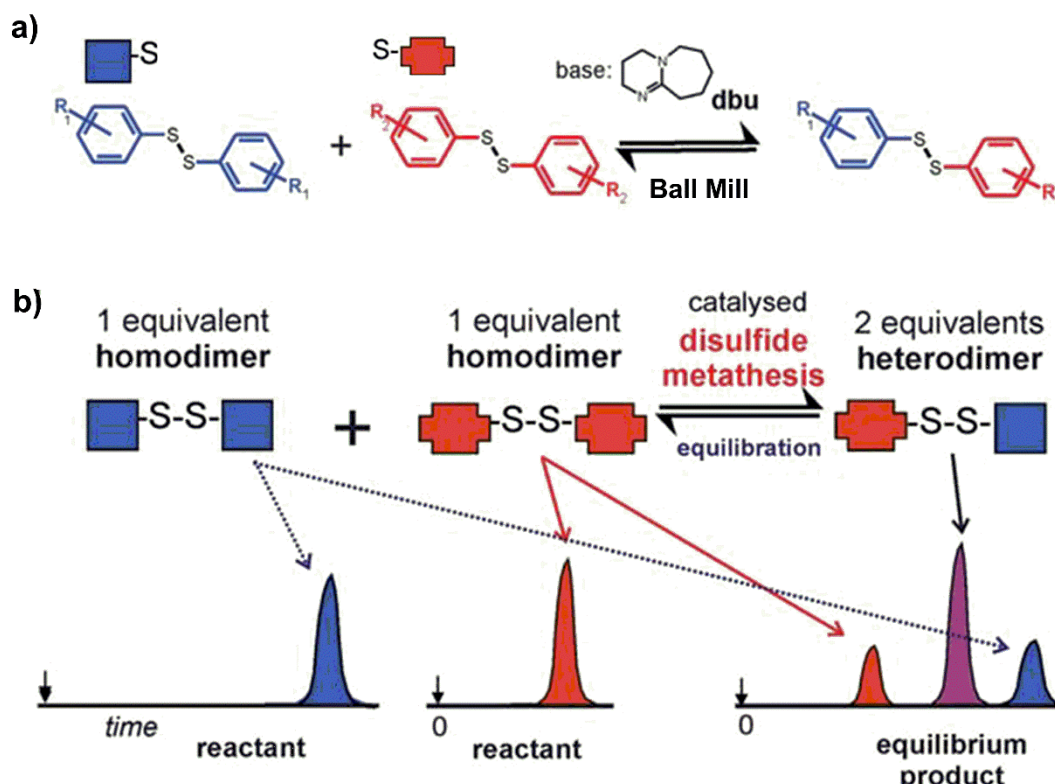


Figure 1.19 Mechanochemical and thermodynamic controlled synthesis of dynamic covalent systems of system chemistry.

1.5 Ball Milling in Organic Synthesis

In synthetic chemistry, ball milling techniques have been used to do the chemical reactions *via* breaking and making of covalent molecular bonds.^{99, 100} Pioneering works on ball milling mechanochemistry were reported by the groups of Toda¹⁰¹ and Kaupp.¹⁰² High efficient mixing of two solid reagents is the key process for the reactions under solvent-free condition.^{103, 104}

In 1989, Toda and co-workers reported the synthesis of 1,1'-bi-2-naphthol in presence of $\text{FeCl}_3 \cdot 6\text{H}_2\text{O}$ under solvent free conditions, starting from 2-naphthol.¹⁰¹ The process was found to be efficient and completed in 8 min.¹⁰⁵ However, the same reaction could be done in 144 h by traditional hand grinding.

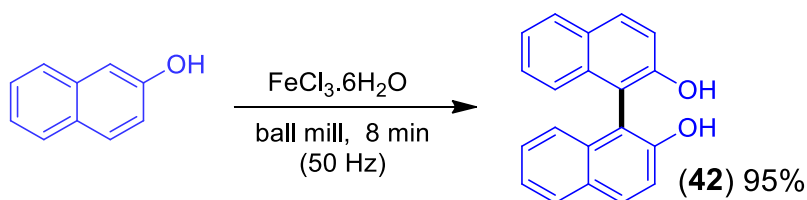


Fig. 1.20. Solvent free oxidative homocoupling reaction of 2-naphthol.

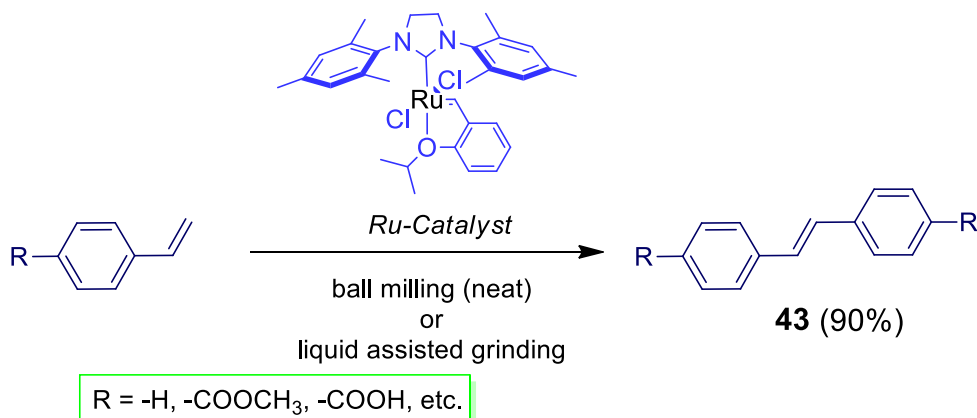


Figure 1.21. Solvent free Ru-catalyzed mechanochemical olefin metathesis.¹⁰⁶

Recently, Friščić and co-workers reported Ru-catalyzed mechanochemical reaction, which is an efficient approach for Hoveyda–Grubbs catalyzed olefin metathesis including cross-metathesis and ring-closing metathesis reactions (Fig. 1.21). The methodology was established to be applicable for both solid and liquid olefins.¹⁰⁶

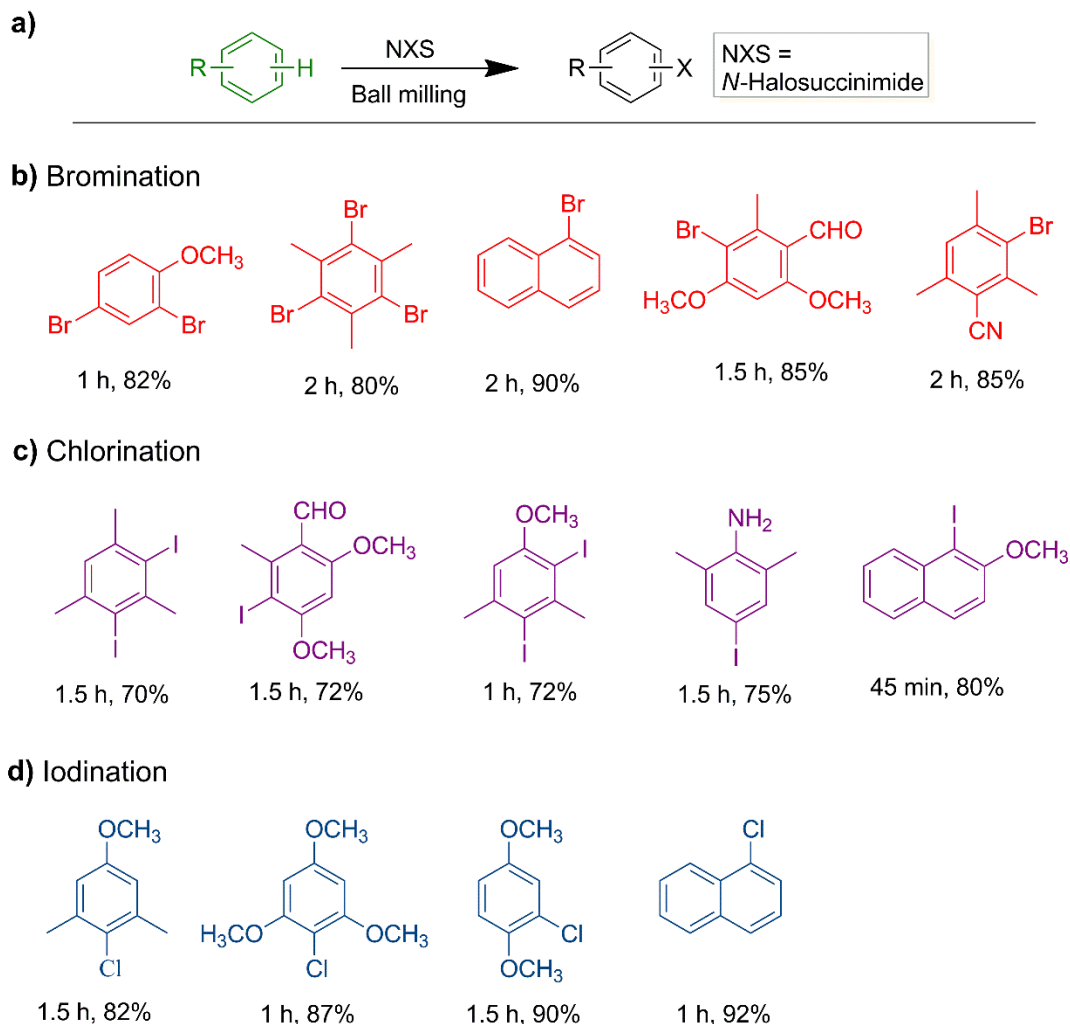
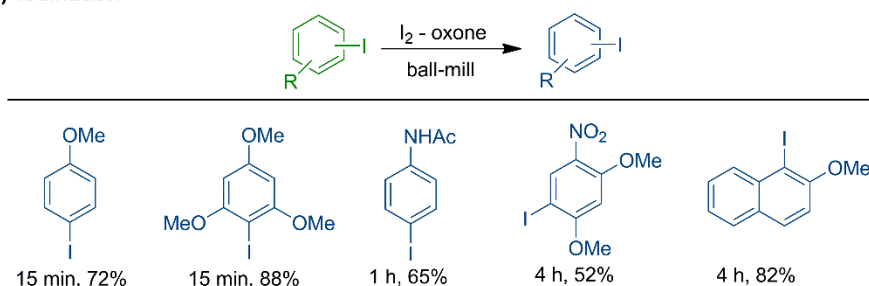


Figure 1.22. Solvent free ball milling aryl halogenation reactions.⁸⁷

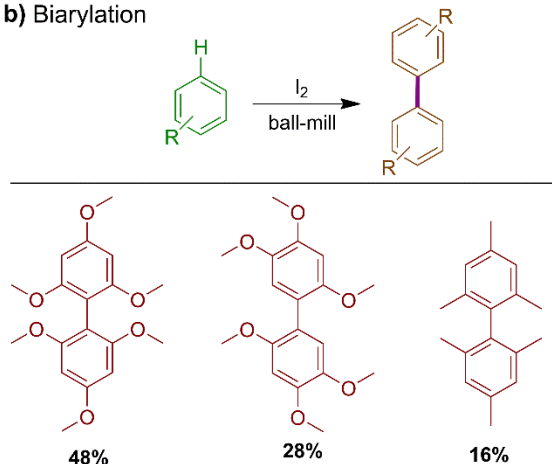
Recently, Mal and co-workers have also explored organic reaction methodology under solvent free ball milling condition. A greener methodology (Fig. 1.22a) of aryl halogenation (bromination and iodination) on aromatic compounds have been demonstrated using respective *N*-halosuccinimides in absence of any catalyst/additives under ball-milling condition (Fig. 1.22b, 1.22c). However, for chlorination ceric ammonium nitrate was used as additive (Fig. 1.22d).⁸⁷

A simple, efficient, environment friendly methodology for electrophilic aryl-iodination of electron rich arenes was reported using I₂-oxone (KHSO₅) in ball-milling condition (Fig. 1.23a). In addition, iodine could be used as catalyst for metal free biaryl coupling (Fig. 1.23b) of few electron rich substrates. One-pot multistep synthesis has been demonstrated in one substrate (Fig. 1.23c).¹⁰⁷

a) Iodination



b) Biarylation



c) Multistep Synthesis

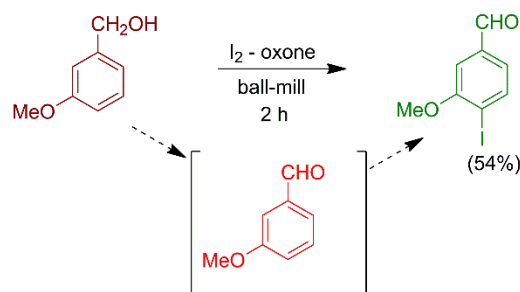


Figure 1.23. Solvent free ball milling for: a) Aryl iodination using I₂-oxone. b) Biaryl coupling and c) Multistep synthesis.¹⁰⁷

IBX (*o*-iodoxybenzoic acid) is metal free, mild and utile oxidant in synthetic chemistry whose wide applicability is usually impeded by its explosiveness at higher temperature and poor solubility in common organic solvents except DMSO. Mal and co-workers

have demonstrated that under mechanical ball milling IBX turned out to be green oxidant for oxidation of alcohol to aldehydes (Fig. 1.24). The reactions worked under solvent-free condition, at room temperature and in a range of reactions (Fig. 1.25). Eventually, the waste produced from the reactions was reusable for multiple-cycle (Fig. 1.26).⁸⁶

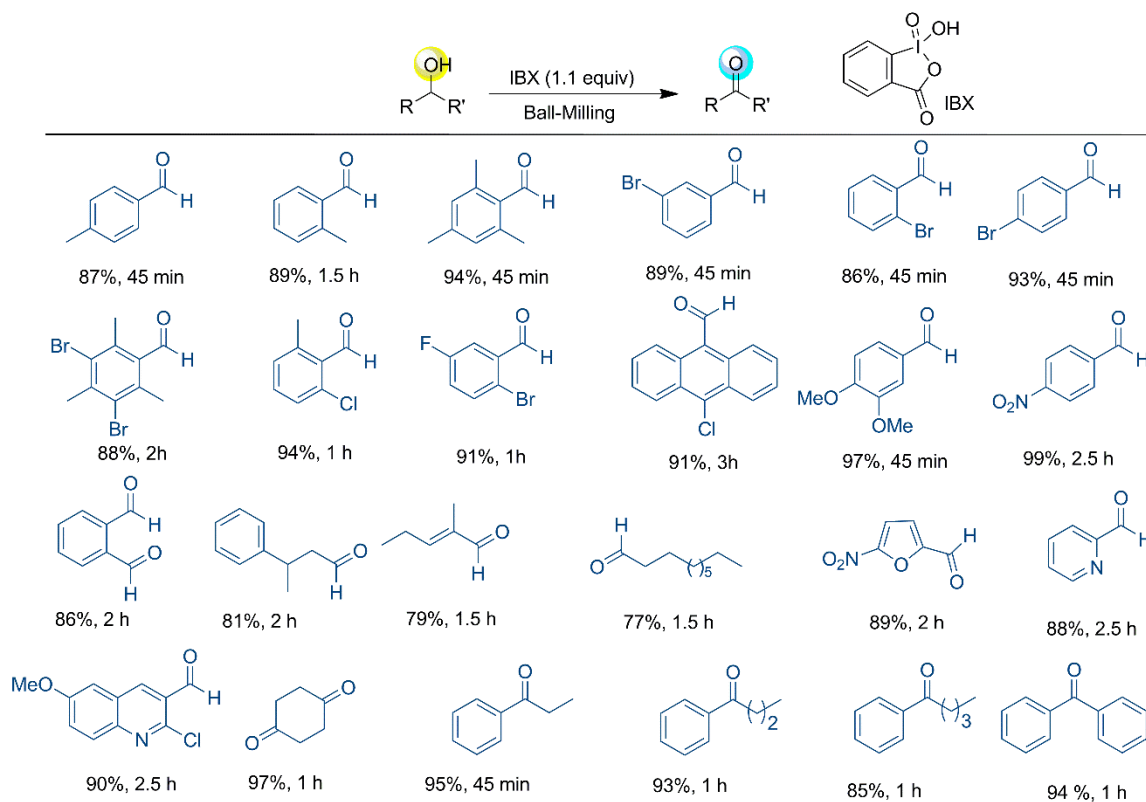


Figure 1.24. Alcohol oxidation using IBX under ball milling.⁸⁶

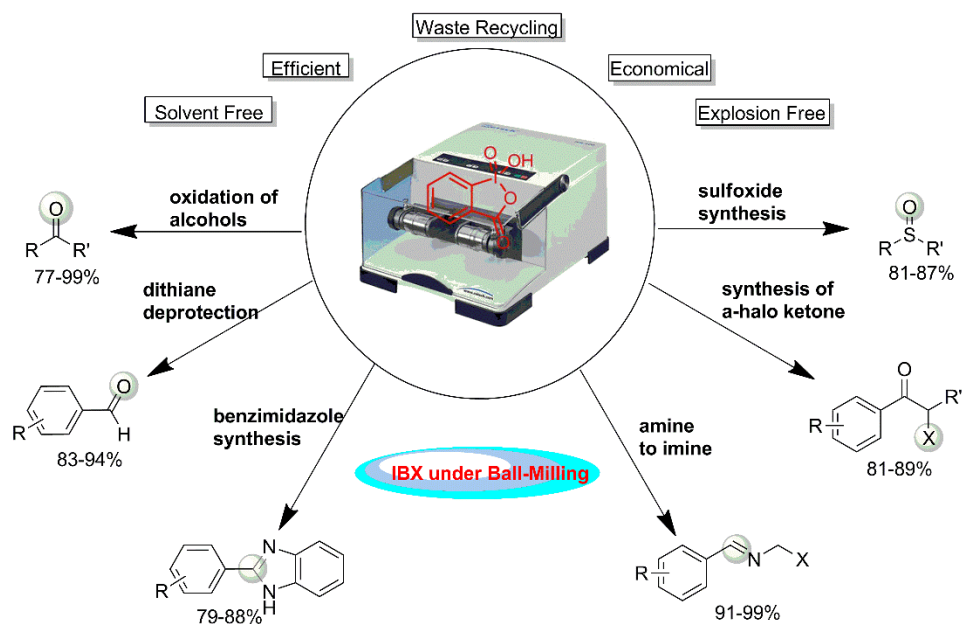


Figure 1.25. Scope of reactions demonstrated using IBX under ball milling.⁸⁶

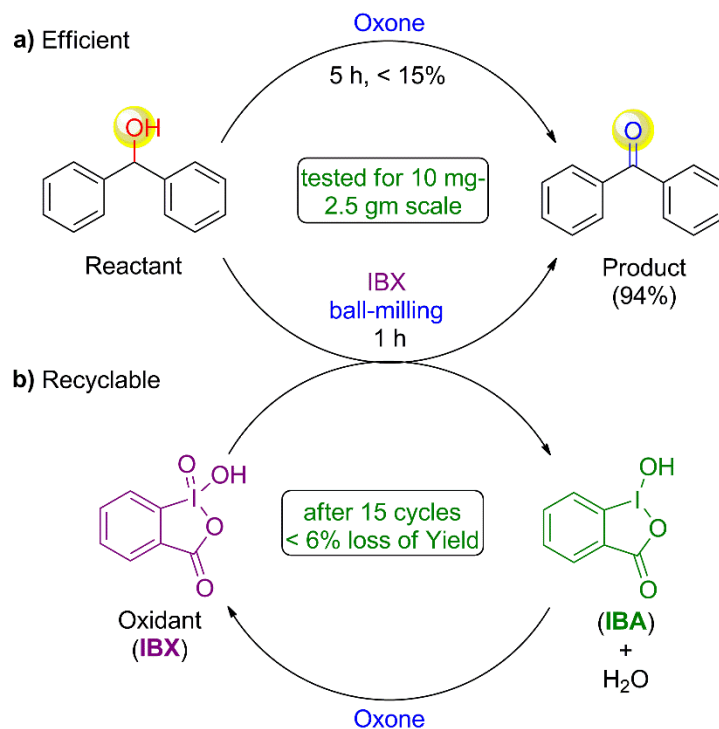


Figure 1.26. a) Efficiency of the IBX oxidation methodology for benzhydrol to benzophenone. b) Overview of recycling process on waste IBA and oxone.⁸⁶

A metal free oxidative amidation methodology via organocatalysis has been established using TBAI-TBHP combination (Fig. 1.27). This example can be considered as C-H activation of aldehydes under ball milling condition. This TBAI-TBHP combination is mild, non-toxic and led to the amide derivative in very good yield.¹⁰⁸

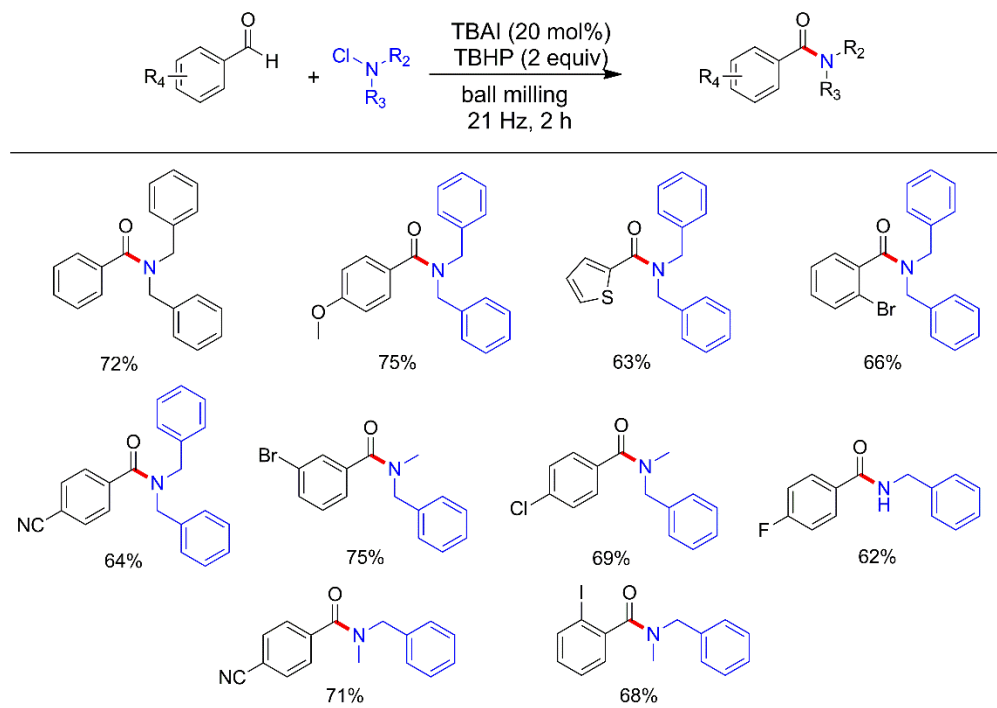


Figure 1.27. Ball milling mediated metal free oxidative amidation methodology.¹⁰⁸

Mal and co-workers have shown that a contact explosive mixture could lead to a high yielding reaction at maximum contact (solvent free ball milling) of the reactants. Conceptually, by selecting an appropriate reaction condition, it was possible to transform a highly exothermic reaction mixture (explosive) into a successful chemical reaction. An acid-salt sodium bisulphate was used to control the reactivity of contact-explosive primary amines-phenyliodine diacetate (Fig. 1.28a). As a proof of the concept,

mechanochemical cross dehydrogenative coupling (CDC) for oxidative amidation of aldehydes *via* C-H activation was considered (Fig. 1.28b).¹⁰⁹

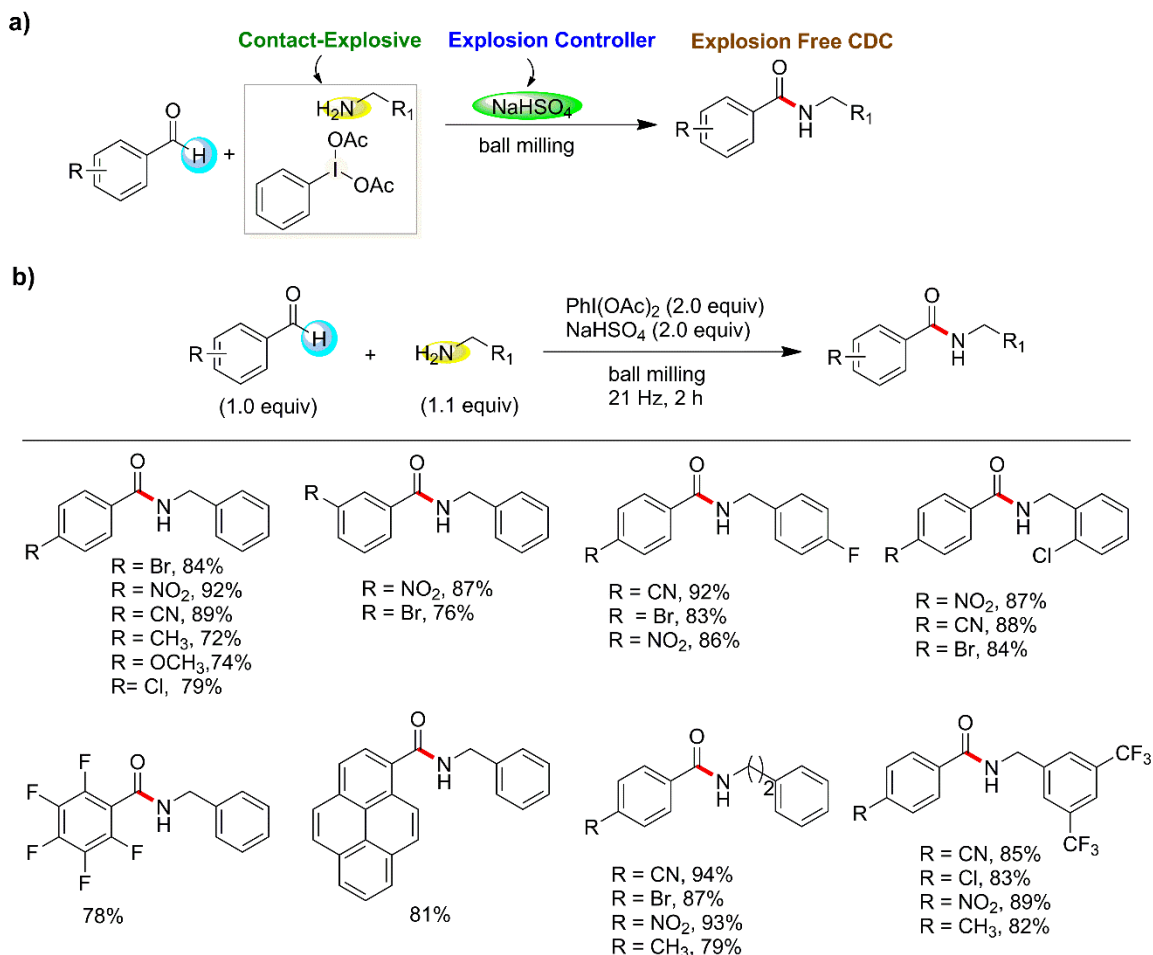


Figure 1.28. Transformation of contact-explosives primary amines and Iodine(III) into a successful chemical reaction under ball milling condition.¹⁰⁹

1.6 CONCLUSION

In last few years, mechanochemistry,^{81-84, 93, 110-112} as a solvent-free synthesis method, has gained great interest to the researchers due to its advantages over traditional solution-based methods.⁸⁵ The core benefit of mechanochemistry is traditional workup can be avoided, easy to perform, less hazardous reaction conditions, etc.^{86, 87, 107, 108} This

advantages have huge implications to green processes, shown to be economical, time efficient and environment friendly. Quantitative conversion, less by products and minimum/no purification bring extra importance to this method. Although, the research on mechanochemistry have received significant advancement during the last decade to have development on environmentally sustainable and more selective processes, still there is long way to achieve the goals on sustainable energy development. In addition, controlling the temperature, moisture contamination for sensitive reactions, handling volatile substances are major disadvantages of the mechanochemical reactions.

Overall, herein a comprehensive account is presented on subcomponent self-assembly to organic synthesis under the research area of mechanochemistry. Thus a linking has been done on supramolecular chemistry to small molecular chemistry.

1.7 NOTES AND REFERENCES

1. C. Bruns and J. F. Stoddart, in *Beauty in Chemistry*, ed. L. Fabbrizzi, Springer Berlin Heidelberg, 2012, vol. 323, ch. 296, pp. 19-72.
2. K. N. Raymond and C. J. Brown, *Top. Curr. Chem.*, 2012, **323**, 1-18.
3. T. Mitra, K. E. Jelfs, M. Schmidtman, A. Ahmed, S. Y. Chong, D. J. Adams and A. I. Cooper, *Nature Chem.*, 2013, **5**, 276-281.
4. J. Rotzler and M. Mayor, *Chem. Soc. Rev.*, 2013, **42**, 44-62.
5. R. Chakrabarty, P. S. Mukherjee and P. J. Stang, *Chem. Rev.*, 2011, **111**, 6810-6918.
6. N. Giuseppone, *Acc. Chem. Res.*, 2012, **45**, 2178-2188.
7. K. Ruiz-Mirazo, C. Briones and A. de la Escosura, *Chem. Rev.*, 2014, **114**, 285-366.

8. Q.-F. Sun, J. Iwasa, D. Ogawa, Y. Ishido, S. Sato, T. Ozeki, Y. Sei, K. Yamaguchi and M. Fujita, *Science*, 2010, **328**, 1144-1147.
9. N. Ponnuswamy, F. B. L. Cougnon, J. M. Clough, G. D. Pantoş and J. K. M. Sanders, *Science*, 2012, **338**, 783-785.
10. S. K. Samanta, J. W. Bats and M. Schmittel, *Chem. Commun.*, 2014, **50**, 2364-2366.
11. X. Su and I. Aprahamian, *Chem. Soc. Rev.*, 2014, **43**, 1963-1981.
12. M. M. Safont-Sempere, G. Fernández and F. Würthner, *Chem. Rev.*, 2011, **111**, 5784-5814.
13. M. L. Saha and M. Schmittel, *Org. Biomol. Chem.*, 2012, **10**, 4651-4684.
14. A. M. Castilla, W. J. Ramsay and J. R. Nitschke, *Acc. Chem. Res.*, 2014, **ASAP article**, DOI: 10.1021/ar5000924.
15. J. R. Nitschke, *Acc. Chem. Res.*, 2007, **40**, 103-112.
16. K.-C. Sham, S.-M. Yiu and H.-L. Kwong, *Inorg. Chem.*, 2013, **52**, 5648-5650.
17. A. M. Castilla, W. J. Ramsay and J. R. Nitschke, *Acc. Chem. Res.*, 2014, **47**, 2063-2073.
18. H. Bunzen, Nonappa, E. Kalenius, S. Hietala and E. Kolehmainen, *Chem. Eur. J.*, 2013, **19**, 12978-12981.
19. X.-P. Zhou, Y. Wu and D. Li, *J. Am. Chem. Soc.*, 2013, **135**, 16062-16065.
20. X.-P. Zhou, J. Liu, S.-Z. Zhan, J.-R. Yang, D. Li, K.-M. Ng, R. W.-Y. Sun and C.-M. Che, *J. Am. Chem. Soc.*, 2012, **134**, 8042-8045.
21. T. K. Ronson, S. Zarra, S. P. Black and J. R. Nitschke, *Chem. Commun.*, 2013, **49**, 2476-2490.

22. C. Talotta, C. Gaeta, Z. Qi, C. A. Schalley and P. Neri, *Angew. Chem. Int. Ed.*, 2013, **52**, 7437–7441.
23. S. Mukherjee and P. S. Mukherjee, *Chem. Commun.*, 2014, **50**, 2239-2248.
24. J.-F. Ayme, J. E. Beves, C. J. Campbell and D. A. Leigh, *Chem. Soc. Rev.*, 2013, **42**, 1700-1712.
25. P. Mal, D. Schultz, K. Beyeh, K. Rissanen and J. R. Nitschke, *Angew. Chem. Int. Ed.*, 2008, **47**, 8297-8301.
26. M. E. Belowich and J. F. Stoddart, *Chem. Soc. Rev.*, 2012, **41**, 2003-2024.
27. K. Osowska and O. Š. Miljanić, *Angew. Chem., Int. Ed.*, 2011, **50**, 8345-8349.
28. C. Giri, F. Topic, P. Mal and K. Rissanen, *Dalton Trans.*, 2014, **43**, 17889-17892.
29. C. Giri, F. Topić, P. Mal and K. Rissanen, *Dalton Trans.*, 2014, **43**, 15697-15699.
30. S. Fischmann and U. Lüning, *Isr. J. Chem.*, 2013, **53**, 87-96.
31. K. Acharyya, S. Mukherjee and P. S. Mukherjee, *J. Am. Chem. Soc.*, 2013, **135**, 554-557.
32. C. S. Wood, T. K. Ronson, A. M. Belenguer, J. J. Holstein and J. R. Nitschke, *Nature Chem.*, 2015, **7**, 354-358.
33. A. J. McConnell, C. S. Wood, P. P. Neelakandan and J. R. Nitschke, *Chem. Rev.*, 2015.
34. T. R. Cook and P. J. Stang, *Chem. Rev.*, 2015, **115**, 7001-7045.
35. T. R. Cook, Y.-R. Zheng and P. J. Stang, *Chem. Rev.*, 2013, **113**, 734-777.
36. D. A. Leigh, R. G. Pritchard and A. J. Stephens, *Nature Chem.*, 2014, **6**, 978-982.

37. D. Leigh, U. Lewandowska, B. Lewandowski and M. Wilson, in *Molecular Machines and Motors*, eds. A. Credi, S. Silvi and M. Venturi, Springer International Publishing, 2014, vol. 354, ch. 546, pp. 111-138.
38. B. Lewandowski, G. De Bo, J. W. Ward, M. Pappmeyer, S. Kuschel, M. J. Aldegunde, P. M. E. Gramlich, D. Heckmann, S. M. Goldup, D. M. D'Souza, A. E. Fernandes and D. A. Leigh, *Science*, 2013, **339**, 189-193.
39. E. Mattia and S. Otto, *Nature Nanotech.*, 2015, **10**, 111-119.
40. Z. He, W. Jiang and C. A. Schalley, *Chem. Soc. Rev.*, 2015, **44**, 779-789.
41. A. Herrmann, *Chem. Soc. Rev.*, 2014, **43**, 1899-1933.
42. K. Osowska and O. Š. Miljanić, *Synlett*, 2011, 1643-1648.
43. A. C. Fahrenbach, C. J. Bruns, H. Li, A. Trabolsi, A. Coskun and J. F. Stoddart, *Acc. Chem. Res.*, 2013, **47**, 482-493.
44. C. J. Bruns and J. F. Stoddart, *Nat Nano*, 2013, **8**, 9-10.
45. R. S. Forgan, J.-P. Sauvage and J. F. Stoddart, *Chem. Rev.*, 2011, **111**, 5434-5464.
46. L. Fang, M. A. Olson, D. Benitez, E. Tkatchouk, W. A. Goddard, 3rd and J. F. Stoddart, *Chem. Soc. Rev.*, 2010, **39**, 17-29.
47. M. C. Thompson and D. H. Busch, *J. Am. Chem. Soc.*, 1964, **86**, 3651-3656.
48. M. C. Thompson and D. H. Busch, *J. Am. Chem. Soc.*, 1962, **84**, 1762-1763.
49. G. Zhang and M. Mastalerz, *Chem. Soc. Rev.*, 2014, **43**, 1934-1947.
50. A. Wilson, G. Gasparini and S. Matile, *Chem. Soc. Rev.*, 2014, **43**, 1948-1962.
51. M. L. Saha, N. Mittal, J. W. Bats and M. Schmittel, *Chem. Commun.*, 2014, **50**, 12189-12192.
52. J. R. Nitschke, *Chem. Soc. Rev.*, 2014, **43**, 1798-1799.

53. M. Han, D. M. Engelhard and G. H. Clever, *Chem. Soc. Rev.*, 2014, **43**, 1848-1860.
54. M. Schmittel and V. Kalsani, *Top. Curr. Chem.*, 2005, **245**, 1-53.
55. T. J. Hubin and D. H. Busch, *Coord. Chem. Rev.*, 2000, **200–202**, 5-52.
56. J. R. Nitschke, *Angew. Chem. Int. Ed.*, 2004, **43**, 3073-3075.
57. D. Schultz and J. R. Nitschke, *Angew. Chem. Int. Ed.*, 2006, **45**, 2453-2456.
58. S. Zarra, D. M. Wood, D. A. Roberts and J. R. Nitschke, *Chem. Soc. Rev.*, 2014, Ahead of Print.
59. Y. Inokuma, M. Kawano and M. Fujita, *Nature Chem.*, 2011, **3**, 349-358.
60. Y. Inokuma, T. Arai and M. Fujita, *Nature Chem.*, 2010, **2**, 780-783.
61. D. Fujita and M. Fujita, *ACS Central Science*, 2015, **1**, 352-353.
62. B. M. Schmidt, T. Osuga, T. Sawada, M. Hoshino and M. Fujita, *Angew. Chem. Int. Ed.*, 2016, **55**, 1561-1564.
63. A. K. Bar, R. Chakrabarty, G. Mostafa and P. S. Mukherjee, *Angew. Chem. Int. Ed.*, 2008, **47**, 8455-8459.
64. S. R. Halper, M. R. Malachowski, H. M. Delaney and S. M. Cohen, *Inorg. Chem.*, 2004, **43**, 1242-1249.
65. J. M. Sutton, E. Rogerson, C. J. Wilson, A. E. Sparke, S. J. Archibald and R. W. Boyle, *Chem. Commun.*, 2004, **0**, 1328-1329.
66. M. Schmittel and A. Ganz, *Chem. Commun.*, 1997, **0**, 999-1000.
67. M. Schmittel, V. Kalsani, P. Mal and J. W. Bats, *Inorg. Chem.*, 2006, **45**, 6370-6377.

68. M. Schmittl, V. Kalsani, D. Fenske and A. Wiegrefe, *Chem. Commun.*, 2004, 490-491.
69. V. Kalsani, H. Bodenstedt, D. Fenske and M. Schmittl, *Eur. J. Inorg. Chem.*, 2005, 1841-1849.
70. V. Kalsani, H. Ammon, F. Jaeckel, J. P. Rabe and M. Schmittl, *Chem. Eur. J.*, 2004, **10**, 5481-5492.
71. M. Schmittl, V. Kalsani, C. Michel, P. Mal, H. Ammon, F. Jaeckel and J. P. Rabe, *Chem. Eur. J.*, 2007, **13**, 6223-6237.
72. M. Schmittl, B. He and P. Mal, *Org. Lett.*, 2008, **10**, 2513-2516.
73. M. Schmittl and P. Mal, *Chem. Commun.*, 2008, 960-962.
74. K. S. Chichak, S. J. Cantrill, A. R. Pease, S.-H. Chiu, G. W. V. Cave, J. L. Atwood and J. F. Stoddart, *Science*, 2004, **304**, 1308-1312.
75. S. J. Cantrill, K. S. Chichak, A. J. Peters and J. F. Stoddart, *Acc. Chem. Res.*, 2005, **38**, 1-9.
76. J. E. Beves, B. A. Blight, C. J. Campbell, D. A. Leigh and R. T. McBurney, *Angew. Chem. Int. Ed.*, 2011, **50**, 9260-9327.
77. T. Hasell, X. Wu, J. T. A. Jones, J. Bacsá, A. Steiner, T. Mitra, A. Trewin, D. J. Adams and A. I. Cooper, *Nature Chem.*, 2010, **2**, 750-755.
78. J. R. Holst, A. Trewin and A. I. Cooper, *Nature Chem.*, 2010, **2**, 915-920.
79. J.-F. Ayme, J. E. Beves, D. A. Leigh, R. T. McBurney, K. Rissanen and D. Schultz, *Nature Chem.*, 2012, **4**, 15-20.
80. P. Mal, B. Breiner, K. Rissanen and J. R. Nitschke, *Science*, 2009, **324**, 1697-1699.

81. R. S. Varma, *Green Chem.*, 2014, **16**, 2027-2041.
82. G. Cravotto, E. C. Gaudino and P. Cintas, *Chem. Soc. Rev.*, 2013, **42**, 7521-7534.
83. D. Braga, L. Maini and F. Grepioni, *Chem. Soc. Rev.*, 2013, **42**, 7638-7648.
84. S. L. James, C. J. Adams, C. Bolm, D. Braga, P. Collier, T. Friscic, F. Grepioni, K. D. M. Harris, G. Hyett, W. Jones, A. Krebs, J. Mack, L. Maini, A. G. Orpen, I. P. Parkin, W. C. Shearouse, J. W. Steed and D. C. Waddell, *Chem. Soc. Rev.*, 2012, **41**, 413-447.
85. S. Ley, M. O'Brien and R. Denton, *Synthesis*, 2011, 1157-1192.
86. T. K. Achar, S. Maiti and P. Mal, *RSC Adv.*, 2014, **4**, 12834-12839.
87. A. Bose and P. Mal, *Tetrahedron Lett.*, 2014, **55**, 2154-2156.
88. P. J. Walsh, H. Li and C. A. de Parrodi, *Chem. Rev.*, 2007, **107**, 2503-2545.
89. M. K. Beyer and H. Clausen-Schaumann, *Chem. Rev.*, 2005, **105**, 2921-2948.
90. K. Tanaka and F. Toda, *Chem. Rev.*, 2000, **100**, 1025-1074.
91. A. Stolle, T. Szuppa, S. E. S. Leonhardt and B. Ondruschka, *Chem. Soc. Rev.*, 2011, **40**, 2317-2329.
92. B. İçli, N. Christinat, J. Tönnemann, C. Schüttler, R. Scopelliti and K. Severin, *J. Am. Chem. Soc.*, 2009, **131**, 3154-3155.
93. T. Friščić, I. Halasz, P. J. Beldon, A. M. Belenguer, F. Adams, S. A. J. Kimber, V. Honkimäki and R. E. Dinnebier, *Nature Chem.*, 2013, **5**, 66-73.
94. M. Ferguson, N. Giri, X. Huang, D. Apperley and S. L. James, *Green Chem.*, 2014, **16**, 1374-1382.
95. S.-Y. Hsueh, K.-W. Cheng, C.-C. Lai and S.-H. Chiu, *Angew. Chem. Int. Ed.*, 2008, **47**, 4436-4439.

96. C.-C. Hsu, N.-C. Chen, C.-C. Lai, Y.-H. Liu, S.-M. Peng and S.-H. Chiu, *Angew. Chem. Int. Ed.*, 2008, **47**, 7475-7478.
97. A. M. Belenguer, T. Friscic, G. M. Day and J. K. M. Sanders, *Chem. Sci.*, 2011, **2**, 696-700.
98. Q. Ji, R. C. Lirag and O. S. Miljanic, *Chem. Soc. Rev.*, 2014, **43**, 1873-1884.
99. E. Gaffet, F. Bernard, J.-C. Niepce, F. Charlot, C. Gras, G. Le Caer, J.-L. Guichard, P. Delcroix, A. Mocellin and O. Tillement, *J. Mater. Chem.*, 1999, **9**, 305-314.
100. M. K. Beyer and H. Clausen-Schaumann, *Chem. Rev.*, 2005, **105**, 2921-2948.
101. F. Toda, K. Tanaka and S. Iwata, *J. Org. Chem.*, 1989, **54**, 3007-3009.
102. G. Kaupp, *Top. Curr. Chem.*, 2005, **254**, 95.
103. G. Kaupp, *CrystEngComm*, 2003, **5**, 117-133.
104. G. Rothenberg, A. P. Downie, C. L. Raston and J. L. Scott, *J. Am. Chem. Soc.*, 2001, **123**, 8701-8708.
105. J. M. K. Shayesteh, M. Haghighi and H. Eskandari, *Asian J. Chem.*, 2010, **22**, 2106-2116.
106. J.-L. Do, C. Mottillo, D. Tan, V. Štrukil and T. Friščić, *J. Am. Chem. Soc.*, 2015, **137**, 2476-2479.
107. S. Maiti and P. Mal, *Synth. Commun.*, 2014, **44**, 3461-3469.
108. T. K. Achar and P. Mal, *J. Org. Chem.*, 2015, **80**, 666-672.
109. T. K. Achar and P. Mal, *Adv. Synth. Catal.*, 2015, **357**, 3977-3985.
110. J. Li, C. Nagamani and J. S. Moore, *Acc. Chem. Res.*, 2015, **48**, 2181-2190.
111. J. Ribas-Arino and D. Marx, *Chem. Rev.*, 2012, **112**, 5412-5487.

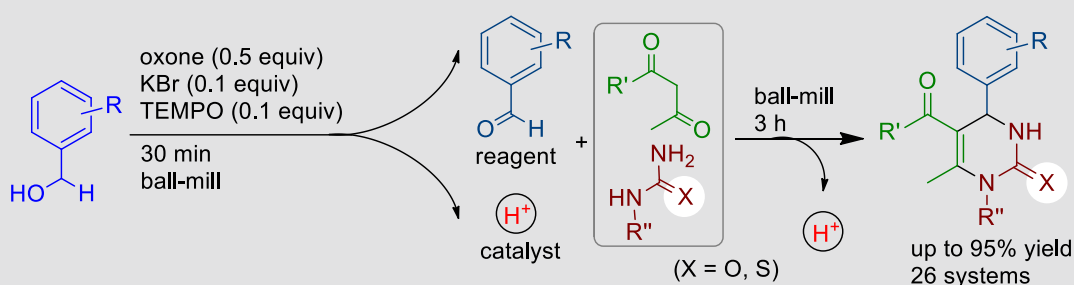
112. J. Ribas-Arino, M. Shiga and D. Marx, *Angew. Chem. Int. Ed.*, 2009, **48**, 4190-4193.

CHAPTER 2

Subcomponent Approach towards the Synthesis of Dihydropyrimidones via Mechano-Milling and its Biological Application

2.1 ABSTRACT

A mechanochemical system: multi-step, multi-component via subcomponent



We report here unique example of system chemistry on small molecules through covalent mechanochemistry. As a model system Multicomponent Biginelli reaction was performed *via* subcomponent synthesis. Reactions were done as solvent free, metal free and mechanochemically (ball milling) at room temperature. Benzaldehydes was formed as a product during Br^+ catalyzed oxidation of benzyl alcohols and H^+ as a by-product which were further promoted as component and catalyst, respectively, for further transformation to dihydropyrimidones within the same reaction pot. A DHPM derivative i.e., Monastrol is a cell-permeable small molecule and serves as potent anticancer drug, was also synthesized using this methodology.

2.2 INTRODUCTION

In system chemistry subcomponent self-assembly¹⁻⁵ is a synthetic approach where ligands of the metallo-supramolecular complexes are produced *in situ* from their subcomponents. The study of

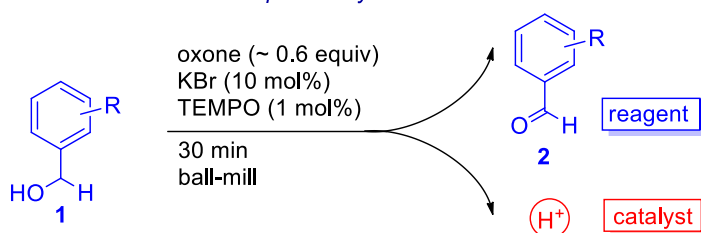
systems chemistry⁶⁻⁸ offers primary understandings into the self-sorting principles⁹⁻¹⁴ of molecular networks which eventually assist us to gain new systems¹⁵ with functions and properties unlike any conventional materials.^{16, 17} Also, This technique has established to be a promising method for synthesis of high-purity metal-complexes from complex mixtures of reactants using minimum number of reaction-steps.^{18, 19} On the other hand, understanding of system chemistry amongst small molecules in metal free systems have not been explored, if any.

Recently, mechanochemistry,²⁰⁻²⁵ as a solvent-free synthesis, has drawn a significant interest due to its benefits over conventional solution-based methods.²⁶ The potential benefit of the mechanochemical synthesis is to avoid traditional workup.²⁷⁻³⁰ This advantage has significant influences to green processes, shown to be economical, time efficient and environmentally benign. Quantitative conversion, less by products and minimum purification bring additional importance to this method. The mechanochemical synthesis of small organic molecules is well explored³¹ which also includes multi-step synthesis.²⁹

Considering these aspects, we are demonstrating a unique example of covalent (metal free) approach in system chemistry in which subcomponent, catalyst were synthesized and used for cascaded post-synthetic transformations for multicomponent Biginelli reaction (Fig. 2.1) within a single ball-milling pot. Aiming to introduce environmentally benign synthesis of small molecules towards development of drug discovery we are reporting here solvent free ball milling (mechano milling) synthesis of dihydropyrimidone (DHPMs) at room temperature. DHPMs have shown a diverse range of biological activities such as antimicrobial,³² antiviral,³³ anti-inflammatory³⁴, anti-hypertensive,³⁵ potassium channel antagonists³⁶ and antioxidant activity.³⁷ Monastrol(**5da**) (Fig. 2.6), the most active DHPM derivative has established as potent anticancer drug and found to be allosteric inhibitor of human kinesin Eg5, leading to mitotic arrest and subsequent

apoptotic cell death.^{38, 39} Different analogues of Monastrol and Oxo-Monastrol were also found to be effective on various cancer cell lines,^{40, 41} which led to the attention for efficient pharmacophore variation of DHPMs for synthesis of novel Monastrol analogues.

a) Reaction initiation: subcomponent synthesis



b) Cascaded transformation: multicomponent reaction

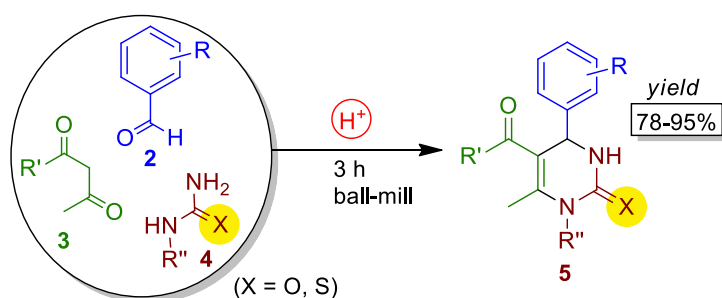


Figure 2.1. System chemistry model. a) Subcomponent synthesis and b) followed by multicomponent transformation.

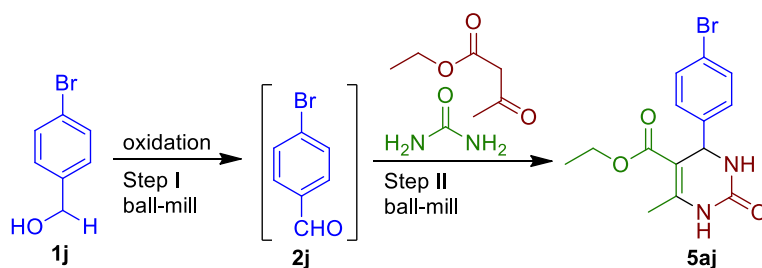
Furthermore, we are also reporting here the antioxidant property of DHPM derivatives (Monastrol analogues) via radical (2,2-diphenyl-1-picrylhydrazyl or DPPH, hydroxyl, nitric oxide and superoxide) scavenging studies.

2.3 RESULT AND DISCUSSION

Br⁺ catalyzed oxidation reaction using TBAB,⁴² NBS^{43, 44} in presence of oxone⁴⁵ are very popular. Now a days metal free oxidation reactions are common in pharmaceutical industries to avoid toxic metal contamination in drugs. In Fig. 2.1a, Br⁺ catalyzed, green and solvent free mechanochemical oxidation of alcohols to aldehydes is described. Reactions were done using

combination of catalytic amount of potassium bromide (KBr) - oxone ($2\text{KHSO}_5 \cdot \text{KHSO}_4 \cdot \text{K}_2\text{SO}_4$)- 2,2,6,6-tetramethylpiperidin-1-yl-oxy radical (TEMPO).⁴⁶

Table 2.1. Optimization of reaction condition



Entry	Step I (condition)	Yield of 2c (%) ^a	Step II	Yield of 5ac (%)
1	IBX ^b (1.1 equiv) 1 h	94	> 4 h	no reaction
2	NBS (1.5 equiv) 30 min	99	> 4 h	Trace (< 3)
3	oxone (1 equiv) TBAB ^c (10 mol%) TEMPO (10 mol%) 30 min	100	3.5 h	81
4	oxone (1 equiv) KBr (10 mol%) TEMPO (10 mol%) 30 min	100	3.5 h	91
5	oxone (0.6-0.7 equiv) KBr (10 mol%) TEMPO (1 mol%) 30 min	100	3.5 h	92

^aYields were determined by ¹H NMR analysis. ^bIBX is 2-Iodoxybenzoic acid. ^cTBAB is tetrabutyl ammonium bromide.

Aldehydes obtained from first step were used as a component, and by-product H^+ was the catalyst for follow up Biginelli reaction (Fig. 2.1b). First step of the reaction was conceived as a covalent type of subcomponent synthesis. However, second step may be an example of self-sorting in which dihydropyrimidones (DHPMs) were obtained using benzaldehydes, 1,3-dicarbonyls (ethyl acetoacetate or acetyl acetone) and urea (or thiourea) as components. Both steps were done in one-pot and the total system can be considered as an example of system chemistry under the area of covalent mechanochemistry.⁴⁷⁻⁴⁹

Table 2.1 exemplifies optimization of reaction conditions. During optimization, progress of the reactions were checked by TLC (thin layer chromatography) or 1H NMR. In a typical run, milling apparatus was stopped and a small portions of sample was collected from reaction-jar and examined. Once reaction was finished, solid-mass was taken in a flask, washed with appropriate solvents and filtered off. Most appropriate condition (entry 5) was identified in which both reaction steps cooperatively led to final products in reasonable yields. Generally, multicomponent Biginelli reaction works in presence of acid or base as a catalyst. But in our strategy, no catalyst was required to be added externally to perform the reaction.

KBr-oxone-TEMPO mediated oxidation of benzyl alcohols was reported by Togo and coworkers for 24 h in different solvents like CH_3CN -water, dichloromethane or ethyl acetate.⁴⁶ Over oxidation could not be controlled and significant amount of benzoic acid was formed in several cases. This kind of shortcomings are very common in the solution phase oxidation chemistry. However, using this methodology, using 1 mol% TEMPO in 30 minutes under solvent free ball milling condition the oxidation was achieved in near quantitative conversion. In general, it is likely that under constrained media the maximum possible concentration of reacting partners putting the system in high stress and hence it could lead to uncontrollable oxidation of newly

formed aldehydes to corresponding acids. Contrastingly, the described methodology for alcohol oxidation (Fig. 2.1a) might serve as an significant documentation in which a solution based oxidation reaction was achieved under solvent free ball milling condition, in higher efficiency, better yields and no over oxidized products.

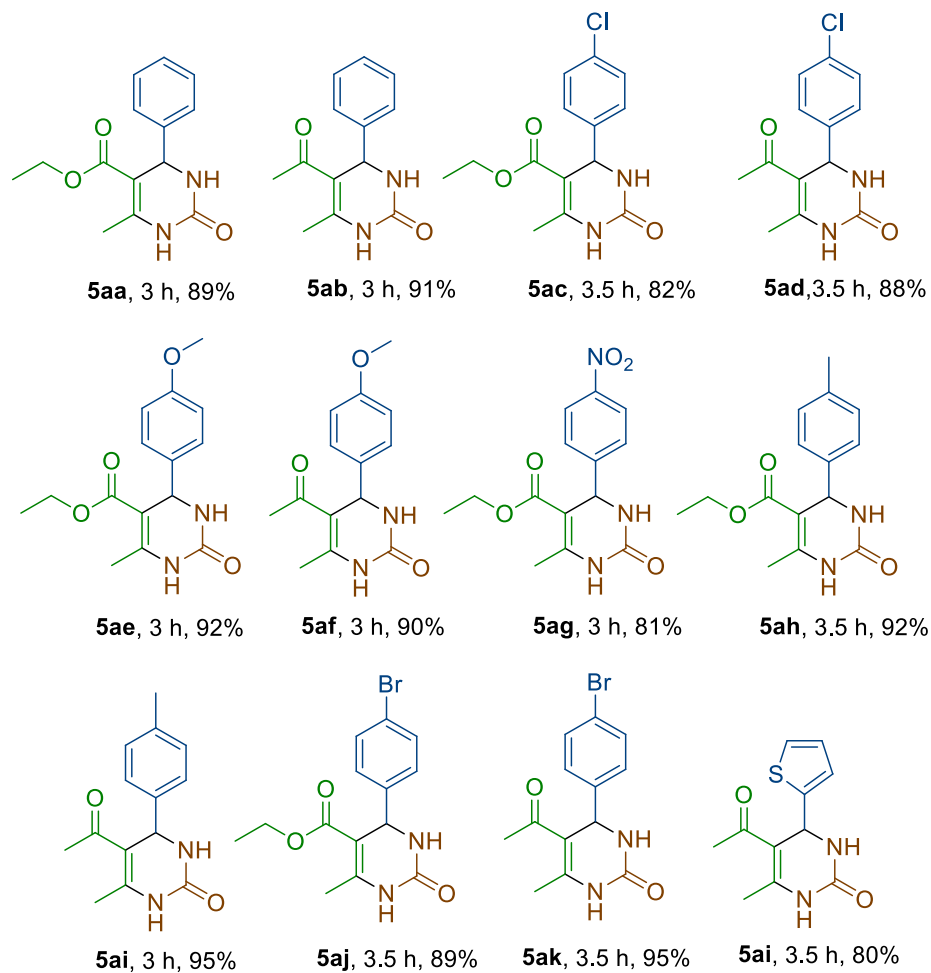


Figure 2.2. Overall (two steps) yields of DHPMs, reaction time for the second step (additional 30 min for the first step) and compounds identification numbers are shown here.

Efficacy for this two-step mechanochemical methodology of DHPMs synthesis looks highly promising. Products were isolated in very good to excellent yields at relatively smaller reaction

time (Fig. 2.2). This methodology works for wide range of electron rich (**5ae**, **5af**, **5ah** and **5ai**), electron deficient (**5ag**) aromatic and thiophenyl aldehydes (**5al**).

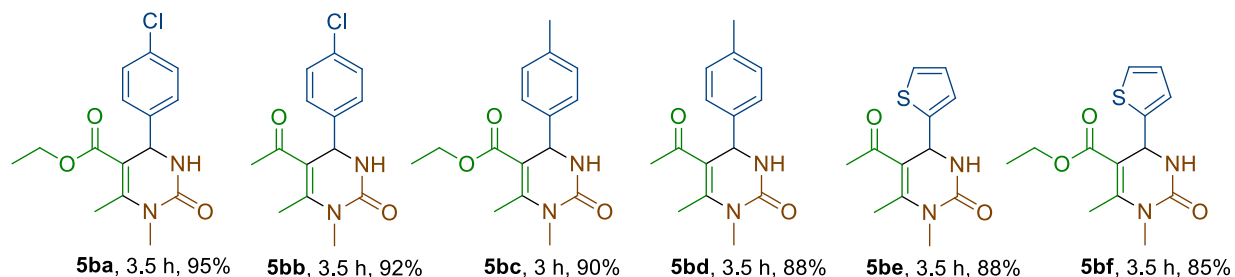


Figure 2.3. Regioselective DHPMs using *N*-methyl urea

Regio-selectivity⁵⁰ for synthesis of DHPMs using *N*-methyl urea is also established (Fig. 2.3).⁵¹

The reactions are controlled by steric effect and that led to single regio-isomer in all cases.

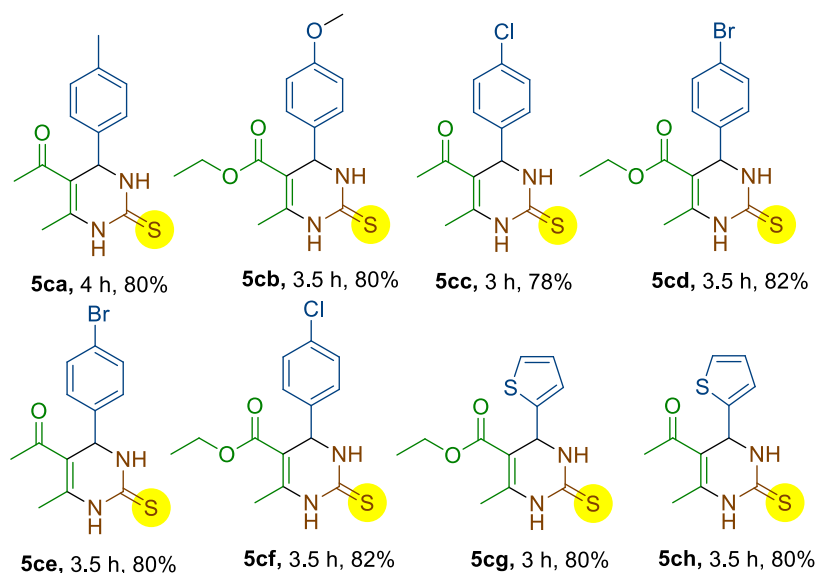


Figure 2.4. DHPMs using thio-urea.

Furthermore, the reactions with thio-urea also resulted in DHPMs with good yield (Fig. 2.4).

Collection of two consecutive thermodynamically stable reaction systems of small molecules was described here using system chemistry approach under mechanomilling. Complete success

for two steps (DHPM synthesis) is depended upon active participation of products (aldehydes) and by-products (H^+) of first step. As shown in Table 2.1, mechano-milling oxidation of alcohols to aldehydes were successful using 2-iodoxybenzoic acid (IBX, entry 1),²⁷*N*-bromosuccinimide (NBS, entry 2) and oxone-KBr-TEMPO (entry 3). As representative examples shown in Fig. 2.5, analysis of the 1H NMR spectra for NBS and oxone-KBr-TEMPO mediated oxidations reactions are clean and high yielding. Unfortunately, second step was unsuccessful using two oxidations systems (IBX and NBS) because, the by-products were not efficient enough as catalyst for Biginelli reaction. Notably, by-products were 2-iodosobenzoic acid (IBA) and succinimide from reactions using IBX and NBS, respectively.

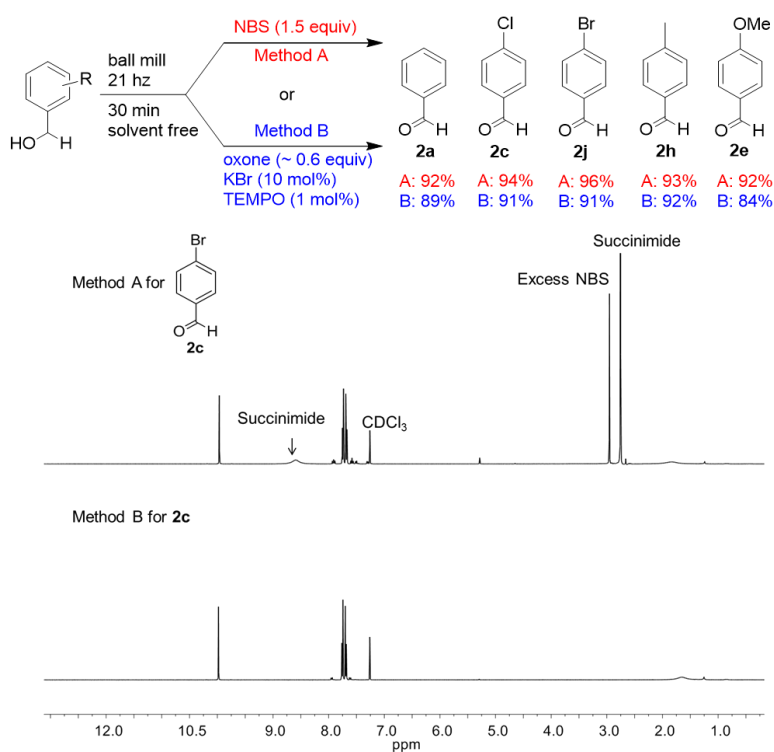


Figure 2.5. a) Efficiency of NBS (method A) and oxone-KBr-TEMPO (method B) mediated oxidations and b) – c) respective 1H NMR spectra (in $CDCl_3$).

To the best of our knowledge solvent free NBS mediated oxidations of alcohols to aldehydes under mechanochemical condition presented herein are new. The products obtained from this

reactions were sufficient pure (Fig. 4) to be used directly for synthetic transformations. This methodology is green, economical and adapts in to milder reaction condition. We hope this methodology will serve as an important addition to organic synthesis and industries.

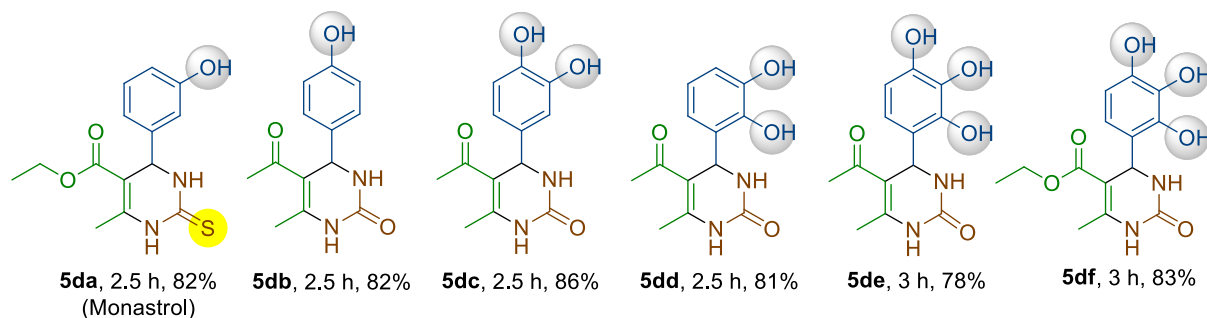


Figure 2.6. Monastrol and Oxo-Monastrol derivatives synthesized from hydroxyl aromatic aldehydes.

After the synthesis, we have focused our attention towards development of anticancer drug with antioxidant properties. It is established that the organic compounds with phenols have potential to do radical scavenging activities⁵². A rational approach for selection of radical scavengers requires a knowledge of the mechanisms. It may be practical to have simple procedures for estimating the appropriateness of a radical scavenger for a given composition. Our first choice was phenolic compounds. In general, the radical scavenging effect is determined by the reactivity of both the scavenger itself and the radicals that it produces⁵³. In phenolic derivatives phenoxyl radical can easily accept one electron to become phenoxide anion⁵⁴. Consequently, we targeted to synthesize the compounds from polyhydroxy phenolic aldehydes as one of the building blocks. The oxo-Monastrol derivatives (**5db-5df**, Fig. 2.6) contain one or more hydroxyl group and could have antioxidant properties. Compounds **5dd-5df** are synthesized from salisaldehyde derivatives and may lead to intramolecular imine-amide tautomeric equilibrium⁵⁵ between flexible structure **I** and rigid structure **II** (Fig. 2.7). This imine-amide tautomerism via O-H...N hydrogen bonding for oxo-Monastrols (**5dd-5df**) may decrease the electrophilicity of the

phenyl ring electronically (oxygen is more electronegative than nitrogen). In addition, structure **II** (Fig. 2.7) becoming more planar and rigid due to formation of a six-membered ring at the bridge of pyrimidone and phenyl rings. Therefore binding with DNA through minor groove is expected to get enhanced *via* intercalation⁵⁶.

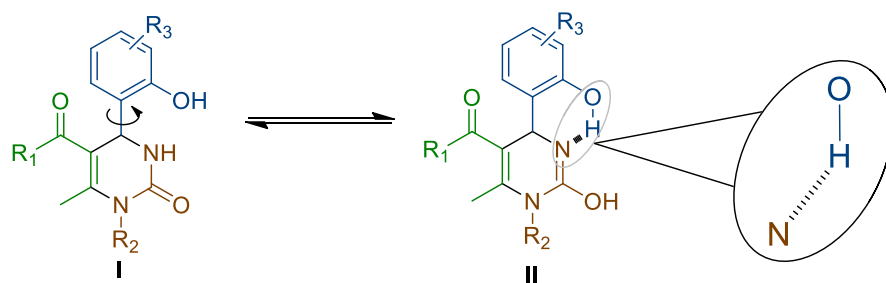


Figure 2.7. Imine-amide tautomeric equilibrium in **5dd-5df**.

Antioxidant Activity

Free radicals such as superoxide, hydroxyl and nitric oxide are often generated as by-products of biological processes and can cause damage to lipids, proteins and DNA. Antioxidants are naturally occurring or synthetic compounds which have power to scavenge free radicals and thus preventing radical-induced cellular damage⁵⁷. Due to the chemical diversity of the antioxidant compounds, a single antioxidant assay does not reflect their total antioxidant capacity (TAC). Several methods, differing in their chemistry (generation of different radicals and/or target molecules), and detection of end points have been developed for measuring the TAC of the compounds. The antioxidant action of a test sample is mediated by hydrogen atom transfer (HAT) and single electron transfer (SET) reactions as well as their combinations *via* sequential proton loss and electron transfer (SPLET)⁵⁸. Herein, we evaluated antioxidant activity of oxo-Monastrol derivatives by four different radical (DPPH, hydroxyl, nitric oxide, and superoxide) scavenging assay with Gallic acid (GA) as a reference compound.

DPPH Radical Scavenging Activity

An initial screening, the DPPH radical scavenging assay was performed with all synthesized compounds to select potential candidates to be able to capture free radicals³⁷. Oxo-Monastrol derivatives and Gallic acid scavenged the DPPH[•] (DPPH radical) as concentration dependent manner (Fig. 2.12, supporting information) and IC₅₀ values are summarized in Table 2.2.

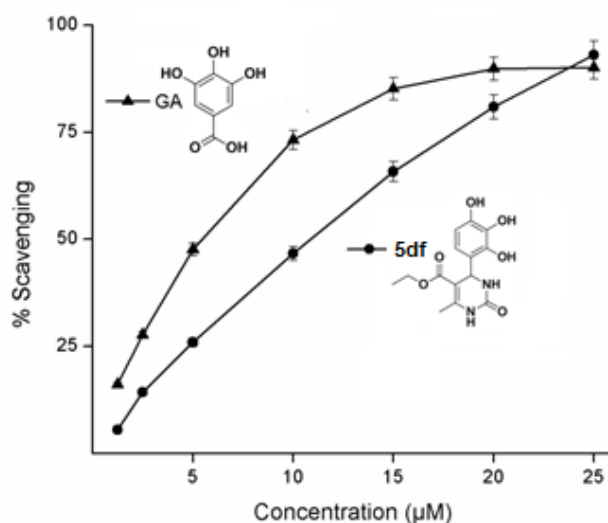


Figure 2.8. DPPH radical scavenging activity of compound 5df and GA. Experiment was performed in triplicate and the results were expressed as mean values \pm standard deviations.

Compound **9a** having a hydroxyl group at para- position showed very poor DPPH radical scavenging activity (IC₅₀ = 21.9 mM), whereas hydroxyl group at meta- position (**5da**, Monastrol) exhibited relatively higher activity (IC₅₀ = 6.0 mM). The activity was found to be significantly increased (mM to µM level) for **5dc** and **5dd**. However, activity was not found to be further increased in **5de** and **5df** (IC₅₀ = 11.6 µM and 11.0 µM, respectively), having three hydroxyl groups, suggesting hydroxyl group at ortho-position (salisaldehyde derivatives) are probably involved in hydrogen bonding with *N*-atom in DHPM moiety and therefore does not take part in DPPH radical scavenging activity. Same trend was also found in compound **5dc**(IC₅₀

= 12.4 μM) and **5dd** (IC_{50} = 51.6 μM). These results suggest that DPPH radicals scavenging activity of these DHPM derivatives depend not only the number of hydroxyl group but also depend on their position, and are not influenced by any other group present in pyrimidone ring. Among these compounds, **5df** was found to be most effective and its activity was comparable with standard Gallic acid (Fig. 2.8).

Table 2.2. Concentration of DHPMs and Gallic acid necessary to scavenge free radicals by 50% (IC_{50})

Substrate	DPPH ^a	$\cdot\text{O}_2^{-b}$	$\cdot\text{OH}^a$	$\text{NO}^{\cdot a}$
5da	$6.0 \times 10^3 \pm 0.18$	3.5 ± 0.05	111.5 ± 1.55	186.0 ± 1.57
5db	$21.9 \times 10^3 \pm 0.56$	1.0 ± 0.02	207.3 ± 1.18	139.8 ± 0.71
5dc	12.4 ± 0.54	2.0 ± 0.08	136.2 ± 1.51	156.3 ± 1.08
5dd	51.6 ± 1.25	1.5 ± 0.06	169.9 ± 3.01	151.3 ± 1.43
5de	11.6 ± 0.62	1.3 ± 0.03	178.3 ± 1.58	137.0 ± 1.64
5df	11.0 ± 0.71	1.0 ± 0.04	237.3 ± 2.17	134.1 ± 0.92
GA	05.2 ± 0.14	2.6 ± 0.07	86.3 ± 0.22	99.2 ± 1.16

^a IC_{50} in μM ; ^b IC_{50} in mM. All tests were performed in triplicate and the results were expressed as mean values \pm standard deviations.

Superoxide Radical Scavenging Activity

Superoxide radical is principally derived from the oxygen that is consumed in various metabolic reactions⁵⁹. Although superoxide is not highly toxic to cell but its effect can be magnified because it produces other types of free radicals and oxidizing agents that can induce cellular damage⁶⁰. However, superoxide radicals are produced more in cancer cells⁶¹ and therefore control of elevated level of superoxide radical is essential to protect the normal cells during cancer development. In our study, all tested compound showed concentration-dependent $\cdot\text{O}_2^{-}$ radical scavenging activity (Figure 2.13, supporting information). The activity of all compounds

was found to be two to three times higher than standard Gallic acid, except Monastrol (**5da**, Table 2.2). Compound **5db** having para-hydroxyl group showed 3.5 time higher activity than meta-hydroxyl containing Monastrol. Compared to **5db**, activity was found to be decreased after addition of another hydroxyl group at meta- position (compound **5dc**). Conversely, ortho and meta-hydroxyl group containing **5dd** showed relatively higher activity than meta and para-hydroxyl bearing compound **5dc**. In addition, three hydroxyl (ortho, meta and para) containing compounds **5de** and **5df** showed higher activity than two hydroxyl containing compounds **5dc** and **5dd** but the activity was not found to be higher than para-hydroxyl containing **5db**. These results suggest that para-hydroxyl group is most important for superoxide radical scavenging activity of the novel derivatives. Altogether, compounds **5db** and **5df** were found to be most potent among the tested compounds whereas the least potent Monastrol showed comparable activity to Gallic acid (Fig. 2.9).

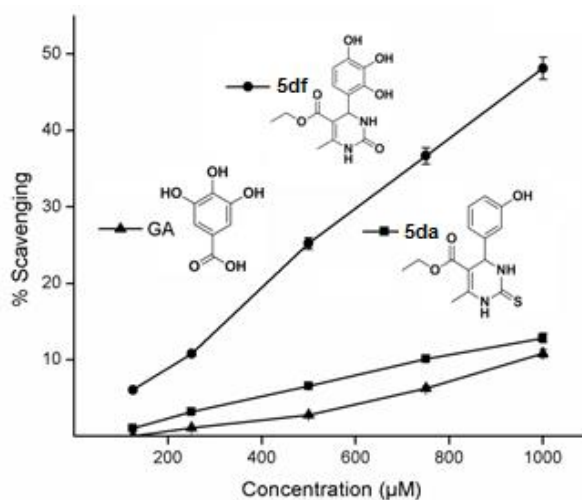


Figure 2.9. Superoxide radical scavenging activity of compound **5da**, **5df** and GA. Experiment was performed in triplicate and the results were expressed as mean values \pm standard deviations.

Hydroxyl Radical Scavenging Activity

Hydroxyl radical is formed by the reaction of $O_2^{\cdot-}$ with H_2O_2 in the presence of Fe^{2+} or Cu^+ (catalyst). This radical is most reactive oxygen species causing lipid peroxidation and enormous biological damage⁶². Therefore it is most favourable for cancer treatment if anticancer drugs can scavenge hydroxyl radical as well. In this study, all the tested compounds showed concentration-dependent $\cdot OH$ scavenging activity (Fig. 2.14, supporting information). The activity of these compounds was found within comparable range (111.5 – 237.3 μM) in respect to standard Gallic acid (86.3 μM , Table 2). Compared to **8db**, activity was found to be decreased with addition of one (**8dc** and **8dd**) or two hydroxyl group (**5de** and **5df**). Remarkably, this activity was found to be reversed trend of superoxide radical scavenging assay. However in comparison to each other, highest superoxide radical scavenging compound **5df** showed lowest $\cdot OH$ scavenging activity, while the least superoxide radical scavenger Monastrol (**5da**) exhibited highest $\cdot OH$ scavenging activity (Fig. 2.10).

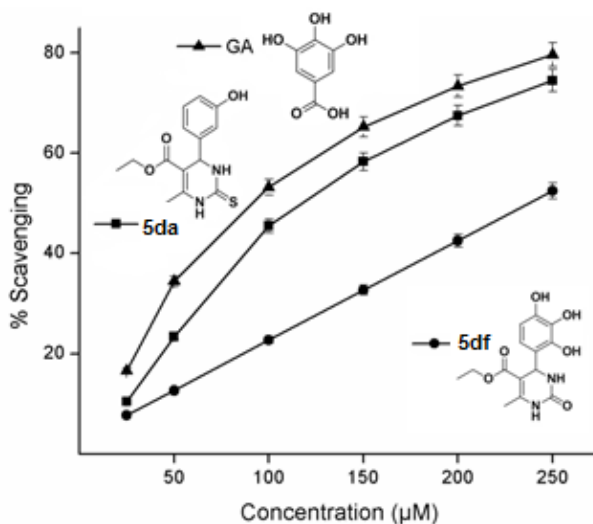


Figure 2.10. Hydroxyl radical scavenging activity of compound **5da**, **5df** and GA. Experiment was performed in triplicate and the results were expressed as mean values \pm standard deviations.

Nitric Oxide Radical (NO[•]) Scavenging Activity

NO[•] is a short-lived, endogenously produced gas that acts as a signalling molecule in the cells and has an important role in various inflammatory processes^{63, 64}. Its sustained production is toxic to tissues and can cause DNA damage *via* the generation of peroxynitrite (ONOO⁻) and N₂O₃⁶⁴. Over past decades, NO has focussed as a molecule of interest in carcinogenesis and tumor development. However, there is considerable controversy and confusion in understanding its role in cancer biology⁶⁴. NO may have both genotoxic and angiogenic properties. It appears that high levels of NO may be cytostatic or cytotoxic for tumor cells, whereas low level activity can have the opposite effect and promote tumour growth⁶³. Therefore it will be favourable for cancer treatment if anticancer drug can beneficially scavenge NO[•] and thereby diminish the controversy role NO in cancer biology. Our results showed concentration-dependent NO[•] scavenging activity by all the tested compounds (Fig. 2.15, supporting information) and the IC₅₀ values are presented in Table 1. The tested compounds showed a moderate to good nitric oxide radical scavenging activity in respect to standard Gallic acid (IC₅₀ = 99.2 μM). However, a significant change in NO[•] scavenging activity was observed with variation of number and position of hydroxyl groups, but we can't describe conclusively because activities of the all compounds were found to be very close to each other (Table 1). Overall, compound **5df** was found to be most potent (IC₅₀ = 134.1 μM), while Monastrol (**5da**) (IC₅₀=186.0 μM) showed lowest nitric oxide radical scavenging activity among them (Fig. 2.11).

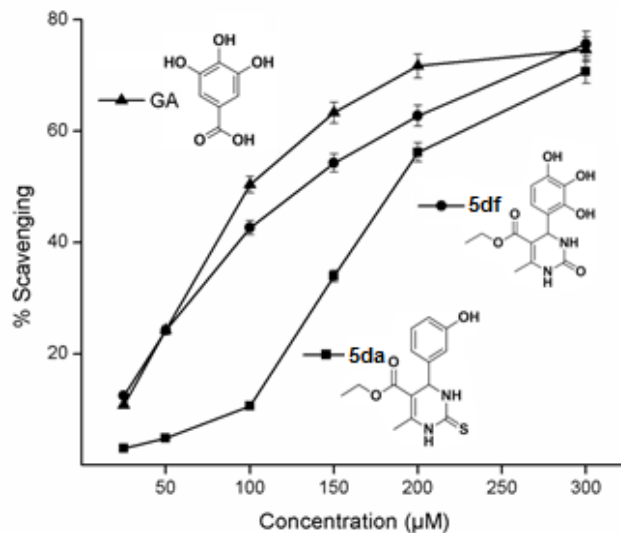


Figure 2.11. Nitric oxide radical scavenging activity of compound **5da**, **5df** and GA. Experiment was performed in triplicate and the results were expressed as mean values \pm standard deviations.

2.4 CONCLUSION

In summary, we presented here a novel approach of system chemistry for thermodynamically stable small molecules under the area of covalent mechanochemistry. This strategy represents a new level of complexity in mechanochemical reactions using ball-milling in which subcomponents were synthesized and used for post-synthetic transformations in a multicomponent reaction within the same reaction pot. Interestingly, we have also shown for the first time that a by-product obtained from a reaction system is used as a catalyst for another reaction. We believe this environmental friendly and economical methodology will be an important addition to drug discovery and development,⁶⁵ because DHPMs are well known to have diverse biological activities⁶⁶ including anticancer properties.^{38, 67} Finally, the system chemistry we described here for small molecules may branches out to a new field of study in covalent mechanochemistry.⁴⁷⁻⁴⁹ In addition, free radical scavenging activity were investigated

for oxo-Monastrol analogues. Compounds **5dc-5df** were found to be promising free radical scavengers, being comparable potent as known antioxidant Gallic acid.

2.5 EXPERIMENTAL SECTION

Methods: The ball milling (21 Hz) experiments were performed at room temperature and under open atmosphere. NMR spectra were recorded on 400 MHz instrument at 298 K. The chemical shift values are reported in parts per million (δ , ppm) and referred to the residual dimethyl sulfoxide (2.50 ppm for ^1H and 40.0 for ^{13}C). The peak patterns are designated as follows: s, singlet; d, doublet; t, triplet; q, quartet; m, multiplet; dd, doublet of doublets; td, triplet of doublets; br s, broad singlet. The coupling constants (J) are reported in hertz (Hz). High-resolution mass spectrometry (HRMS) were conducted on ESI-TOF (time of flight) mass spectrometer. Infrared spectral data are reported in wavenumber (cm^{-1}). Melting points of the compounds were determined using digital melting point apparatus and are uncorrected.

General procedure for synthesis of ethyl-4-(4-bromophenyl)-6-methyl-2-oxo-1,2,3,4-tetrahydropyrimidine-5-carboxylate (5aj) under ball-milling. *p*-Bromobenzylalcohol (100 mg, 0.53 mmol), oxone (228mg, 0.37 mmol), potassium bromide (6 mg, 0.05 mmol), TEMPO (0.8 mg, 0.005 mmol), and one ball (5 mm diameter, stainless steel) were transferred to a milling jar (10 mL, stainless steel). The ball-milling operation was performed for 30 minutes and the reaction was monitored by TLC/ ^1H NMR spectroscopy. After complete conversion of alcohol to the same jar ethyl acetoacetate (69 mg, 0.53 mmol) and urea (33 mg, 0.58 mmol) were added. When the reaction was completed, the reaction mixture was extracted with dichloromethane. Column chromatographic purification using 40% ethyl acetate/hexane afforded 172 mg (95%) of

5aj. $R_f = 0.30$ (40% ethyl acetate/hexane); colorless powder; mp: 223-225 °C (lit. ⁶⁸ 225-226 °C); ¹H NMR (400 MHz, DMSO-*d*₆) δ 1.09 (t, 3H, $J = 7.2$ Hz), 2.24 (s, 3H), 3.98 (q, 2H, $J = 7.2$ Hz), 5.12 (d, 1H, $J = 3.2$ Hz), 7.18 (d, 2H, $J = 8.4$ Hz), 7.52 (d, 2H, $J = 8.4$ Hz), 7.75 (s, 1H), 9.23 (s, 1H); ¹³C NMR (100 MHz, DMSO-*d*₆) δ 14.1, 17.8, 53.5, 59.3, 98.8, 120.3, 128.6, 131.4, 144.2, 148.8, 152.0, 165.3; HRMS observed 339.0335 (calculated for C₁₄H₁₅N₂O₃Br [M+H]⁺ 339.0339).

Ethyl-6-methyl-2-oxo-4-phenyl-1,2,3,4-tetrahydro-pyrimidine-5-carboxylate (5aa): $R_f = 0.30$ (40% ethyl acetate/hexane); colorless powder; yield 173 mg (89%); mp: 201-203 °C (lit. ⁶⁹ 202-203 °C); ¹H NMR (400 MHz, DMSO-*d*₆) δ 1.07 (t, 3H, $J = 7.2$ Hz), 2.24 (s, 3H), 3.95 (q, 2H, $J = 7.2$ Hz), 5.14 (d, 1H, $J = 3.2$ Hz), 7.22-7.33 (m, 5H), 7.71 (s, 1H), 9.16 (s, 1H); ¹³C NMR (100 MHz, DMSO-*d*₆) δ 14.2, 17.9, 54.1, 59.3, 99.4, 126.3, 127.4, 128.5, 144.9, 148.4, 152.3, 165.5; HRMS observed 261.1245 (calculated for C₁₄H₁₆N₂O₃ [M+H]⁺ 261.1234).

5-Acetyl-6-methyl-4-phenyl-3,4-dihydropyrimidin-2(1H)-one (5ab): $R_f = 0.28$ (40% ethyl acetate/hexane); colorless powder; yield 197 mg (91%); mp: 233-235 °C (lit. ⁶⁹ 233-234 °C); ¹H NMR (400 MHz, DMSO-*d*₆) δ 2.10 (s, 3H), 2.28 (s, 3H), 5.25 (d, 1H, $J = 3.2$ Hz), 7.23-7.34 (m, 5H), 7.80 (s, 1H), 9.15 (s, 1H); ¹³C NMR (100 MHz, DMSO-*d*₆) δ 19.0, 30.4, 53.9, 109.7, 126.5, 127.5, 128.7, 144.3, 148.3, 152.3, 194.5; HRMS observed 231.1140 (calculated for C₁₃H₁₄N₂O₂ [M+H]⁺ 231.1128).

Ethyl 4-(4-chlorophenyl)-6-methyl-2-oxo-1,2,3,4-tetrahydropyrimidine-5-carboxylate (5ac): $R_f = 0.30$ (40% ethyl acetate/hexane); colorless powder; yield 193 mg (92%); mp: 208-210 °C (lit. ⁶⁹ 210-211 °C); ¹H NMR (400 MHz, DMSO-*d*₆) δ 1.07 (t, 3H, $J = 7.2$ Hz), 2.25 (s, 3H), 3.95 (q, 2H, $J = 7.2$ Hz), 5.14 (d, 1H, $J = 3.2$ Hz), 7.23 (d, 2H, $J = 8.4$ Hz), 7.37 (d, 2H, $J = 8.4$ Hz), 7.76 (s, 1H), 9.22 (s, 1H); ¹³C NMR (100 MHz, DMSO-*d*₆) δ 14.1, 17.8, 53.5, 59.3, 98.9, 128.2,

128.4, 131.8, 143.8, 148.8, 152.0, 165.3; HRMS observed 295.0836 (calculated for $C_{14}H_{15}N_2O_3Cl[M+H]^+$ 295.0844).

5-Acetyl-4-(4-chlorophenyl)-6-methyl-3,4-dihydropyrimidin-2(1H)-one (5ad): $R_f = 0.30$ (50% ethyl acetate/hexane); colorless powder; yield 166 mg (94%); mp: 240-241 °C (lit. ⁷⁰ 258-260 °C); 1H NMR (400 MHz, DMSO- d_6) δ 2.12 (s, 3H), 2.29 (s, 3H), 5.25 (d, 1H, $J = 3.6$ Hz), 7.24-7.39 (m, 4H), 7.85 (s, 1H), 9.22 (s, 1H); ^{13}C NMR (100 MHz, DMSO- d_6) δ 19.0, 30.5, 53.1, 109.6, 128.4, 128.5, 131.9, 143.2, 148.5, 152.1, 194.2; HRMS observed 265.0711 (calculated for $C_{13}H_{13}N_2O_2Cl[M+H]^+$ 265.0738).

Ethyl-4-(4-methoxyphenyl)-6-methyl-2-oxo-1,2,3,4-tetrahydropyrimidine-5-carboxylate

(5ae): $R_f = 0.30$ (60% ethyl acetate/hexane); colorless powder; yield 196 mg (92%); mp: 201-203 °C (lit. ⁶⁹ 200-201 °C); 1H NMR (400 MHz, DMSO- d_6) δ 1.08 (t, 3H, $J = 7.2$ Hz), 2.23 (s, 3H), 3.71 (s, 3H), 3.95 (q, 2H, $J = 7.2$ Hz), 5.08 (d, 1H, $J = 3.2$ Hz), 6.86 (d, 2H, $J = 8.8$ Hz), 7.13 (d, 2H, $J = 8.8$ Hz), 7.64 (s, 1H), 9.12 (s, 1H); ^{13}C NMR (100 MHz, DMSO- d_6) δ 14.2, 17.9, 53.4, 55.2, 59.3, 99.7, 113.8, 127.5, 137.1, 148.1, 152.3, 158.6, 165.5; HRMS observed 291.1354 (calculated for $C_{15}H_{18}N_2O_4[M+H]^+$ 291.1339).

5-Acetyl-4-(4-methoxyphenyl)-6-methyl-3,4-dihydropyrimidin-2(1H)-one (5af): $R_f = 0.26$ (60% ethyl acetate/hexane); colorless powder; yield 173 mg (90%); mp: 170-171 °C (lit. ⁷¹ 169-171 °C); 1H NMR (400 MHz, DMSO- d_6) δ 2.07 (s, 3H), 2.27 (s, 3H), 3.72 (s, 3H), 5.19 (d, 1H, $J = 3.2$ Hz), 6.87 (d, 2H, $J = 8.8$ Hz), 7.14 (d, 2H, $J = 8.8$ Hz), 7.73 (s, 1H), 9.12 (s, 1H); ^{13}C NMR (100 MHz, DMSO- d_6) δ 18.9, 30.2, 53.4, 55.1, 109.7, 113.9, 127.7, 136.4, 147.9, 152.2, 158.6, 194.5; HRMS observed 261.1240 (calculated for $C_{14}H_{16}N_2O_3[M+H]^+$ 261.1234).

Ethyl-6-methyl-4-(4-nitrophenyl)-2-oxo-1,2,3,4-tetrahydropyrimidine-5-carboxylate

(5ag): $R_f = 0.30$ (60% ethyl acetate/hexane); colorless powder; yield 164 mg (81%); mp: 209-211 °C (lit.⁶⁹ 208-209 °C); ¹H NMR (400 MHz, DMSO- d_6) δ 1.07 (t, 3H, $J = 7.2$ Hz), 2.26 (s, 3H), 3.96 (q, 2H, $J = 7.2$ Hz), 5.27 (d, 1H, $J = 2.8$ Hz), 7.49 (d, 2H, $J = 8.8$ Hz), 7.87 (s, 1H), 8.12 (d, 2H, $J = 8.8$ Hz), 9.33 (s, 1H); ¹³C NMR (100 MHz, DMSO- d_6) δ 14.1, 17.9, 53.7, 59.5, 98.3, 123.9, 127.7, 146.8, 149.4, 151.8, 152.0, 165.1; HRMS observed 306.1074 (calculated for $C_{14}H_{15}N_3O_5$ [M+H]⁺ 306.1084).

Ethyl-6-methyl-2-oxo-4-(p-tolyl)-1,2,3,4-tetrahydropyrimidine-5-carboxylate (5ah): $R_f =$

0.37 (40% ethyl acetate/hexane); colorless powder; yield 103 mg (92%); mp: 215-217 °C (lit.⁶⁹ 214-216 °C); ¹H NMR (400 MHz, DMSO- d_6) δ 1.09 (t, 3H, $J = 7.2$ Hz), 2.23 (s, 3H), 2.25 (s, 3H), 4.96 (q, 4H, $J = 7.2$ Hz), 5.10 (d, 1H, $J = 3.6$ Hz), 7.11 (s, 4H), 7.66 (s, 1H), 9.13 (s, 1H); ¹³C NMR (100 MHz, DMSO- d_6) δ 14.1, 17.8, 20.7, 53.7, 59.3, 99.5, 126.2, 129.0, 136.5, 142.0, 148.2, 152.3, 165.4; HRMS observed 275.1333 (calculated for $C_{15}H_{18}N_2O_3$ [M+H]⁺ 275.1390).

5-Acetyl-6-methyl-4-(p-tolyl)-3,4-dihydropyrimidin-2(1H)-one (5ai): $R_f = 0.30$ (60% ethyl

acetate/hexane); colorless powder; yield 95 mg (95%); mp: 255-257 °C (lit.⁷⁰ 256-257 °C); ¹H NMR (400 MHz, DMSO- d_6) δ 2.07 (s, 3H), 2.25 (s, 3H), 2.26 (s, 3H), 5.20 (d, 1H, $J = 3.6$ Hz), 7.12 (s, 4H), 7.75 (s, 1H), 9.12 (s, 1H); ¹³C NMR (100 MHz, DMSO- d_6) δ 18.9, 20.7, 30.3, 53.7, 109.7, 126.5, 129.2, 136.7, 141.4, 148.1, 152.3, 194.6; HRMS observed 245.1238 (calculated for $C_{14}H_{16}N_2O_2$ [M+H]⁺ 245.1285).

Ethyl-4-(4-bromophenyl)-6-methyl-2-oxo-1,2,3,4-tetrahydropyrimidine-5-carboxylate

(5aj): $R_f = 0.30$ (40% ethyl acetate/hexane); colorless powder; yield 172 mg (95%); mp: 223-225 °C (lit.⁶⁸ 225-226 °C); ¹H NMR (400 MHz, DMSO- d_6) δ 1.09 (t, 3H, $J = 7.2$ Hz), 2.24 (s, 3H), 3.98 (q, 2H, $J = 7.2$ Hz), 5.12 (d, 1H, $J = 3.2$ Hz), 7.18 (d, 2H, $J = 8.4$ Hz), 7.52 (d, 2H, $J = 8.4$

Hz), 7.75 (s, 1H), 9.23 (s, 1H); ^{13}C NMR (100 MHz, DMSO- d_6) δ 14.1, 17.8, 53.5, 59.3, 98.8, 120.3, 128.6, 131.4, 144.2, 148.8, 152.0, 165.3; HRMS observed 339.0335 (calculated for $\text{C}_{14}\text{H}_{15}\text{N}_2\text{O}_3\text{Br}$ $[\text{M}+\text{H}]^+$ 339.0339).

5-Acetyl-4-(4-bromophenyl)-6-methyl-3,4-dihydropyrimidin-2(1H)-one (5ak): $R_f = 0.30$ (50% ethyl acetate/hexane); colorless powder; yield 152 mg (92%); mp: 239-241 °C (lit. ³⁴ 232-233 °C); ^1H NMR (400 MHz, DMSO- d_6) δ 2.12 (s, 3H), 2.28 (s, 3H), 5.24 (d, 1H, $J = 3.6$ Hz), 7.19 (d, 2H, $J = 8.4$ Hz), 7.52 (d, 2H, $J = 8.4$ Hz), 7.84 (s, 1H), 9.21 (s, 1H); ^{13}C NMR (100 MHz, DMSO- d_6) δ 19.4, 30.9, 53.6, 110.0, 120.8, 129.1, 131.9, 144.1, 149.0, 152.5, 194.6; HRMS observed 309.0213 (calculated for $\text{C}_{13}\text{H}_{13}\text{N}_2\text{O}_2\text{Br}$ $[\text{M}+\text{H}]^+$ 309.0233).

5-Acetyl-6-methyl-4-(thiophen-2-yl)-3,4-dihydropyrimidin-2(1H)-one (5al): $R_f = 0.37$ (40% ethyl acetate/hexane); colorless powder; yield 92 mg (88%); mp: 208-210 °C; ^1H NMR (400 MHz, DMSO- d_6) δ 2.17 (s, 3H), 2.25 (s, 3H), 5.51 (d, 1H, $J = 3.2$ Hz), 6.90-6.94 (m, 2H), 7.35 (dd, 1H, $J_1 = 3.6$ Hz, $J_2 = 1.2$ Hz), 7.94 (s, 1H), 9.28 (s, 1H); ^{13}C NMR (100 MHz, DMSO- d_6) δ 19.0, 30.3, 49.4, 110.8, 124.2, 125.1, 127.0, 148.5, 148.7, 152.5, 194.2; HRMS observed 253.0491 (calculated for $\text{C}_{11}\text{H}_{12}\text{N}_2\text{OS}$ $[\text{M}+\text{H}]^+$ 253.0464).

Ethyl-4-(4-chlorophenyl)-1,6-dimethyl-2-oxo-1,2,3,4-tetrahydropyrimidine-5-carboxylate

(5ba): $R_f = 0.30$ (30% ethyl acetate/hexane); colorless powder; yield 205 mg (95%); mp: 128-130 °C (lit. ⁷² 130-131 °C); ^1H NMR (400 MHz, DMSO- d_6) δ 1.10 (t, 3H, $J = 7.2$ Hz), 2.486 (s, 3H), 3.09 (s, 3H), 4.02 (q, 2H, $J = 7.2$ Hz), 5.14 (d, 1H, $J = 4$ Hz), 7.23 (d, 2H, $J = 8.4$ Hz), 7.38 (d, 2H, $J = 8.4$ Hz), 7.98 (d, 1H, $J = 4$ Hz); ^{13}C NMR (100 MHz, DMSO- d_6) δ 14.1, 16.1, 29.8, 51.9, 59.7, 102.0, 128.1, 128.5, 131.9, 143.1, 151.0, 152.9, 165.5; HRMS observed 309.1021 (calculated for $\text{C}_{15}\text{H}_{17}\text{N}_2\text{O}_3\text{Cl}$ $[\text{M}+\text{H}]^+$ 309.1000).

5-Acetyl-4-(4-chlorophenyl)-1,6-dimethyl-3,4-dihydropyrimidin-2(1H)-one (5bb): $R_f = 0.28$ (40% ethyl acetate/hexane); colorless powder; yield 180 mg (92%); mp: 142-144 °C (lit. ⁷³ 149-151 °C); ¹H NMR (400 MHz, DMSO-d₆) δ 2.12 (s, 3H), 2.43 (s, 3H), 3.08 (s, 3H), 5.21 (d, 1H, $J = 3.6$ Hz), 7.25 (d, 2H, $J = 8.4$ Hz), 7.39 (d, 2H, $J = 8.4$ Hz), 8.06 (d, 1H, $J = 3.6$ Hz); ¹³C NMR (100 MHz, DMSO-d₆) δ 17.0, 30.0, 30.6, 52.1, 112.3, 128.5, 128.8, 132.3, 142.4, 150.3, 153.2, 195.9; HRMS observed 279.0897 (calculated for C₁₄H₁₅N₂O₂Cl[M+H]⁺ 279.0895).

Ethyl-1,6-dimethyl-2-oxo-4-(p-tolyl)-1,2,3,4-tetrahydropyrimidine-5-carboxylate(5bc): $R_f = 0.36$ (45% ethyl acetate/ hexane); colorless powder; yield 106 mg (90%); mp: 113-115 °C (lit. ⁷³ 119-120 °C); ¹H NMR (400 MHz, DMSO-d₆) δ 1.12 (t, 3H, $J = 7.2$ Hz), 2.25 (s, 3H), 2.47 (s, 3H), 3.08 (s, 3H), 4.02 (q, 2H, $J = 7.2$ Hz), 5.10 (d, 1H, $J = 3.6$ Hz), 7.10 (dd, 4H, $J_1 = 8.4$ Hz, $J_2 = 2.8$ Hz), 7.90 (d, 1H, $J = 3.6$); ¹³C NMR (100 MHz, DMSO-d₆) δ 14.1, 16.1, 20.7, 29.8, 52.1, 59.6, 102.7, 126.0, 129.0, 136.6, 141.1, 150.4, 153.2, 165.7; HRMS observed 289.1554 (calculated for C₁₆H₂₀N₂O₃ [M+H]⁺ 289.1547).

5-Acetyl-1,6-dimethyl-4-(p-tolyl)-3,4-dihydropyrimidin-2(1H)-one (5bd): $R_f = 0.30$ (40% ethyl acetate/ hexane); colorless powder; yield 93 mg (88%); mp: 135-137 °C (lit. ⁷³ 138-140 °C); ¹H NMR (400 MHz, DMSO-d₆) δ 2.08 (s, 3H), 2.26 (s, 3H), 2.43 (s, 3H), 3.07 (s, 3H), 5.15 (d, 1H, $J = 4$ Hz), 7.12 (s, 4H), 7.99 (d, 1H, $J = 4$ Hz); ¹³C NMR (100 MHz, DMSO-d₆) δ 16.6, 20.7, 29.7, 30.3, 52.5, 112.3, 126.3, 129.2, 136.8, 140.4, 149.6, 153.1, 195.8; HRMS observed 259.1463 (calculated for C₁₄H₁₈N₂O₂ [M+H]⁺ 259.1441).

5-Acetyl-1,6-dimethyl-4-(thiophen-2-yl)-3,4-dihydropyrimidin-2(1H)-one (5be): $R_f = 0.37$ (40% ethyl acetate/ hexane); pale yellow powder; yield 98 mg (88%); mp: 174-178 °C; ¹H NMR (400 MHz, DMSO-d₆) δ 2.19 (s, 3H), 2.42 (s, 3H), 3.09 (s, 3H), 5.45 (d, 1H, $J = 4.0$ Hz), 6.96-6.93 (m, 1H), 7.37 (dd, 1H, $J_1 = 4.4$, $J_2 = 1.6$ Hz), 8.16 (d, 1H, $J = 4.0$ Hz); ¹³C NMR (100 MHz,

DMSO- d_6) δ 16.9, 30.1, 30.6, 48.7, 113.6, 124.6, 125.4, 127.2, 148.0, 150.2, 153.4, 196.3; IR (KBr) $\tilde{\nu}$ 3275, 3127, 2962, 1695, 1617, 1383, 1359, 1341, 1249, 1196, 1068, 949, 765, 736 cm^{-1} ; HRMS observed 251.0746 (calculated for $\text{C}_{12}\text{H}_{15}\text{N}_2\text{O}_2\text{S}$ $[\text{M}+\text{H}]^+$ 251.0849).

Ethyl -1,6-dimethyl-2-oxo-4-(thiophen-2-yl)-1,2,3,4-tetrahydropyrimidine-5-carboxylate

(5bf): $R_f = 0.37$ (30% ethyl acetate/ hexane); brown powder; yield 106 mg (85%); mp: 155-158 $^{\circ}\text{C}$ (lit.⁷⁴ 158-159 $^{\circ}\text{C}$); ^1H NMR (400 MHz, DMSO- d_6) δ 1.19 (t, 3H, $J = 7.2$ Hz), 2.46 (s, 3H), 3.09 (s, 3H), 4.10 (q, 2H, $J = 7.2$ Hz), 5.40 (d, 1H, $J = 4.0$ Hz), 6.87 (d, 1H, $J = 3.2$ Hz), 6.92-6.94 (m, 1H), 7.34 (dd, 1H, $J_1 = 4.8$, $J_2 = 0.8$ Hz), 8.11 (d, 1H, $J = 4.0$ Hz); ^{13}C NMR (100 MHz, DMSO- d_6) δ 165.6, 153.7, 151.4, 148.3, 127.2, 125.2, 124.0, 103.6, 60.2, 48.6, 30.3, 16.4, 14.6; IR (KBr) $\tilde{\nu}$ 3228, 3107, 2925, 1623, 1356, 1343, 1302, 1252, 1190, 1050, 713 cm^{-1} ; HRMS observed 281.0851 (calculated for $\text{C}_{13}\text{H}_{17}\text{N}_2\text{O}_3\text{S}$ $[\text{M}+\text{H}]^+$ 281.0954).

1-(6-Methyl-2-thioxo-4-(p-tolyl)-1,2,3,4-tetrahydropyrimidin-5-yl)ethanone (5ca): $R_f = 0.30$

(40% ethyl acetate/ hexane); colorless powder; yield 85 mg (80%); mp: 190-192 $^{\circ}\text{C}$ (lit.⁷⁵ 183-185 $^{\circ}\text{C}$); ^1H NMR (400 MHz, DMSO- d_6) δ 2.12 (s, 3H), 2.26 (s, 3H), 2.31 (s, 3H), 5.24 (d, 1H, $J = 3.6$ Hz), 7.09-7.15 (m, 4H), 9.70 (s, 1H), 10.23 (s, 1H); ^{13}C NMR (100 MHz, DMSO- d_6) δ 18.3, 20.7, 30.4, 53.7, 110.5, 126.6, 129.3, 137.1, 140.1, 144.5, 174.1, 195.0; HRMS observed 261.1052 (calculated for $\text{C}_{14}\text{H}_{16}\text{N}_2\text{OS}$ $[\text{M}+\text{H}]^+$ 261.1056).

Ethyl-4-(4-methoxyphenyl)-6-methyl-2-thioxo-1,2,3,4-tetrahydropyrimidine-5-carboxylate

(5cb): $R_f = 0.26$ (40% ethyl acetate/ hexane); colorless powder; yield 186 mg (85%); mp: 146-148 $^{\circ}\text{C}$ (lit.⁷¹ 150-152 $^{\circ}\text{C}$); ^1H NMR (400 MHz, DMSO- d_6) δ 1.10 (t, 3H, $J = 7.2$ Hz), 2.28 (s, 3H), 3.72 (s, 3H), 3.99 (q, 2H, $J = 7.2$ Hz), 5.11 (d, 1H, $J = 3.6$ Hz), 6.89 (d, 2H, $J = 8.4$ Hz),

7.12 (d, 2H, $J = 8.4$ Hz), 9.58 (s, 1H), 10.27 (s, 1H); ^{13}C NMR (100 MHz, DMSO- d_6) δ 14.4, 17.5, 53.8, 55.5, 59.9, 101.3, 114.2, 128.0, 136.0, 145.1, 159.1, 165.5, 174.4; HRMS observed 307.1187 (calculated for $\text{C}_{15}\text{H}_{19}\text{N}_2\text{O}_3\text{S}$ $[\text{M}+\text{H}]^+$ 307.1144).

1-(4-(4-chlorophenyl)-6-methyl-2-thioxo-1,2,3,4-tetrahydropyrimidin-5-yl)ethanone (5cc):

$R_f = 0.30$ (30% ethyl acetate/ hexane); off white powder; yield 153 mg (78%); mp: 190-192 °C (lit. 76 192-194 °C); ^1H NMR (400 MHz, DMSO- d_6) δ 2.17 (s, 3H), 2.23 (s, 3H), 5.28 (d, 1H, $J = 4$ Hz), 7.23 (d, 2H, $J = 8.4$ Hz), 7.1 (d, 2H, $J = 8.4$ Hz), 9.76 (s, 1H), 10.32 (s, 1H); ^{13}C NMR (100 MHz, DMSO- d_6) δ 18.7, 30.9, 53.4, 110.7, 128.8, 129.0, 132.6, 142.2, 145.3, 174.6, 196.1; HRMS observed 281.0531 (calculated for $\text{C}_{13}\text{H}_{14}\text{ClN}_2\text{OS}$ $[\text{M}+\text{H}]^+$ 281.0510).

Ethyl-4-(4-bromophenyl)-6-methyl-2-thioxo-1,2,3,4-tetrahydropyrimidine-5-carboxylate

(5cd): $R_f = 0.28$ (30% ethyl acetate/ hexane); colorless powder; yield 155 mg (82%); mp: 178-180 °C; ^1H NMR (400 MHz, DMSO- d_6) δ 1.10 (t, 3H, $J = 7.2$ Hz), 2.28 (s, 3H), 4.01 (q, 2H, $J = 7.2$ Hz), 5.14 (d, 1H, $J = 3.6$ Hz), 7.16 (d, 2H, $J = 8.4$ Hz), 7.56 (d, 2H, $J = 8.4$ Hz), 9.66 (s, 1H), 10.37 (s, 1H); ^{13}C NMR (100 MHz, DMSO- d_6) δ 14.3, 17.5, 53.8, 60.0, 100.6, 121.1, 129.0, 131.8, 143.1, 145.7, 165.3, 174.6; IR (KBr) $\tilde{\nu}$ 3326, 3171, 3103, 2981, 1669, 1577, 1464, 1176, 1121 cm^{-1} ; HRMS observed 355.0156 (calculated for $\text{C}_{14}\text{H}_{16}\text{BrN}_2\text{O}_2\text{S}$ $[\text{M}+\text{H}]^+$ 355.0110).

1-(4-(4-Bromophenyl)-6-methyl-2-thioxo-1,2,3,4-tetrahydropyrimidin-5-yl)ethanone (5ce):

$R_f = 0.30$ (30% ethyl acetate/ hexane); brown colored powder; yield 139 mg (80%); mp: 212-215 °C; ^1H NMR (400 MHz, DMSO- d_6) δ 2.18 (s, 3H), 2.33 (s, 3H), 5.27 (s, 1H), 7.17 (d, 2H, $J = 7.6$ Hz), 7.55 (d, 2H, $J = 7.6$ Hz), 9.77 (s, 1H), 10.33 (s, 1H); ^{13}C NMR (100 MHz, DMSO- d_6) δ 18.6, 30.4, 53.8, 110.6, 121.1, 129.1, 131.9, 142.6, 145.3, 174.6, 196.0; IR (KBr) $\tilde{\nu}$ 3283, 3177, 2992, 2924, 1618, 1581, 1458, 1361, 1329, 1183, 1011 cm^{-1} ; HRMS observed 325.0044 (calculated for $\text{C}_{13}\text{H}_{14}\text{BrN}_2\text{OS}$ $[\text{M}+\text{H}]^+$ 324.0005).

Ethyl-4-(4-chlorophenyl)-6-methyl-2-thioxo-1,2,3,4-tetrahydropyrimidine-5-carboxylate

(5cf): $R_f = 0.30$ (30% ethyl acetate/ hexane); colorless powder; yield 179 mg (82%); mp: 186-189 °C (lit. ⁷⁶ 192-194 °C; ¹H NMR (400 MHz, DMSO- d_6) δ 1.10 (t, 3H, $J = 7.2$ Hz), 2.29 (s, 3H), 4.01 (d, 2H, $J = 7.2$ Hz), 5.17 (d, 1H, $J = 3.6$ Hz), 7.22 (d, 2H, $J = 8.4$ Hz), 7.42 (d, 2H, $J = 8.4$ Hz), 9.66 (s, 1H), 10.37 (s, 1H); ¹³C NMR (100 MHz, DMSO- d_6) δ 14.3, 17.5, 53.8, 60.0, 100.6, 128.6, 128.9, 132.6, 142.7, 145.7, 165.3, 174.6; HRMS observed 311.0653 (calculated for $C_{14}H_{16}ClN_2O_2S$ $[M+H]^+$ 311.0616).

Ethyl-6-methyl-4-(thiophen-2-yl)-2-thioxo-1,2,3,4-tetrahydropyrimidine-5-carboxylate

(5cg): $R_f = 0.37$ (25% ethyl acetate/ hexane); colorless powder; yield 100 mg (80%); mp: 202-204 °C; ¹H NMR (400 MHz, DMSO- d_6) δ 1.16 (t, 3H, $J = 7.2$ Hz), 2.27 (s, 3H), 4.08 (q, 2H, $J = 7.2$ Hz), 5.42 (d, 1H, $J = 3.6$ Hz), 6.90 (d, 1H, $J = 2.8$ Hz), 6.96 (m, 1H), 7.40 (d, 1H, $J = 4.4$ Hz), 9.77 (s, 1H), 10.46 (s, 1H); ¹³C NMR (100 MHz, DMSO- d_6) δ 14.4, 17.4, 49.6, 60.1, 101.5, 124.5, 125.7, 127.1, 145.7, 147.3, 165.1, 175.0; IR (KBr) $\tilde{\nu}$ 3305, 3101, 2986, 2899, 1667, 1571, 1458, 1333, 1277, 1254, 1162, 1115, 1028, 739 cm^{-1} ; HRMS observed 283.0452 (calculated for $C_{12}H_{15}N_2O_2S_2$ $[M+H]^+$ 283.0569).

1-(6-methyl-4-(thiophen-2-yl)-2-thioxo-1,2,3,4-tetrahydropyrimidin-5-yl)ethanone(5ch): R_f

= 0.30 (30% ethyl acetate/ hexane); brown color powder; yield 88 mg (80%); mp: 220-222 °C; ¹H NMR (400 MHz, DMSO- d_6) δ 2.21 (s, 3H), 2.30 (s, 3H), 5.53 (d, 1H, $J = 3.6$ Hz), 6.92-6.96 (m, 2H), 7.40 (d, 1H, $J = 4.4$ Hz), 9.83 (s, 1H), 10.40 (s, 1H); ¹³C NMR (100 MHz, DMSO- d_6) δ 18.5, 30.6, 49.5, 111.6, 124.9, 125.9, 127.2, 145.0, 147.3, 174.9, 194.7; IR (KBr) $\tilde{\nu}$ 3271, 3165, 2961, 2925, 2854, 1665, 1570, 1451, 1413, 1361, 1160, 1115, 784, 761, 707 cm^{-1} ; HRMS observed 253.0491 (calculated for $C_{11}H_{13}N_2OS_2$ $[M+H]^+$ 253.0464).

Ethyl-4-(3-hydroxyphenyl)-6-methyl-2-thioxo-1,2,3,4-tetrahydropyrimidine-5-carboxylate

(5da): Colorless powder; yield 189 mg (84%); mp: 183-185 °C (lit. ⁶⁹ 184-185 °C); ¹H NMR (400 MHz, DMSO-d₆) δ 1.10 (t, 3H, *J* = 7.2 Hz), 2.28 (s, 3H), 3.99 (q, 2H, *J* = 7.2 Hz), 5.09 (d, 1H, *J* = 3.6 Hz), 6.64-6.66 (m, 3H), 7.10-7.13 (m, 1H), 9.45 (s, 1H), 9.58 (s, 1H), 10.27 (s, 1H); ¹³C NMR (100 MHz, DMSO-d₆) δ 14.1, 17.3, 54.1, 59.8, 101.0, 113.4, 114.7, 117.1, 129.6, 144.9, 145.0, 157.6, 165.3, 174.3; HRMS observed 293.0948 (calculated for C₁₄H₁₆N₂O₃S [M+H]⁺ 293.0954).

5-Acetyl-4-(4-hydroxyphenyl)-6-methyl-3,4-dihydropyrimidin-2(1H)-one (5db): Colorless

powder; yield 184 mg (82%); mp: 235-237 °C (lit. ⁷⁰ 236-238 °C); ¹H NMR (400 MHz, DMSO-d₆) δ 2.05 (s, 3H), 2.26 (s, 3H), 5.14 (d, 1H, *J* = 3.2 Hz), 6.68 (d, 2H, *J* = 8.4 Hz), 7.02 (d, 2H, *J* = 8.4 Hz), 7.68 (s, 1H), 9.09 (s, 1H), 9.39 (s, 1H); ¹³C NMR (100 MHz, DMSO-d₆) δ 18.9, 30.1, 55.6, 109.7, 115.2, 127.8, 134.8, 147.7, 152.2, 156.7, 194.6; HRMS observed 247.1081 (calculated for C₁₄H₁₆N₂O₃S [M+H]⁺ 274.1077).

5-Acetyl-4-(3,4-dihydroxyphenyl)-6-methyl-3,4-dihydropyrimidin-2(1H)-one

(5dc): Colorless powder; yield 164 mg (86%); mp: 240-242 °C; ¹H NMR (400 MHz, DMSO-d₆) δ 2.04 (s, 3H), 2.25 (s, 3H), 5.07 (d, 1H, *J* = 3.2 Hz), 6.49-6.52 (m, 1H), 6.64-6.66 (m, 2H), 7.65 (s, 1H), 8.84 (s, 1H), 8.88 (s, 1H), 9.07 (s, 1H); ¹³C NMR (100 MHz, DMSO-d₆) δ 18.8, 30.1, 53.8, 109.6, 114.0, 115.4, 117.5, 135.4, 144.7, 145.2, 147.4, 152.1, 194.7; IR (KBr) $\tilde{\nu}$ 3293, 1684, 1618, 1518, 1458, 1363, 1285, 1243, 1115 cm⁻¹; HRMS observed 263.1036 (calculated for C₁₄H₁₆N₂O₃S [M+H]⁺ 263.1026).

5-Acetyl-4-(2,3-dihydroxyphenyl)-6-methyl-3,4-dihydropyrimidin-2(1H)-one

(5dd): Colorless powder; yield 155 mg (81%); mp: 217-219 °C; ¹H NMR (400 MHz, DMSO-d₆) δ 1.66 (s, 3H), 2.27 (s, 3H), 4.56 (s, 1H), 6.62-6.72 (m, 3H), 7.06 (s, 1H), 7.42 (s, 1H), 9.01 (s,

1H); ^{13}C NMR (100 MHz, DMSO- d_6) δ 23.7, 29.0, 47.0, 50.0, 83.1, 115.3, 118.8, 120.2, 126.7, 139.1, 145.8, 154.8, 204.2; IR (KBr) $\tilde{\nu}$ 3437, 3348, 3073, 1715, 1652, 1593, 1472, 1366, 1284, 1253, 1212, 1094 cm^{-1} ; HRMS observed 263.1035 (calculated for $\text{C}_{14}\text{H}_{16}\text{N}_2\text{O}_3\text{S}$ $[\text{M}+\text{H}]^+$ 263.1026).

5-Acetyl-6-methyl-4-(2,3,4-trihydroxyphenyl)-3,4-dihydropyrimidin-2(1H)-one

(5de): Colorless powder; yield 142 mg (78%); mp: 200-202 $^\circ\text{C}$; ^1H NMR (400 MHz, DMSO- d_6) δ 1.65 (s, 3H), 2.25 (s, 3H), 4.50 (s, 1H), 6.33 (d, 1H, $J = 8$ Hz), 6.47 (d, 1H, $J = 8$ Hz), 6.98 (s, 1H), 7.37 (s, 1H), 8.13 (s, 1H), 9.00 (s, 1H); ^{13}C NMR (100 MHz, DMSO- d_6) δ 24.1, 29.4, 47.3, 50.6, 83.3, 108.3, 118.3, 118.4, 133.5, 140.3, 146.1, 155.3, 204.8; IR (KBr) $\tilde{\nu}$ 3358, 3254, 1716, 1644, 1495, 1339, 1250, 1156, 1117, 1023 cm^{-1} ; HRMS observed 279.0998 (calculated for $\text{C}_{14}\text{H}_{16}\text{N}_2\text{O}_3\text{S}$ $[\text{M}+\text{H}]^+$ 279.0975).

Ethyl-6-methyl-2-oxo-4-(2,3,4-trihydroxyphenyl)-1,2,3,4-tetrahydropyrimidine-5-

carboxylate (5df): Colorless powder; yield 151 mg (83%); mp: 180-182 $^\circ\text{C}$; ^1H NMR (400 MHz, DMSO- d_6) δ 1.20 (t, 3H, $J = 8$ Hz), 1.75 (s, 3H), 4.13-4.16 (m, 2H), 4.32-4.34 (m, 2H), 6.33 (d, 1H, $J = 8$ Hz), 6.44 (d, 1H, $J = 8$ Hz), 7.08 (d, 1H, $J = 4$ Hz), 7.48 (s, 1H), 8.13 (s, 1H), 9.98 (s, 1H); ^{13}C NMR (100 MHz, DMSO- d_6) δ 14.1, 24.1, 60.5, 82.7, 108.1, 117.5, 117.7, 133.2, 139.8, 145.8, 154.7, 168.7; IR (KBr) $\tilde{\nu}$ 3407, 3363, 1733, 1655, 1492, 1327, 1200, 1154, 1092, 1059, 1024 cm^{-1} ; HRMS observed 309.1088 (calculated for $\text{C}_{14}\text{H}_{16}\text{N}_2\text{O}_3\text{S}$ $[\text{M}+\text{H}]^+$ 309.1081).

Antioxidant activity studies

Four different assays were used to evaluate the antioxidant activity of Monastrol and its novel derivatives. Stock solution of compounds was prepared in DMSO for DPPH and NO^\bullet radical scavenging assay. However, DMSO itself can scavenge $\bullet\text{OH}$ radical ⁷⁷ and can generate

superoxide anion radicals in alkaline solution⁷⁸. Hence, stock solution of compounds was prepared in 10 mM NaOH solution for hydroxyl and superoxide radical scavenging assay to escape interference of DMSO. All tests were performed in triplicate and the results were expressed as mean values \pm standard deviations.

DPPH radical scavenging assay

The capacity of compounds to scavenge the free radical DPPH was monitored according to previously described method.⁷⁹ An aliquot of the samples (0.5 ml) was mixed with an equal volume of 0.04 mM DPPH solution (in 95% MeOH) and incubated for 30 min at room temperature in the dark. The reduction of the DPPH radical was determined by measuring the absorption at 517 nm using methanol as the blank. DPPH radical scavenging activity was expressed as the percentage inhibition was calculated using the following formula:

% inhibition = $[(A_C - A_S)/A_C] \times 100$, where A_C is the absorbance in absence of the test samples and A_S is the absorbance in the presence of the test samples.

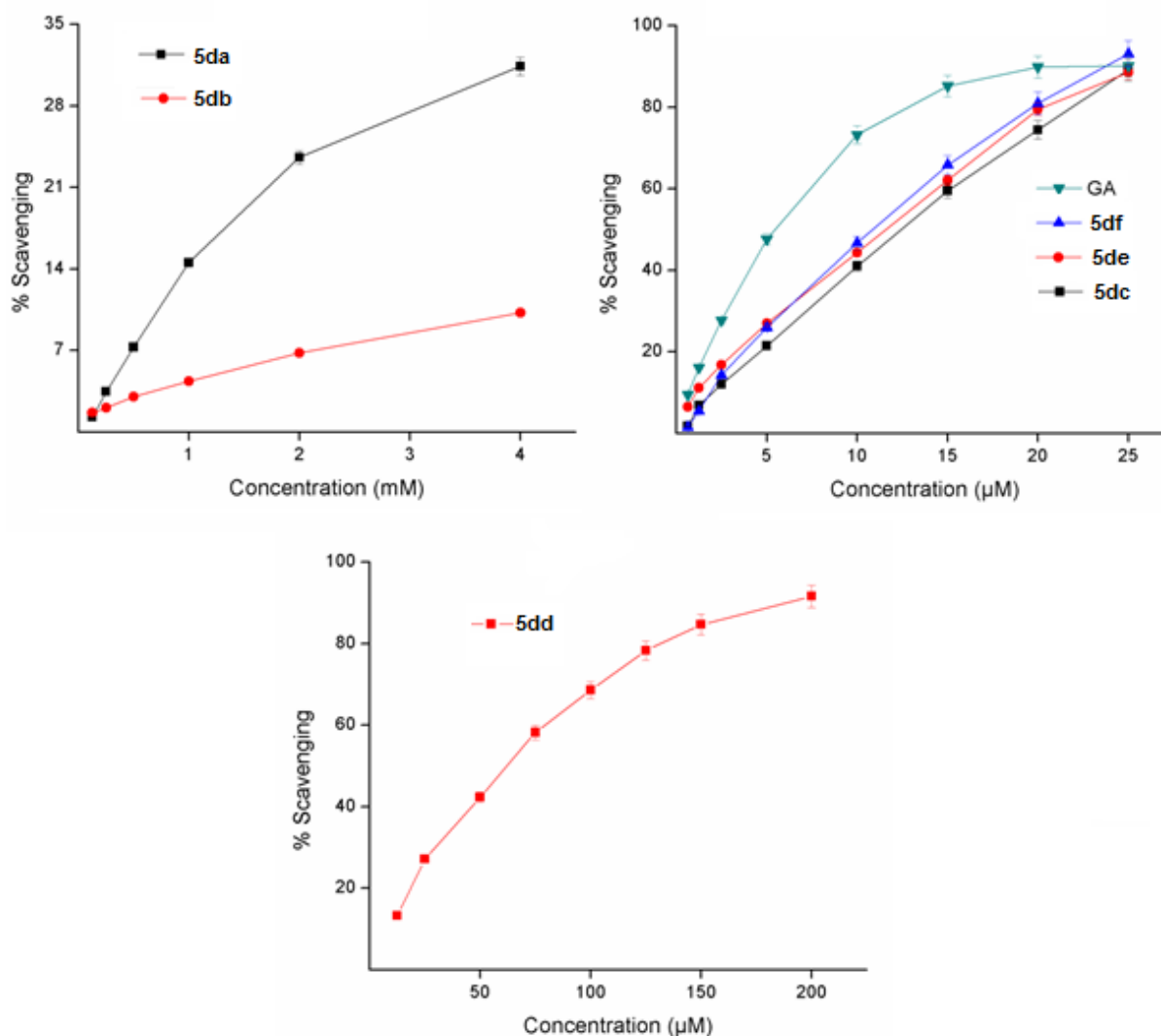


Figure 2.12. DPPH radical scavenging activity of DHPMs and Gallic acid (GA)

Superoxide radical scavenging assay

The superoxide radical ($\cdot\text{O}_2^-$) scavenging activity was assayed by measuring the auto-oxidation inhibition rate of pyrogallol according to previously described method with minor modifications⁸⁰. Freshly prepared 50 µL pyrogallol (15 mM, in 1 mM HCl) was added to various concentrations of samples in 650 µL of 50 mM Tris-HCl buffer, pH 7.4. The inhibition rate of

pyrogallol auto-oxidation was measured by monitoring the absorbance at 325 nm every 30 s over a period of 3 min. The superoxide radical scavenging activity was calculated as:

% Inhibition = $[(\Delta A_C/T - \Delta A_S/T)/\Delta A_C/T] \times 100$, where ΔA_C is the increase in absorbance of the mixture without the sample, ΔA_S is increase in absorbance with the sample and $T = 3$ min.

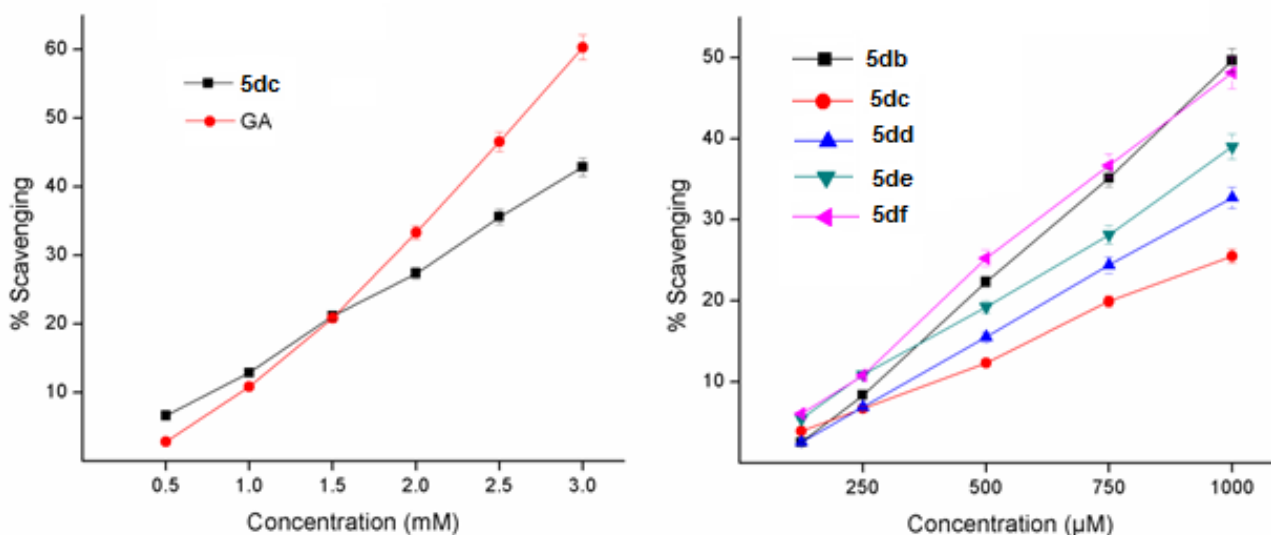


Figure 2.13. Superoxide radical scavenging activity of DHPMs and Gallic acid (GA)

Hydroxyl radical scavenging assay

The assay was carried out according to previously described benzoic acid hydroxylation method⁸¹. The benzoic acid is hydroxylated by $\cdot\text{OH}$ formed by Fenton reaction at C3 or C4 position of the aromatic ring and emitting fluorescence which decreases in presence of an hydroxyl radical scavenger. Briefly, 0.2 mL of sodium benzoate (10 mM) and 0.2 mL of $\text{FeSO}_4 \cdot 7\text{H}_2\text{O}$ (10 mM) and EDTA (10 mM) were mixed with sample in phosphate buffer (pH 7.4, 0.1 M) to give a total volume of 1.8 mL. Finally, 0.2 mL of H_2O_2 solution (10 mM) was added, and incubated at 37°C for 2h. After incubation, the fluorescence was measured at 407 nm

emission with excitation at 305 nm. Hydroxyl radical scavenging activity was calculated using the following formula:

% inhibition = $[(F_C - F_S)/F_C] \times 100$, where F_C and F_S are the fluorescence intensity in absence and presence of the sample, respectively.

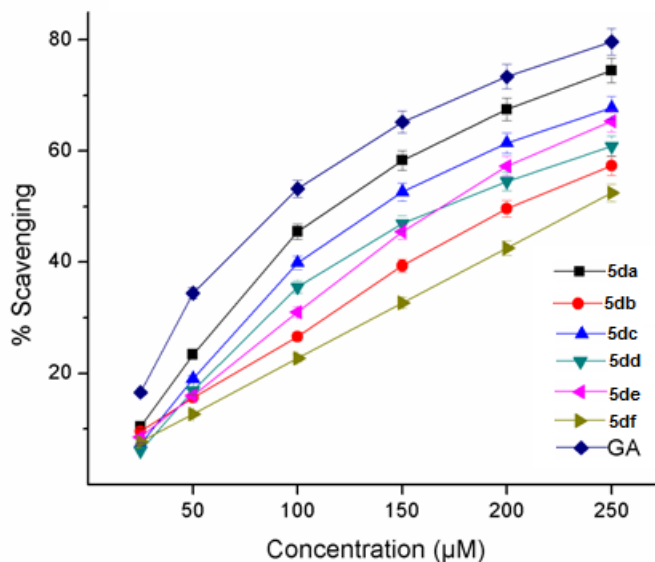


Figure 2.14. Hydroxyl radical scavenging activity of DHPMs and Gallic acid (GA)

Nitric oxide radical scavenging assay

The assay was carried out according to previously described method⁷⁹. The reaction mixture contained 200 μl of 10 mM SNP (Sodium nitroprusside) in phosphate buffered saline (pH 7.4) and the 100 μl of various concentrations of the samples. After incubation for 150 min at 25 °C, 0.35 mL sulfanilic acid (0.33% in 20% glacial acetic acid) was added and allowed to stand for 5 min. In this mixture, 0.35 ml NEED (naphthylethylenediaminedihydrochloride, 0.1% w/v) was added and incubated for 30 min at 25 °C. The pink chromophore, generated during diazotization

of nitrite ions with sulfanilic acid and subsequent coupling with NEED was measured at 540 nm.

The nitric oxide radical scavenging activity was calculated using the following equation:

% inhibition = $[(A_C - A_S)/A_C] \times 100$, where A_S is the absorbance in the presence of the test samples and A_C is the absorbance in absence of the sample.

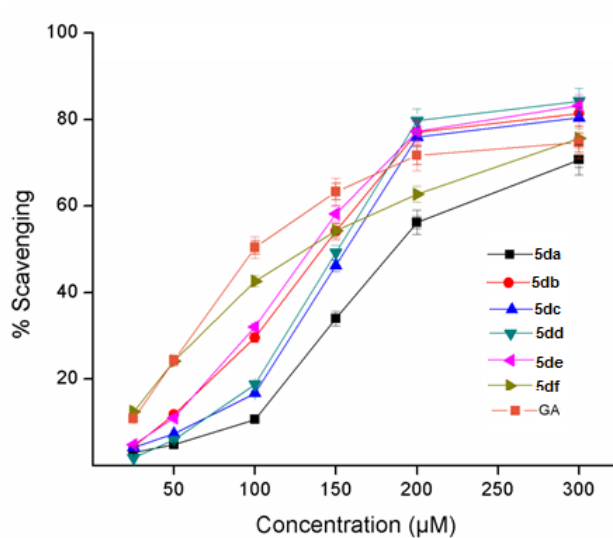
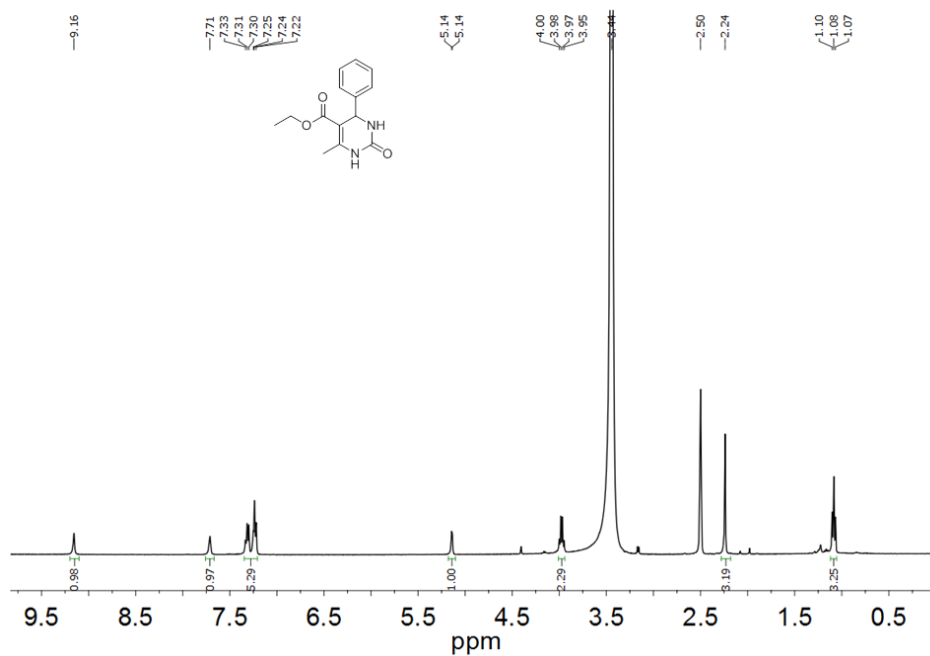
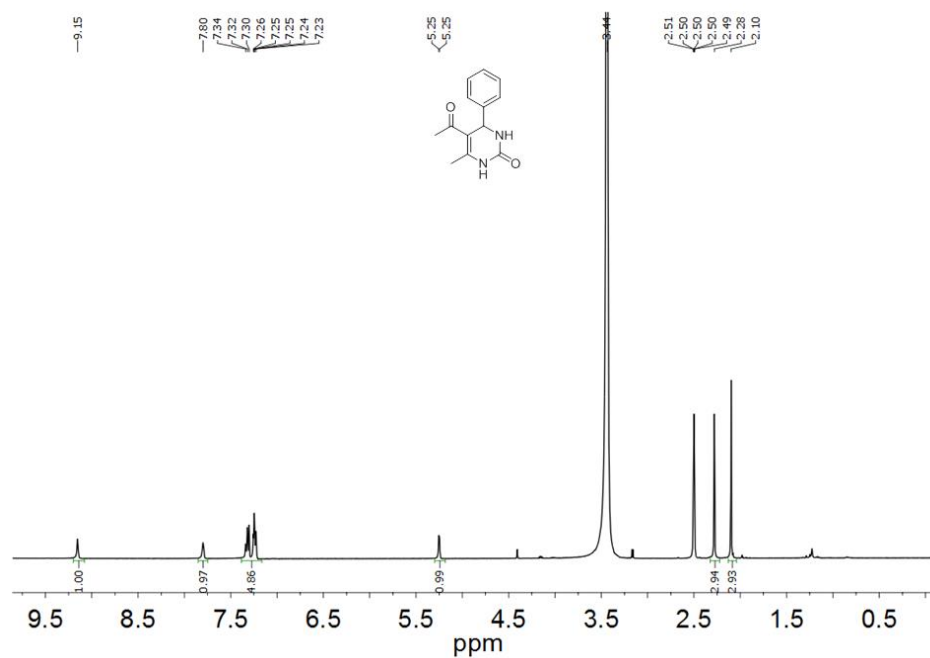
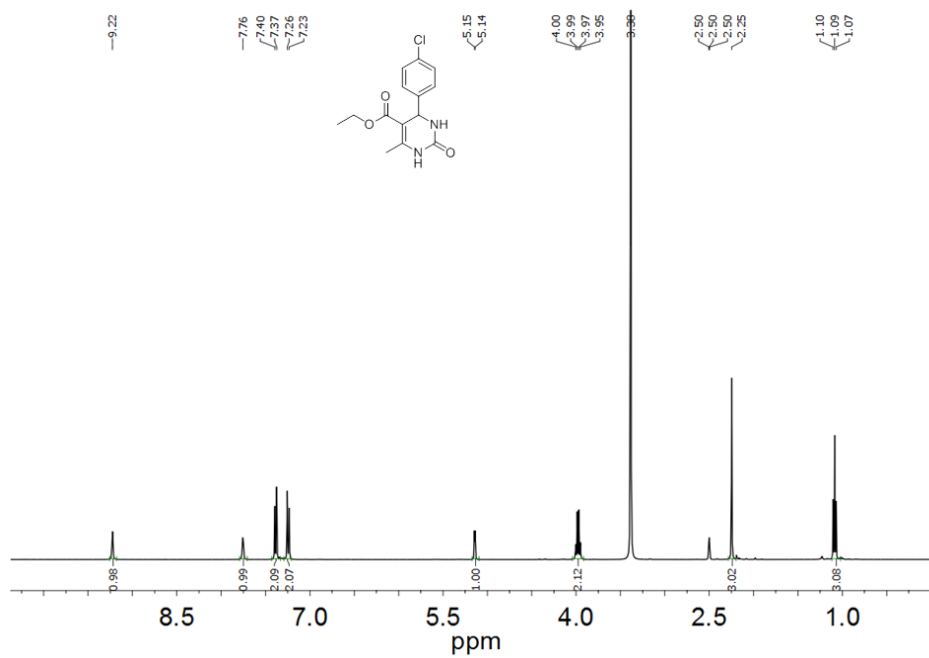
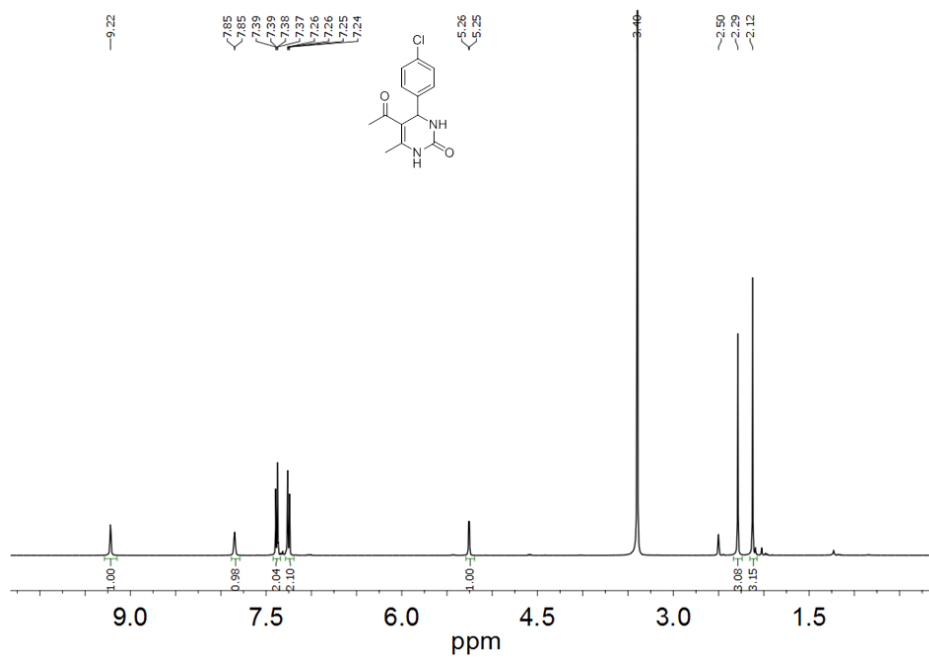


Figure 2.15. Nitric oxide radical scavenging activity of DHPMs and Gallic acid (GA)

^1H and ^{13}C NMR spectra the compoundsFigure 2.16. ^1H NMR spectrum of (5aa).Figure 2.17. ^1H NMR spectrum of (5ab).

Figure 2.18. ^1H NMR spectrum of (5ac).Figure 2.19. ^1H NMR spectrum of (5ad).

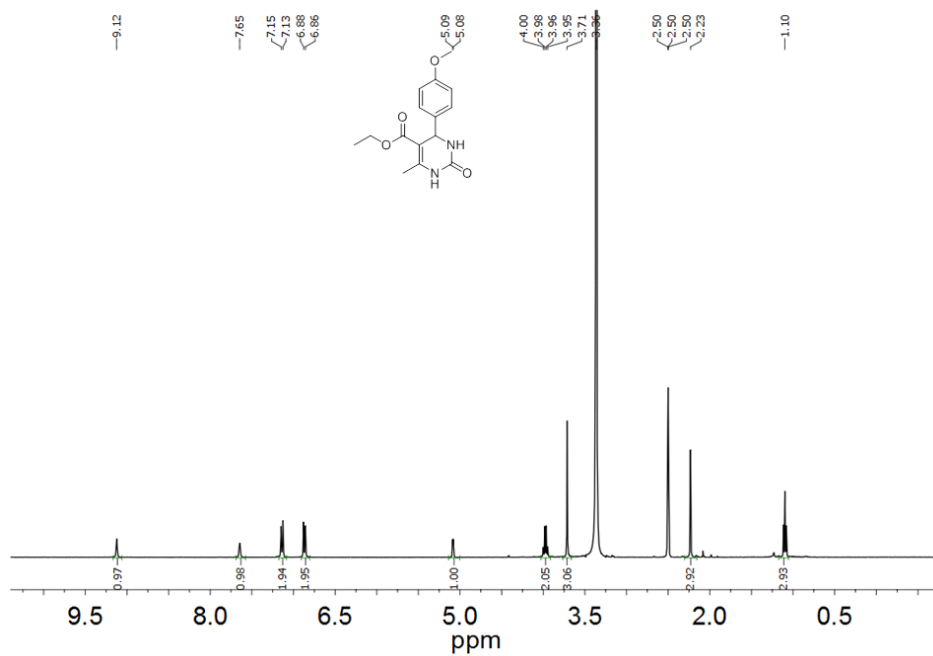


Figure 2.20. ^1H NMR spectrum of (5ae).

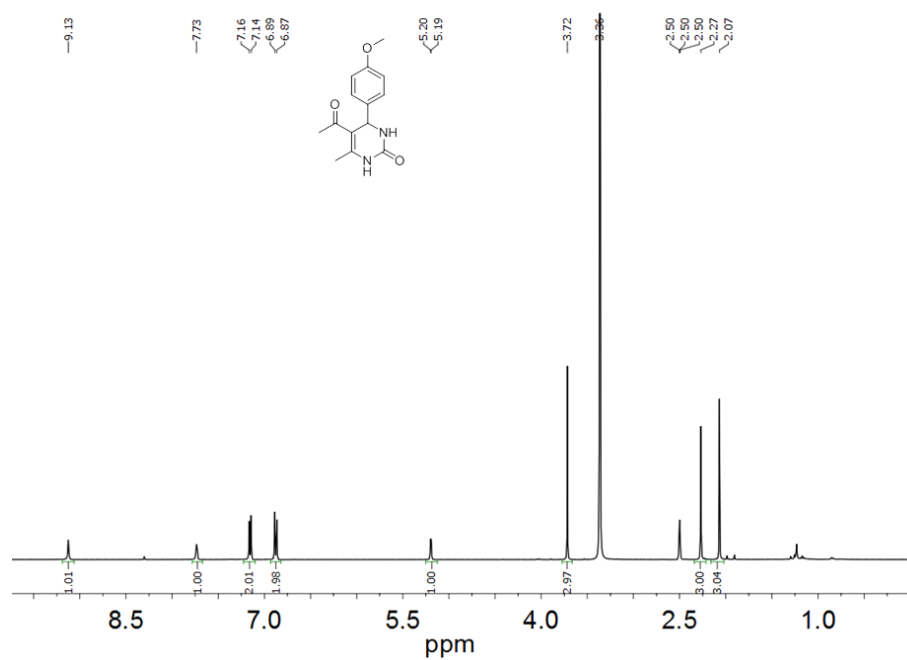
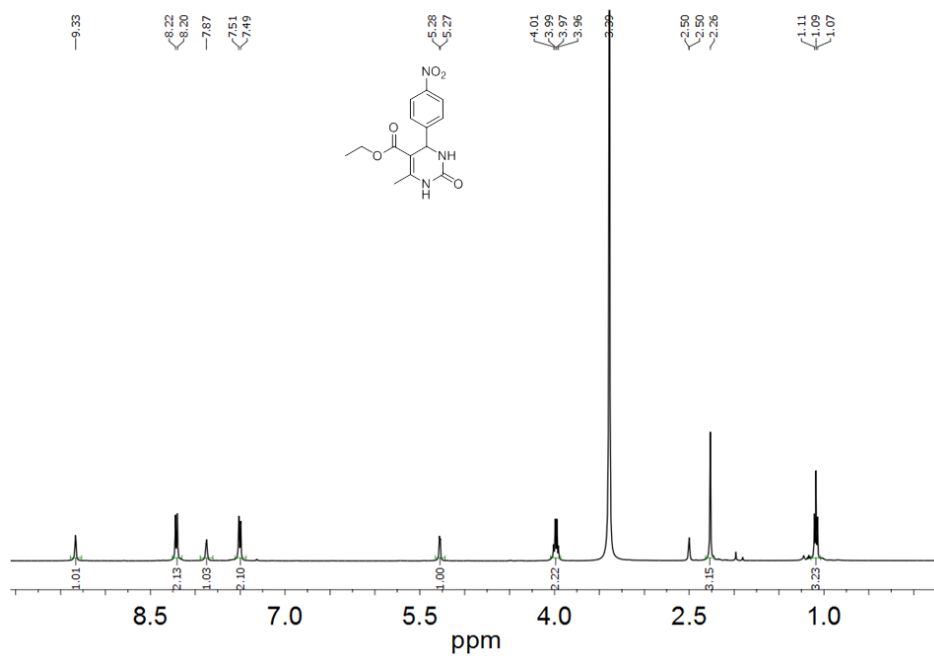
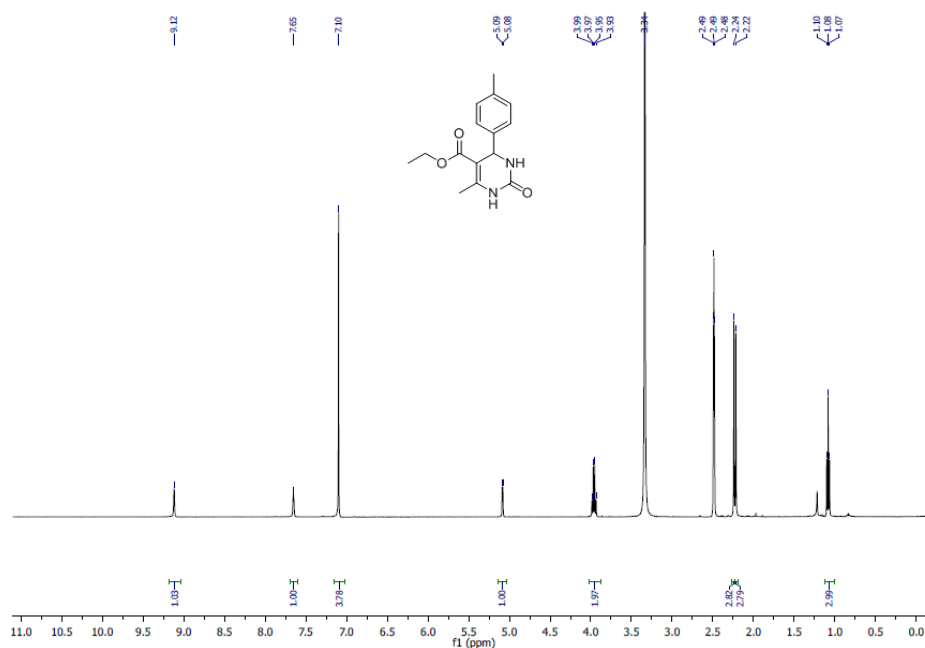


Figure 2.21. ^1H NMR spectrum of (5af).

Figure 2.22. ^1H NMR spectrum of (5ag).Figure 2.23. ^1H NMR spectrum of (5ah).

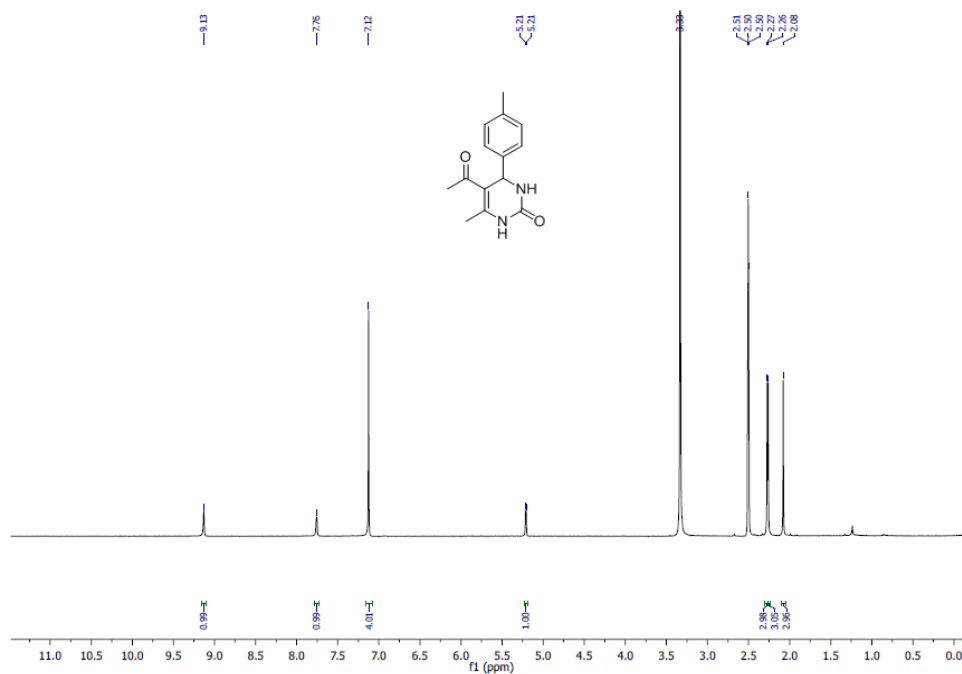


Figure 2.24. ^1H NMR spectrum of (5ai).

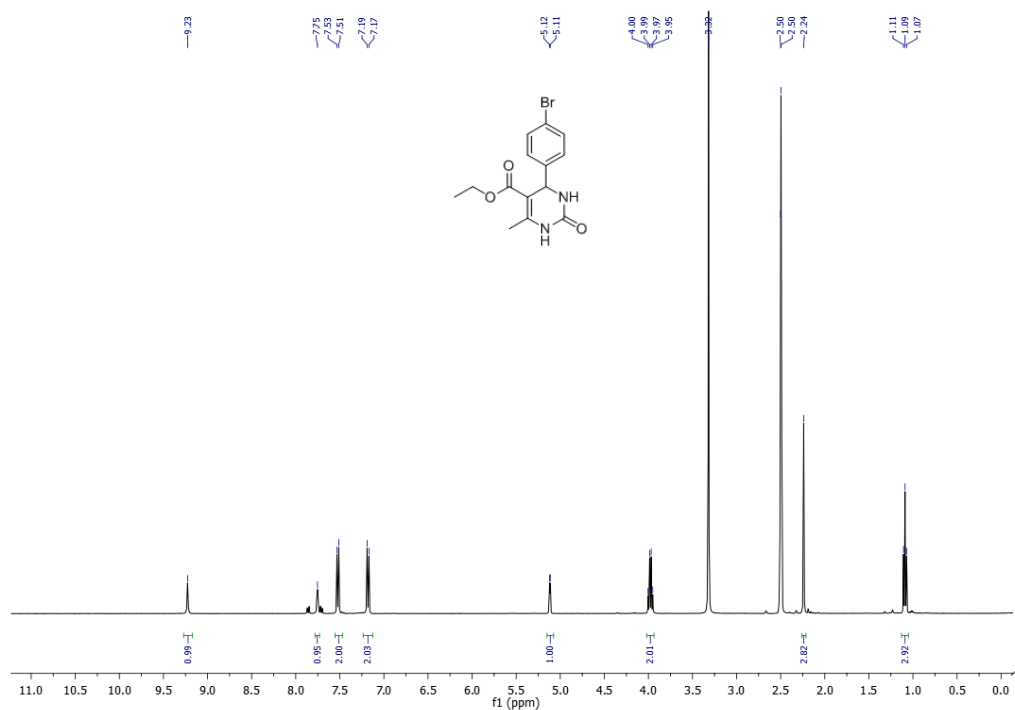
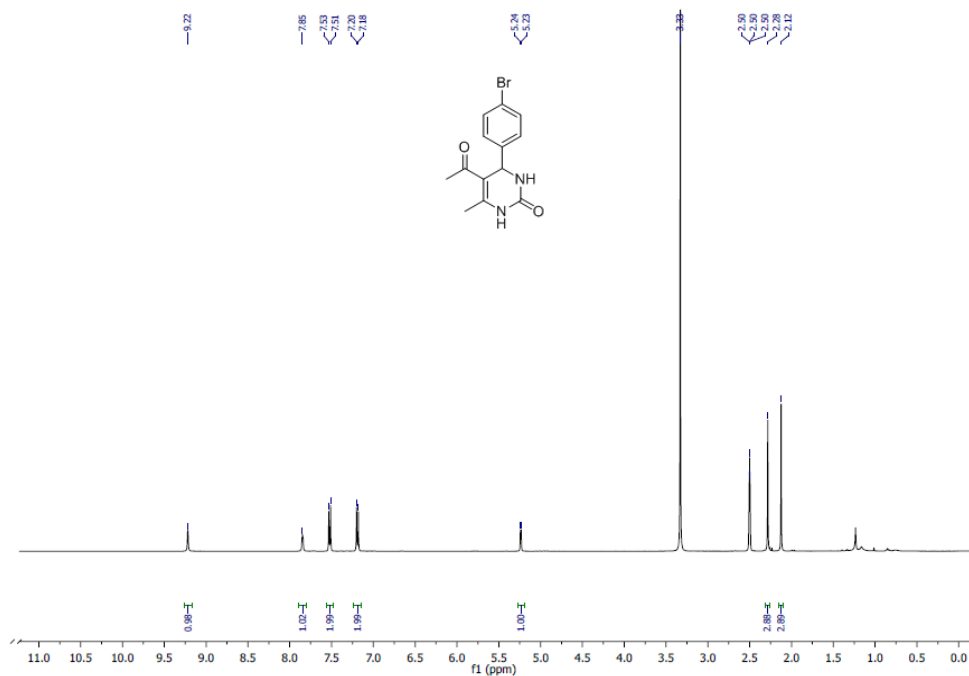
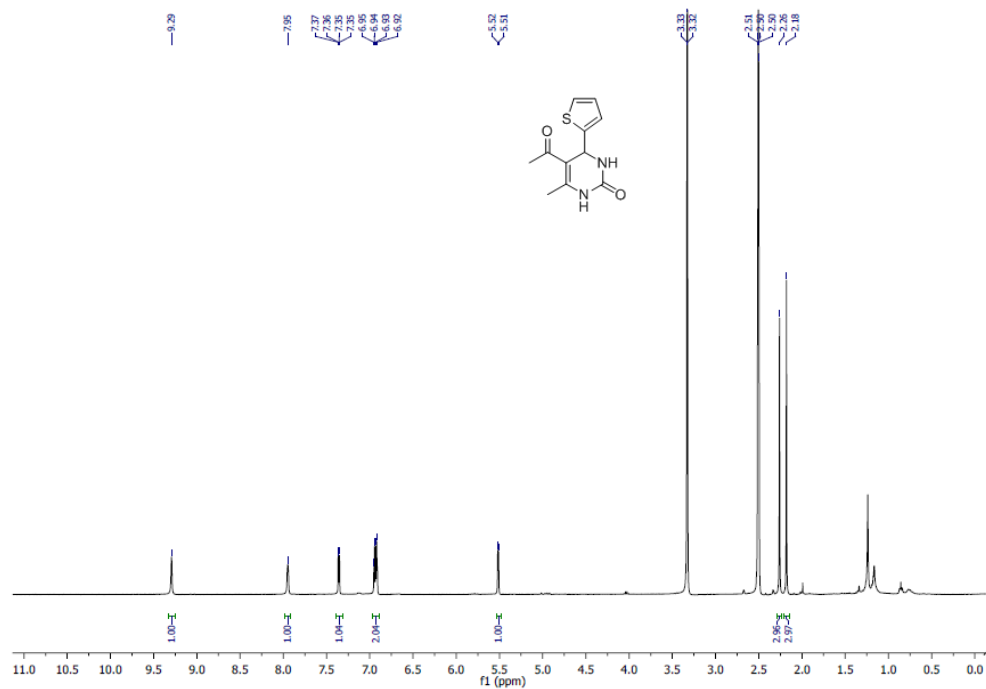


Figure 2.25. ^1H NMR spectrum of (5aj).

Figure 2.26. ^1H NMR spectrum of (5ak).Figure 2.27. ^1H NMR spectrum of (5al).

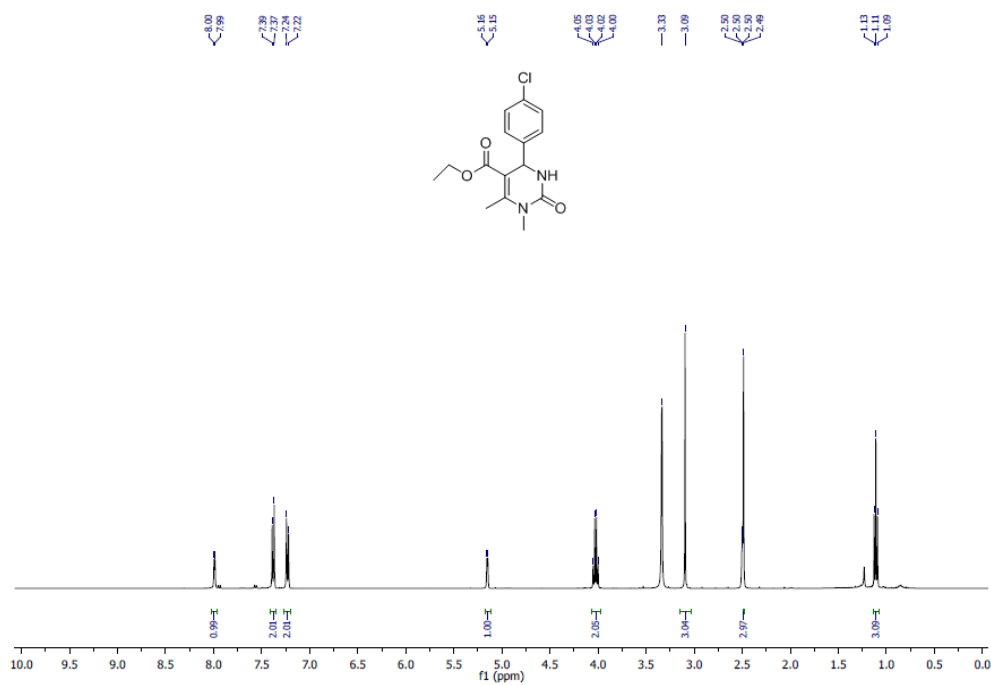


Figure 2.28. ¹H NMR spectrum of (5ba).

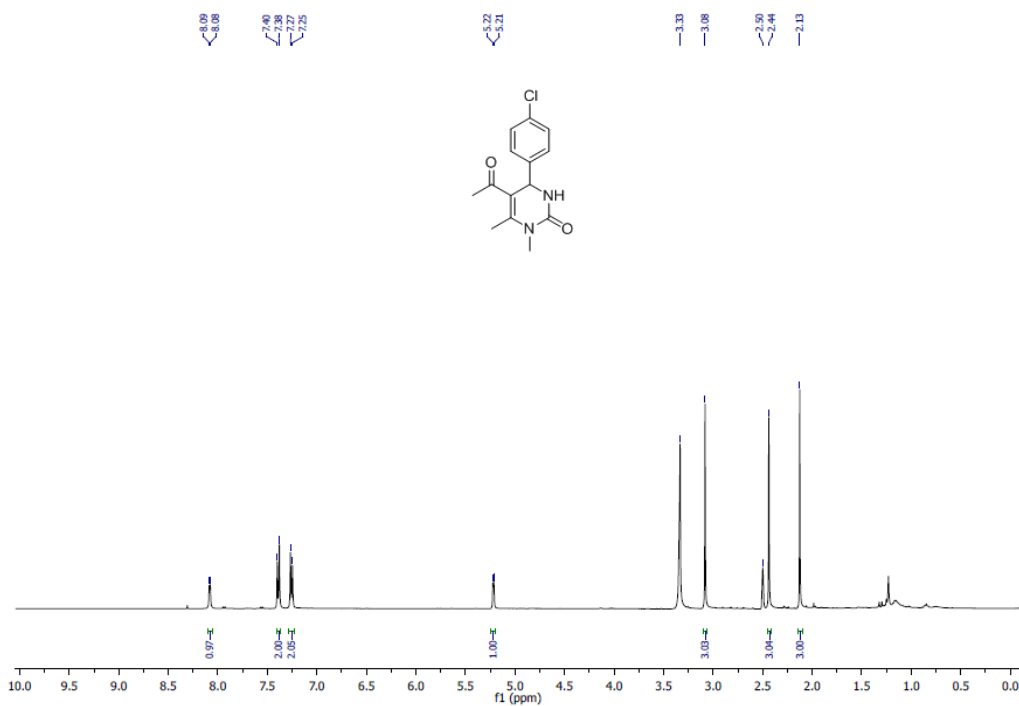
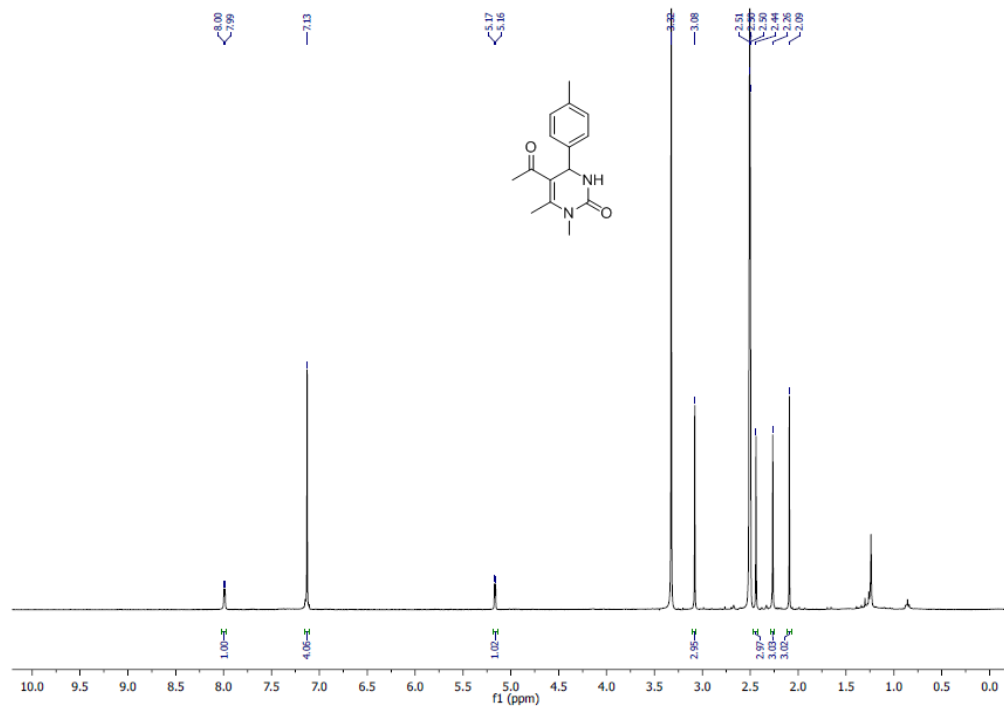
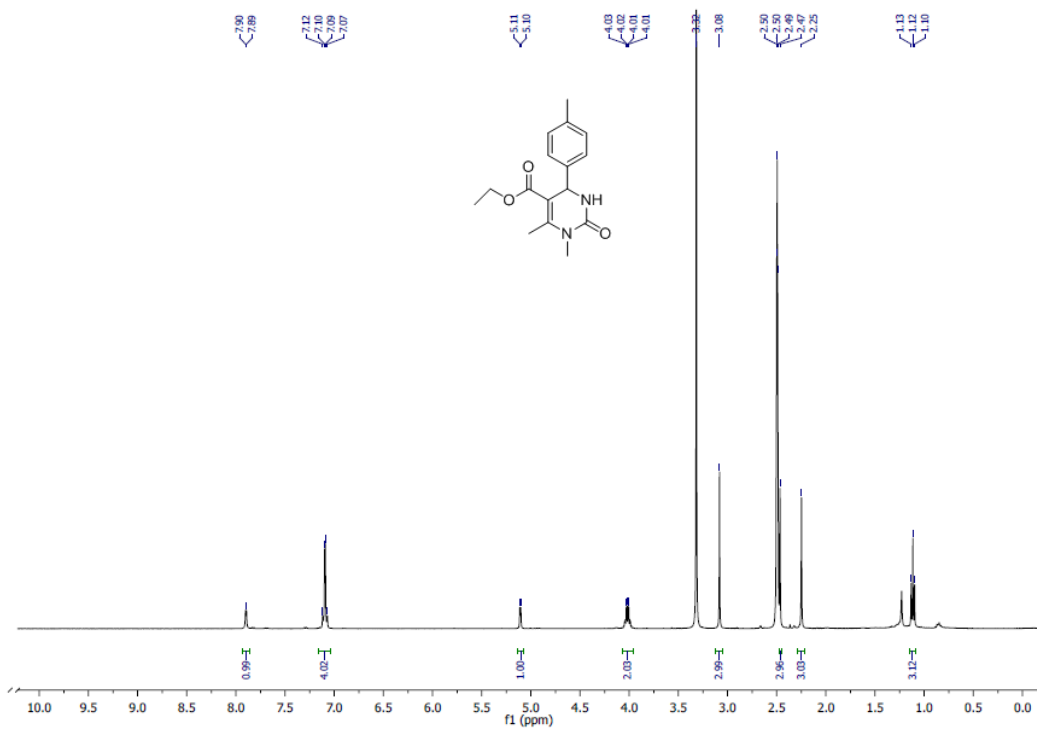


Figure 2.29. ¹H NMR spectrum of (5bb).



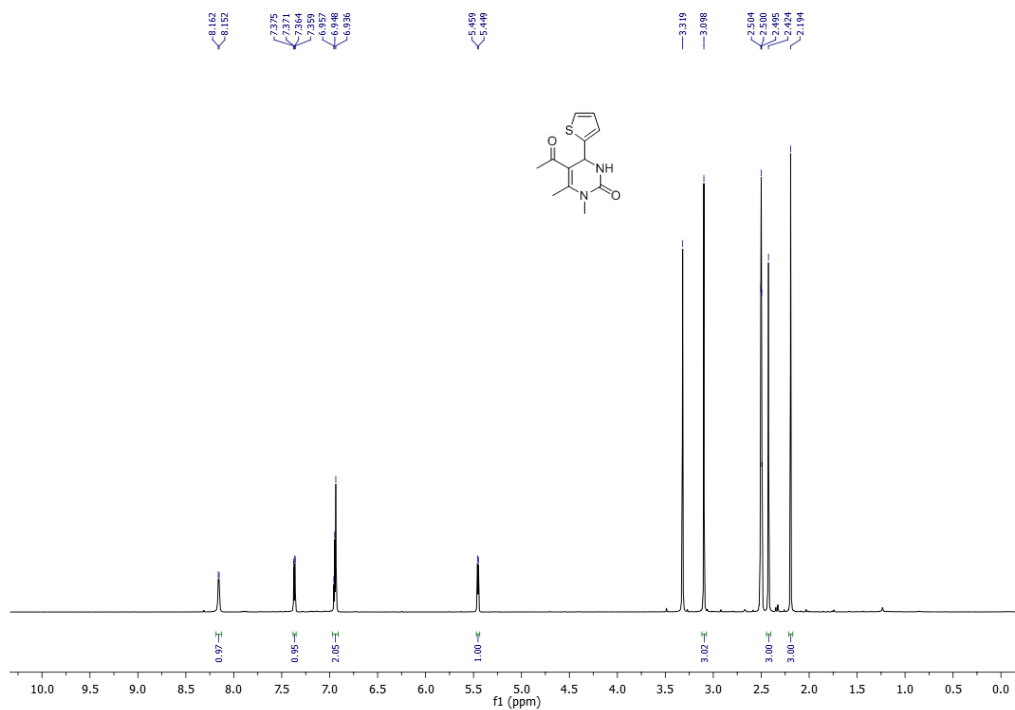


Figure 2.32. ¹H NMR spectrum of (5be).

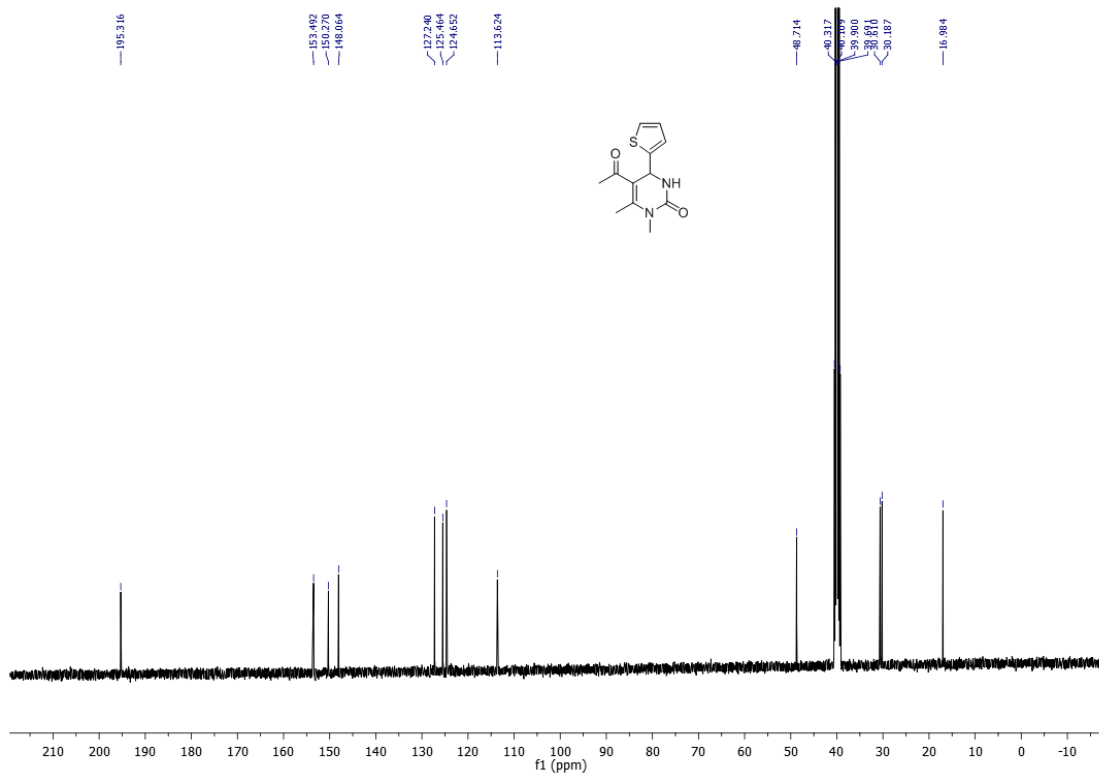
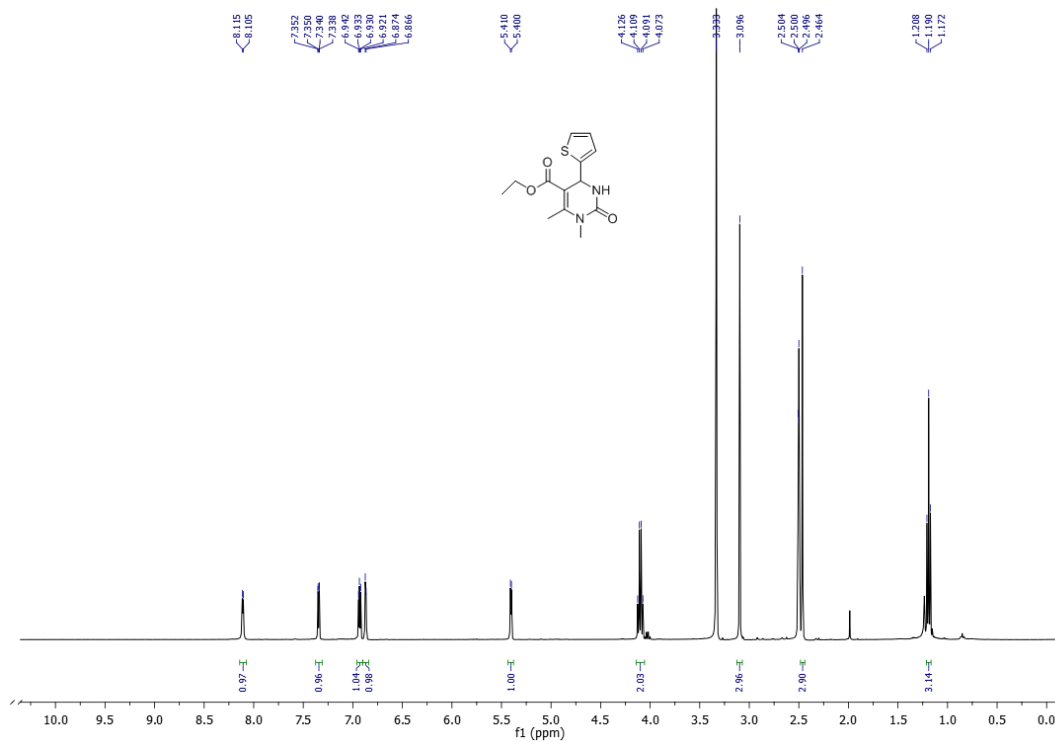
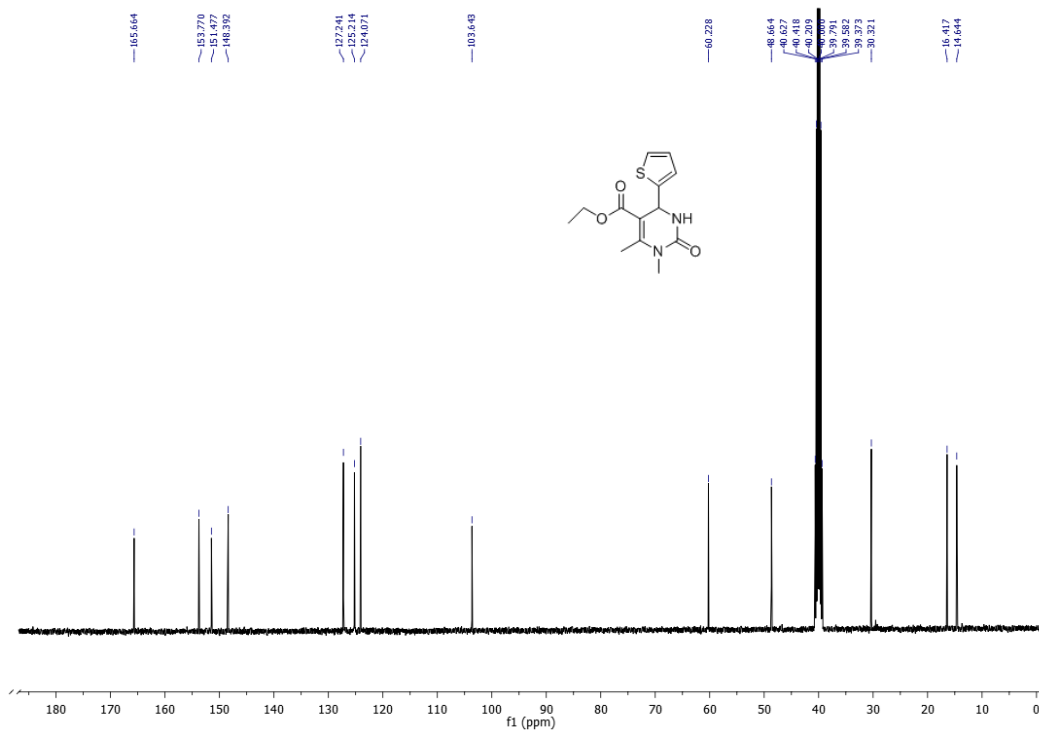


Figure 2.33. ¹³C NMR spectrum of (5be).

Figure 2.34. ¹H NMR spectrum of (5bf).Figure 2.35. ¹³C NMR spectrum of (5bf).

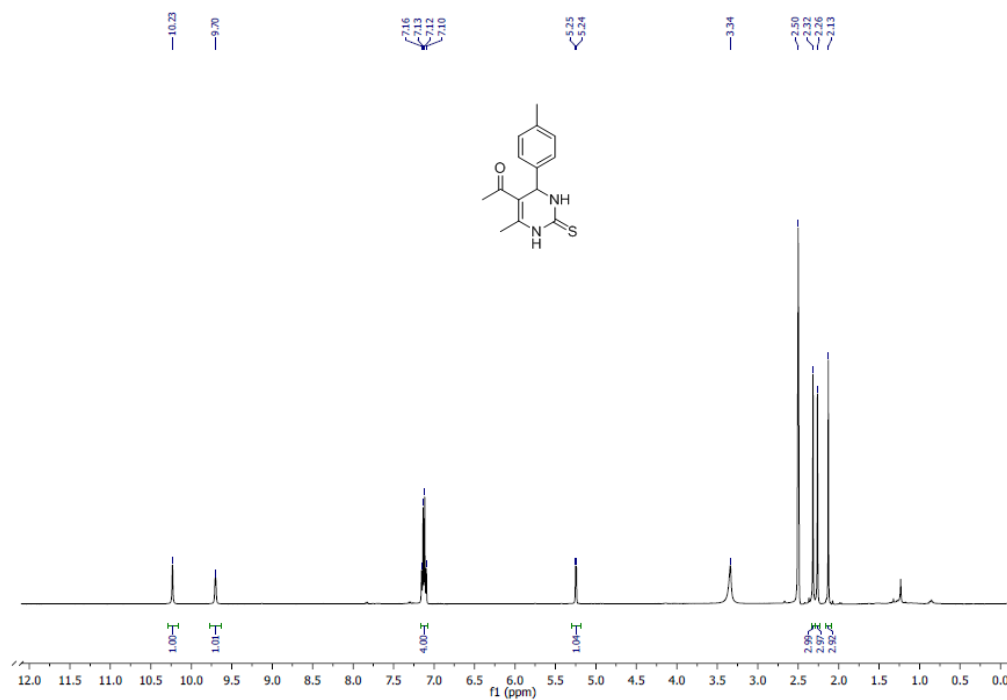


Figure 2.36. ^1H NMR spectrum of **(5ca)**.

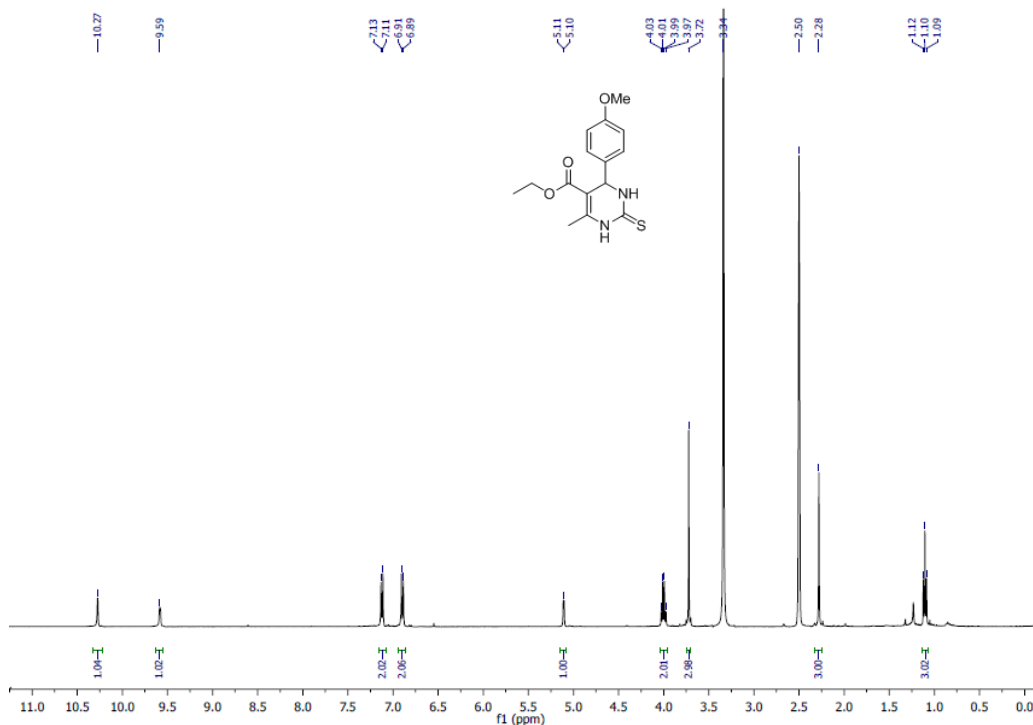
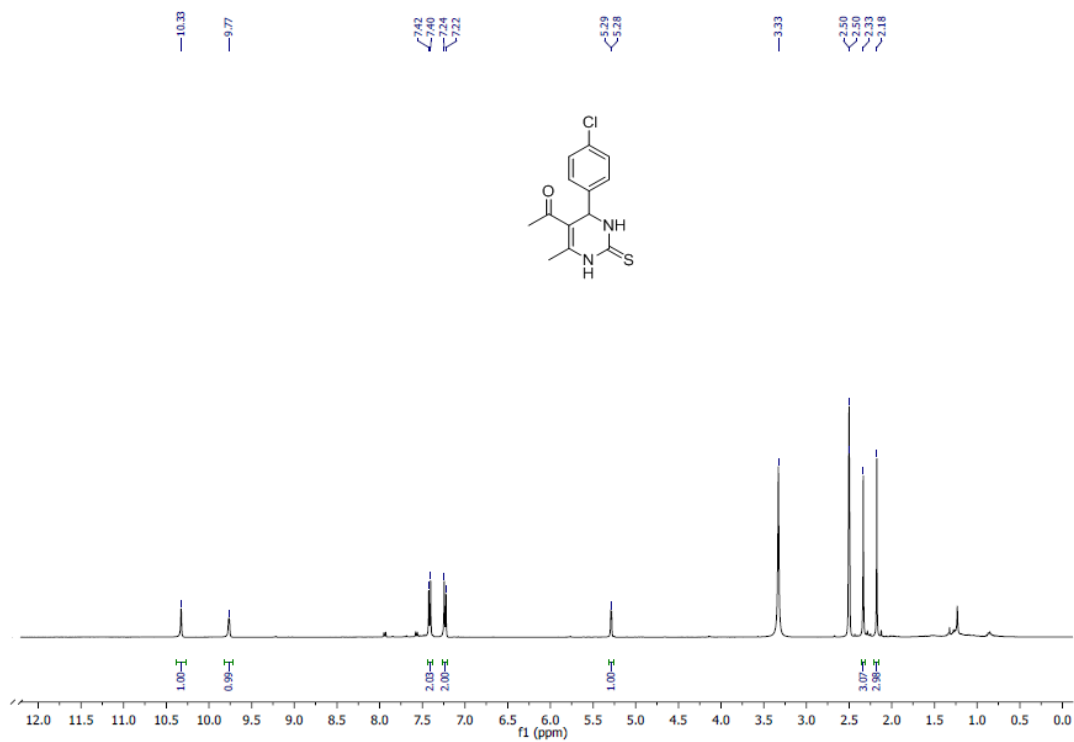
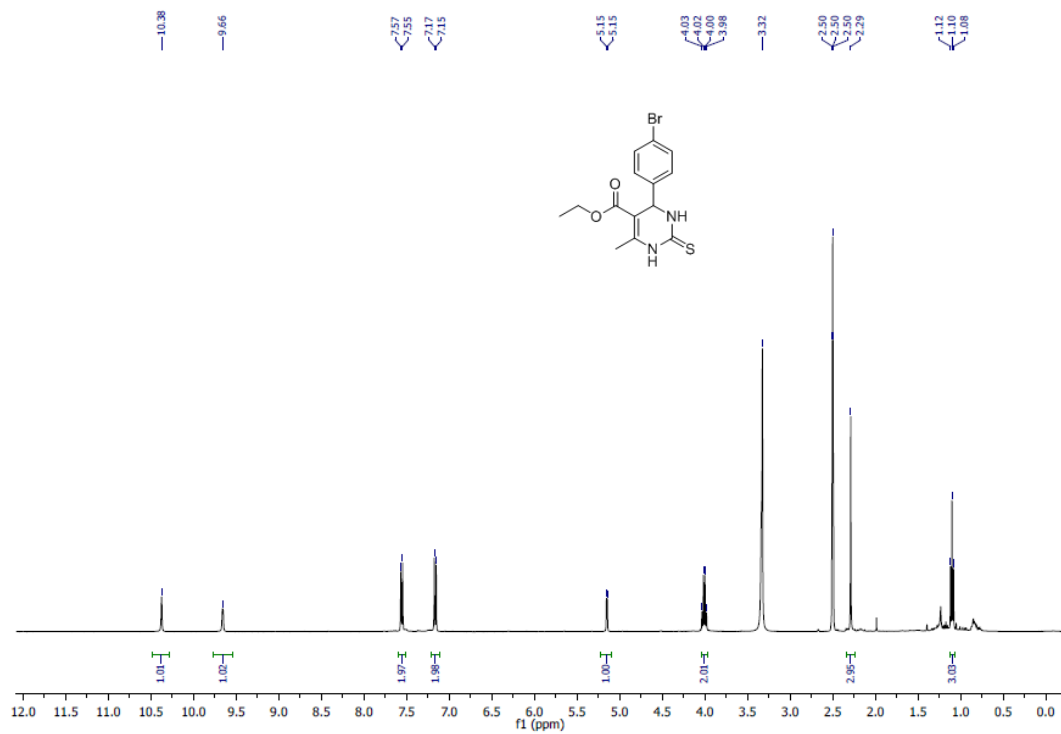


Figure 2.37. ^1H NMR spectrum of **(5cb)**.

Figure 2.38. ¹H NMR spectrum of (5cc).Figure 2.39. ¹H NMR spectrum of (5cd).

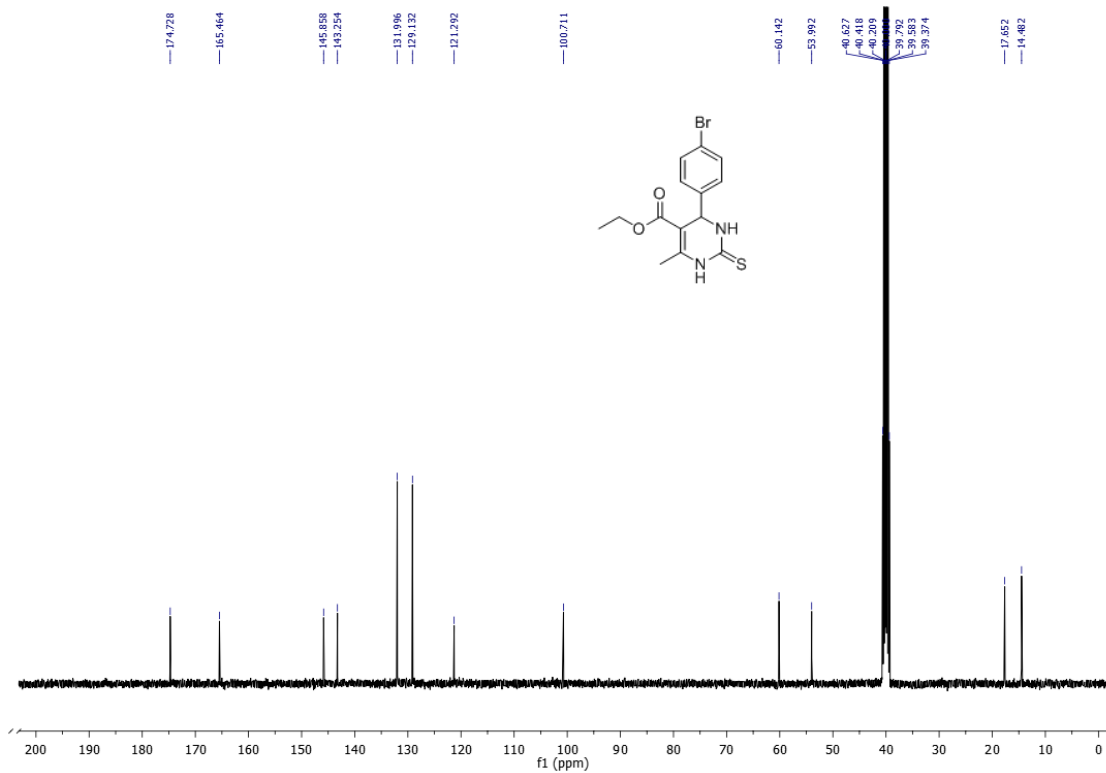


Figure 2.40. ^{13}C NMR spectrum of **(5cd)**.

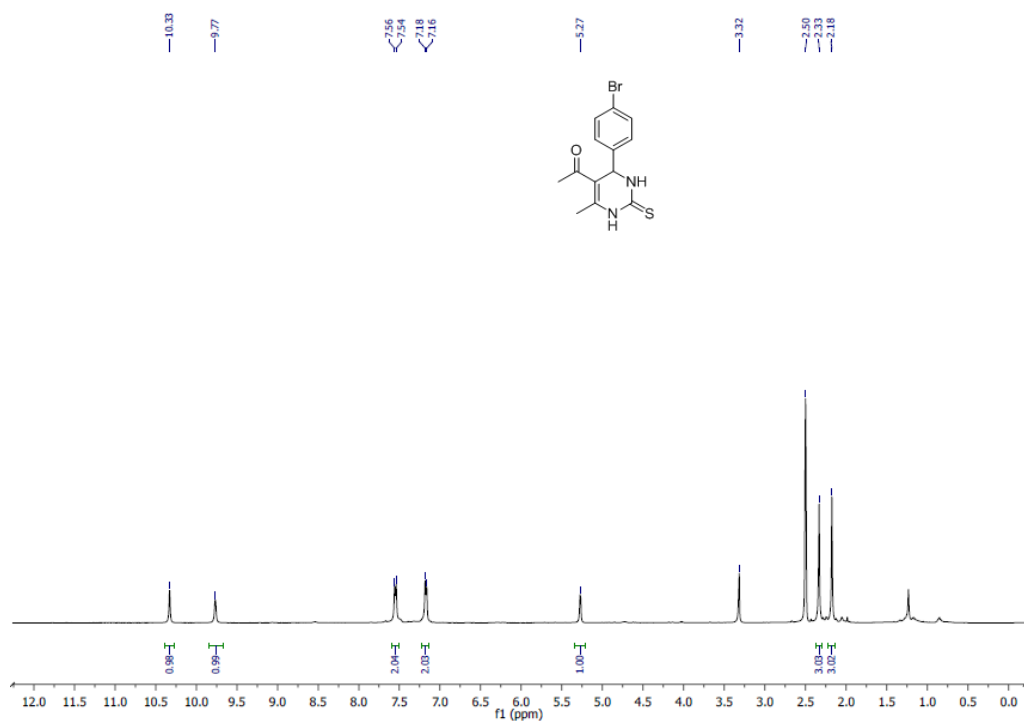
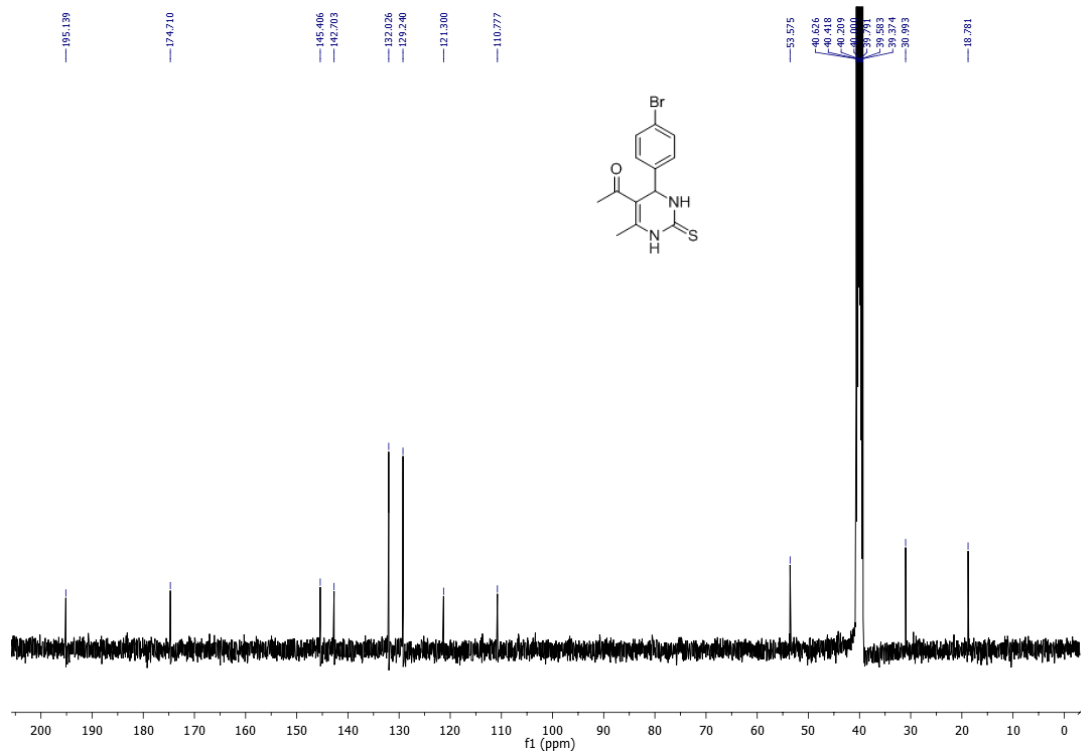
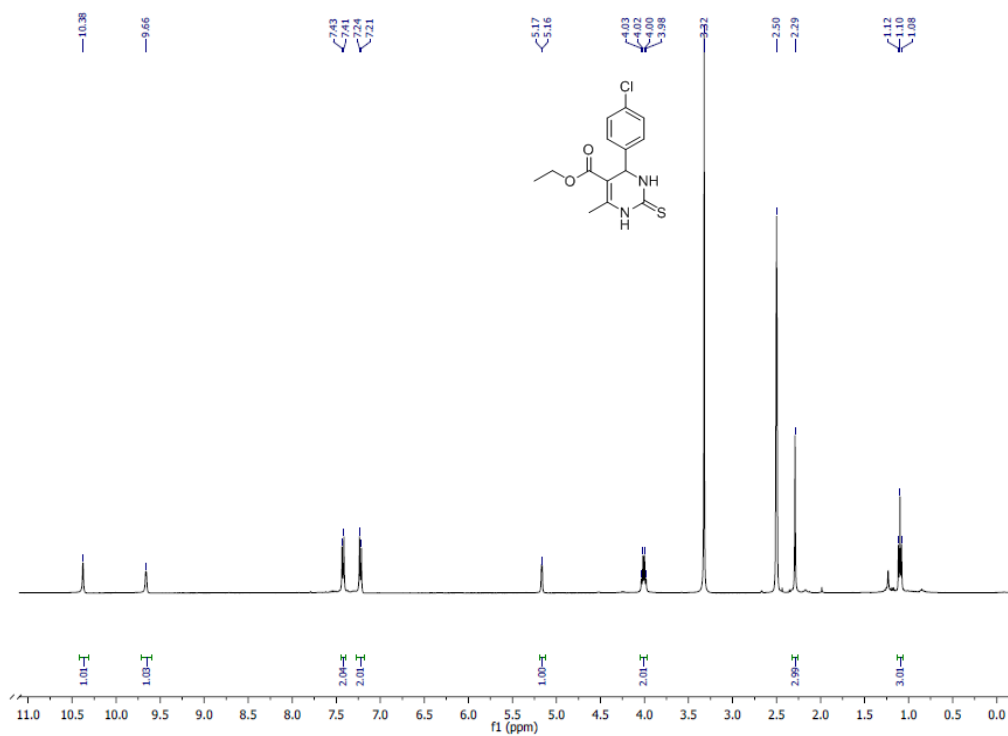
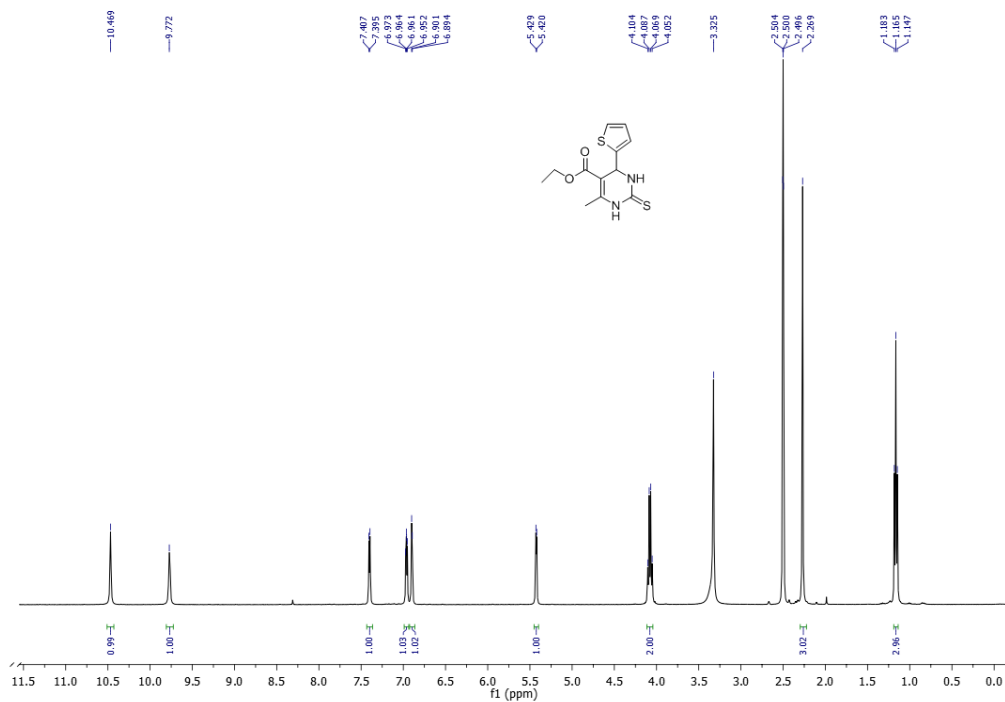
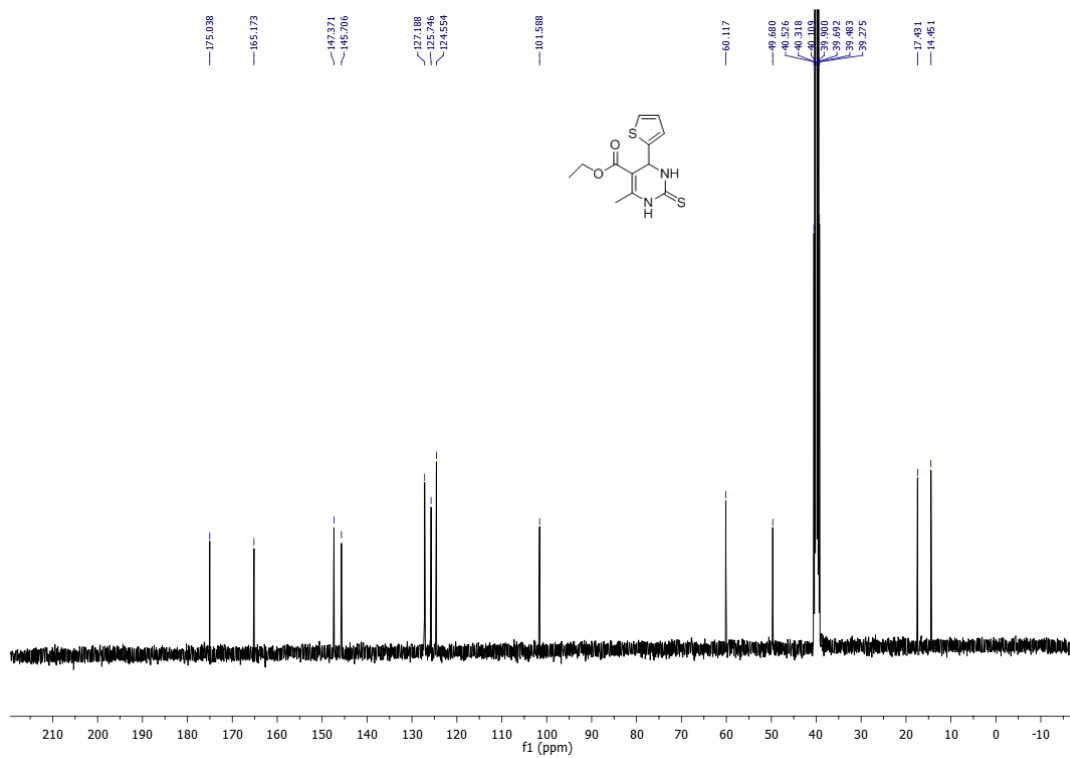
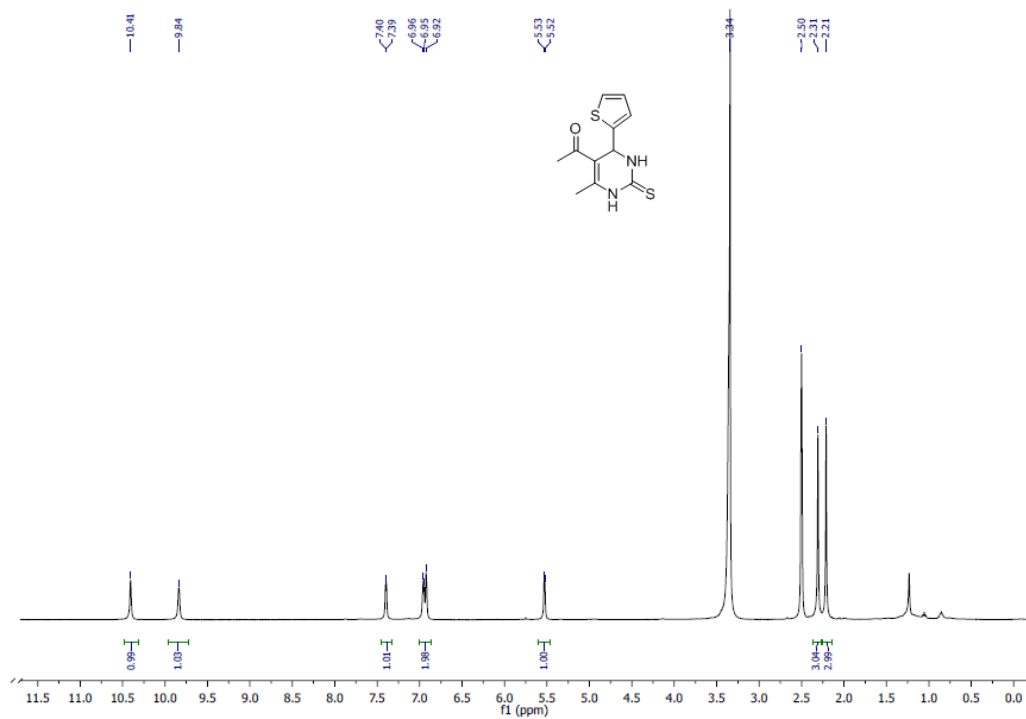
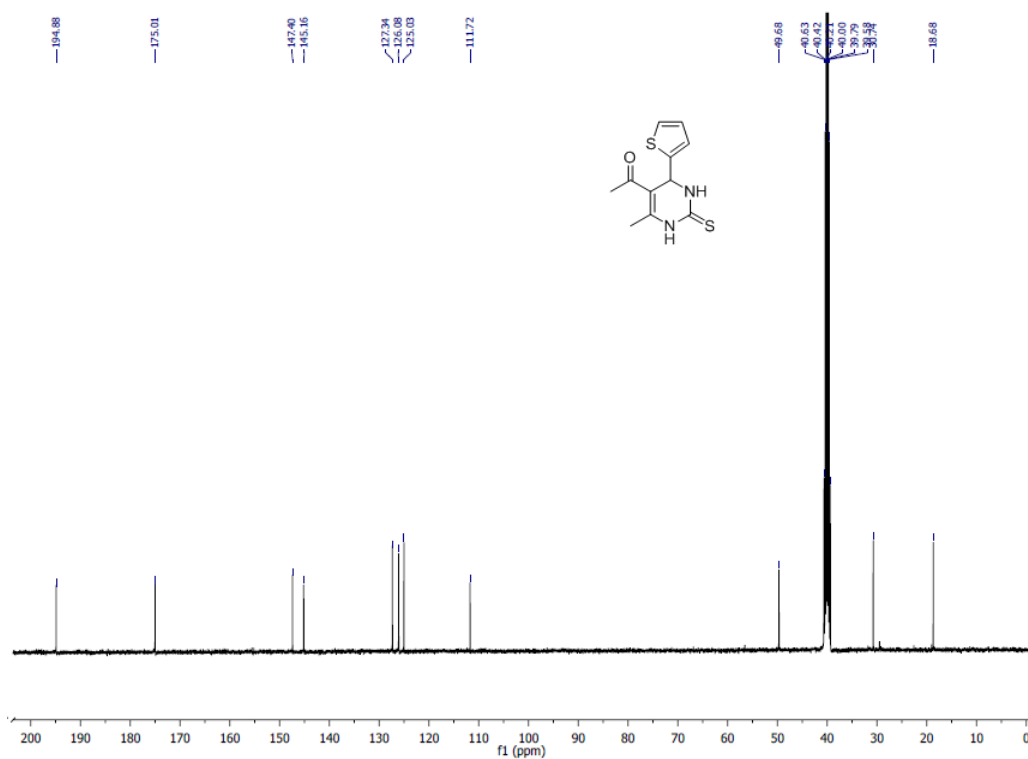


Figure 2.41. ^1H NMR spectrum of **(5ce)**.

Figure 2.42. ^{13}C NMR spectrum of (**5ce**).Figure 2.43. ^1H NMR spectrum of (**5cf**).

Figure 2.44. ^1H NMR spectrum of (5cg).Figure 2.45. ^{13}C NMR spectrum of (5cg).

Figure 2.46. ¹H NMR spectrum of (5ch).Figure 2.47. ¹³C NMR spectrum of (5ch).

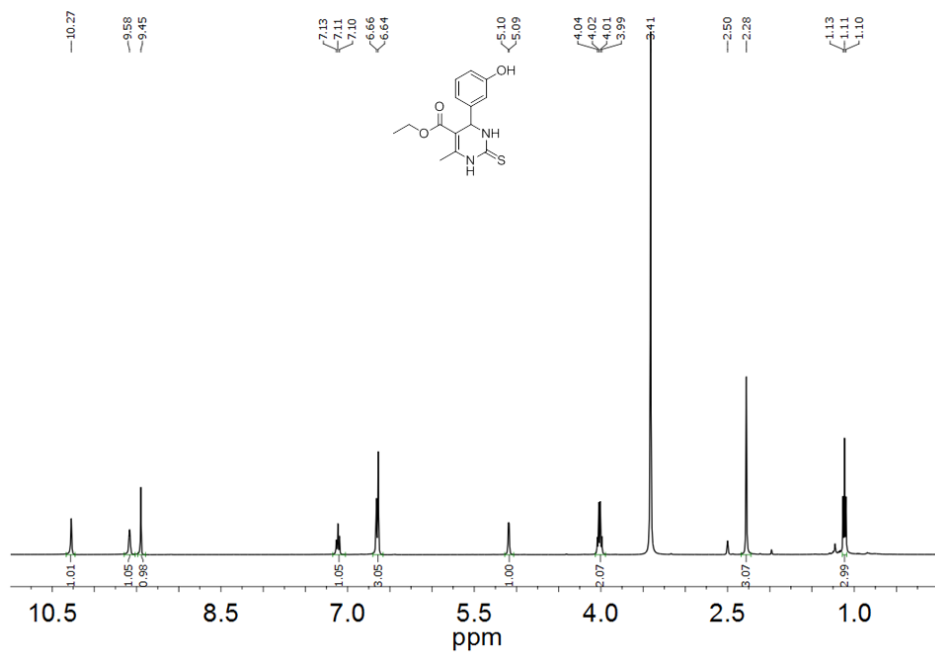


Figure 2.48. ¹H NMR spectrum of (5da).

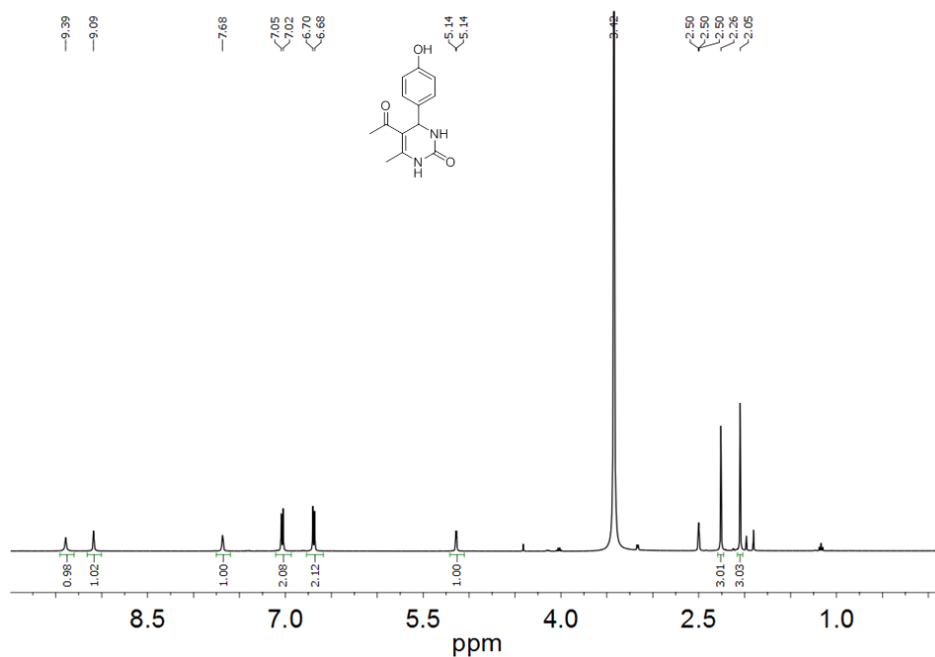
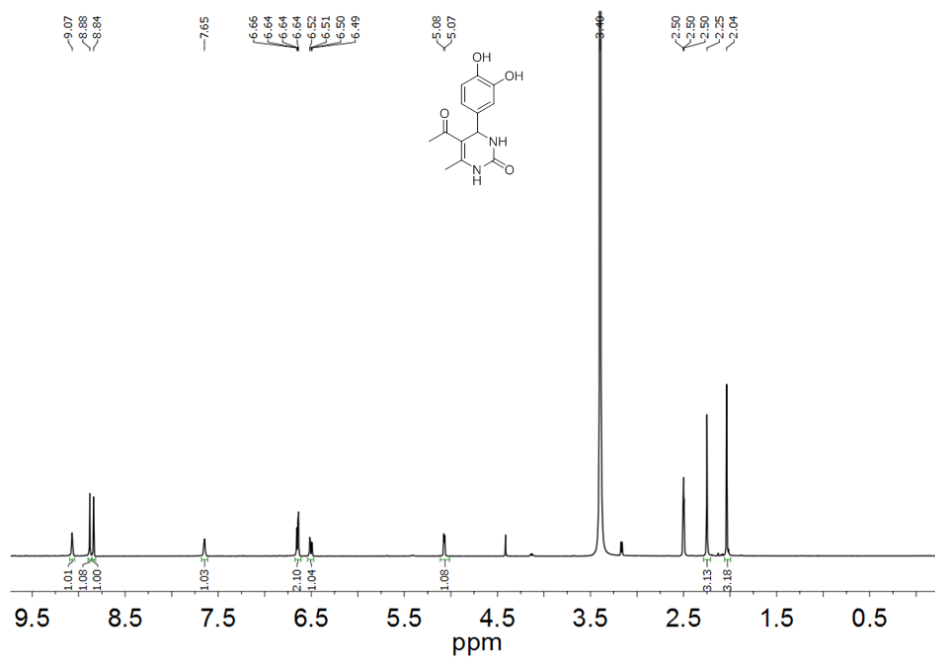
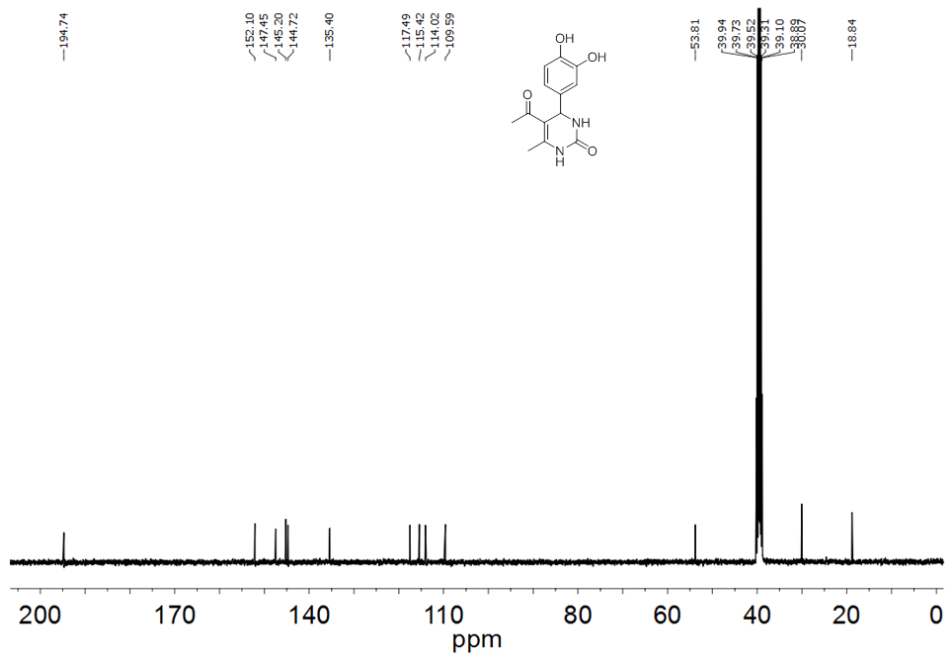


Figure 2.49. ¹H NMR spectrum of (5db).

Figure 2.50. ^1H NMR spectrum of (5dc).Figure 2.51. ^{13}C NMR spectrum of (5dc).

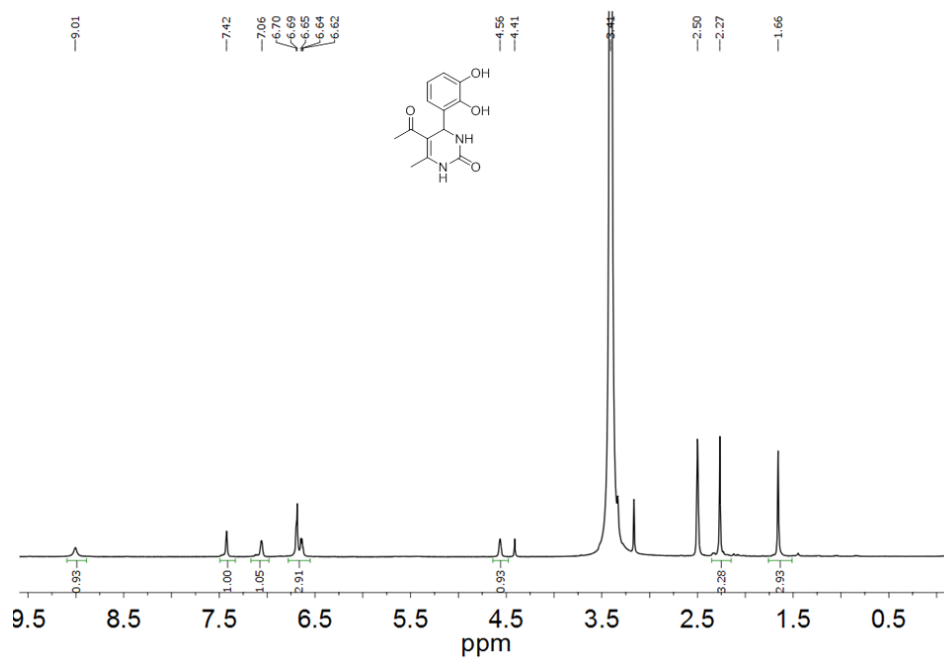


Figure 2.52. ^1H NMR spectrum of (5dd).

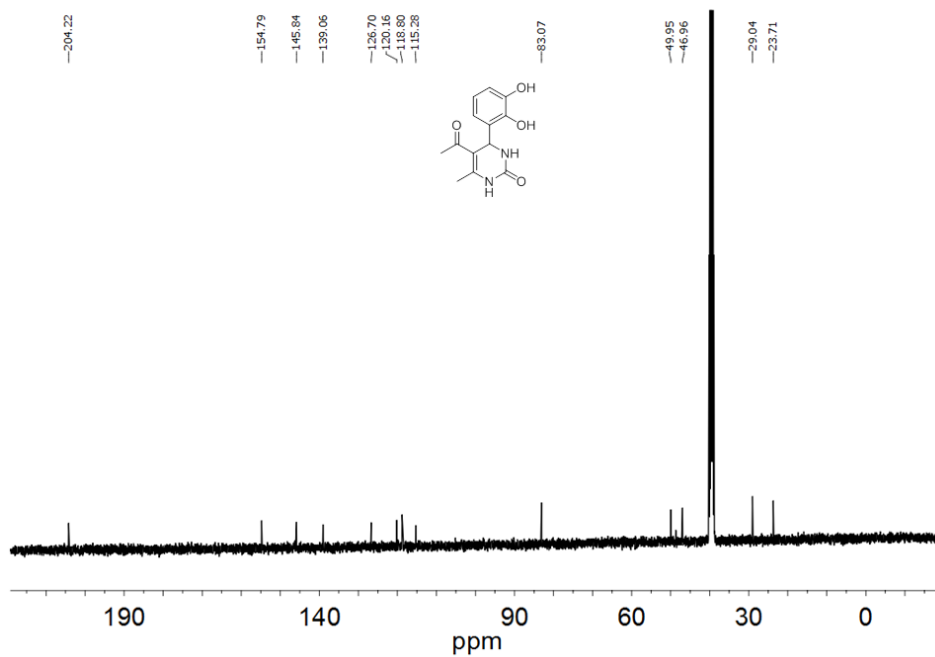
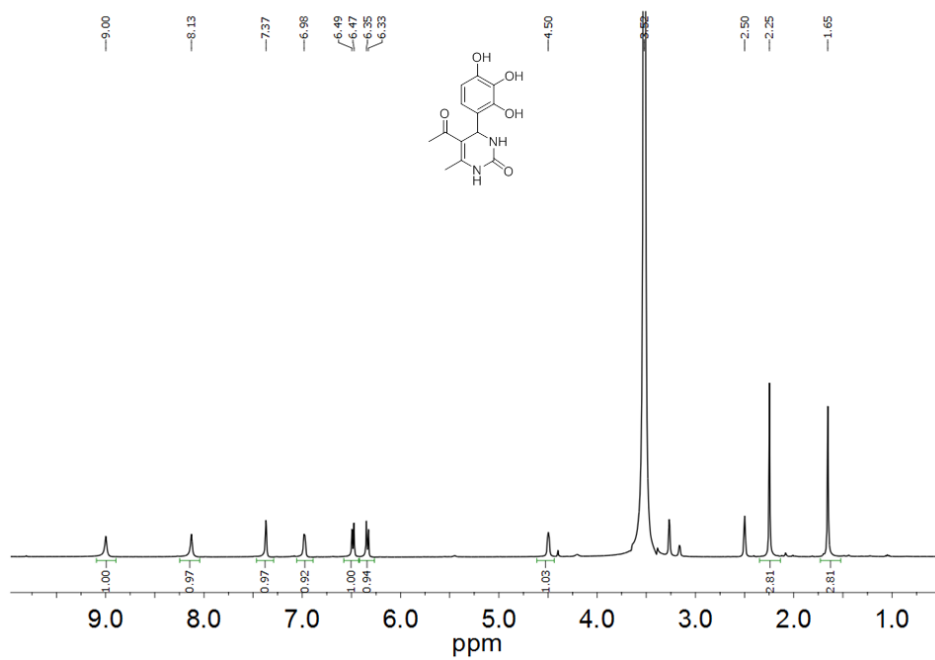
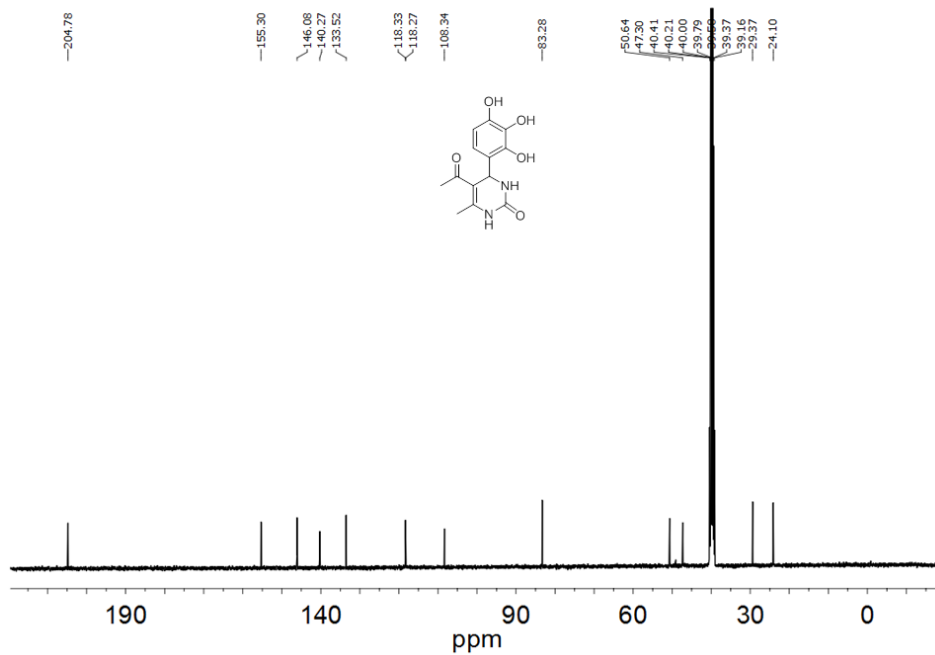


Figure 2.53. ^{13}C NMR spectrum of (5dd).

Figure 2.54. ^1H NMR spectrum of (5de).Figure 2.55. ^{13}C NMR spectrum of (5de).

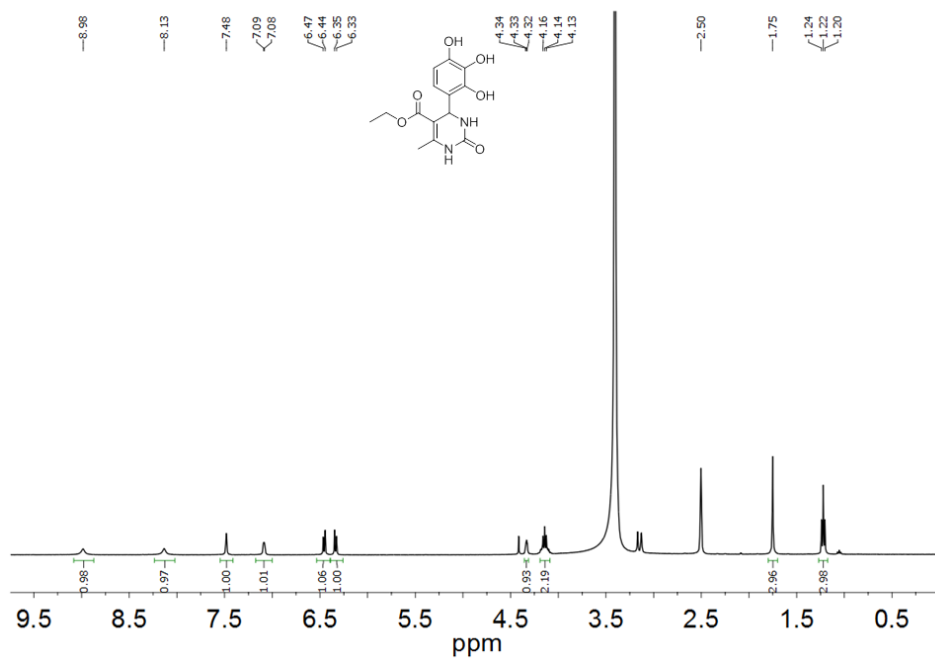


Figure 2.56. ^1H NMR spectrum of (**5df**).

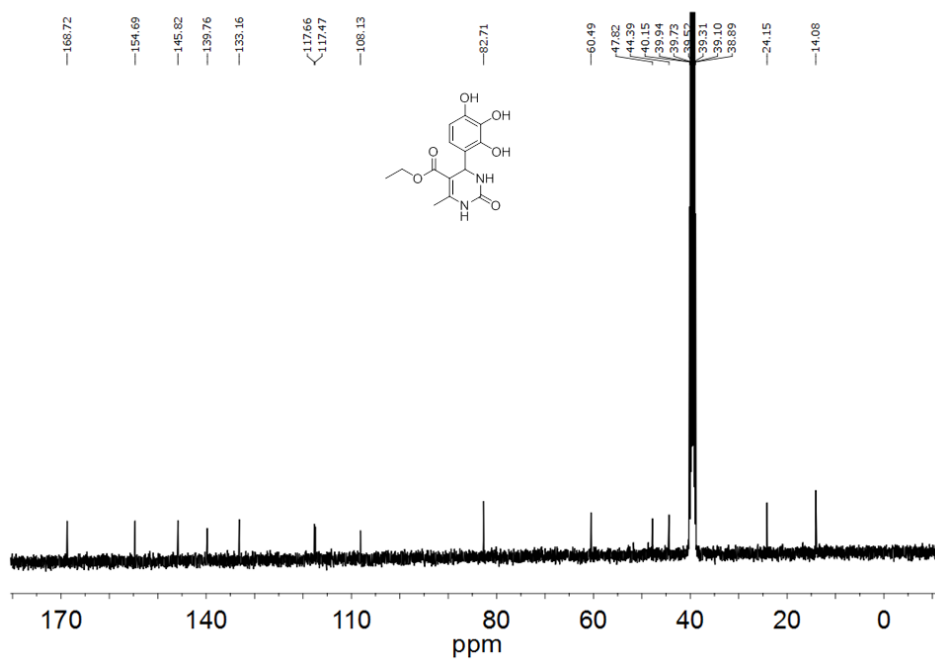


Figure 2.57. ^{13}C NMR spectrum of (**5df**).

2.6 NOTES AND REFERENCES

1. P. D. Frischmann, V. Kunz, V. Stepanenko and F. Würthner, *Chem. Eur. J.*, 2015, **21**, 2766-2769.
2. A. M. Castilla, W. J. Ramsay and J. R. Nitschke, *Acc. Chem. Res.*, 2014, **47**, 2063-2073.
3. H. Bunzen, Nonappa, E. Kalenius, S. Hietala and E. Kolehmainen, *Chem. Eur. J.*, 2013, **19**, 12978-12981.
4. X.-P. Zhou, Y. Wu and D. Li, *J. Am. Chem. Soc.*, 2013, **135**, 16062-16065.
5. D. H. Ren, D. Qiu, C. Y. Pang, Z. Li and Z. G. Gu, *Chem. Commun.*, 2014, **51**, 788-791.
6. N. Giuseppone, *Acc. Chem. Res.*, 2012, **45**, 2178-2188.
7. J. R. Nitschke, *Nature*, 2009, **462**, 736-738.
8. R. F. Ludlow and S. Otto, *Chem. Soc. Rev.*, 2008, **37**, 101-108.
9. M. L. Saha, N. Mittal, J. W. Bats and M. Schmittel, *Chem. Commun.*, 2014, **50**, 12189-12192.
10. D. Lewing, H. Koppetz and F. E. Hahn, *Inorg. Chem.*, 2015, **54**, 7653-7659.
11. K. Pandurangan, J. A. Kitchen, S. Blasco, E. M. Boyle, B. Fitzpatrick, M. Feeney, P. E. Kruger and T. Gunnlaugsson, *Angew. Chem. Int. Ed.*, 2015, **54**, 4566-4570.
12. J. E. Beves, J. J. Danon, D. A. Leigh, J.-F. Lemonnier and I. J. Vitorica-Yrezabal, *Angew. Chem. Int. Ed.*, 2015, **54**, 7555-7559.
13. R. Chakrabarty, P. S. Mukherjee and P. J. Stang, *Chem. Rev.*, 2011, **111**, 6810-6918.
14. K. Acharyya, S. Mukherjee and P. S. Mukherjee, *J. Am. Chem. Soc.*, 2013, **135**, 554-557.
15. K. Ruiz-Mirazo, C. Briones and A. de la Escosura, *Chem. Rev.*, 2014, **114**, 285-366.
16. E. R. Kay, D. A. Leigh and F. Zerbetto, *Angew. Chem. Int. Ed.*, 2007, **46**, 72-191.

17. B. Lewandowski, G. De Bo, J. W. Ward, M. Papmeyer, S. Kuschel, M. J. Aldegunde, P. M. E. Gramlich, D. Heckmann, S. M. Goldup, D. M. D'Souza, A. E. Fernandes and D. A. Leigh, *Science*, 2013, **339**, 189-193.
18. C. Giri, F. Topic, M. Cametti and K. Rissanen, *Chem. Sci.*, 2015, **6**, 5712-5718.
19. C. Giri, P. K. Sahoo, R. Puttreddy, K. Rissanen and P. Mal, *Chem. Eur. J.*, 2015, **21**, 6390–6393.
20. R. S. Varma, *Green Chem.*, 2014, **16**, 2027-2041.
21. G. Cravotto, E. C. Gaudino and P. Cintas, *Chem. Soc. Rev.*, 2013, **42**, 7521-7534.
22. D. Braga, L. Maini and F. Grepioni, *Chem. Soc. Rev.*, 2013, **42**, 7638-7648.
23. S. L. James, C. J. Adams, C. Bolm, D. Braga, P. Collier, T. Friscic, F. Grepioni, K. D. M. Harris, G. Hyett, W. Jones, A. Krebs, J. Mack, L. Maini, A. G. Orpen, I. P. Parkin, W. C. Shearouse, J. W. Steed and D. C. Waddell, *Chem. Soc. Rev.*, 2012, **41**, 413-447.
24. T. Friščić, I. Halasz, P. J. Beldon, A. M. Belenguer, F. Adams, S. A. J. Kimber, V. Honkimäki and R. E. Dinnebier, *Nature Chem.*, 2013, **5**, 66-73.
25. P. Balaz, M. Achimovicova, M. Balaz, P. Billik, Z. Cherkezova-Zheleva, J. M. Criado, F. Delogu, E. Dutkova, E. Gaffet, F. J. Gotor, R. Kumar, I. Mitov, T. Rojac, M. Senna, A. Streletskii and K. Wieczorek-Ciurowa, *Chem. Soc. Rev.*, 2013, **42**, 7571-7637.
26. S. Ley, M. O'Brien and R. Denton, *Synthesis*, 2011, 1157-1192.
27. T. K. Achar, S. Maiti and P. Mal, *RSC Adv.*, 2014, **4**, 12834-12839.
28. T. K. Achar and P. Mal, *J. Org. Chem.*, 2015, **80**, 666-672.
29. S. Maiti and P. Mal, *Synth. Commun.*, 2014, **44**, 3461-3469.
30. A. Bose and P. Mal, *Tetrahedron Lett.*, 2014, **55**, 2154-2156.

31. A. Stolle, T. Szuppa, S. E. S. Leonhardt and B. Ondruschka, *Chem. Soc. Rev.*, 2011, **40**, 2317-2329.
32. E. Rajanarendar, M. N. Reddy, K. R. Murthy, K. G. Reddy, S. Raju, M. Srinivas, B. Praveen and M. S. Rao, *Bioorg. Med. Chem. Lett.*, 2010, **20**, 6052-6055.
33. S. J. Stray, C. R. Bourne, S. Punna, W. G. Lewis, M. G. Finn and A. Zlotnick, *Proc. Natl. Acad. Sci. U. S. A.*, 2005, **102**, 8138-8143.
34. S. N. Mokale, S. S. Shinde, R. D. Elgire, J. N. Sangshetti and D. B. Shinde, *Bioorg. Med. Chem. Lett.*, 2010, **20**, 4424-4426.
35. O. Alam, S. A. Khan, N. Siddiqui, W. Ahsan, S. P. Verma and S. J. Gilani, *Eur. J. Med. Chem.*, 2010, **45**, 5113-5119.
36. J. Lloyd, H. J. Finlay, W. Vacarro, T. Hyunh, A. Kover, R. Bhandaru, L. Yan, K. Atwal, M. L. Conder, T. Jenkins-West, H. Shi, C. Huang, D. Li, H. Sun and P. Levesque, *Bioorg. Med. Chem. Lett.*, 2010, **20**, 1436-1439.
37. D. L. da Silva, F. S. Reis, D. R. Muniz, A. L. T. G. Ruiz, J. E. de Carvalho, A. A. Sabino, L. V. Modolo and Â. de Fátima, *Bioorg. Med. Chem.*, 2012, **20**, 2645-2650.
38. T. U. Mayer, T. M. Kapoor, S. J. Haggarty, R. W. King, S. L. Schreiber and T. J. Mitchison, *Science*, 1999, **286**, 971-974.
39. Z. Maliga, T. M. Kapoor and T. J. Mitchison, *Chem. Biol.*, 2002, **9**, 989-996.
40. U. Soumyanarayanan, V. Bhat, S. Kar and J. Mathew, *Org. Med. Chem. Lett.*, 2012, **2**, 23.
41. D. Russowsky, R. F. S. Canto, S. A. A. Sanches, M. G. M. D'Oca, Â. de Fátima, R. A. Pilli, L. K. Kohn, M. A. Antônio and J. E. de Carvalho, *Bioorg. Chem.*, 2006, **34**, 173-182.

42. H. Hussain, I. R. Green and I. Ahmed, *Chem. Rev.*, 2013, **113**, 3329-3371.
43. S. Adimurthy and P. U. Patoliya, *Synth. Commun.*, 2007, **37**, 1571-1577.
44. J.-C. Fan, Z.-C. Shang, J. Liang, X.-H. Liu and Y. Liu, *J. Phys. Org. Chem.*, 2008, **21**, 945-953.
45. V. V. Zhdankin, in *Hypervalent Iodine Chemistry*, John Wiley & Sons Ltd, 2013, pp. 145-336.
46. K. Moriyama, M. Takemura and H. Togo, *J. Org. Chem.*, 2014, **79**, 6094-6104.
47. J. Ribas-Arino and D. Marx, *Chem. Rev.*, 2012, **112**, 5412-5487.
48. J. Ribas-Arino, M. Shiga and D. Marx, *Angew. Chem. Int. Ed.*, 2009, **48**, 4190-4193.
49. J. Wang, T. B. Kouznetsova, Z. Niu, M. T. Ong, H. M. Klukovich, A. L. Rheingold, T. J. Martinez and S. L. Craig, *Nature Chem.*, 2015, **7**, 323-327.
50. C. O. Kappe, *J. Org. Chem.*, 1997, **62**, 7201-7204.
51. Q. Chen, L.-L. Jiang, C.-N. Chen and G.-F. Yang, *J. Heterocycl. Chem.*, 2009, **46**, 139-148.
52. R. W. Owen, A. Giacosa, W. E. Hull, R. Haubner, B. Spiegelhalder and H. Bartsch, *Eur. J. Cancer*, 2000, **36**, 1235-1247.
53. E. T. Denisov and I. V. Khudyakov, *Chem. Rev.*, 1987, **87**, 1313-1357.
54. X.-B. Wang, Q. Fu and J. Yang, *J. Phys. Chem. A*, 2010, **114**, 9083-9089.
55. M. Oliverio, P. Costanzo, M. Nardi, I. Rivalta and A. Procopio, *ACS Sustainable Chem. Eng.*, 2014, **2**, 1228-1233.
56. M. Ahmad, M. Afzal, S. Tabassum, B. Kalińska, J. Mrozinski and P. K. Bharadwaj, *Eur. J. Med. Chem.*, 2014, **74**, 683-693.
57. B. Halliwell, *Nutr. Rev.*, 1997, **55**, S44-S49.

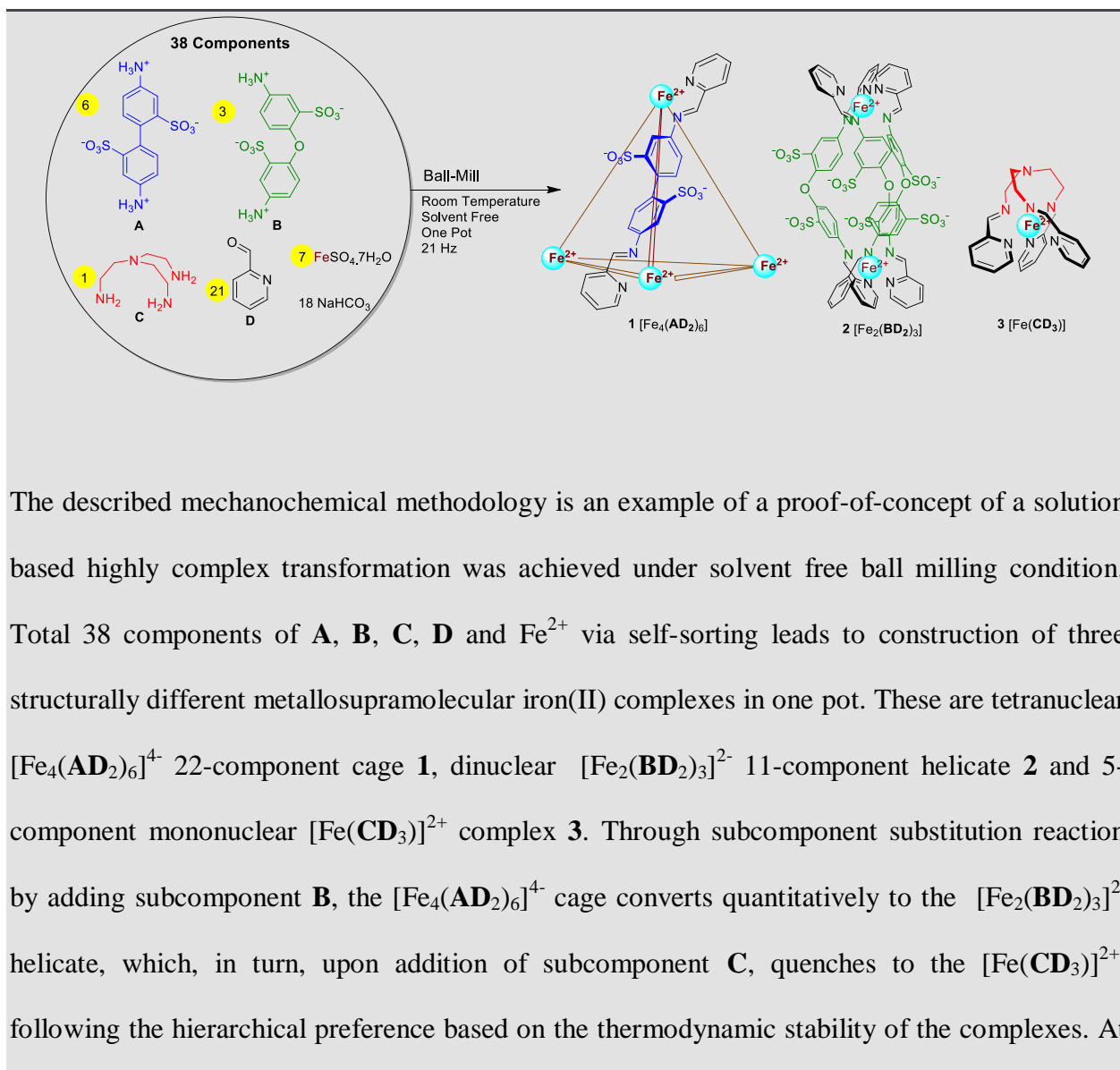
58. R. L. Prior, X. Wu and K. Schaich, *J. Agric. Food. Chem.*, 2005, **53**, 4290-4302.
59. C. Gorrini, I. S. Harris and T. W. Mak, *Nat. Rev. Drug. Discov.*, 2013, **12**, 931-947.
60. K. A. Conklin, *J. Nutr.*, 2004, **134**, 3201S-3204S.
61. M. F. Mccarty and F. Contreras, *Frontiers in Oncology*, 2014, **4**.
62. E. Rollet-Labelle, M.-J. Grange, C. Elbim, C. Marquetty, M.-A. Gougerot-Pocidallo and C. Pasquier, *Free Radical Biol. Med.*, 1998, **24**, 563-572.
63. W. Xu, L. Z. Liu, M. Loizidou, M. Ahmed and I. G. Charles, *Cell Res*, 2002, **12**, 311-320.
64. S. K. Choudhari, M. Chaudhary, S. Bagde, A. R. Gadbail and V. Joshi, *World J. Surg. Oncol.*, 2013, **11**, 118.
65. P. A. Wender, V. A. Verma, T. J. Paxton and T. H. Pillow, *Acc. Chem. Res.*, 2008, **41**, 40-49.
66. C. O. Kappe, *Eur. J. Med. Chem.*, 2000, **35**, 1043-1052.
67. M. Gartner, N. Sunder-Plassmann, J. Seiler, M. Utz, I. Vernos, T. Surrey and A. Giannis, *Chembiochem*, 2005, **6**, 1173-1177.
68. K. K. Pasunooti, H. Chai, C. N. Jensen, B. K. Gorityala, S. Wang and X.-W. Liu, *Tetrahedron Lett.*, 2011, **52**, 80-84.
69. S. D. Sharma, P. Gogoi and D. Konwar, *Green Chem.*, 2007, **9**, 153-157.
70. S. Chitra and K. Pandiarajan, *Tetrahedron Lett.*, 2009, **50**, 2222-2224.
71. A. J. McConnell, C. S. Wood, P. P. Neelakandan and J. R. Nitschke, *Chem. Rev.*, 2015, **115**, 7729-7793.
72. S. Putatunda, S. Chakraborty, S. Ghosh, P. Nandi, S. Chakraborty, P. C. Sen and A. Chakraborty, *Eur. J. Med. Chem.*, 2012, **54**, 223-231.

73. S. Besoluk, M. Kucukislamoglu, M. Nebioglu, M. Zengin and M. Arslan, *J. Iranian Chem. Soc.*, 2008, **5**, 62-66.
74. K. Singh, D. Arora, D. Falkowski, Q. Liu and R. S. Moreland, *Eur. J. Org. Chem.*, 2009, 3258-3264.
75. T. N. Glasnov, H. Tye and C. O. Kappe, *Tetrahedron*, 2008, **64**, 2035-2041.
76. L. M. Ramos, B. C. Guido, C. C. Nobrega, J. R. Corrêa, R. G. Silva, H. C. B. de Oliveira, A. F. Gomes, F. C. Gozzo and B. A. D. Neto, *Chem. Eur. J.*, 2013, **19**, 4156-4168.
77. X. Li, *Food Chem.*, 2013, **141**, 2083-2088.
78. X. Qiao, S. Chen, L. Tan, H. Zheng, Y. Ding and Z. Ping, *Magn. Reson. Chem.*, 2001, **39**, 207-211.
79. S. Maity, S. Chatterjee, P. S. Variyar, A. Sharma, S. Adhikari and S. Mazumder, *J. Agric. Food. Chem.*, 2013, **61**, 3443-3450.
80. X. Li, *J. Agric. Food. Chem.*, 2012, **60**, 6418-6424.
81. L. Ismaili, A. Nadaradjane, L. Nicod, C. Guyon, A. Xicluna, J. F. Robert and B. Refouvelet, *Eur. J. Med. Chem.*, 2008, **43**, 1270-1275.

CHAPTER 3

Mechanochemical Self-Sorting and Subcomponent Substitutions in Metallosupramolecular Complexes and its Application in CF₃I Encapsulation

3.1 ABASTRACT



ambient condition, complete encapsulation of active gaseous substrate trifluoroiodomethane (CF_3I) was observed by the metallo-organic supramolecular anionic cage $[\text{Fe}_4(\text{AD}_2)_6]^{4-}$ in water. The binding constant were calculated by relative comparison with benzene encapsulation.

3.2 INTRODUCTION

The metal ion assisted sub-component self-assembly¹⁻⁵ is an integral part of self-sorting reactions⁶⁻¹⁰ in which ligands of the metallo-supramolecular complexes are formed *in situ* from their sub-components. This concept has proved to offer a promising method for synthesis of high-purity products from complex mixtures of starting materials.¹¹⁻¹³ The metal-ion assisted subcomponent self-assembly of a rigid aromatic linear bis-amine, pyridine-2-carboxaldehyde and iron(II) resulting in tetrahedral M_4L_6 cage in water reported by Nitschke and us opened a new page on supramolecular tetrahedral complexes.¹⁴ Recently, by exploiting the same dynamic imine chemistry,¹⁵⁻¹⁷ we have used this concept to prepare the smallest possible tetrahedral M_4L_6 cage complex¹⁸ and for the anion-controlled formation of an aminated-(bis)imine Fe(II)-complex.¹⁹ In all the above mentioned cases the dynamic behavior of the imine bond is the key factor to control the self-assembly process.²⁰⁻²²

In last few years, mechanochemistry,²³⁻²⁸ as a solvent-free synthesis method, has drawn a great interest due to its advantages over traditional solution-based methods.²⁹ The core benefit of mechanochemistry is to avoid traditional workup.³⁰⁻³³ This advantage has huge implications to green processes, shown to be economical, time efficient and environment friendly. Quantitative conversion, less by products and no purification bring extra importance to this method. The mechanochemical synthesis of small organic molecules is well explored,³⁴ including also multi-step synthesis,^{32, 35} olefin metathesis³⁶ etc. Recently, James and coworkers have demonstrated the

synthesis of small mononuclear Zn^{II} , Cu^{II} and Ni^{II} salen/salophen complexes via subcomponent self-assembly both in liquid assisted grinding and solvent free condition.³⁷ The study of self-assembly,³⁸ system chemistry,³⁹ self-sorting or complex transformation⁴⁰ remains a poorly developed area of mechanochemistry.⁴¹ In solvent free condition maximum concentration putting the system under high stress and thus it never could be expected, that the specific self-assembly takes place in those extreme conditions.

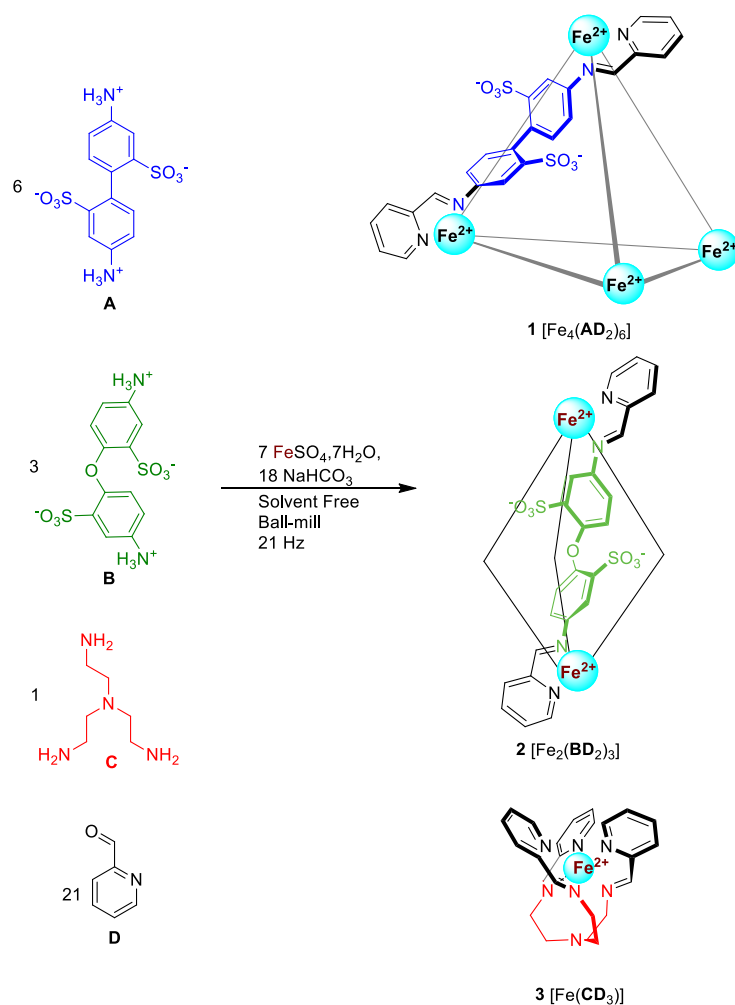


Figure 3.1. The one-pot solvent free synthesis of 22-component $[\text{Fe}_4(\text{AD}_2)_6]^{4+}$ **1**, 11-component $[\text{Fe}_2(\text{BD}_2)_3]^{2-}$ **2** and 5-component $[\text{Fe}(\text{CD}_3)]^{2+}$ **3**. A slight excess of 2-formylpyridine (**D**) was used (1.1 equivalent)

The recent development of fluorinated compounds in organic synthesis has drawn a significant interest due to its potential application in pharmaceutical and agrochemical industry.⁴²⁻⁴⁵ the fluorination of the organic compounds has been explored through trifluoromethylation using trifluoriodomethane (CF₃I).⁴⁶⁻⁴⁸ This gaseous substrate CF₃I is very much insoluble in most of the solvents. Thus, in practice, experimentation with CF₃I is not convenient. It is also difficult to control the gaseous CF₃I concentration, at varying temperature. Therefore, it is a challenging task to find a suitable media for storage and direct use of CF₃I. Recently, CF₃I was isolated as liquid after forming halogen bonded complex with tetramethylguanidine (TMG).⁴⁹ After which this complex was explored to demonstrate arene trifluoromethylation reaction.

Gas storage capacity by the Metal–organic frameworks (MOFs) and organic hosts molecules are well-known.⁵⁰⁻⁵⁷ The advancement towards gas absorption separation and their use in solid state are rapidly growing.^{58, 59} However, host- and gaseous-guest complexation studies by metallo-organic supramolecular complexes are relatively little done. Due to dynamic in nature, host-guest complexation studied can be easily monitored in solution for the metallo-supramolecular complexes, which is advantages compare to MOFs. Using metal-ion assisted sub-component self-assembly approach the synthesis of a tetrahedral **M₄L₆** cage in aqueous media has been reported by Nitschke and us.⁶⁰ Afterwards, the host-guest chemistry of the same tetrahedral cage was demonstrated by exploring its potential as a container molecule for white phosphorus.⁶¹ Recent research interest has grown to encapsulate Freon gases due to their green-house effect.^{62, 63} Surprisingly, encapsulation attempt has not done on active gaseous reagent (CF₃I), which is very similar to Freon.

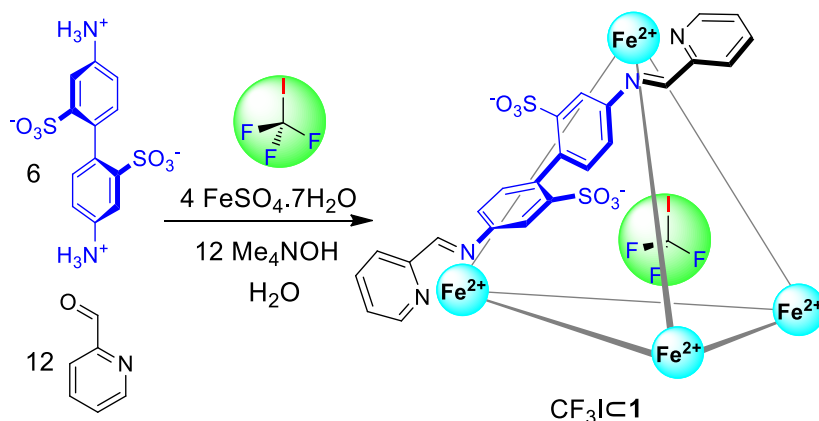


Figure 3.2. General Scheme for synthesis and encapsulation of CF_3I in water by the cage **1**

3.3 RESULT & DISCUSSION

Herein we demonstrate an unprecedented example, that mechanochemistry, under one-pot solvent free ball-milling conditions, offers a very efficient route to prepare three distinct, structurally different, water soluble metallosupramolecular iron complexes from their respective sub-components via self-sorting from 38 components. These metallosupramolecular complexes are a tetrahedral $[\text{Fe}_4(\text{AD}_2)_6]$ cage **1** (22 components), a dinuclear $[\text{Fe}_2(\text{BD}_2)_3]$ triple helicate **2** (11 components) and a mononuclear $[\text{Fe}(\text{CD}_3)]$ complex **3** (5 components) (Figure 3.1), where AD_2 , BD_2 and CD_3 are the *bis*-, *bis*- and *tris*-Schiff base ligands formed *in situ* during the one-pot reaction.

The one-pot solvent-free ball-milling reaction emulates the same solution reaction⁶⁴ where a mixture of six equivalents of 4,4'-diaminobiphenyl-2,2'-disulfonic acid **A**, three equivalents of 6,6'-oxybis(3-ammoniobenzenesulfonate) **B**, one equivalent of tris(2-aminoethyl)amine **C**, 21 equivalents of 2-formyl pyridine **D**, 18 equivalents of sodium bicarbonate, together with seven equivalents of iron(II) sulphate heptahydrate are mixed together, however here they were mechanically milled without any solvent in a ball-mill (21 Hz) resulting in the same three

metallo-supramolecular complexes **1**, **2** and **3** as in solution. Individually, under the same ball-milling conditions, the supramolecular complexes **1**, **2** and **3** were also produced from their respective sub-components, **A + D** for **1**, **B + D** for **2** and **C + D** for **3**.

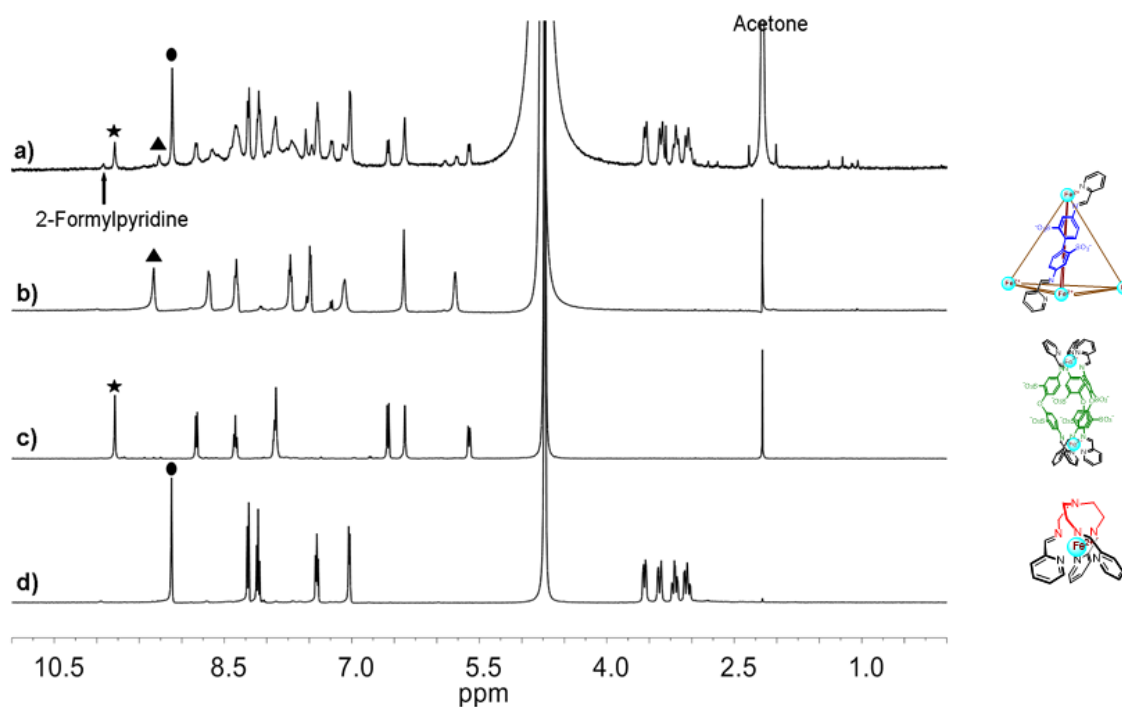


Figure 3.3. ^1H NMR spectra of the complexes obtained under solvent free ball milling condition a) **1**, **2** and **3** from the one-pot reaction; Individual reactions b) **1**, c) **2**, d) **3**.

The one-pot and individual reactions were performed under ambient conditions and monitored during the initial synthesis tests using ^1H NMR spectroscopy. During monitoring the ball-milling apparatus was stopped and a small portion of the sample was extracted from reaction chamber and the ^1H NMR spectrum recorded in D_2O . The final synthesis was done in a fixed time and the products were removed and placed on a paper filter and washed with a minimum quantity of acetone to remove the excess pyridine-2-aldehyde (1.1 equiv). The complexes were characterized and their purity verified comparing against the ^1H NMR spectra of a standard

sample of the same complexes synthesized in water. The cage **1** was originally synthesized in water in 20 h at 50 °C,⁶⁴ however, in here the solvent-free ball-milling reaction times are 2 h for **1**, 1 h for **2** and 0.5 h for **3**, respectively. The one-pot synthesis of **1**, **2** and **3** took 2 h.

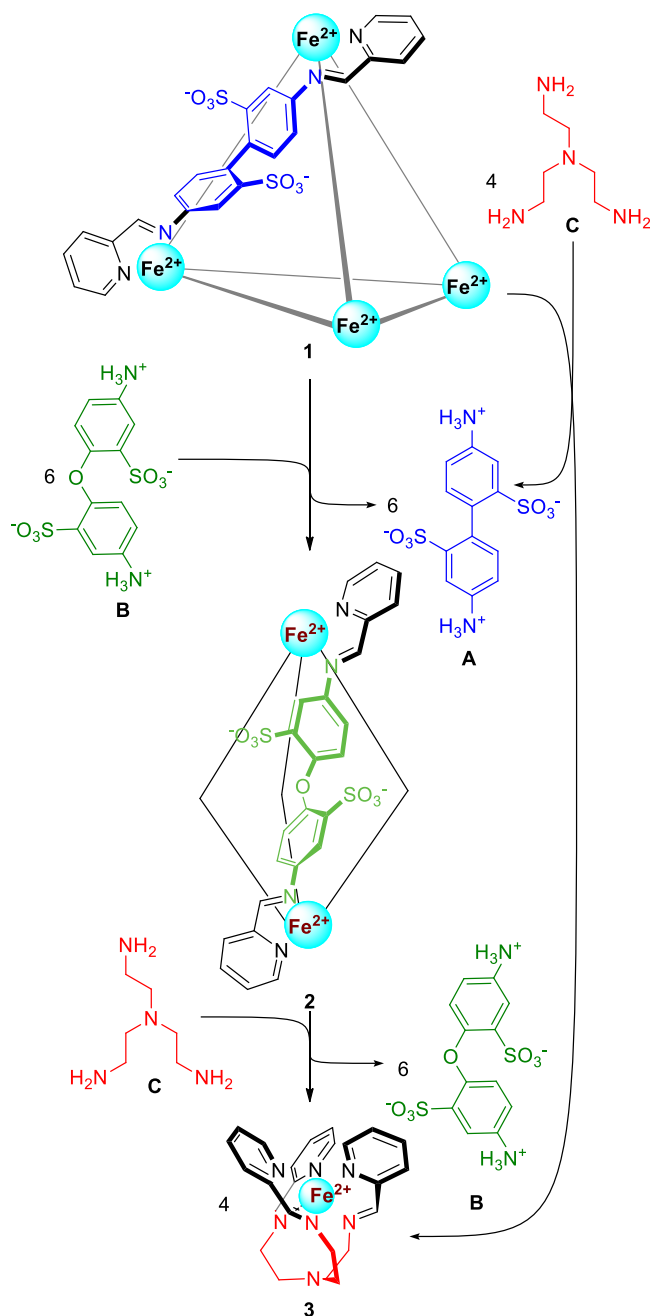


Figure 3.4. The solvent free post-assembly transformation (substitution) reaction^{65, 66} of **1** and **2** leading to **3**.

Previous studies in solution⁶⁴ have established that complexes **1**, **2** and **3** can undergo transformation to thermodynamically more stable structure upon appropriate subcomponent substitution reaction. The role of the solvent has been considered to be crucial within the transformation from thermodynamically less stable complex to the thermodynamically more stable complex, like **1**→**2**. However, under solvent-free conditions, due to restrictions of the molecular movements, the concept of dynamic chemistry has not been explored or defined. However it has been anticipated that under ball-milling conditions the products formed are thermodynamically controlled.

The well-defined differences in the thermodynamical stability of **1**, **2** and **3** enables post-assembly transformation (substitution)⁴⁰ chemistry to progress in a predictable, hierarchical path also under solvent-free ball-milling conditions. The addition of the tris-amine sub-component **C** to either **1** or **2** under ball-milling conditions yielded **3**, with ejection of diamine sub-components **A** or **B**, respectively. Similarly adding **B** into **1** resulted in **2**, which could then sub-sequentially be transformed into **3** upon addition of **C** (Figure 3.4).

Our focus on the competition among the iron complexes includes the flexibility/rigidity of their backbones and the entropy associated with degrees of freedom of mono-, di- and tetra- iron (II) complexes. The geometries of **1**, **2** and **3** derive from the flexibilities of their respective amine subcomponents: To maximize entropy, each imine ligand will generate the smallest self-assembled structure possible in which all iron(II) ions are hexa-coordinate and all imine nitrogen atoms are coordinated to iron(II). As can be seen from the structural analysis of the iron complexes, the number of building blocks presents in the systems are 22, 11 and 5 for **1**, **2** and **3**, respectively. Therefore the relative thermodynamic stability of the complexes could be as follows, $\mathbf{3} > \mathbf{2} > \mathbf{1}$. Thus the experimental outcome shown in Figure 3.4 may be justified.

Many self-sorting methodologies^{8, 12, 67} are known in ‘systems biology’.⁶⁸ However, the study of ‘systems chemistry’^{13, 69, 70} provides primary insights into the self-sorting principles⁷¹ of molecular networks which ultimately assist us to acquire new systems⁷² with properties and functions unlike any conventional materials.^{73, 74} In other words, dynamic self-sorting approach can enable an easy access to certain materials of interests by changing inputs in either sub- or multi-component systems.⁷⁵⁻⁷⁷ To the best of our knowledge, this is the first example of a sub-component self-assembly under solvent free condition in which both cationic (**1** and **2**) and anionic (**3**) complexes were generated together.

The reversible trapping of active hydrophobic CF₃I within the central cavity of a self-assembled metallo-supramolecular complex in water by exploring purely hydrophobic effect. We believe that the present system may be an unprecedented example of 100% encapsulation of a gaseous guest into the cage **1**. Further, storage and controlled release of the CF₃I molecule could be possible in water.

The iron(II) centers are located at the vertices of the tetrahedron and the bis-imine-ligands connecting them through six edges. The presence of twelve sulfonate groups (two from each ligand), at the exterior of the cage, was responsible for good water solubility (34 g/L). However, the aromatic rings provide a hydrophobic cavity. From the X-ray data, the average Fe–Fe separation is found to be 12.9 Å which make the cavity volume available 141 Å³ for guest encapsulation. Therefore, the encapsulation of suitable guests are done due to hydrophobic effects by following Rebek’s 40% rule, which is optimal for a gas binding by organic host.⁷⁸ SF₆ occupied 53% void of the cage during the encapsulation.⁷⁹

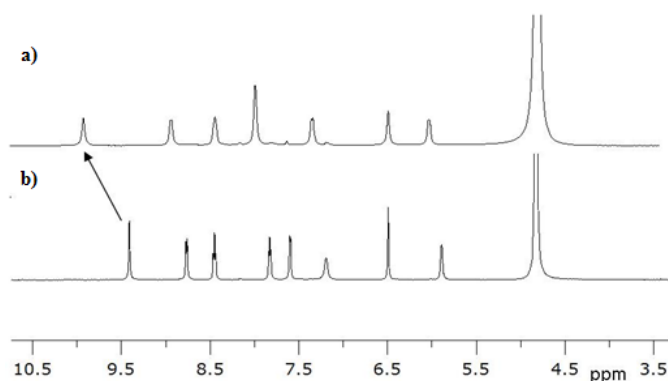


Figure 3.5. Selective region of the ^1H NMR spectrum in D_2O a) $\text{CF}_3\text{I}@1$ and b) **1**.

CF_3I is a colorless, odorless gas and water solubility of CF_3I is estimated to be $3.36 \times 10^{-2} \text{ M}^{-1}$ at 25°C . Slow bubbling of CF_3I through a solution of **1** in D_2O resulted in the formation of $\text{CF}_3\text{I}@1$ as observed by the analysis of ^1H NMR (Fig. 3.5). The aromatic protons of $[\text{CF}_3\text{I}@1]$ displayed a significant downfield shift relative to those observed in the spectrum of guest-free **1** (Fig. 3.5a and 3.5b). The ^1H NMR spectrum indicated complete ($\sim 100\%$) encapsulation of CF_3I onto the cage **1** in water. Signals corresponding to both encapsulated and free CF_3I were observed in the ^{19}F NMR spectrum as well (Fig. 3.6a), confirming the encapsulation. We have observed a downfield shift in ^{19}F NMR spectrum as well in water.

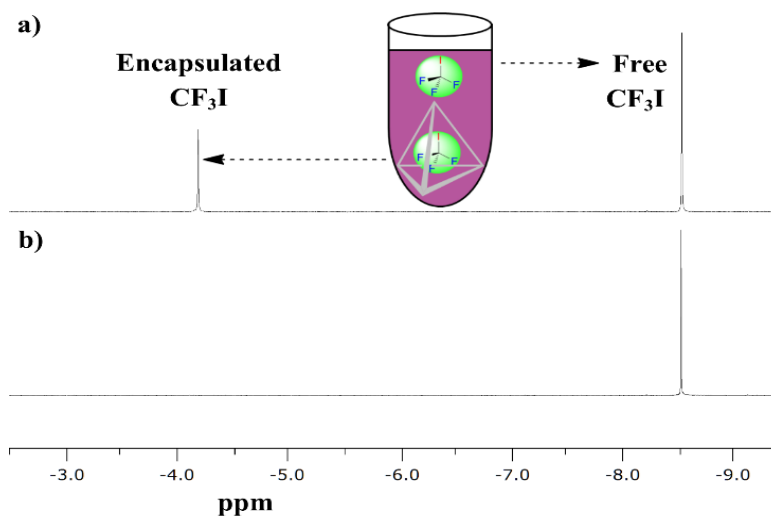


Figure 3.6. a) ^{19}F NMR of $\text{CF}_3\text{I}@1$; b) CF_3I in water.

The gas encapsulation studies by M_4L_6 cage **1** has been achieved up to 24% for Xenon⁸⁰ and 75% for SF₆.⁷⁹ The green-house gas SF₆ occupies 53% of the cavity volume (141 Å³) which is greater than the optimal value (40%) for Host-Guest encapsulation by a gas molecule.⁷⁸ However, Xenon with smaller volume (30% occupancy) even makes it difficult to bind with the cage **1**. Thus, the binding constant of Xenon is much smaller (16 mol⁻¹) compare to SF₆ (1.3 × 10⁴ M⁻¹).

Binding constant determination by direct use of ¹H NMR spectroscopy could not be possible due to the following reasons: solubility of CF₃I in water varies with temperature, concentration of host-molecule and equilibrium vapour pressure of the CF₃I-cage-aqueous solution. Raymond and co-workers have developed a successful competitive binding experiments method to overcome similar problem.⁸¹ Later Nitschke group have applied this method successfully to determine the thermodynamic as well as kinetic binding constant of a series of guests.⁸² Herein, in order to determine the binding constant following steps were followed:

- Solubility of CF₃I in water was estimated.(Experimental Section)
- 100% encapsulation of CF₃I was made with cage **1**
- The saturated solution of both benzene (HG_{benzene}) and CF₃I (HG_{CF3I}) were prepared in presence of cage **1**
- Equilibrium between the two host-guest adducts HG_{benzene} and HG_{CF3I} was established: HG_{benzene} + G_{CF3I} ⇌ HG_{CF3I} + G_{benzene}

- However, when the aqueous solution was saturated with these guests, because of their strong binding, no empty host was observed by NMR spectroscopy. For this equilibrium, the corresponding equilibrium constant (K_{rel}) is given by

$$K_{rel} = \frac{[HG]_{CF_3I}}{[HG]_{Benzene}} \times \frac{[G]_{Benzene}}{[G]_{CF_3I}}$$

$$= \frac{[HG]_{CF_3I}}{[HG]_{Benzene}} \times \frac{S_{Max}(Benzene)}{S_{Max}(CF_3I)} = \frac{K_{CF_3I}}{K_{Benzene}}$$

- Following equilibration, integration of the 1H NMR signals provided the $HG_{CF_3I}/HG_{benzene}$ ratio. Figure 3.7 shows the 1H NMR spectrum of host **1** in an aqueous solution saturated with benzene and trifluoroiodomethane. Two sets of resonances can be discerned, one for the benzene \subset **1** complex and the other for trifluoroiodomethane \subset **1**. The ratio of these two species, after correction for the water solubility of the respective guests, provides K_{rel} , which is the ratio of the binding constants of the two guests. The binding constant for the trifluoroiodomethane guest, K_{a,CF_3I} , was calculated from K_{rel} and $K_{a,benzene}$, since the binding constant of guest (benzene) is known. Using the three methods outlined above, we were able to determine the values of K_a for the trifluoroiodomethane guest. The binding constant of CF_3I is K_{CF_3I}

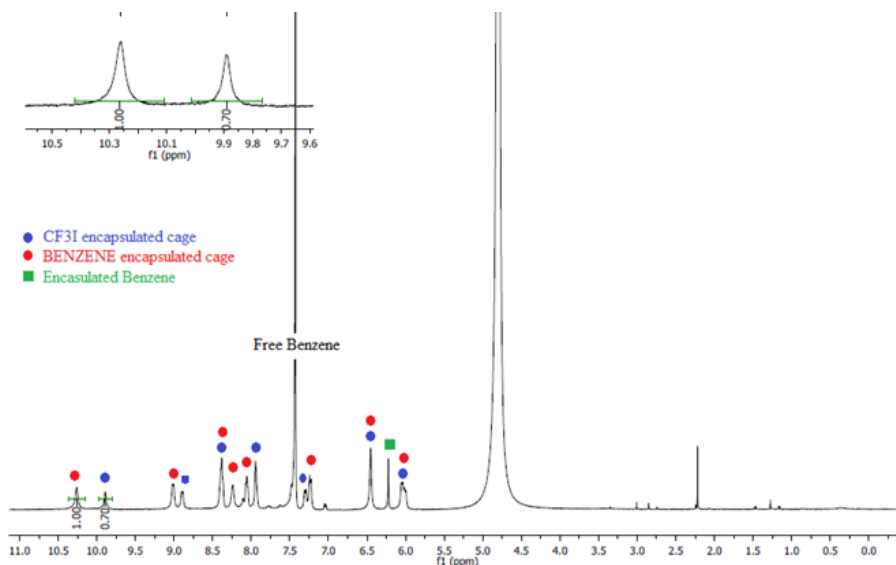


Figure 3.7. ^1H NMR of trifluoroiodomethane \subset 1 and benzene \subset 1, an equilibrium mixture of both.

$$K_{CF_3I} = K_{Benzene} \times \frac{[HG]_{CF_3I}}{[HG]_{Benzene}} \times \frac{S_{Max}(Benzene)}{S_{Max}(CF_3I)}$$

$$= 3 \times 10^3 \times 41 / 59 \times 2.29 \times 10^{-2} / 3.36 \times 10^{-2} = 1.42 \times 10^3$$

3.4 CONCLUSION

In conclusion, an unprecedented example of self-sorting of three distinct iron(II) complexes under solvent free mechano milling condition has been demonstrated. These three distinct structures were obtained from 38 subcomponents in one-pot at room temperature. However, the complexes were switchable to more stable systems upon subcomponent substitution under solvent free condition. We anticipate that the described mechanochemical methodology can be rationalized as a proof-of-concept of system chemistry under solvent free condition. We have also shown that the complete encapsulation of CF_3I in the suitable iron cage molecule. The binding of sparingly water soluble CF_3I to the cage molecule is due to hydrophobic effect (binding constant $1.42 \times 10^3 \text{ M}^{-1}$). Thus, CF_3I can be made water-soluble. Recently, under the area of

mechanochemistry, the solid-state reaction or solvent free synthesis is growing rapidly.⁸³

⁸⁴ We have found out that CF₃I can also be stored in the solid-state and we are currently exploring the possible trifluoromethylation reactions in the solid state by using caged-CF₃I.

3.5 EXPERIMENTAL SECTION

General Methods. The mechano-milling (21 Hz) experiments were executed under open atmosphere and at room temperature (27 °C) in a ball milling instrument. The NMR spectra were recorded on 400 MHz instrument at 27 °C and D₂O was used as solvent until and unless specified.

Procedure for the synthesis of iron(II) tetranuclear cage 1¹⁴ under mechano-milling. 4,4'-Diaminobiphenyl-2,2'-disulfonic acid (purity 70%, balance water, 100 mg, 0.20 mmol), 2-formylpyridine (43.5 mg, 0.40 mmol), sodium bicarbonate (33.6 mg, 0.40 mmol), and iron(II) sulfate heptahydrate (37.6 mg, 0.14 mmol) were added to a 10 mL Teflon jar. It was tightly capped and milling operation (21 Hz) was started and continued for 2 h. After which purple colored solid mass was dissolved in D₂O and NMR spectra were recorded. ¹H NMR (400 MHz, 300 K, D₂O): δ = 9.34 (s, 12H, imine), 8.71 (d, *J* = 7.6 Hz, 12H, 3-pyridine), 8.41 (t, *J* = 7.6 Hz, 12H, 4-pyridine), 7.78 (t, *J* = 6.4 Hz, 12H, 5-pyridine), 7.54 (d, *J* = 5.0 Hz, 12H, 6-pyridine), 7.14 (d, *J* = 6.8 Hz, 12H, 6,6'-benzidine), 6.45 (s, 12H, 3,3'-benzidine), 5.85 (d, *J* = 6.4 Hz, 12H, 5,5'-benzidine); ¹³C NMR (100 MHz, 300 K, D₂O): δ = 176.1, 157.9, 155.8, 150.2, 143.2, 139.8, 136.0, 132.2, 132.0, 130.0, 121.8, 120.9 ppm.

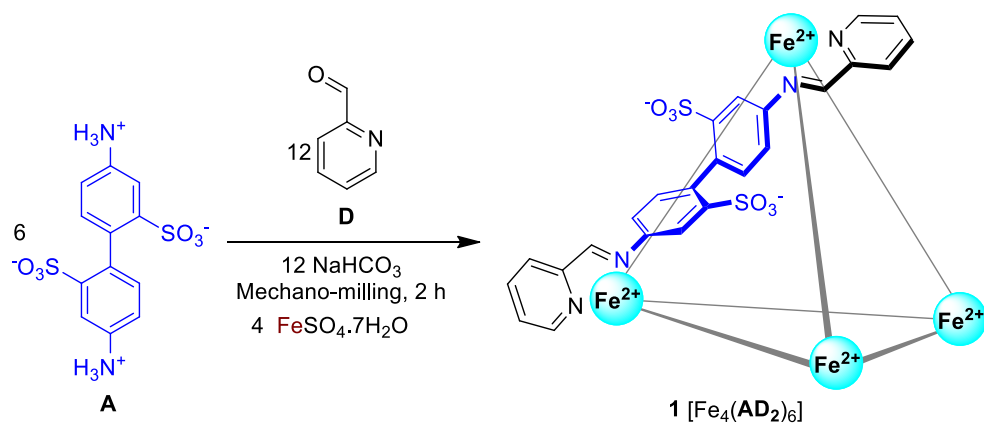


Figure 3.8. Preparation of complex **1** under mechano-milling.

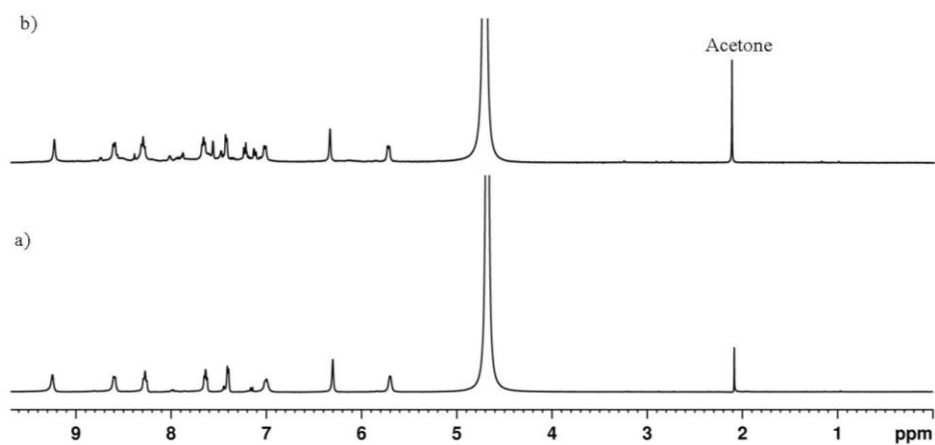


Figure 3.9. ¹H NMR of cage **1** synthesized under solvent free mechano milling; a) recrystallized from water; b) crude material was washed with acetone only in D₂O.

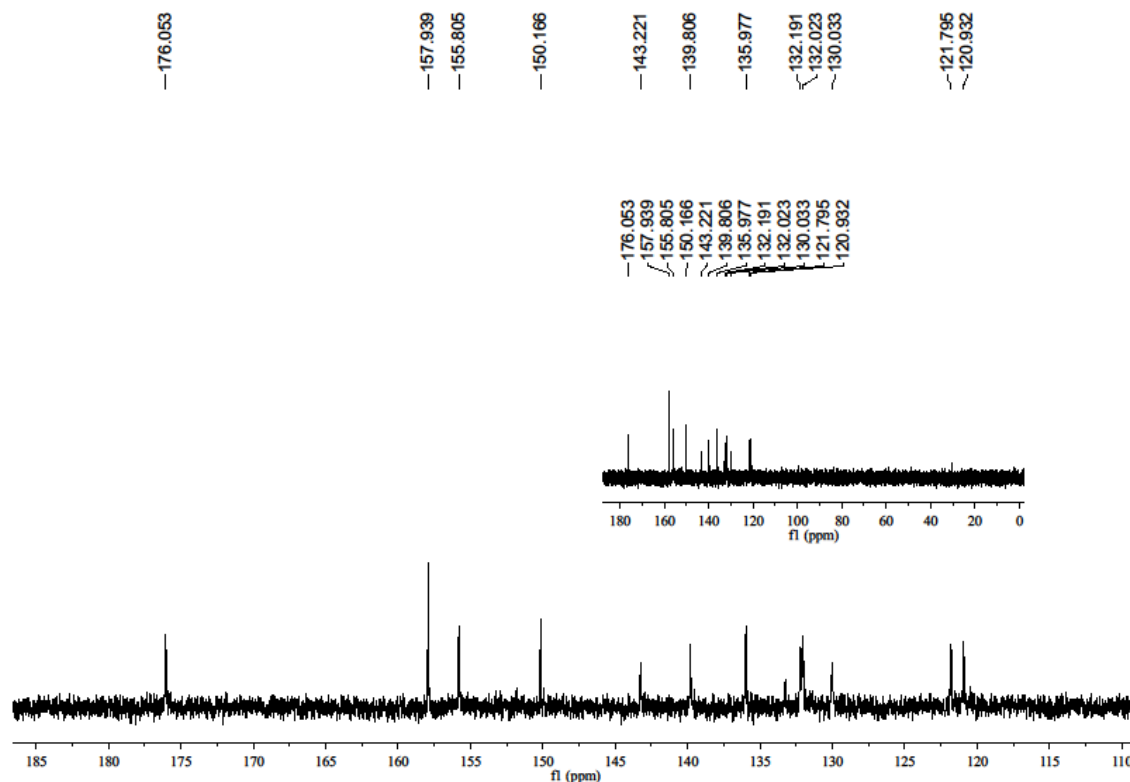


Figure 3.10. ^{13}C NMR of cage 1 synthesized in solid state by mechano-milling in D_2O .

Procedure for the synthesis of iron(II) dinuclear helicate 2^{64} under mechano-milling. 4,4'-diaminobiphenyl ether-2,2'-disulfonic acid B (450 mg, purity 70% and balance water, 1.0 mmol), 2-formylpyridine D (214 mg, 2.0 mmol), sodium bicarbonate (168 mg, 2.0 mmol), and iron(II) sulfate heptahydrate (186 mg, 0.67 mmol) were added to a 10 mL of a Teflon jar. It was tightly capped and milling operation (21 Hz) was started and continued for 1 h. After that the purple colored solid mass was dissolved in D_2O and NMR spectra were recorded.; ^1H NMR (400 MHz, 300 K, D_2O): δ = 9.86 (s, 6 H, imine), 8.90 (d, J = 7.6 Hz, 6 H, 3- pyridine), 8.46 (t, J = 7.6 Hz, 6 H, 4-pyridine), 7.98-7.96 (m, 12 H, 4-, 5-pyridine), 6.65 (d, J = 8.8 Hz, 6 H, 6,6'-benzidine), 6.45 (d, J = 1.6 Hz, 6 H, 3,3'-benzidine), 5.69 (dd, J = 6.8, 1.6 Hz, 6 H, 5,5'-benzidine); ^{13}C NMR (125 MHz, 300 K, D_2O): δ = 174.5, 156.7, 156.3, 155.4, 147.3, 140.2, 134.8, 133.1, 132.0, 126.0, 123.0, 122.7.

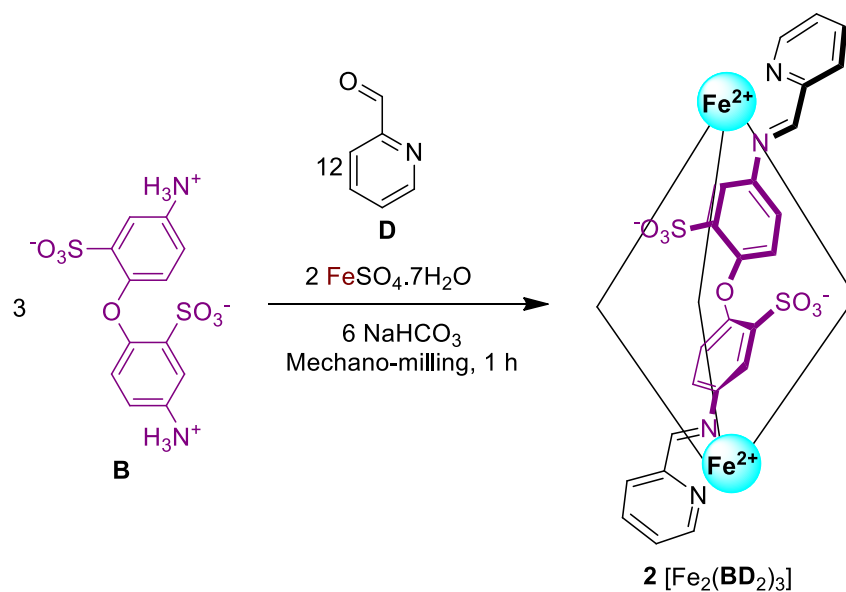


Figure 3.11. Preparation of complex dinuclear iron(II) helicate **2** under solvent free condition.

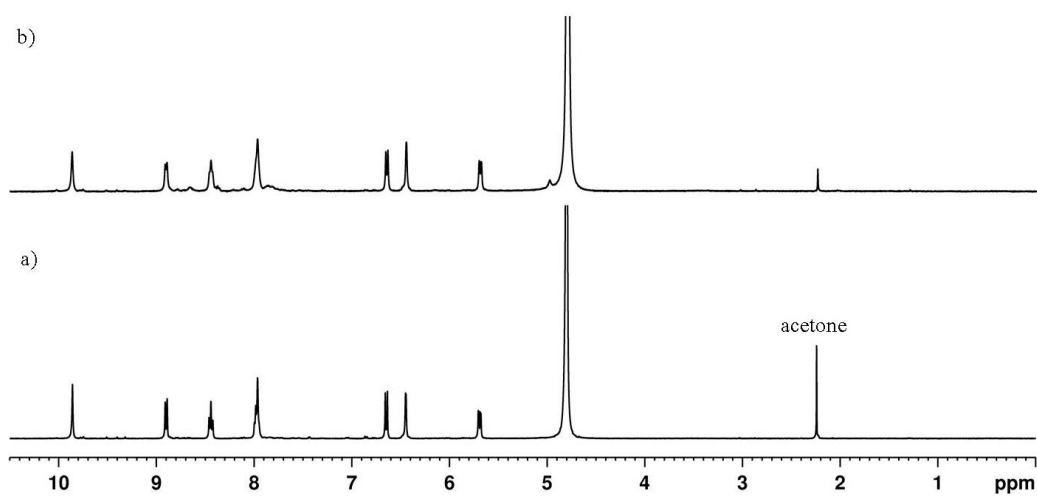


Figure 3.12. ^1H NMR (in D_2O) spectrum of helicate **2** synthesized under mechano-milling a) recrystallized from water; b) crude material was washed with acetone.

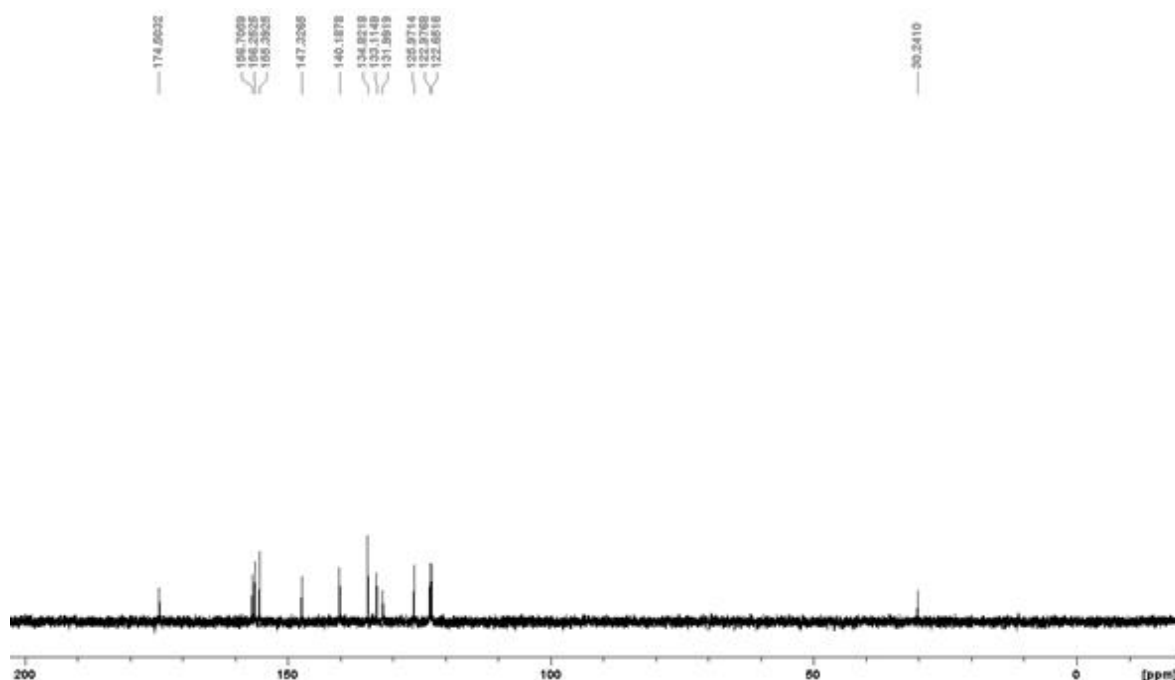


Figure 3.13. ^{13}C NMR spectrum (in D_2O) of helicate **2** synthesized in under mechano-milling.

Procedure for the synthesis of iron(II) mononuclear complex 1^{85} under mechano-milling.

Tris(2-aminoethyl)amine (26.0 mg, 0.18 mmol), pyridine-2-carbaldehyde (58 mg, 0.54 mmol), and iron(II) sulfate heptahydrate (50 mg, 0.18 mmol) were added to a 10 mL of a Teflon jar. It was tightly capped and milling operation (21 Hz) was started and continued for 30 min. ^1H NMR was recorded in D_2O ; ^1H NMR (400 MHz, 300 K, D_2O): δ = 9.19 (s, 3 H, imine), 8.29 (d, J = 7.7 Hz, 3 H, 3- pyridine), 8.17 (t, J = 7.7 Hz, 3 H, 4-pyridine), 7.48 (t, J = 6.5, 3 H, 5-pyridine), 7.10 (d, J = 5.0 Hz, 3 H, 6-pyridine), 3.63 (dd, J = 11.4, 2.5 Hz, 3 H, $-\text{CH}_2-$), 3.45 (dd, J = 14.7, 2.48 Hz, 3 H, $-\text{CH}_2-$), 3.27 (dt, J = 3.3, 11.9 Hz, 3 H, $-\text{CH}_2-$) 3.13 (dt, J = 3.3, 13.4 Hz, 3 H, $-\text{CH}_2-$); ^{13}C NMR (100 MHz, 300 K, D_2O): δ = 171.0, 157.1, 153.4, 138.0, 127.9, 127.5, 58.4, 53.2.

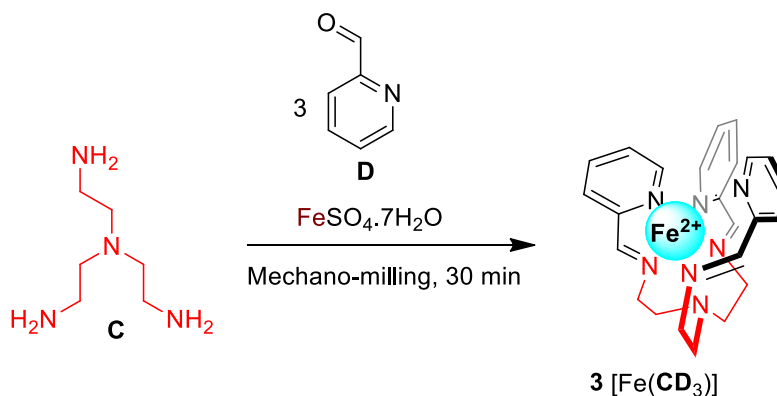


Figure 3.14. Preparation of mononuclear iron(II) complex **3**.

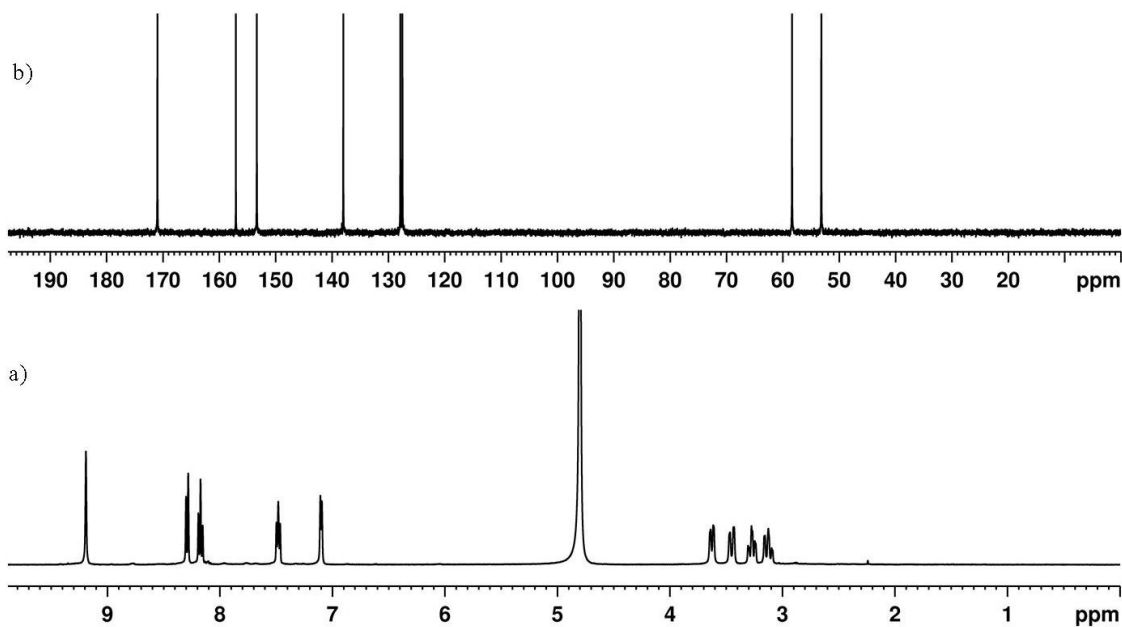


Figure 3.15. a) ^1H NMR spectrum of mononuclear **3** synthesized under mechano-milling; b) ^{13}C NMR of **3** in D_2O .

Simultaneous one pot synthesis of all complexes 1, 2 and 3.⁶⁴ Tris(2-ethylamino)amine **A** (1.46 mg, 10.0 μmol), 4,4'-diaminobiphenylether-2,2'-disulfonic acid **B** (4.5 mg, 80% balance water, 6.6 μmol), 4,4'-diaminobiphenyl-2,2'-disulfonic acid **C** (4.6 mg, assumed 75%, 6.6 μmol), sodium bicarbonate (5.0 mg, 60 μmol), $\text{FeSO}_4 \cdot 7\text{H}_2\text{O}$ (6.5 mg, 23.3 μmol) and 2-formyl

pyridine (6.7 μL , 70 μmol) were added to a 10 mL of a Teflon jar. It was tightly capped and milling operation (21 Hz) was started and continued for 30 min. ^1H NMR was recorded in D_2O (Figure 3.16).

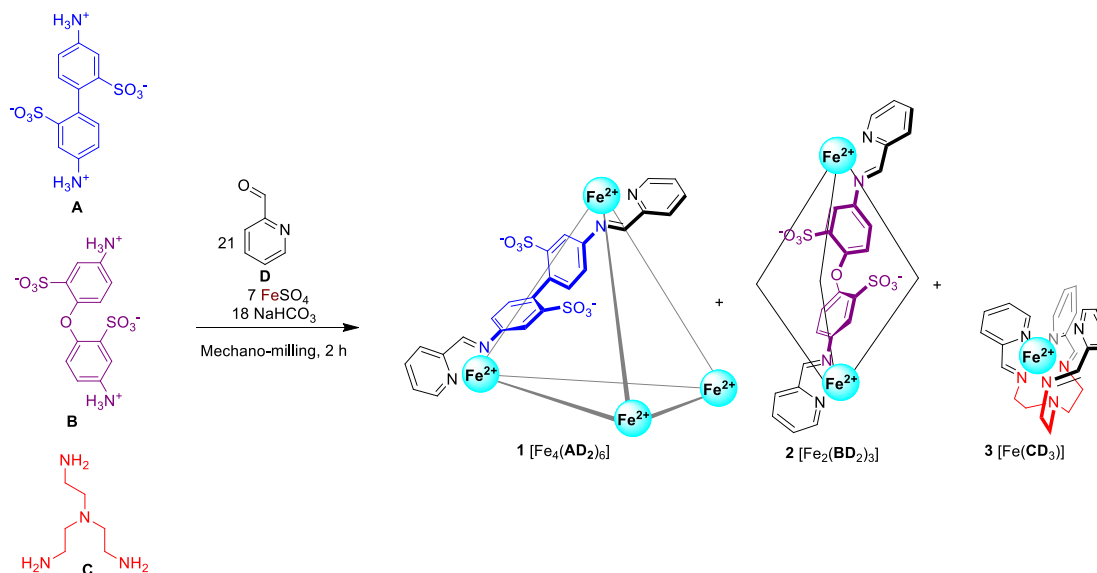


Figure 3.16. One pot mechanochemical synthesis of the complexes **1**, **2** and **3**.

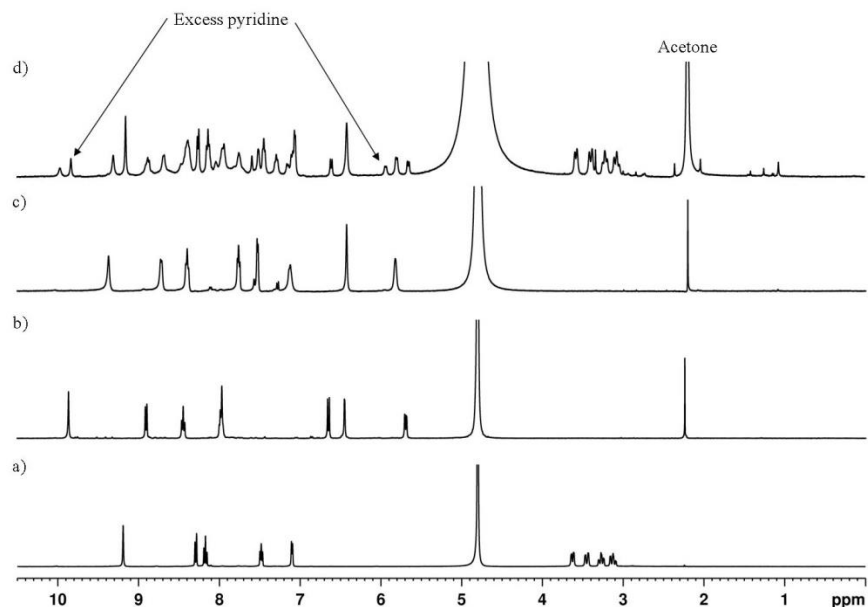


Figure 3.17. ^1H NMR of iron complex of a) mononuclear complex **3** b) dinuclear helicate **2** c) tetranuclear cage **1** d) complexes **1**, **2** and **3** synthesized together under mechano-milling condition.

Transformation of 1 into 2 upon substitution with B. **1** (4.0 mg, 0.94 μmol), 4,4'-diaminobiphenyl ether-2,2'-disulfonate **B** (4.0 mg, 80%, balance water, 8.9 μmol) and NaHCO_3 (1.5 mg, 17.9 μmol) were added to a 10 mL of a Teflon jar. After that the milling operation was continued for 2 h. ^1H NMR was recorded for the reaction mixture and the appearance was noted of ^1H resonances corresponding to **2**, free 4,4'-diaminobiphenyl-2,2'-disulfonic acid (**A**).

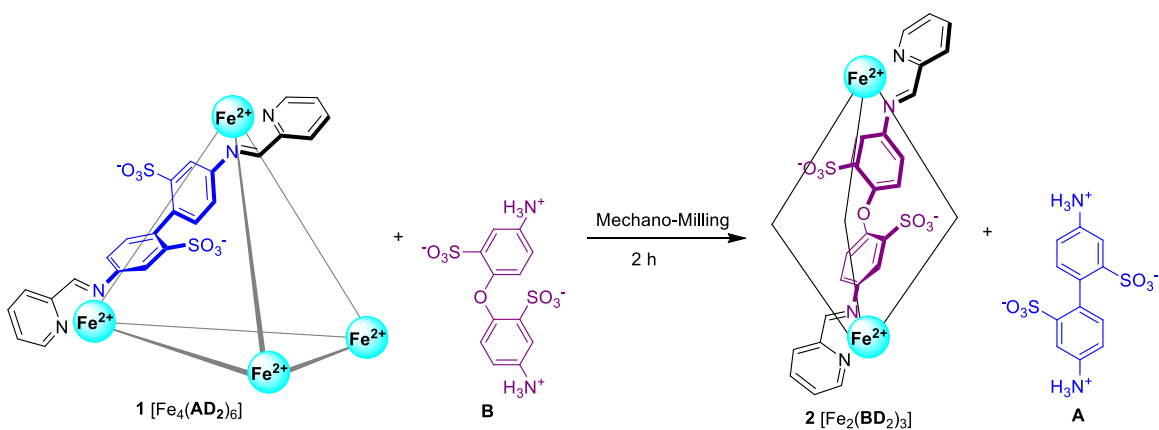


Figure 3.18. Solvent free transformation of tetranuclear cage **1** to dinuclear helicate **2**.

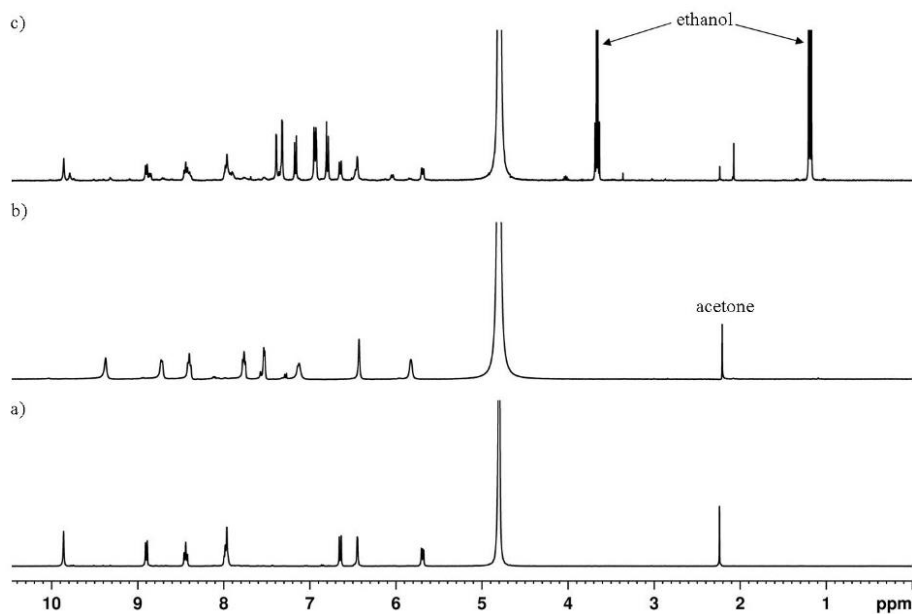


Figure 3.19. ^1H NMR spectra of a) dinuclear helicate; **2** b) tetranuclear cage **1**; c) reaction mixture for the transformation of tetranuclear cage **1** to dinuclear helicate **2**.

Conversion of 1 into 3 by reaction with C. **1** (4.0 mg, 0.94 μmol), and tris(2-ethylamino)amine **C** (0.86 mg, 5.8 μmol) and 15 mg of silica gel (column chromatography grade, 100-200 mesh, to avoid stickiness at the milling ball) were added into a 10 mL of a Teflon jar. Milling operation was started and continued for 1 h. Afterwards, all the crude materials were dissolved in D_2O , filtered and ^1H NMR spectra was recorded. The appearance was noted of ^1H resonances corresponding to **3**, free 4,4'-diaminobiphenyl-2,2'-disulfonic acid (**A**).

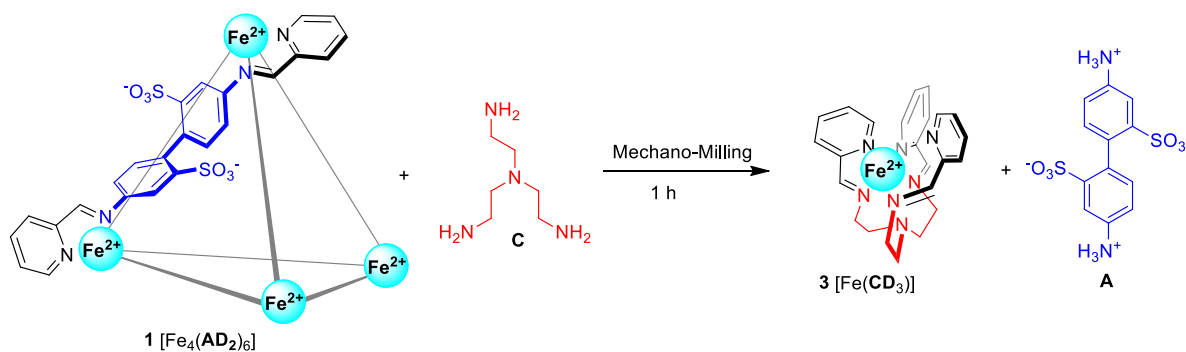


Figure 3.20. Solvent free synthesis of dinuclear helicate **2** from tetranuclear cage **1**.

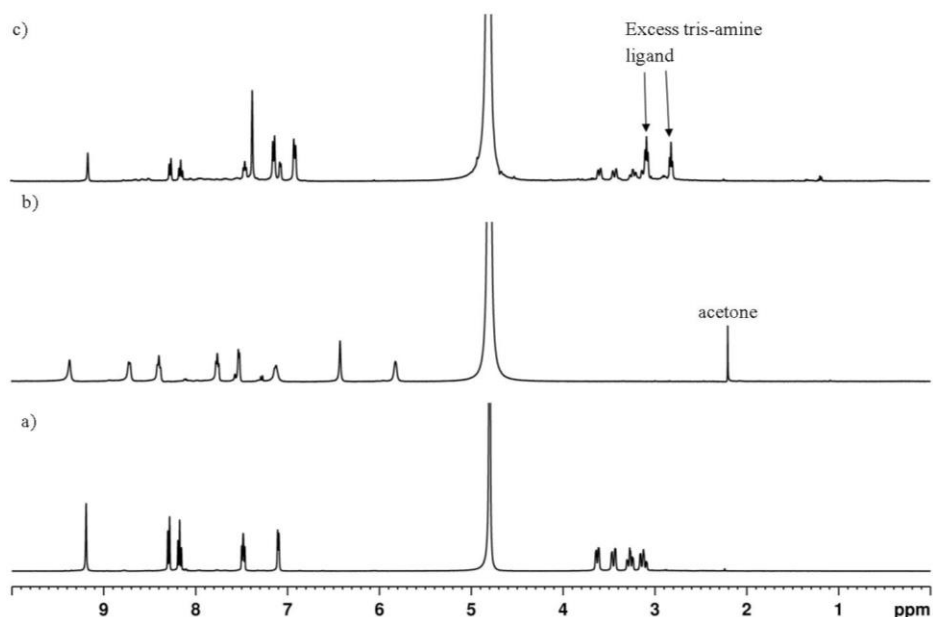


Figure 3.21. ^1H NMR spectra of a) mononuclear complex **3** b) tetranuclear cage **1** c) reaction mixture for the transformation of **3** to **2**.

Conversion of 2 into 3 by reaction with C. **2** (4.0 mg, 2.2 μmol), and tris(2-ethylamino)amine **C** (0.86 mg, 5.8 μmol) and 15 mg of silica gel were added to a 10 mL of a Teflon jar. Milling operation was started and continued for 1 h. Afterwards, all the crude materials were dissolved in D_2O , filtered and ^1H NMR spectra was recorded. The appearance was noted of ^1H resonances corresponding to **3**, free 4,4'-diaminobiphenyl ether-2,2'-disulfonate (**B**).

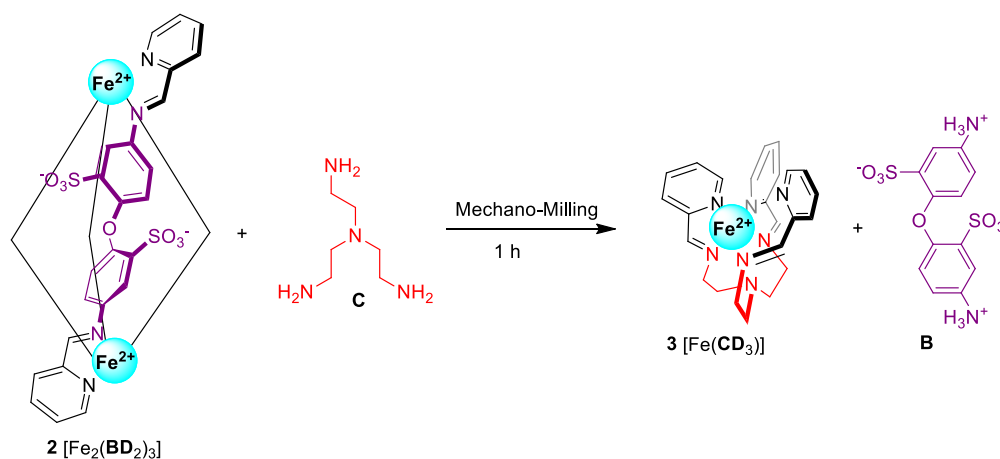


Figure 3.22. From dinuclear helicite **2** to mononuclear complex **3** under solvent free condition.

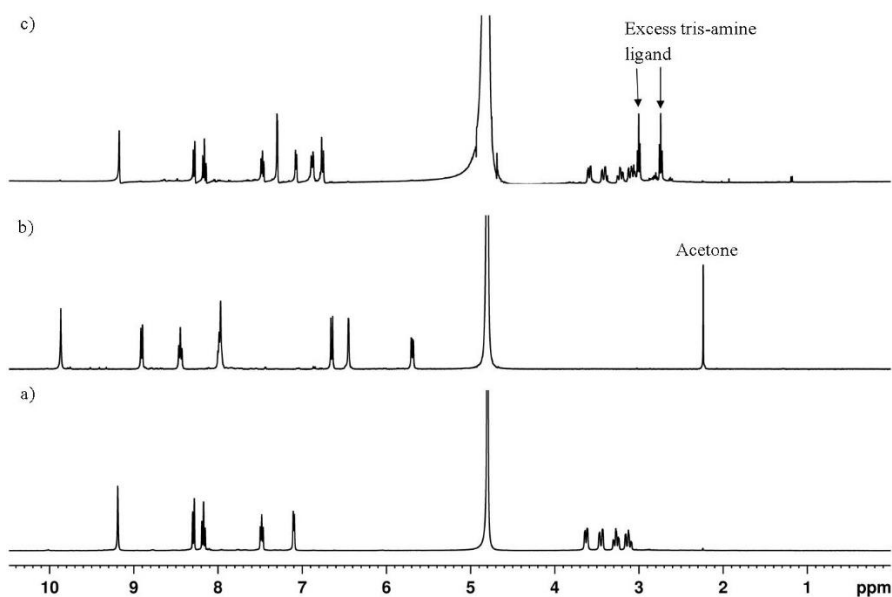


Figure 3.23. ^1H NMR spectra of a) mononuclear complex **3**; b) dinuclear helicite **2**; c) reaction mixture after the transformation from **2** to **3**.

General Methods. CF₃I was purchased from Sigma-Aldrich and used without further purification. NMR solvents were purchased from Fluorochem. ¹H and ¹⁹F NMR spectra were recorded on a Bruker 400 MHz spectrometer. ¹³C NMR spectra were recorded by using ^tBuOH as reference. Chemical shifts are reported in parts per million (ppm).

Preparation of CF₃I⋅1** complex.**

Cage **1** (4.0 mg, 0.75 μmol) was loaded into a J-Young NMR tube, then D₂O (0.5 mL) was added and CF₃I was bubbled through the solution for fifteen minutes, the tube was then sealed under an atmosphere of CF₃I. ¹H NMR was recorded. One new set of signal was formed due to complete incorporation of CF₃I into **1**, leading to complete formation of CF₃I⋅**1**. CF₃I⋅**1**. ¹H NMR (400 MHz, 300 K, D₂O) δ = 9.85 (s, 12 H, imine), 8.87 (d, 12 H, 3- pyridine), 8.39 (t, 12 H, 4-pyridine), 7.94 (t, 12 H 6,6'-benzidine, m, 12 H, 5-pyridine), 7.31 (d, 12 H, 6-pyridine), 6.46 (s, 12 H, 3,3'-benzidine), 6.01 (d, 12 H, 5,5'-benzidine), 2.23 (s, acetone) ppm; ¹³C NMR (125 MHz, 300 K, D₂O, referenced to 2-methyl- 2-propanol at 30.29 ppm as internal standard): δ = 215.5 (carbonyl of acetone), 174.7, 157.0, 156.1, 151.6, 142.8, 140.0, 136.1, 133.5, 133.2, 131.8, 122.8, 121.1, 69.8 (C-OH: 2-methyl-2-propanol), 53.9 (dichloromrthane, dissolved in water), 30.3 (methyls of 2-methyl-2-propanol), 29.6 (methyls of acetone) ppm. ¹⁹F NMR (376 MHz; 300 K; D₂O) δ -4.19 (1F, s, CF₃I_{bound}), -8.54 (1F, s, CF₃I_{free}).

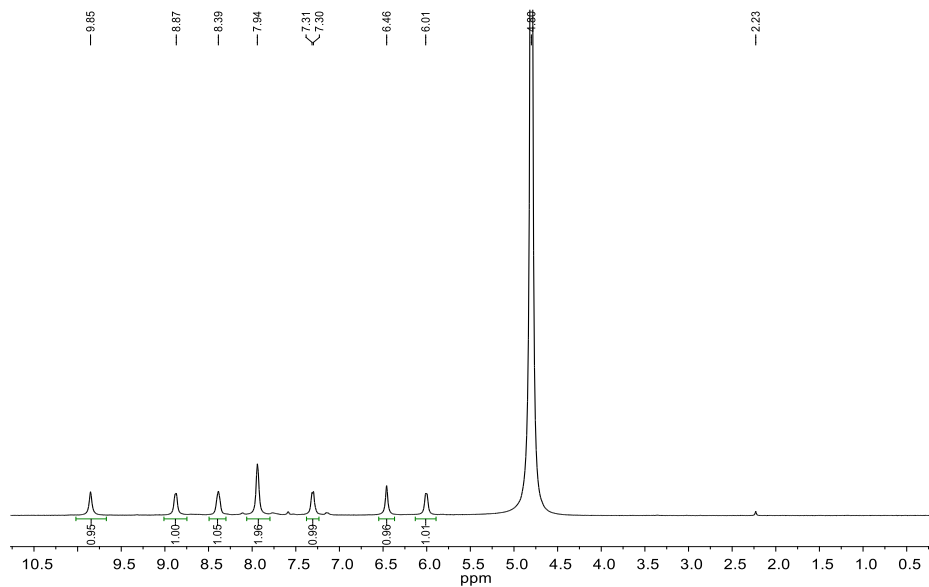


Figure 3.24. ^1H NMR of $\text{CF}_3\text{I-1}$

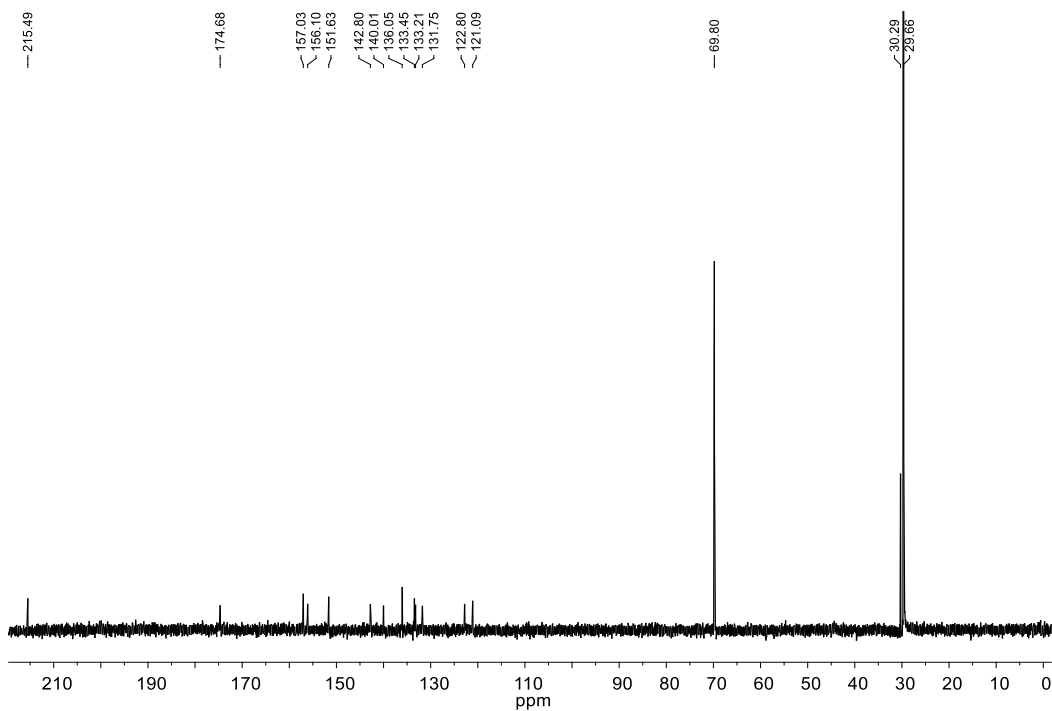


Figure 3.25. ^{13}C NMR of $\text{CF}_3\text{I-1}$

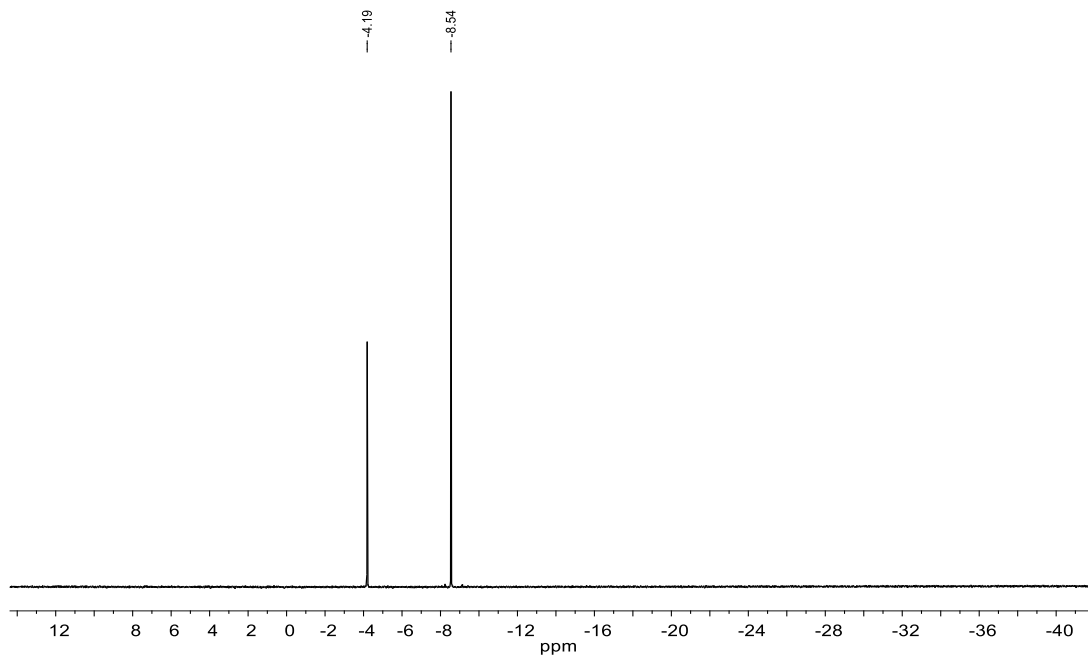


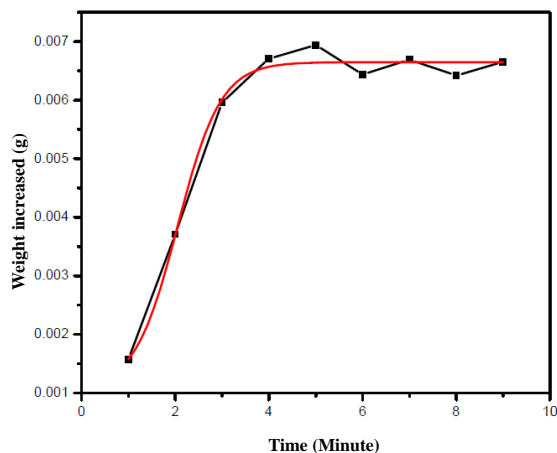
Figure 3.26. ^{19}F NMR of CF_3I

S_{MAX} Calculation

For S_{MAX} Calculation 1st we have degassed the water under vacuum and with this water we have continued the experiment by the following way,

1. Take the weight of a vial + cap + needle
2. Add ~1 ml water in vial, Take the weight of a vial + cap + needle + water
3. Bubble CF_3I slowly for one minute and take the weight, repeat the process upto 8-9 times.

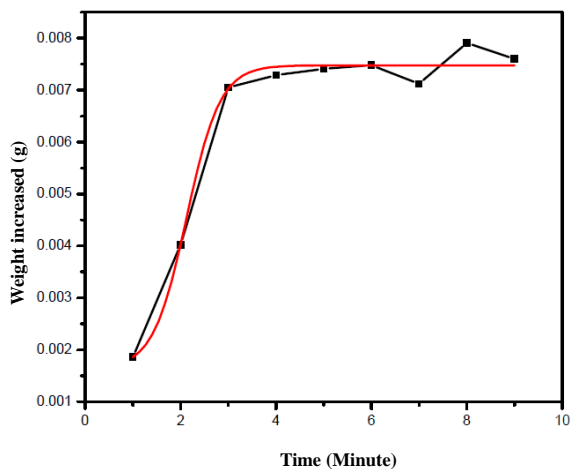
We have calculated the S_{MAX} by averaging all the following data.



Weight of water taken 1.01922g

Average weight increased 0.00665g

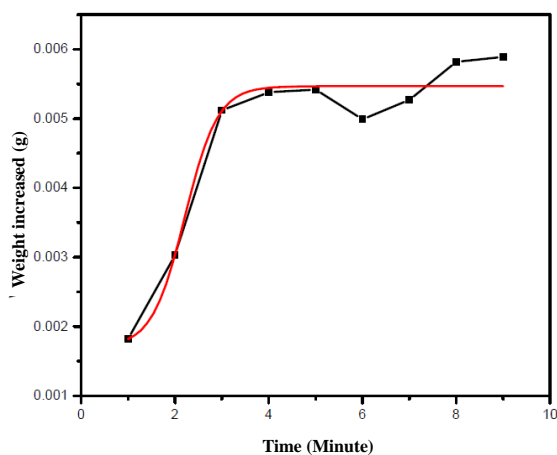
CF₃I solubility/g is 0.00652



Weight of water taken 0.85694 g

Average weight increased 0.00546 g

CF₃I solubility/g is 0.00649



Weight of water taken 1.1789 g

Average weight increased 0.00748 g

CF₃I solubility/g is 0.00634

Figure 3.27. Set I to III. Solubility curve of CF₃I in water: with increasing weigh

From the above three data Average $S_{\text{MAX}} = 0.00645 \text{ g/ml}$

$$= 3.36 \times 10^{-2} \text{ (M) [Mol wt of CF}_3\text{I}=195.9]$$

CF₃I Binding Constant Calculation

As earlier we have observed that, there was 8% encapsulation of CF₃I after 12h in presence of Benzene and it's slowly decreased with time. After 3 days it became 1%. It may be due to release of CF₃I from NMR tube (as CF₃I is less soluble in water). We have attached the NMR below.

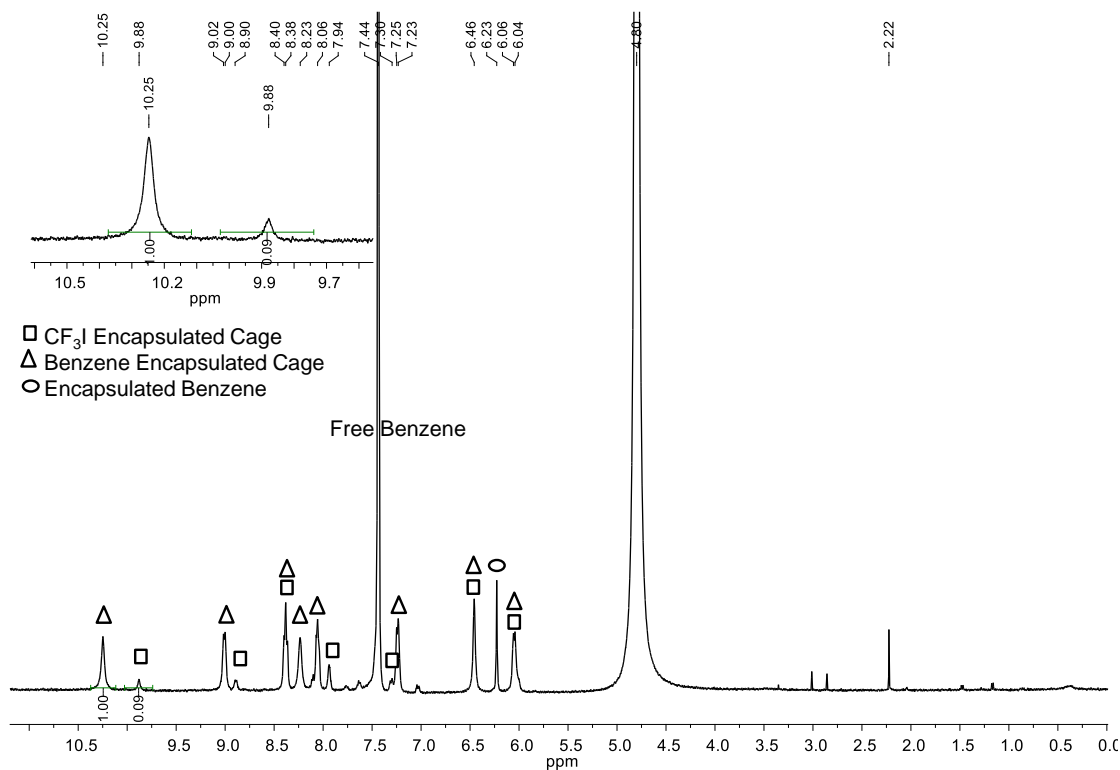


Figure 3.28. ¹H NMR of CF₃I and benzene, under open atmosphere.

We have repeated the experiment again in a J-young NMR tube. After 12 h we have checked the NMR and found that there was 41% CF₃I encapsulation and it's almost unchanged after 24 h. we have attached the NMR below.

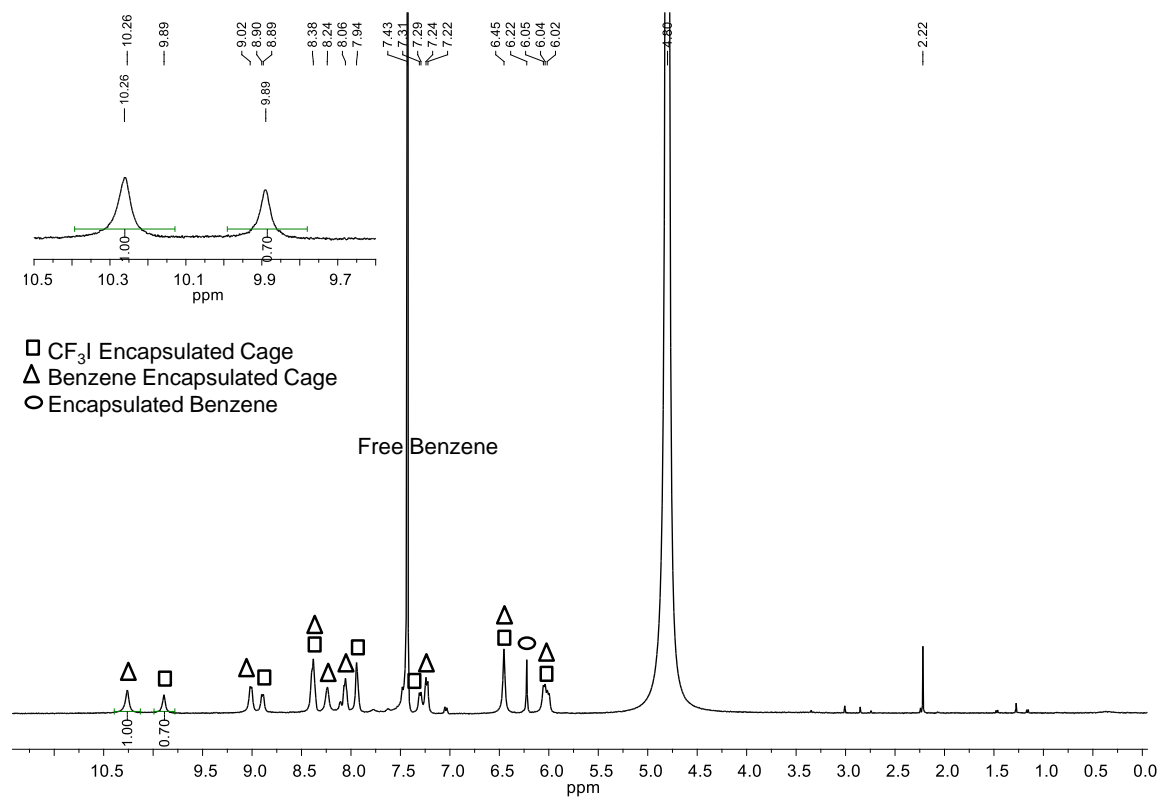


Figure 3.29. ¹H NMR of CF₃I⊂1 and benzene⊂1 mixture under equilibrium.

If the binding constant of CF₃I is K_{CF_3I} , Then

$$\begin{aligned}
 K_{CF_3I} &= K_{Benzene} \times \frac{[HG]_{CF_3I}}{[HG]_{Benzene}} \times \frac{S_{Max\ Benzene}}{S_{Max\ CF_3I}} \\
 &= 3 \times 10^3 \times 41 / 59 \times 2.29 \times 10^{-2} / 3.36 \times 10^{-2} \\
 &= 1.42 \times 10^3
 \end{aligned}$$

3.6 NOTES AND REFERENCES

1. P. D. Frischmann, V. Kunz, V. Stepanenko and F. Würthner, *Chem. Eur. J.*, 2015, **21**, 2766-2769.
2. A. M. Castilla, W. J. Ramsay and J. R. Nitschke, *Acc. Chem. Res.*, 2014, **47**, 2063-2073.
3. H. Bunzen, Nonappa, E. Kalenius, S. Hietala and E. Kolehmainen, *Chem. Eur. J.*, 2013, **19**, 12978-12981.
4. X.-P. Zhou, Y. Wu and D. Li, *J. Am. Chem. Soc.*, 2013, **135**, 16062-16065.
5. D. H. Ren, D. Qiu, C. Y. Pang, Z. Li and Z. G. Gu, *Chem. Commun.*, 2014, **51**, 788-791.
6. Z. He, W. Jiang and C. A. Schalley, *Chem. Soc. Rev.*, 2015, **44**, 779-789.
7. C. Talotta, C. Gaeta, Z. Qi, C. A. Schalley and P. Neri, *Angew. Chem. Int. Ed.*, 2013, **52**, 7437–7441.
8. M. L. Saha and M. Schmittel, *Org. Biomol. Chem.*, 2012, **10**, 4651-4684.
9. M. M. Safont-Sempere, G. Fernández and F. Würthner, *Chem. Rev.*, 2011, **111**, 5784-5814.
10. S. Mukherjee and P. S. Mukherjee, *Chem. Commun.*, 2014, **50**, 2239-2248.
11. J.-F. Ayme, J. E. Beves, C. J. Campbell and D. A. Leigh, *Chem. Soc. Rev.*, 2013, **42**, 1700-1712.
12. T. Mitra, K. E. Jelfs, M. Schmidtman, A. Ahmed, S. Y. Chong, D. J. Adams and A. I. Cooper, *Nature Chem.*, 2013, **5**, 276-281.
13. N. Giuseppone, *Acc. Chem. Res.*, 2012, **45**, 2178-2188.
14. P. Mal, D. Schultz, K. Beyeh, K. Rissanen and J. R. Nitschke, *Angew. Chem. Int. Ed.*, 2008, **47**, 8297-8301.
15. M. E. Belowich and J. F. Stoddart, *Chem. Soc. Rev.*, 2012, **41**, 2003-2024.

16. K. Osowska and O. Š. Miljanić, *Angew. Chem., Int. Ed.*, 2011, **50**, 8345-8349.
17. J.-M. Lehn, *Angew. Chem. Int. Ed.*, 2015, 10.1002/anie.201409399.
18. C. Giri, F. Topic, P. Mal and K. Rissanen, *Dalton Trans.*, 2014, **43**, 17889-17892.
19. C. Giri, F. Topić, P. Mal and K. Rissanen, *Dalton Trans.*, 2014, **43**, 15697-15699.
20. S. Fischmann and U. Lüning, *Isr. J. Chem.*, 2013, **53**, 87-96.
21. K. Acharyya, S. Mukherjee and P. S. Mukherjee, *J. Am. Chem. Soc.*, 2013, **135**, 554-557.
22. S. K. Samanta, J. W. Bats and M. Schmittel, *Chem. Commun.*, 2014, **50**, 2364-2366.
23. R. S. Varma, *Green Chem.*, 2014, **16**, 2027-2041.
24. G. Cravotto, E. C. Gaudino and P. Cintas, *Chem. Soc. Rev.*, 2013, **42**, 7521-7534.
25. D. Braga, L. Maini and F. Grepioni, *Chem. Soc. Rev.*, 2013, **42**, 7638-7648.
26. S. L. James, C. J. Adams, C. Bolm, D. Braga, P. Collier, T. Friscic, F. Grepioni, K. D. M. Harris, G. Hyett, W. Jones, A. Krebs, J. Mack, L. Maini, A. G. Orpen, I. P. Parkin, W. C. Shearouse, J. W. Steed and D. C. Waddell, *Chem. Soc. Rev.*, 2012, **41**, 413-447.
27. T. Friščić, I. Halasz, P. J. Beldon, A. M. Belenguer, F. Adams, S. A. J. Kimber, V. Honkimäki and R. E. Dinnebier, *Nature Chem.*, 2013, **5**, 66-73.
28. P. Balaz, M. Achimovicova, M. Balaz, P. Billik, Z. Cherkezova-Zheleva, J. M. Criado, F. Delogu, E. Dutkova, E. Gaffet, F. J. Gotor, R. Kumar, I. Mitov, T. Rojac, M. Senna, A. Streletskii and K. Wieczorek-Ciurowa, *Chem. Soc. Rev.*, 2013, **42**, 7571-7637.
29. S. Ley, M. O'Brien and R. Denton, *Synthesis*, 2011, 1157-1192.
30. T. K. Achar, S. Maiti and P. Mal, *RSC Adv.*, 2014, **4**, 12834-12839.
31. T. K. Achar and P. Mal, *J. Org. Chem.*, 2015, **80**, 666-672.
32. S. Maiti and P. Mal, *Synth. Commun.*, 2014, **44**, 3461-3469.
33. A. Bose and P. Mal, *Tetrahedron Lett.*, 2014, **55**, 2154-2156.

34. A. Stolle, T. Szuppa, S. E. S. Leonhardt and B. Ondruschka, *Chem. Soc. Rev.*, 2011, **40**, 2317-2329.
35. G.-W. Wang, *Chem. Soc. Rev.*, 2013, **42**, 7668-7700.
36. J.-L. Do, C. Mottillo, D. Tan, V. Strukil and T. Friscic, *J. Am. Chem. Soc.*, 2015, **10.1021/jacs.5b00151**.
37. M. Ferguson, N. Giri, X. Huang, D. Apperley and S. L. James, *Green Chem.*, 2014, **16**, 1374-1382.
38. J. Antesberger, G. W. V. Cave, M. C. Ferrarelli, M. W. Heaven, C. L. Raston and J. L. Atwood, *Chem. Commun.*, 2005, 892-894.
39. E. Mattia and S. Otto, *Nature Nanotech.*, 2015, **10**, 111-119.
40. Y.-R. Zheng, W.-J. Lan, M. Wang, T. R. Cook and P. J. Stang, *J. Am. Chem. Soc.*, 2011, **133**, 17045-17055.
41. J. G. Hernandez, I. S. Butler and T. Friscic, *Chem. Sci.*, 2014, **5**, 3576-3582.
42. R. S. Keri, M. R. Patil, S. A. Patil and S. Budagumpi, *Eur. J. Med. Chem.*, 2015, **89**, 207-251.
43. R. Kato, *Chem. Rev.*, 2004, **104**, 5319-5346.
44. C. Vila and M. Rueping, *Green Chem.*, 2013, **15**, 2056-2059.
45. P. Kirsch, *Modern Fluoroorganic Chemistry: Synthesis Reactivity and Applications*, Wiley Online Library, 2004.
46. P. Gao, X.-R. Song, X.-Y. Liu and Y.-M. Liang, *Chem. Eur. J.*, 2015, **ASAP Article**, 10.1002/chem.201406432.
47. C. Alonso, E. Martínez de Marigorta, G. Rubiales and F. Palacios, *Chem. Rev.*, 2015, **115**, 1847-1935.

48. M. S. Winston, W. J. Wolf and F. D. Toste, *J. Am. Chem. Soc.*, 2014, **136**, 7777-7782.
49. W.-J. Yoo and C.-J. Li, *J. Org. Chem.*, 2006, **71**, 6266-6268.
50. G. Zhu and H. Ren, in *Porous Organic Frameworks*, Springer, 2015, pp. 57-85.
51. Y.-B. Zhang, H. Furukawa, N. Ko, W. Nie, H. J. Park, S. Okajima, K. E. Cordova, H. Deng, J. Kim and O. M. Yaghi, *J. Am. Chem. Soc.*, 2015.
52. M. Zhang, H. Li, Z. Perry and H.-C. Zhou, *Metal-Organic Framework Materials*, 2014, 283.
53. C. Qian, X. Zhang, J. Li, F. Xu, Y. Zhang and Q. Shen, *Organometallics*, 2009, **28**, 3856-3862.
54. L. Zhang, S. Su, H. Wu and S. Wang, *Tetrahedron*, 2009, **65**, 10022-10024.
55. Y. Li, F. Jia and Z. Li, *Chem. Eur. J.*, 2013, **19**, 82-86.
56. Y. Ruan, P. W. Peterson, C. M. Hadad and J. D. Badjic, *Chem. Commun.*, 2014, **50**, 9086-9089.
57. Q.-Q. Wang, V. W. Day and K. Bowman-James, *Org. Lett.*, 2014, **16**, 3982-3985.
58. R. Sure, R. Tonner and P. Schwerdtfeger, *J. Comput. Chem.*, 2015, **36**, 88-96.
59. B. Zhou, J. Du, Y. Yang and Y. Li, *Org. Lett.*, 2013, **15**, 2934-2937.
60. P. Mal, D. Schultz, K. Beyeh, K. Rissanen and J. R. Nitschke, *Angew. Chem. Int. Ed. Engl.*, 2008, **47**, 8297-8301.
61. F. Grellepois, *J. Org. Chem.*, 2013, **78**, 1127-1137.
62. J. Z. Dong Yang, Yanxia Zhao, Yibo Lei, Liping Cao, Xiao-Juan Yang, Martin Davi, and C. J. Nader de Sousa Amadeu, Zhibin Zhang, Yao-Yu Wang, and Biao Wu*, *Angew. Chem. Int. Ed.*, 2015, **54**, 8658-8661.

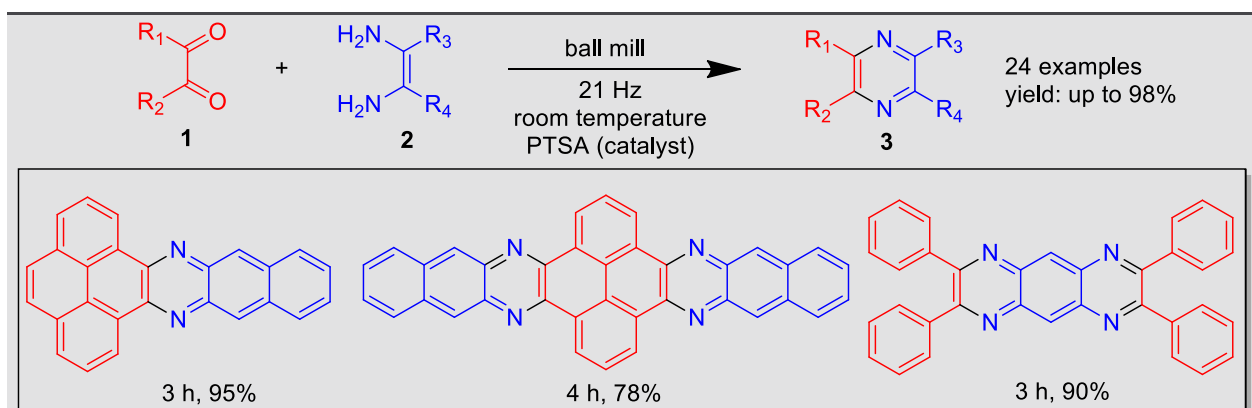
63. T.-H. Chen, I. Popov, W. Kaveevivitchai, Y.-C. Chuang, Y.-S. Chen, O. Daugulis, A. J. Jacobson and O. Š. Miljanić, *Nat Commun*, 2014, **5**, 1-8.
64. P. Mal and J. R. Nitschke, *Chem. Commun.*, 2010, **46**, 2417-2419.
65. Y.-R. Zheng, W.-J. Lan, M. Wang, T. R. Cook and P. J. Stang, *J. Am. Chem. Soc.*, 2011, **133**, 17045-17055.
66. D. A. Roberts, A. M. Castilla, T. K. Ronson and J. R. Nitschke, *J. Am. Chem. Soc.*, 2014, **136**, 8201-8204.
67. M. M. Safont-Sempere, G. Fernández and F. Würthner, *Chem. Rev.*, 2011, **111**, 5784-5814.
68. J. Snoep and H. Westerhoff, in *Systems Biology*, eds. L. Alberghina and H. V. Westerhoff, Springer Berlin Heidelberg, 2005, vol. 13, ch. 61, pp. 13-30.
69. J. R. Nitschke, *Nature*, 2009, **462**, 736-738.
70. R. F. Ludlow and S. Otto, *Chem. Soc. Rev.*, 2008, **37**, 101-108.
71. R. Chakrabarty, P. S. Mukherjee and P. J. Stang, *Chem. Rev.*, 2011, **111**, 6810-6918.
72. K. Ruiz-Mirazo, C. Briones and A. de la Escosura, *Chem. Rev.*, 2014, **114**, 285-366.
73. E. R. Kay, D. A. Leigh and F. Zerbetto, *Angew. Chem. Int. Ed.*, 2007, **46**, 72-191.
74. B. Lewandowski, G. De Bo, J. W. Ward, M. Papmeyer, S. Kuschel, M. J. Aldegunde, P. M. E. Gramlich, D. Heckmann, S. M. Goldup, D. M. D'Souza, A. E. Fernandes and D. A. Leigh, *Science*, 2013, **339**, 189-193.
75. J. Brinkmann, E. Cavatorta, S. Sankaran, B. Schmidt, J. van Weerd and P. Jonkheijm, *Chem. Soc. Rev.*, 2014, **43**, 4449-4469.
76. A. Herrmann, *Chem. Soc. Rev.*, 2014, **43**, 1899-1933.

77. M. M. J. Smulders, I. A. Riddell, C. Browne and J. R. Nitschke, *Chem. Soc. Rev.*, 2013, **42**, 1728-1754.
78. D. Ajami and J. Rebek, *Angew. Chem. Int. Ed.*, 2008, **47**, 6059-6061.
79. I. A. Riddell, M. M. J. Smulders, J. K. Clegg and J. R. Nitschke, *Chem. Commun.*, 2011, **47**, 457-459.
80. R. Garcia-Alvarez, P. Crochet and V. Cadierno, *Green Chem.*, 2013, **15**, 46-66.
81. S. M. Biros, R. G. Bergman and K. N. Raymond, *J. Am. Chem. Soc.*, 2007, **129**, 12094-12095.
82. M. M. Smulders, S. Zarra and J. R. Nitschke, *J. Am. Chem. Soc.*, 2013, **135**, 7039-7046.
83. C. Giri, P. K. Sahoo, R. Puttreddy, K. Rissanen and P. Mal, *Chem. Eur. J.*, 2015, **21**, 6390-6393.
84. H. Morimoto, R. Fujiwara, Y. Shimizu, K. Morisaki and T. Ohshima, *Org. Lett.*, 2014.
85. D. Schultz and J. R. Nitschke, *Chem. Eur. J.*, 2007, **13**, 3660-3665.

CHAPTER 4

Mechanochemical Synthesis, Photophysical Properties, and X-ray Structures of N-Heteroacenes

4.1 ABASTRACT



Syntheses of pyrazaacenes were achieved under solvent free ball milling condition as easy, high yielding, time-efficient and environmentally benign. The described mechanochemical methodology is an example of a proof-of-concept in which solution based tedious, poor yielding and difficult. Synthesized compounds also include pyrazaacenes (*N*-heteroacenes) of octacene analogues containing pyrene as a building block. Compounds were sparingly soluble in major solvents and column purifications could be avoided after solvent free synthesis. The UV-Vis absorption spectra of pyrazaacene shows an intense absorption in near IR region. The single crystal X-Ray analysis of the crystal lattice of selected pyrazaacene derivatives show pair-wise π - π interactions and some C-H $\cdots\pi$ interactions which could account some of the photophysical features in the solid state.

4.2 INTRODUCTION

The recent advancement in synthesis of extended pi-conjugated acene molecules with exciting optoelectronic properties has gained significant interest in material science. Generally, acenes are considered as most comprehensive class of fused polycyclic aromatic hydrocarbons,¹ described by the fewest localized Clar resonant sextets per number of aromatic rings.² Uses of these materials varying the range from applications as moth repellents to precursors for synthetic dyes like alizarin.³ Also, these molecules have gained attention due to their electronic properties such as field effect transistors (FETs), organic light emitting diodes (OLEDs), photovoltaic cells, etc. Unfortunately, acenes are highly unstable and incorporation of hetero atom increases their stability. These heteroacenes display improved stability as compared to their hydrocarbon analogues because making C-N bond is much easier than the C-C bond.⁴ Due to electron deficient in nature, low band gaps and high thermal stability heteroacenes have appeared to be potential choices as n-type semiconducting materials over acenes.^{5,6}

Herein, we mainly focus our attention on the synthesis of pyrazaacenes i.e., nitrogen containing heteroacenes having either pyrene building block or contains pyrene-fused oligoazaacenes. In general, pyrazaacenes are synthesized by considering on two popular methods (1) cyclocondensation reactions between 1,2-diaminoarenes and 1,2-diketones, (2) substitution reaction of 1,2-diaminoarenes with dihydroxy acenes and followed by oxidation. However, these pyrazaacenes are synthesized by following the cyclocondensation method, because C=N bonds are easily constructed through this reaction. Major disadvantages of the literature known syntheses of pyrazaacenes are associated with practicing of hazardous reaction condition, low yielding and therefore very few methods are available on pyrazaacenes synthesis.

Recently, ball-milling mechanochemistry,⁷⁻⁹ as a solvent-free synthetic methodology, has drawn significant interest to the chemists due to its benefits over traditional solution-based methods.¹⁰ The advantages of mechanochemistry are substantial and well documented in literature.^{11, 12} This has huge significance to green processes, time efficient, environmentally benign and shown to be economical. Minimum purification, towards quantitative conversion and production of less by products bring extra importance to this method.¹³⁻¹⁶ Under the area of mechanochemistry, recently, we have reported multistep synthesis, synthetic methodologies and self-sorting reactions. Also, we have anticipated that ball milling methodology^{7, 15} may possibly be used as a supply of mechanical energy and reactions could be done in greener way for the synthesis of heteroacenes. Taking into consideration all these aspects, we have designed a straightforward route *via* mechanochemistry to prepare pyrazaacenes in limited synthetic steps and in high yields.

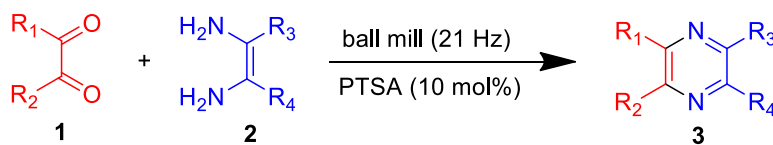
4.3 RESULTS AND DISCUSSION

Synthesis

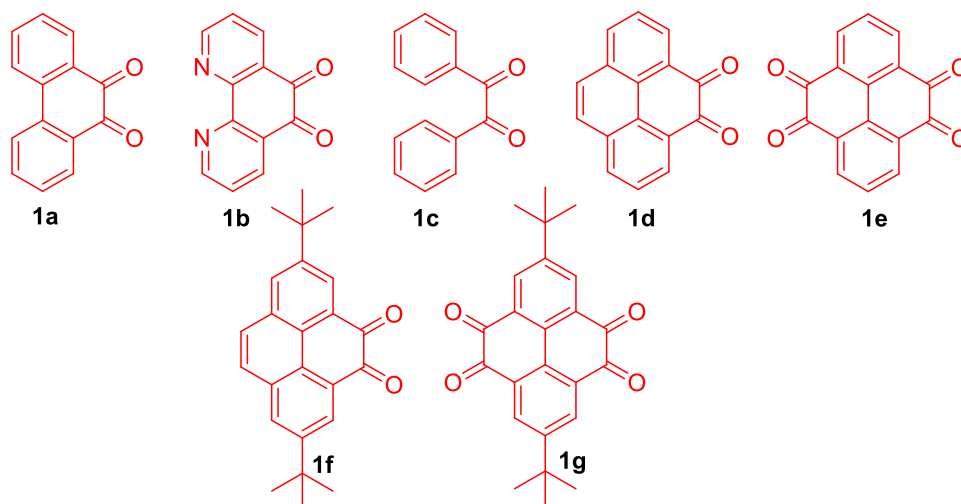
Mechanochemical (ball-milling) synthesis of heteroacenes from respective precursors are shown in Fig.4.1. 1,2-Dicarbonyl compounds (**1**) and 1,2-diaminoarenes (**2**) were used as precursors for the solvent free cyclocondensation reaction. The reactions were carried out under solvent-free condition and at room temperature in which *p*-toluene sulfonic acid (PTSA) was used as catalyst. While optimization, the progress of reactions were monitored by thin layer chromatography (TLC) or ¹H NMR. In a standard run, the milling instrument was stopped and a small parts of the sample was collected from reaction-jar and analyzed. Once the reaction was completed, the

solid-mass was collected in a flask, washed with appropriate solvent and filtered off. The substrates scope of this methodology was verified and the results are shown in Fig. 4.2.

a) this work: solvent free cyclocondensation reaction



b) 1,2-dicarbonyl compounds



c) 1,2-diamino arenes

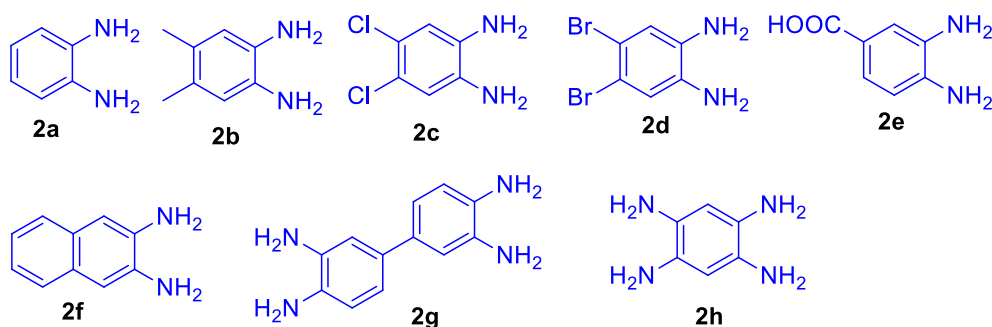


Figure 4.1. Mechanochemical approach of heteroacenes synthesis.

As shown in Fig. 4.2a excellent yields (91-95%) of pyrazaacene derivatives using pyrene-4,5-dione (**1a**) and different diamines were obtained. Similar high yielding reactions were observed for the synthesis of pyrazaacene derivatives using other dicarbonyl or tetracarboxyl derivatives.

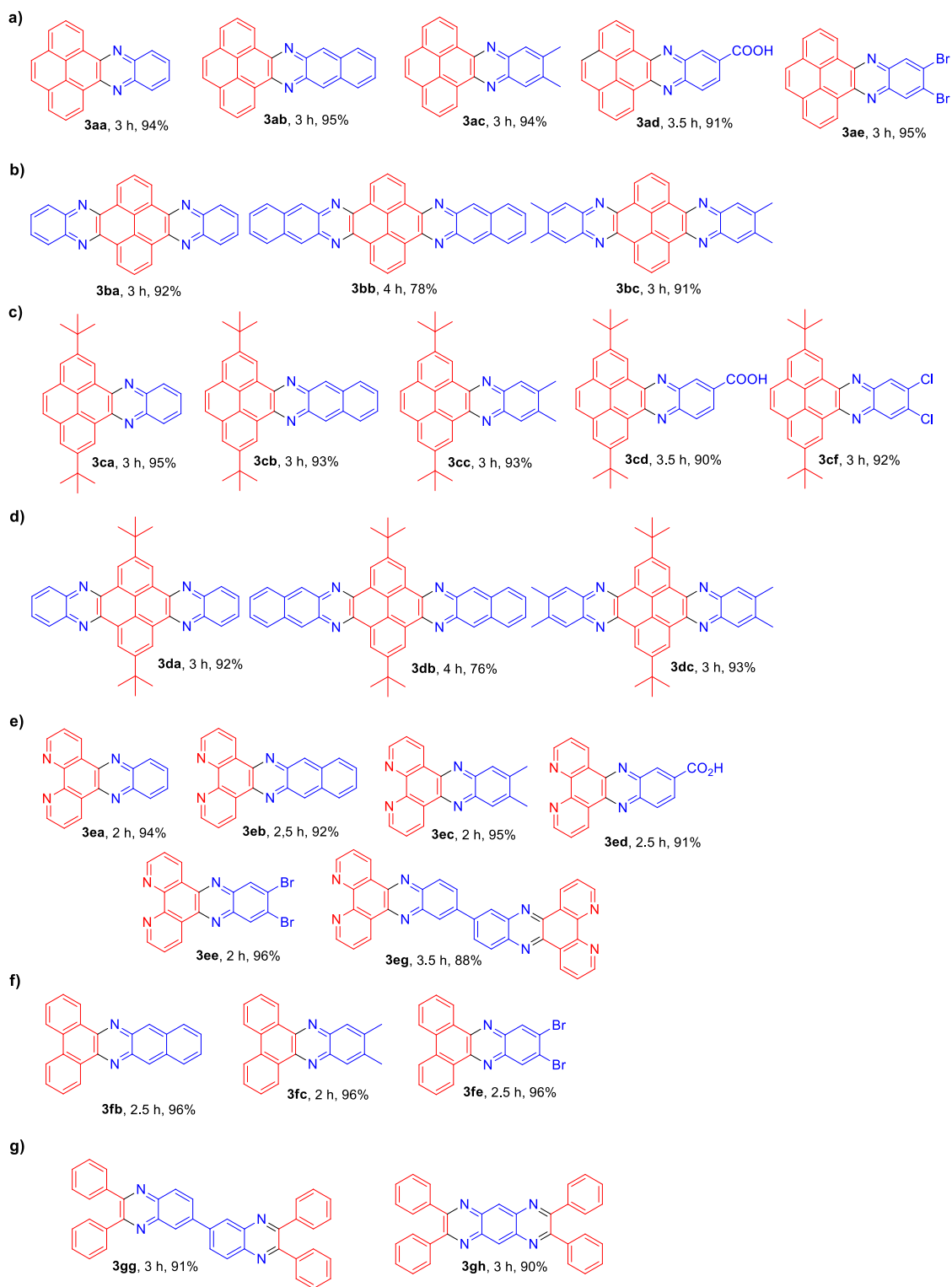
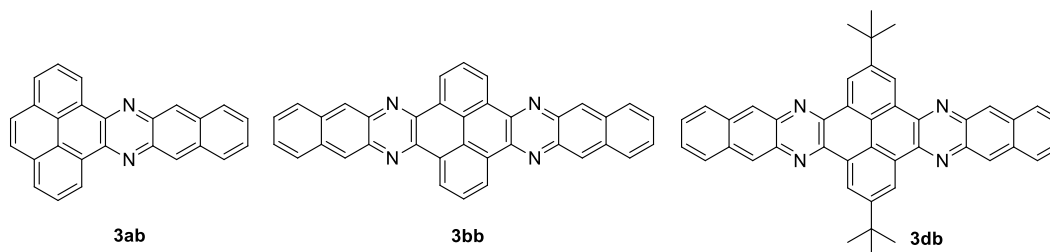


Figure 4.2. Mechanochemically synthesized *N*-heteroacenes are shown with their compound identification number, reaction times and isolated yields.

In major cases single product was obtained and therefore, purification by washing with an appropriate solvents (mainly high polar) led to isolation of analytically pure products (Fig. 4.3, NMR spectra). Using this methodology, we were also able to successfully synthesize the octacene derivatives benzo[*i*]benzo[6',7']quinoxalino[2',3':9,10]phenanthro[4,5-*abc*]phenazine (**3bb**) and 2,13-di-*tert*-butylbenzo[*i*]benzo[6',7']quinoxalino[2',3':9,10]phenanthro[4,5-*abc*]phenazine (**3db**) in good yield. But in case of octacenes (**3bb** and **3db**) the purifications were done by washing with high polar solvents like DMF.

As pyrazene is one of the most important heterocyclic core we extended our methodology to other classes of *N*-heteroacene analogues. Using different 1,2-diketones (Fig.4.1b) like benzil (**1g**), 1,10-phenanthroline-5,6-dione (**1e**) and phenanthrene-5,6-dione (**1f**) we were able to synthesize different classes of *N*-heteroacenes with excellent yields (Fig. 4.2e-g). Similarly, bis-phenazine (**3gh**) and bis-quinoxaline (**3gg**) were also obtained in excellent yields (~ 90%) using [1,1'-biphenyl]-3,3',4,4'-tetraamine (**2g**) and benzene-1,2,4,5-tetraamine (**2h**), respectively.

Commonly used method to synthesize heteroacenes containing pyrazene moiety is reported in refluxing ethanol/acetic acid or acetic acid in presence of oxidant IBX. In all these cases reaction conditions are hazardous, time consuming and often led to very poor yielding reactions.^{17, 18} However our method turned out to be simple, convenient, time-efficient, economical and environment friendly. A comparison table (Table 4.1) has been presented for the synthesis of few heteroacenes using our method and literature methods. After carefully analyzing the literature methods, we believe that our methodology for synthesis of heteroacenes is superior to any existing ones.

Table 4.1. Efficiency of the synthesis via ball milling.

Entry	Compd.	Information ^a	Lit.	This work
1	3ab	A	ref ¹⁹	ball mill
		B	pyridine, reflux, Ar atm, 3 days	RT, 3 h, PTSA catalyst
		C	work-up and then flash chromatography	solid residue washed with ethanol
		D	32	95
2	3bb	A	ref ²⁰	ball mill
		B	pyridine, 120 °C, Ar atm, 3 days	RT, 4 h, PTSA catalyst
		C	solid residue was washed with ethanol and then chloroform	solid residue washed with ethanol and then DMF
		D	40	78
3	3db	A	ref ¹⁷	ball mill
		B	pyridine, 120 °C, Ar atm, 3 days	room temperature, 4 h, PTSA catalyst
		C	solid residue was washed with ethanol and chloroform	solid residue washed with ethanol and followed by DMF
		D	32	76

^a A ref, B reaction condition, C isolation procedure, D isolated yield (%)

¹H NMR spectroscopy

Solvent free syntheses were performed under ambient conditions and ¹H NMR study were helpful to understand efficiency of this described methodology. No purification was done using

any chromatographic technique, however, by washing with minimum quantity of high polar solvents compounds were isolated with high purity to be used for further studies. As representative examples, without any purification the ^1H NMR spectra of the compounds **3aa**, **3cb**, **3ee** and **3gg** are shown in Fig. 4.3. Thus, the efficiency of this ball mill methods for the synthesis of *N*-heteroacenes has been established.

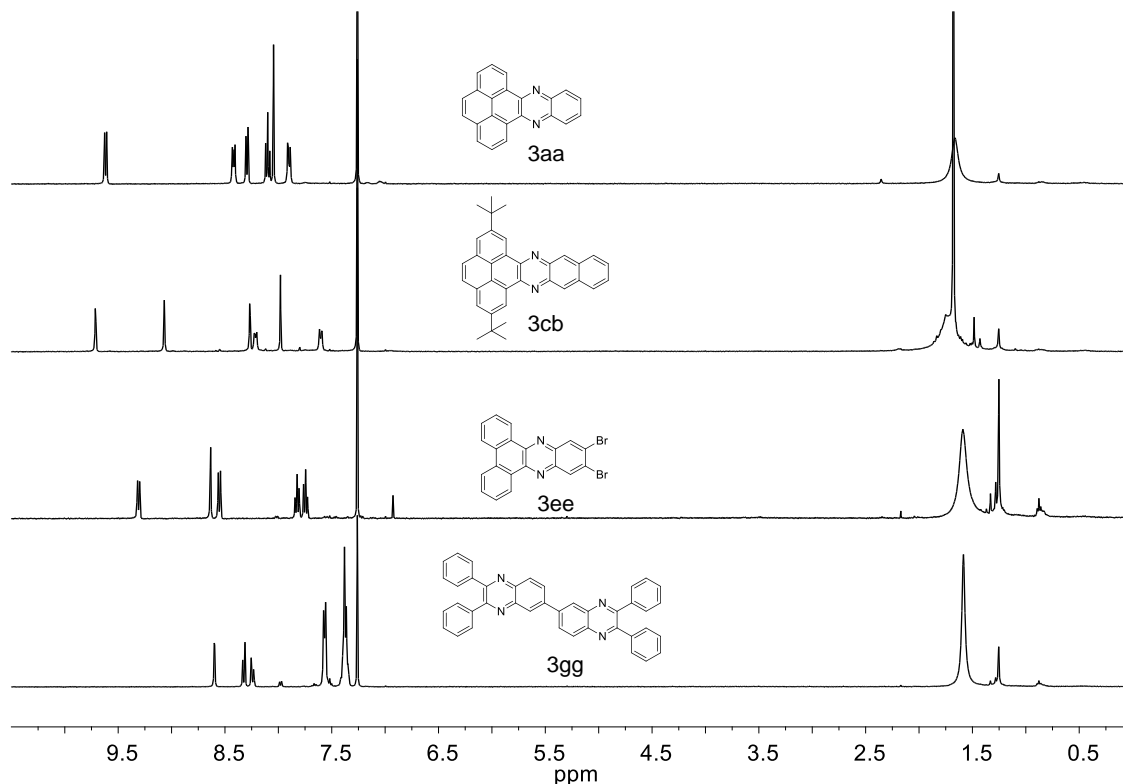


Figure 4.3. ^1H NMR spectra of the compounds **3aa**, **3cb**, **3ee** and **3gg** recorded in CDCl_3 . No purifications are done on this compounds before recording spectra.

Photophysical study.²¹ Absorption and photoluminescence spectra of compounds were recorded in appropriate solvents and selective data are shown in Table 2. The absorption maxima on above 400 nm for the compounds due to $n\text{-}\pi^*$ transition. As expected with increasing conjugation more red-shifted absorptions were observed, for example $\lambda_{\text{max}} \sim 435$ nm for **3aa** and 469 nm for **3ab**.

UV-Vis absorption spectra of pyraazacenes **3aa-3ae** recorded in dichloromethane are shown in Fig. 4.4.

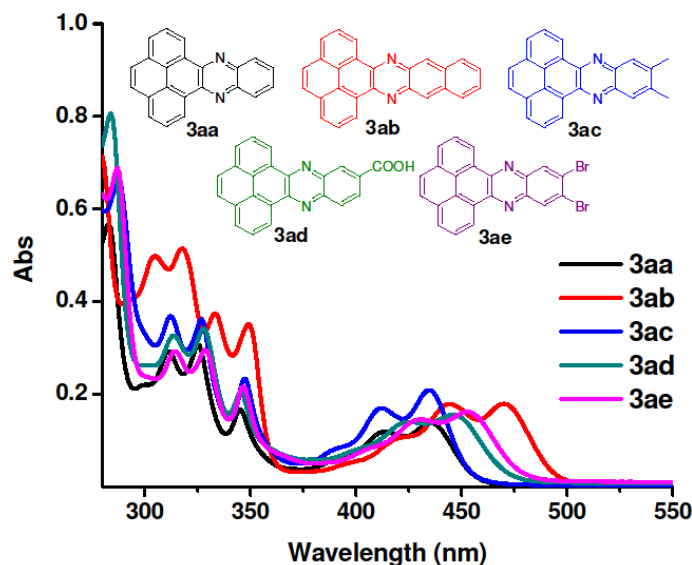


Figure 4.4. UV-Vis absorption spectra of pyraazacenes **3aa-3ae** in dichloromethane (1×10^{-5} M).

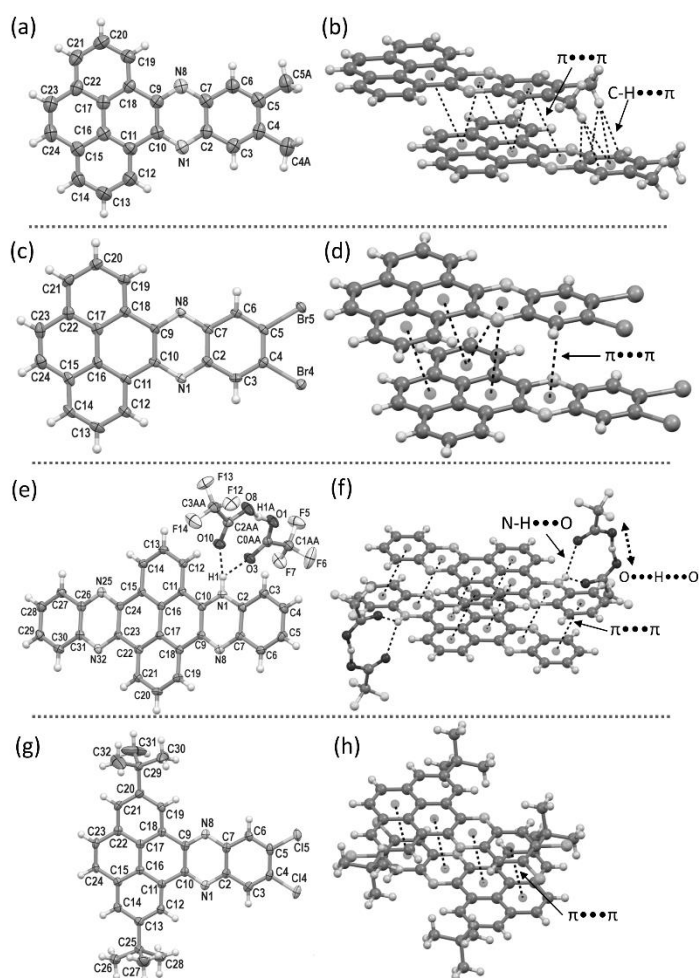
Crystallographic Investigations

The molecular structures of Polycyclic Aromatic Hydrocarbons (PAHs) by itself are less interesting.¹ However, the heteroatom induced PAHs and their solid-state organization featuring enhanced π - π interactions have great deal of interest to understand by X-ray crystallography.²² In solid-state, the extent of π - π and C-H $\cdots\pi$ interactions in *N*-heteroacenes are believed to be further improved by the role of substituents, and any π -disturbance to cause by the inclusion of charged species, *e.g.* anions and protonation. These concepts are explored within the crystal structures of **3ac**, **3ae**, **3ba** and **3cf**, also the forces that drive aromatic rings to cause molecular association by π - π and C-H $\cdots\pi$ interactions.^{21,23}

All the crystal structures show characteristic π - π interactions as shown in Fig. 4.5. Compound **3ac** displays herringbone pattern (Fig. 4.9) with aromatic rings displaced laterally, and are stabilized by pair-wise π - π interactions at centroid-to-centroid distances ranging from 3.562 to 3.786 Å. Additionally, the lateral displacement caused the methyl substituents to stabilize by C-H $\cdots\pi$ interactions [*ca.* 2.780 to 3.022 Å] as shown in Fig. 4.5b. In compound **3ae**, the aromatic rings are displaced such that the bromine substituted benzene ring stacks on pyrazine ring uniquely stabilized by pair-wise π - π interactions [*ca.* 3.532 to 3.849 Å], as shown in Fig. 4.5d. The packing of **3ae** is influenced by the bromine substituents, displaying once again a herringbone solid-state organization stabilized by π - π and Br \cdots Br interactions [*ca.* 3.602 Å]. All the interatomic distances in the crystal packing interactions are shorter than the sum of the van der Waals radii (Fig.4.10).

As shown in Fig. 4.5f, compound **3ba** clearly has the most abundant and efficient π - π interactions [*ca.* 3.608 to 3.808 Å] of all the compounds. This enhanced activity can be accounted due to the protonation at pyrazine nitrogen. The N-H acts as a bifurcated hydrogen bond donor for two trifluoroacetate (TFA) C-O oxygens with slight double character [1.211(3)Å] at distances of 2.726(3) Å [angle N-H \cdots O = 144°] and 2.802(3) Å [angle N-H \cdots O = 115°]. On the other hand, the C-O oxygens [1.273(3) Å] of TFA anions further stabilize by unsymmetrical O \cdots H \cdots O hydrogen bond with distances 1.21(5) Å and 1.23(4) Å [angle O \cdots H \cdots O = 167(4)°], as shown in Fig. 4.5f. Crystal packing extends one-dimensionally further by π - π interactions [*ca.* 3.737 Å], and two dimensionally by weak C-H \cdots O interactions between TFA and aromatic ring hydrogens to generate herringbone [viewed along *a*-axis] or sinusoidal [viewed along *c*-axis] pattern (Fig. 4.11). Despite the C-H \cdots O interactions deviates by 0.122Å from the sum of van der Waals radii and are caused by packing, these interactions are important in crystal packing

stabilization. The efficient π -cloud delocalization between pyrene core with electron-donating *ter*-butyl substituted and pyrazine fused benzene ring having electron-withdrawing chloride substituents resulted in strong π - π interactions in compound **3cf**. The π - π interactions occurs one-dimensionally without aromatic ring displacements (Fig. 4.12), however in inverted fashion to avoid the steric hindrance between the *ter*-butyl groups as shown in Fig. 4.5h. The shortest observed centroid-to-centroid distance is 3.415 Å, and ranges up to 3.698 Å. The crystal packing of compound **3cf** is trivial, and all the observed C-H \cdots π interactions are above the sum of the



van der Waals radii. The Hirshfeld surface plots and 2-D fingerprint analysis are given in supporting information.

Figure 4.5. Left side - X-ray crystal structures of (a) **3ac**, (c) **3ae**, (e) **3ba** and (g) **3cf** with thermal ellipsoids at 50% probability level. Hydrogen atoms are not labelled for clarity. Right side, the corresponding motifs showing π - π interactions.

4.4 CONCLUSION

In summary, we foresee that the benefits of the mechanochemical synthesis of the pyraazacenes are substantial: (a) this could potentially be the most efficient approach for heteroacenes synthesis; (b) room temperature synthesis, lesser reaction time and simplified purification procedure will make the heteroacenes cheaply available for the materials chemistry application. We anticipate that our study may pull substantial attention of researches working on the development of synthetic methodologies using heteroacenes as well as the chemists searching for superior methods in organic mechanochemistry.

4.5 EXPERIMENTAL SECTION

General Methods. Synthesis using ball milling (21 Hz) were performed in the open atmosphere using Retsch MM 200, in 10 mL jar made of ZrO₂ or Stainless steel with One ball of 15 mm Diameter made of ZrO₂ or Stainless steel respectively. NMR spectra were recorded on 400 MHz instrument at 25 °C. The chemical shift values are reported in parts per million (ppm) and referred to the residual chloroform (7.26 ppm for ¹H and 77.16 for ¹³C) and deuterium oxide (4.79 ppm for ¹H). The peak patterns are designated as follows: s, singlet; d, doublet; t, triplet; q, quartet; m, multiplet; dd, doublet of doublets; td, triplet of doublets; br s, broad singlet. The coupling constants (*J*) are reported in hertz (Hz). High-resolution mass spectrometry (HRMS) was conducted on ESI-TOF (time of flight) mass spectrometer. Infrared spectral data are

reported in wavenumber (cm^{-1}). Melting points of the compounds were determined using digital melting point apparatus and are uncorrected.

Procedure for synthesis phenanthro[4,5-*abc*]phenazine 3aa: Pyrene-4,5-dione (**1a**, 50 mg, 0.21 mmol) and *o*-pheynelediamine (**2a**, 23 mg, 0.21 mmol), PTSA (4 mg, 0.021 mmol) and a stainless steel ball were taken in a stainless steel jar (10 mL). Milling was started and continued for 3h. After that the crude reaction mixture was washed with ethanol to isolate product as yellowish solid; yield 94% (62 mg); mp: 257-259 °C; (lit. ²⁴ mp 276.8–277.4 °C); ¹H NMR (400 MHz, CDCl_3) δ 9.59 (dd, $J = 7.7, 0.9$ Hz, 2H), 8.39 (dd, $J = 6.5, 3.4$ Hz, 2H), 8.28 (dd, $J = 7.7, 0.9$ Hz, 2H), 8.10 (t, $J = 7.7$ Hz, 2H), 8.03 (s, 2H), 7.90 (dd, $J = 6.5, 3.4$ Hz, 2H); ¹³C NMR (100 MHz, CDCl_3) δ 143.5, 142.6, 131.6, 130.1, 129.7, 129.7, 129.4, 127.4, 127.0, 126.3, 124; IR (KBr) $\tilde{\nu}$ 3049, 2923, 1624, 1480, 1422, 1359, 1334, 1314, 1292, 1174, 1094, 1063, 830, 763, 713, 630, 587, 426 cm^{-1} ; HRMS observed 305.1088 (calculated for $\text{C}_{22}\text{H}_{12}\text{N}_2$ $[\text{M}+\text{H}]^+$ 305.1073).

Large scale synthesis: Suggested loading of the reactant materials should be less than one third of jar volume (25 mL ZrO_2 jar). Compound **3aa** was also synthesized using 1.2 g Pyrene-4,5-dione, 552 mg *o*-pheynelediamine and PTSA 96 mg. Yield 1.5 g (94%).

Benzo[*i*]phenanthro[4,5-*abc*]phenazine (3ab):¹⁹ Yellow solid; yield 95% (72 mg); mp: >300 °C; (lit. mp not available); ¹H NMR (400 MHz, TFA-*d*) δ 9.62 (d, $J = 7.6$ Hz, 2H), 9.25 (d, $J = 3.2$ Hz, 2H), 8.73 (d, $J = 7.7$ Hz, 2H), 8.52 (dd, $J = 6.3, 3.1$ Hz, 2H), 8.48 (t, $J = 7.7$ Hz, 2H), 8.30 (d, $J = 2.3$ Hz, 2H), 8.17 (dd, $J = 6.5, 2.9$ Hz, 2H); ¹³C NMR (101 MHz, TFA) δ 142.0, 138.1, 136.4, 134.2, 133.1, 132.5, 130.2, 130.1, 129.8, 127.5, 127.3, 125.4, 124.1; IR (KBr) $\tilde{\nu}$ 3049, 2917, 1855, 1624, 1421, 1358, 1294, 1262, 1176, 1098, 874, 829, 737, 716, 486 cm^{-1} ; HRMS observed 355.1241 (calculated for $\text{C}_{26}\text{H}_{14}\text{N}_2$ $[\text{M}+\text{H}]^+$ 355.1230).

11,12-Dimethylphenanthro[4,5-abc]phenazine (3ac): Pale orange solid; yield 94% (67 mg); mp: 238-240 °C; ^1H NMR (400 MHz, CDCl_3) δ 9.54 (d, $J = 7.7$ Hz, 2H), 8.26 (d, $J = 7.7$ Hz, 2H), 8.08-8.05 (m, 4H), 8.02 (s, 2H), 2.58 (s, 6H); ^{13}C NMR (100 MHz, CDCl_3) δ 142.6, 141.7, 140.9, 131.6, 130.0, 128.9, 128.5, 127.3, 126.9, 126.1, 123.7, 20.7; IR (KBr) $\tilde{\nu}$ 3041, 2920, 2848, 1613, 1354, 1295, 1096, 1001, 867, 831, 719, 438 cm^{-1} ; HRMS observed 333.1410 (calculated for $\text{C}_{24}\text{H}_{16}\text{N}_2$ $[\text{M}+\text{H}]^+$ 333.1386).

Phenanthro[4,5-abc]phenazine-11-carboxylic acid (3ad): Orange solid; yield 91% (68 mg); mp: 246-248 °C; ^1H NMR (400 MHz, CDCl_3) δ 9.57 (s, 2H), 9.41 (s, 1H), 8.80 (s, 2H), 8.60 (dd, $J = 22.0, 6.9$ Hz, 2H), 8.25 (s, 2H), 8.19 (q, $J = 9.3$ Hz, 2H); ^{13}C NMR (100 MHz, CDCl_3) δ 170.0, 144.68, 140.7, 138.4, 136.0, 135.8, 134.5, 134.4, 133.2, 132.6, 132.4, 131.0, 128.9, 128.8, 128.7, 128.2, 127.5, 127.4, 126.5, 126.4, 124.8, 124.3, 121.8; IR (KBr) $\tilde{\nu}$ 3050, 2880, 1688, 1680, 1435, 1358, 1283, 1206, 1134, 1023, 832, 801, 714 cm^{-1} ; HRMS observed 349.0993 (calculated for $\text{C}_{23}\text{H}_{12}\text{N}_2\text{O}_2$ $[\text{M}+\text{H}]^+$ 349.0972).

11,12-Dibromophenanthro[4,5-abc]phenazine (3ae): Yellow solid; yield 95% (85 mg); mp: >300 °C; ^1H NMR (400 MHz, CDCl_3) δ 9.43 (s, 2H), 8.87 (s, 2H), 8.50 (d, $J = 6.5$ Hz, 2H), 8.18 (s, 2H), 8.10 (s, 2H); ^{13}C NMR (100 MHz, CDCl_3) δ 141.8, 136.0, 134.0, 132.2, 132.1, 129.9, 128.5, 128.2, 126.5, 126.4, 123.8; IR (KBr) $\tilde{\nu}$ 3063, 3046, 2917, 2843, 1624, 1442, 1353, 1293, 1171, 1099, 1080, 903, 833, 714, 434 cm^{-1} ; HRMS observed 460.9253 (calculated for $\text{C}_{22}\text{H}_{10}\text{Br}_2\text{N}_2$ $[\text{M}+\text{H}]^+$ 460.9283).

Quinoxalino[2',3':9,10]phenanthro[4,5-abc]phenazine (3ba): Pale yellow solid; yield 92% (71 mg); mp: >300 °C; (lit.²⁵ mp >420 °C); ^1H NMR (400 MHz, CDCl_3) δ 9.98 (d, $J = 8.0$ Hz, 4H), 8.79 (dd, $J = 6.4, 3.3$ Hz, 4H), 8.59 (t, $J = 8.0$ Hz, 2H), 8.40 (dd, $J = 6.5, 3.1$ Hz, 4H); ^{13}C

NMR (100 MHz, CDCl₃) δ 130.0, 137.7, 136.4, 132.1, 131.0, 128.9, 126.1, 125.2; IR (KBr) $\tilde{\nu}$ 3053, 3011, 2923, 1957, 1903, 1613, 1479, 1415, 1403, 1356, 1332, 1294, 1231, 1133, 1101, 976, 870, 809, 759, 720, 615, 570, 515, 443 cm⁻¹; HRMS observed 407.1290 (calculated for C₂₈H₁₄N₄ [M+H]⁺ 407.1291).

Benzo[*i*]benzo[6',7']quinoxalino[2',3':9,10]phenanthro[4,5-*abc*]phenazine (3bb):²⁰ Orange solid; yield 78% (71 mg); mp: >300 °C; (lit. mp not available); ¹H NMR (400 MHz, TFA-d₁) δ 9.19 (d, *J* = 8.0 Hz, 4H), 8.52 (s, 4H), 7.19 (t, *J* = 8.0 Hz, 2H), 7.58 (m, 4H), 7.13 (m, 4H); IR (KBr) $\tilde{\nu}$ 3428, 2338, 1677, 1406, 1359, 1327, 1298, 1207, 1178, 1132, 1094, 1022, 897, 869, 805, 774, 721 cm⁻¹; HRMS data could not be obtained due to insoluble nature by the compound.

6,7,15,16-Tetramethylquinoxalino[2',3':9,10]phenanthro[4,5-*abc*]phenazine (3bc): Yellow solid; yield 91% (80 mg); mp: >300 °C; (lit.²⁵ mp >420°C); ¹H NMR (400 MHz, CDCl₃) δ 9.91 (d, *J* = 8.0 Hz, 4H), 8.54 (t, *J* = 8.0 Hz, 2H), 8.50 (s, 4H), 2.78 (s, 12H); ¹³C NMR (101 MHz, CDCl₃) δ 149.6, 137.6, 137.0, 131.0, 130.6, 128.1, 125.2, 124.6, 21.5; IR (KBr) $\tilde{\nu}$ 2976, 2915, 1621, 1474, 1449, 1397, 1353, 1338, 1215, 1112, 1027, 998, 066, 894, 815, 723, 445 cm⁻¹; HRMS observed 463.1916 (calculated for C₃₂H₂₂N₄ [M+H]⁺ 463.1917).

2,7-Di-*tert*-butylphenanthro[4,5-*abc*]phenazine (3ca): Yellow solid; yield 95% (57 mg); mp: >300 °C; ¹H NMR (400 MHz, CDCl₃) δ 9.69 (d, *J* = 4.0 Hz, 2H), 8.44 (q, *J* = 4.0 Hz, 2H), 8.28 (d, *J* = 4.0 Hz, 2H), 8.00 (s, 2H), 7.89 (q, *J* = 4.0 Hz, 2H), 1.67 (s, 18H); ¹³C NMR (101 MHz, CDCl₃) δ 149.9, 144.1, 131.4, 129.8, 129.7, 129.2, 127.5, 126.0, 124.5, 121.7, 35.7, 32.1; IR (KBr) $\tilde{\nu}$ 2961, 2885, 2867, 2333, 1815, 1759, 1612, 1625, 1610, 1477, 1438, 1364, 1353, 1346, 1328, 1259, 1201, 1169, 1112, 1033, 972, 948, 912, 887, 803, 760, 723, 582 cm⁻¹; HRMS observed 417.2355 (calculated for C₃₀H₂₈N₂ [M+H]⁺ 417.2325).

2,7-Di-tert-butylbenzo[i]phenanthro[4,5-abc]phenazine (3cb): Yellow solid; yield 93% (63 mg); mp: >300 °C; ¹H NMR (400 MHz, CDCl₃) δ 9.70 (d, *J* = 4.0 Hz, 2H), 9.03 (s, 2H) 8.28 (d, *J* = 4.0 Hz, 2H), 8.24 (m, 2H), 8.00 (s, 2H), 7.63 (m, 2H), 1.69 (s, 18H); ¹³C NMR (101 MHz, CDCl₃) δ 150.1, 145.3, 139.1, 134.2, 121.5, 129.3, 128.8, 127.7, 127.4, 126.7, 126.6, 124.7, 122.3, 35.7, 32.1; IR (KBr) $\tilde{\nu}$ 3051, 2866, 2743, 2713, 2689, 2668, 2485, 2333, 2324, 1625, 1612, 1552, 1480, 1474, 1436, 1390, 1365, 1344, 1283, 1257, 1236, 1201, 1161, 1109, 1098, 975, 948, 890, 803, 739, 723, 601, 616, 578 cm⁻¹; HRMS observed 467.2509 (calculated for C₃₄H₃₀N₂ [M+H]⁺ 467.2482).

2,7-Di-tert-butyl-11,12-dimethylphenanthro[4,5-abc]phenazine (3cc): Yellow solid; yield 93% (60 mg); mp: >300 °C; ¹H NMR (400 MHz, CDCl₃) δ 9.64 (d, *J* = 4.0 Hz, 2H), 8.25 (d, *J* = 4.0 Hz, 2H), 8.17 (s, 2H), 7.99 (s, 2H), 2.62 (s, 6H), 1.66 (s, 18H); ¹³C NMR (101 MHz, CDCl₃) δ 149.7, 143.2, 141.5, 140.6, 131.3, 129.5, 128.5, 127.4, 125.6, 124.3, 121.3, 35.7, 32.1, 20.7; IR (KBr) $\tilde{\nu}$ 2963, 2868, 2331, 1625, 1612, 1509, 1479, 1444, 1363, 1346, 1327, 1262, 1242, 1225, 1209, 1161, 1123, 1057, 1033, 1000, 964, 887, 866, 804, 724, 624, 601, 577 cm⁻¹; HRMS observed 445.2699 (calculated for C₃₄H₃₀N₂ [M+H]⁺ 445.2638).

2,7-Di-tert-butylphenanthro[4,5-abc]phenazine-11-carboxylic acid (3cd): Yellow solid; yield 90% (61 mg); mp: >300 °C; ¹H NMR (400 MHz, CDCl₃) δ 9.63 (s, 1H), 9.53 (s, 1H), 9.42 (s, 1H), 8.79 (d, *J* = 8.0 Hz, 1H), 8.72 (d, *J* = 8.0 Hz, 1H), 8.59 (s, 1H), 8.53 (s, 1H), 8.15 (m, 2H), 1.66 (s, 9H), 1.62 (s, 9H); ¹³C NMR (101 MHz, CDCl₃) δ 152.5, 152.3, 145.3, 141.3, 138.1, 135.6, 134.1, 133.0, 132.8, 132.3, 132.2, 131.0, 130.9, 128.7, 128.2, 125.9, 124.9, 124.6, 124.4, 124.2, 124.0, 36.0, 31.7, 31.5; IR (KBr) $\tilde{\nu}$ 2661, 2551, 1845, 1690, 1616, 1486, 1442, 1363, 1344, 1302, 1283, 1261, 1226, 1166, 978, 887, 843, 795, 767, 722, 554 cm⁻¹; HRMS observed 461.2249 (calculated for C₃₁H₂₈N₂O₂ [M+H]⁺ 461.2224).

2,7-Di-tert-butyl-11,12-dichlorophenanthro[4,5-abc]phenazine (3cf): Yellow solid; yield 92% (65 mg); mp: >300 °C; ^1H NMR (400 MHz, CDCl_3) δ 9.59 (d, $J = 4.0$ Hz, 2H), 8.53 (s, 2H), 8.31 (d, $J = 4.0$ Hz, 2H), 8.01 (s, 2H), 1.67 (s, 18H); ^{13}C NMR (101 MHz, CDCl_3) δ 152.5, 142.4, 140.6, 134.7, 132.4, 131.9, 128.5, 125.9, 125.2, 124.1, 122.7, 36.0, 31.5; IR (KBr) $\tilde{\nu}$ 2958, 2884, 2866, 1906, 1820, 1810, 1799, 1787, 1759, 1752, 1729, 1610, 1593 1473, 1449, 1406, 1383, 1364, 1330, 1287, 1240, 1219, 1171, 1127, 1111, 1103, 986, 888, 866, 798, 722, 528 cm^{-1} ; HRMS observed 485.1526 (calculated for $\text{C}_{34}\text{H}_{30}\text{N}_2$ $[\text{M}+\text{H}]^+$ 485.1546).

2,11-Di-tert-butylquinoxalino[2',3':9,10]phenanthro[4,5-abc]phenazine (3da):²⁶ Pale yellow solid; yield 92% (64 mg); mp: >300 °C; (lit. mp >300 °C) ^1H NMR (400 MHz, CDCl_3) δ 9.94 (s, 4H), 8.77 (m, 4H), 8.39 (m, 4H), 1.71 (s, 18H); ^{13}C NMR (101 MHz, CDCl_3) δ 155.4, 139.4, 137.2, 136.1, 129.7, 127.1, 125.9, 124.6, 36.7, 31.3; IR (KBr) $\tilde{\nu}$ 2961, 2861, 1951, 1924, 1822, 1709, 1612, 1533, 1479, 1436, 1405, 1383, 1298, 1261, 1184, 1115, 898, 879, 865, 763, 730, 584 cm^{-1} ; HRMS observed 519.2570 (calculated for $\text{C}_{36}\text{H}_{30}\text{N}_4$ $[\text{M}+\text{H}]^+$ 519.2543).

2,13-Di-tert-butylbenzo[i]benzo[6',7']quinoxalino[2',3':9,10]phenanthro[4,5-abc]phenazine (3db):¹⁷ Orange solid; yield 76% (63 mg); mp: >300 °C; (lit. mp not available); ^1H NMR (400 MHz, CDCl_3) δ 9.99 (s, 4H), 9.38 (s, 4H), 8.84 (m, 4H), 7.94 (m, 4H), 1.75 (s, 18H); IR (KBr) $\tilde{\nu}$ 2961, 1984, 1931, 1797, 1674, 1602, 1519, 1380, 1350, 1305, 1277, 1238, 1141, 1111, 1033, 960, 943, 905, 875, 831, 779, 754, 742, 668, 545 cm^{-1} ; HRMS observed 619.2877 (calculated for $\text{C}_{44}\text{H}_{34}\text{N}_4$ $[\text{M}+\text{H}]^+$ 619.2856).

2,11-Di-tert-butyl-6,7,15,16-tetramethylquinoxalino[2',3':9,10]phenanthro[4,5-abc]phenazine (3dc): Orange solid; yield 93% (71 mg); mp: >300 °C; ^1H NMR (400 MHz, CDCl_3) δ 9.91 (s, 4H), 8.52 (s, 4H), 2.79 (s, 12H), 1.72 (s, 18H); ^{13}C NMR (101 MHz, CDCl_3) δ

154.9, 149.4, 138.0, 136.5, 128.7, 126.4, 124.6, 124.4, 36.7, 31.3, 21.4; IR (KBr) $\tilde{\nu}$ 2965, 2912, 2867, 2730, 2558, 2347, 1845, 1823, 1677, 1610, 1477, 1400, 1324, 1302, 1280, 1226, 1185, 1136, 1025, 1001, 899, 886, 865, 784, 732, 562 cm^{-1} ; HRMS observed 575.3190 (calculated for $\text{C}_{40}\text{H}_{38}\text{N}_4$ $[\text{M}+\text{H}]^+$ 575.3169).

Dipyrido[3,2-a:2',3'-c]phenazine (3ea): Orange solid; yield 94% (63 mg); mp: 248-250 °C (lit.²⁷ 246-247 °C); ^1H NMR (400 MHz, CDCl_3) δ 9.67 (dd, $J = 8.1, 1.6$ Hz, 2H), 9.29 (dd, $J = 4.4, 1.5$ Hz, 2H), 8.38 (dd, $J = 6.5, 3.4$ Hz, 2H), 7.95 (dd, $J = 6.5, 3.4$ Hz, 2H), 7.82 (dd, $J = 8.1, 4.4$ Hz, 2H); ^{13}C NMR (100 MHz, CDCl_3) δ 152.8, 148.6, 142.7, 141.4, 134.0, 130.9, 129.8, 127.8, 124.4; HRMS observed 283.1003 (calculated for $\text{C}_{14}\text{H}_{16}\text{N}_2\text{O}_3$ $[\text{M}+\text{H}]^+$ 283.0978).

Benzo[i]dipyrido[3,2-a:2',3'-c]phenazine (3eb):²⁸ Orange solid; yield 92% (72 mg); mp: 272-274 °C; (lit. mp not available); ^1H NMR (400 MHz, CDCl_3) δ 9.60 (d, $J = 7.8$ Hz, 2H), 9.24 (d, $J = 3.5$ Hz, 2H), 8.89 (s, 2H), 8.18 (dd, $J = 6.3, 2.9$ Hz, 2H), 7.78 (dd, $J = 7.9, 4.4$ Hz, 2H), 7.62 (dd, $J = 6.5, 2.9$ Hz, 2H); ^{13}C NMR (100 MHz, CDCl_3) δ 152.7, 148.5, 142.0, 138.8, 134.6, 134.2, 128.7, 128.0, 127.9, 127.3, 124.5; HRMS observed 333.1162 (calculated for $\text{C}_{22}\text{H}_{12}\text{N}_4$ $[\text{M}+\text{H}]^+$ 333.1135).

11,12-Dimethyldipyrido[3,2-a:2',3'-c]phenazine (3ec): White solid; yield 95% (70 mg); mp: 183-185 °C; (lit.²⁹ 183 °C); ^1H NMR (400 MHz, CDCl_3) δ 9.59 (dd, $J = 8.1, 1.4$ Hz, 2H), 9.25 (dd, $J = 4.3, 1.4$ Hz, 2H), 8.03 (s, 2H), 7.78 (dd, $J = 8.1, 4.4$ Hz, 2H), 2.58 (s, 6H); ^{13}C NMR (100 MHz, CDCl_3) δ 152.3, 148.3, 141.9, 141.7, 140.4, 133.6, 128.3, 127.9, 124.1, 20.8; HRMS observed 311.1318 (calculated for $\text{C}_{20}\text{H}_{14}\text{N}_4$ $[\text{M}+\text{H}]^+$ 311.1291).

Dipyrido[3,2-a:2',3'-c]phenazine-11-carboxylic acid (3ed):³⁰ White solid; yield 91% (70 mg); mp: >300 °C; (lit. mp not available); ^1H NMR (400 MHz, CDCl_3) δ 10.12 (t, $J = 7.2$ Hz, 2H),

9.35 – 9.31 (m, 3H), 8.69 – 8.67 (m, 1H), 8.61 (d, $J = 8.9$ Hz, 1H), 8.35 (td, $J = 8.1, 5.2$ Hz, 2H). ^{13}C NMR (100 MHz, CDCl_3) δ 170.3, 148.3, 147.7, 144.5, 141.6, 139.8, 139.3, 139.2, 139.1, 139.0, 138.9, 133.5, 131.2, 131.0, 130.0, 129.0, 128.9, 126.8, 126.8; HRMS observed 327.0893 (calculated for $\text{C}_{19}\text{H}_{10}\text{N}_4\text{O}_2$ $[\text{M}+\text{H}]^+$ 327.0877).

11,12-Dibromodipyrido[3,2-*a*:2',3'-*c*]phenazine (3ee):³¹ White solid; yield 96% (100 mg); mp: >300 °C; (lit. mp not available); ^1H NMR (400 MHz, CDCl_3) δ 10.04 (d, $J = 7.5$ Hz, 2H), 9.32 (d, $J = 4.0$ Hz, 2H), 8.83 (s, 2H), 8.32 (dd, $J = 8.2, 5.1$ Hz, 2H); ^{13}C NMR (100 MHz, CDCl_3) δ 148.9, 142.4, 140.0, 139.9, 139.6, 133.8, 131.1, 129.9, 127.7; HRMS observed 440.9193 (calculated for $\text{C}_{18}\text{H}_8\text{Br}_2\text{N}_4$ $[\text{M}+\text{H}]^+$ 440.9169).

11,11'-Bidipyrido[3,2-*a*:2',3'-*c*]phenazine (3eg): Pale yellow solid; yield 88% (58 mg); mp: >300 °C; (lit.³² mp not available); ^1H NMR (400 MHz, CDCl_3) δ 10.23(d, $J = 7.2$ Hz, 4H), 9.34 (s, 4H), 9.06 (s, 2H), 8.79 (d, $J = 8.8$ Hz, 2H), 8.72 (d, $J = 8.8$ Hz, 2H), 8.38 (s, 4H); ^{13}C NMR (100 MHz, CDCl_3) δ 148.7, 148.5, 143.9, 143.7, 143.6, 140.6, 140.4, 139.8, 139.7, 139.6, 139.3, 133.0, 131.4, 130.5, 130.4, 128.7, 128.0, 128.0; HRMS observed 563.1722 (calculated for $\text{C}_{36}\text{H}_{18}\text{N}_8$ $[\text{M}+\text{H}]^+$ 563.1727).

Tribenzo[*a,c,i*]phenazine (3fb): Yellow solid; yield 96% (76 mg); mp: 291-293 °C (lit.²⁸ mp 293-294 °C); ^1H NMR (400 MHz, CDCl_3) δ 9.25 (d, $J = 7.9$ Hz, 2H), 9.10 (s, 2H), 8.51 (d, $J = 8.0$ Hz, 2H), 8.25-8.24 (m, 2H), 7.95 (t, $J = 7.1$ Hz, 2H), 7.84-7.77 (m, 4H); ^{13}C NMR (100 MHz, CDCl_3) δ 140.2, 136.3, 135.2, 133.8, 131.9, 130.5, 130.3, 129.0, 127.3, 124.5, 124.3, 124.2; HRMS observed 331.1233 (calculated for $\text{C}_{24}\text{H}_{14}\text{N}_2$ $[\text{M}+\text{H}]^+$ 331.1230).

11,12-Dimethyldibenzo[*a,c*]phenazine (3fc):³³ Pale yellow solid; yield 96% (71 mg); mp: 280-282 °C; (lit. mp not available); ^1H NMR (400 MHz, CDCl_3) δ 9.20 (dd, $J = 8.2, 0.9$ Hz, 2H),

8.60 (d, $J = 8.2$ Hz, 2H), 8.33 (s, 2H), 7.97-7.93 (m, 2H), 7.86 (t, $J = 7.6$ Hz, 2H), 2.69 (s, 6H); ^{13}C NMR (100 MHz, CDCl_3) δ 148.3, 138.1, 135.6, 134.1, 133.2, 129.9, 126.3, 124.3, 124.2, 124.1, 21.1; HRMS observed 309.1368 (calculated for $\text{C}_{14}\text{H}_{16}\text{N}_2\text{O}_3$ $[\text{M}+\text{H}]^+$ 309.1386).

11,12-Dibromodibenzo[a,c]phenazine (3fe):³⁴ Pale yellow solid; yield 96% (101 mg); mp: 278-280 °C; (lit.³⁰¹ mp not available); ^1H NMR (400 MHz, CDCl_3) δ 9.33 (d, $J = 7.6$ Hz, 2H), 8.65 (s, 2H), 8.57 (d, $J = 8.0$ Hz, 2H), 7.85 (t, $J = 7.4$ Hz, 2H), 7.77 (t, $J = 7.3$ Hz, 2H); ^{13}C NMR (100 MHz, CDCl_3) δ 143.6, 141.4, 133.5, 132.6, 131.2, 130.0, 128.4, 126.7, 126.5, 123.3; HRMS observed 436.9233 (calculated for $\text{C}_{20}\text{H}_{10}\text{Br}_2\text{N}_2$ $[\text{M}+\text{H}]^+$ 436.9283).

2,2',3,3'-Tetraphenyl-6,6'-biquinoxaline (3gg): Pale yellow solid; yield 96% (66 mg); mp: >300°C (lit.³⁵ >300 °C); ^1H NMR (400 MHz, CDCl_3) δ 8.62 (s, 2H), 8.35 (d, $J = 8.4$ Hz, 2H), 8.26 (d, $J = 8.2$ Hz, 2H), 7.58 (d, $J = 6.0$ Hz, 4H), 7.38 (d, $J = 6.5$ Hz, 10H); ^{13}C NMR (100 MHz, CDCl_3) δ 154.4, 153.9, 141.7, 141.4, 141.2, 139.2, 130.2, 130.1, 129.7, 129.2, 128.5, 127.7; HRMS observed 563.2244 (calculated for $\text{C}_{40}\text{H}_{26}\text{N}_4$ $[\text{M}+\text{H}]^+$ 563.2230).

2,3,7,8-Tetraphenylpyrazino[2,3-g]quinoxaline (3gh):³⁶ Yellow solid; yield 90% (50 mg); mp: 280-282°C (lit. mp not available); ^1H NMR (400 MHz, CDCl_3) δ 9.03 (s, 2H), 7.63 (d, $J = 6.7$ Hz, 8H), 7.45-7.38 (m, 12H); ^{13}C NMR (100 MHz, CDCl_3) δ 155.6, 140.7, 139.1, 130.3, 129.7, 129.1, 128.6; HRMS observed 487.1947 (calculated for $\text{C}_{34}\text{H}_{22}\text{N}_4$ $[\text{M}+\text{H}]^+$ 487.1917).

Fluorescence quantum yield determination. For fluorescence quantum yield determination quinine sulphate³⁷ was used as the standard ($\Phi_{\text{Fl}} = 0.577$ in 0.1 N H_2SO_4 , Irradiation wavelength

$$\frac{\varphi_1}{\varphi_2} = \frac{A_2 n_1^2 \alpha_1}{A_1 n_2^2 \alpha_2}$$

was 350 nm). In a typical measurement, 20 μL of heteroacene stock solution (2.5×10^{-3} M in

DCM) was added to 2.5 mL of solvent. Fluorescence wavelengths from 385 to 650 nm were considered for calculation:

Where ϕ = quantum yield, A = absorbance at given wavelength (350 nm), n = refractive index & α = area under fluorescence spectrum. Indices 1 and 2 designate sample and standard, respectively.

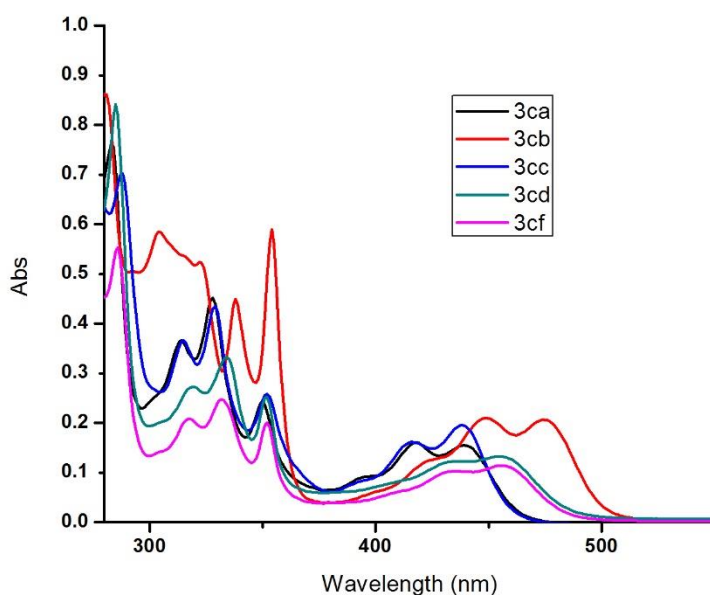


Figure S4.6. UV/vis absorption spectra of pyrazacene (3c analogue) in DCM (1×10^{-5} M) at room temperature.

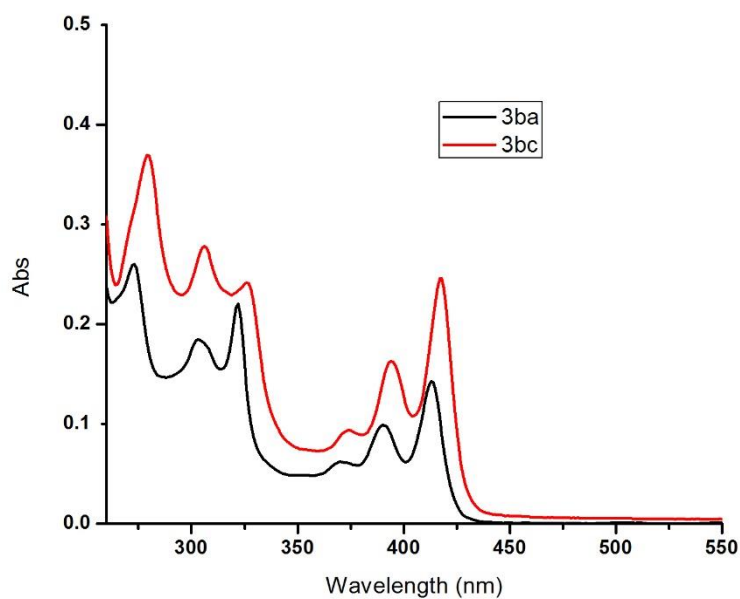


Figure 4.7. UV/vis absorption spectra of pyrazacenece (3b analogue) in DCM (1×10^{-5} M) at room temperature.

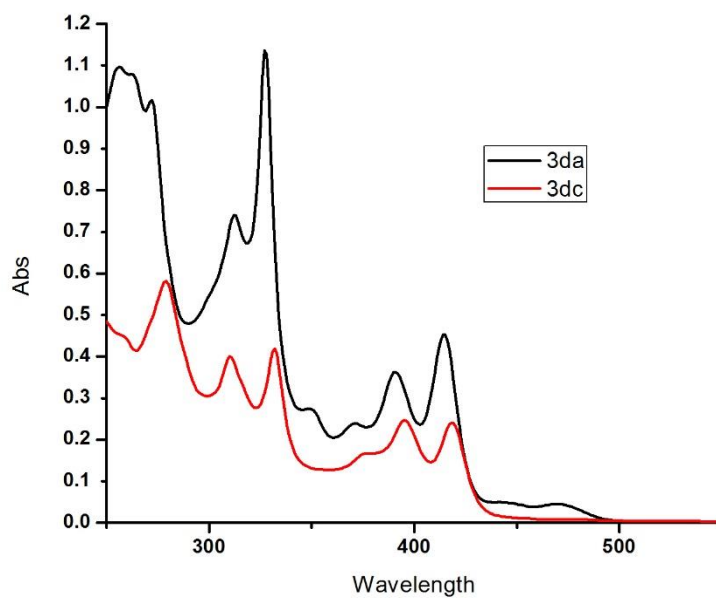


Figure 4.8. UV/vis absorption spectra of pyrazacenece (3d analogue) in DCM (1×10^{-5} M) at room temperature.

Solid-state analysis

General information

The single crystal X-ray diffraction data for **3ac**, **3ba** and **3cf** were collected at room temperature using Bruker-SMART-APEX II D8 diffractometer with Mo-K α ($\lambda = 0.71073$ Å) radiation. The data for **3ae** was collected at room temperature on a single source Agilent SuperNova diffractometer equipped with an Atlas EoS CCD detector using Mo-K α ($\lambda = 0.71073$ Å) radiation. The intensities for data the collected on Bruker diffractometer were corrected for absorption using SADABS with multi-scan absorption correction type method.³⁸ The intensities of **3ae** were corrected for absorption using the empirical absorption using spherical harmonics implemented in SCALE3 ABSPACK scaling algorithm.³⁹ All the structures were solved with direct methods (SHELXS)⁴⁰ and refined by full-matrix least squares on F² using the OLEX2,⁴¹ which utilizes the SHELXL-2013 module.⁴⁰ No attempt was made to locate the hydrogens, and for some hydrogen atoms involved in hydrogen bonds were introduced from difference Fourier maps.

Table 4.2. Crystal data and X-Ray experimental details for **3ac**, **3ae**, **3ba** and **3cf**

	3ac	3ae	3ba	3cf
CCDC Number	1437948	1437949	1437950	1437951
Chemical formula	C ₂₄ H ₁₆ N ₂	C ₂₂ H ₁₀ Br ₂ N ₂	C ₃₂ H ₁₆ F ₆ N ₄ O ₄	C ₃₀ H ₂₆ Cl ₂ N ₂
M_r	332.39	462.14	634.49	485.43
Temperature (K)	296(2)	293(2)	296(2)	296(2)
Crystal system, space group	Monoclinic, <i>P2₁/c</i>	Orthorhombic <i>Pna2₁</i>	Monoclinic <i>P2₁/c</i>	<i>Triclinic</i> <i>P-1</i>
a (Å)	16.4818(9)	24.4623(10)	8.7753(8)	6.8263(16)
b (Å)	5.1869(3)	15.4367(6)	30.793(2)	14.171(3)
c (Å)	19.7604(13)	4.26657(17)	9.5637(7)	14.474(3)
α (°)	90	90	90	116.293(15)
β (°)	107.385(4)	90	95.999(6)	91.512(16)
γ (°)	90	90	90	99.359(16)
Volume (Å³)	1612.14(17)	1611.14(11)	2570.1(3)	1230.9(5)
Z	4	4	4	2
Density (Calculated) mg/m³	1.369	1.905	1.640	1.310
Absorption Coefficient (mm⁻¹)	0.081	5.040	0.139	0.285
F(000)	696	904	1288	508
Crystal size (mm³)	0.12 x 0.10 x 0.10	0.13 x 0.11 x 0.09	0.16 x 0.14 x 0.10	0.12 x 0.12 x 0.01
θ range for data collection (°)	1.30 to 25.00	3.12 to 25.00	2.65 to 25.00	3.04 to 25.00

Reflections collected [R(int)]	10658 [0.0844]	10919 [0.0390]	15804 [0.0679]	16211 [0.1066]
Reflections [I>2sigma(I)]	1156	2391	2883	2787
Data completeness (%)	99.99	99.60	99.99	99.70
Data/ restraints/ parameters	2840/0/237	2590/1/235	4528/0/419	4310/0/313
Goodness-of-fit on F²	1.018	1.027	1.037	1.022
Final R₁ indices [I>2sigma(I)]	R ₁ = 0.0643 wR ₂ = 0.1514	R ₁ = 0.0264 wR ₂ = 0.0595	R ₁ = 0.0475 wR ₂ = 0.1133	R ₁ = 0.0595 wR ₂ = 0.1372
Final R indices [all data]	R ₁ = 0.1723 wR ₂ = 0.2071	R ₁ = 0.0308 wR ₂ = 0.0613	R ₁ = 0.0832 wR ₂ = 0.1363	R ₁ = 0.0999 wR ₂ = 0.1593
Largest diff. peak/hole (e.Å ⁻³)	0.191/ -0.192	0.386/ -0.246	0.216/ -0.335	0.335/ -0.276

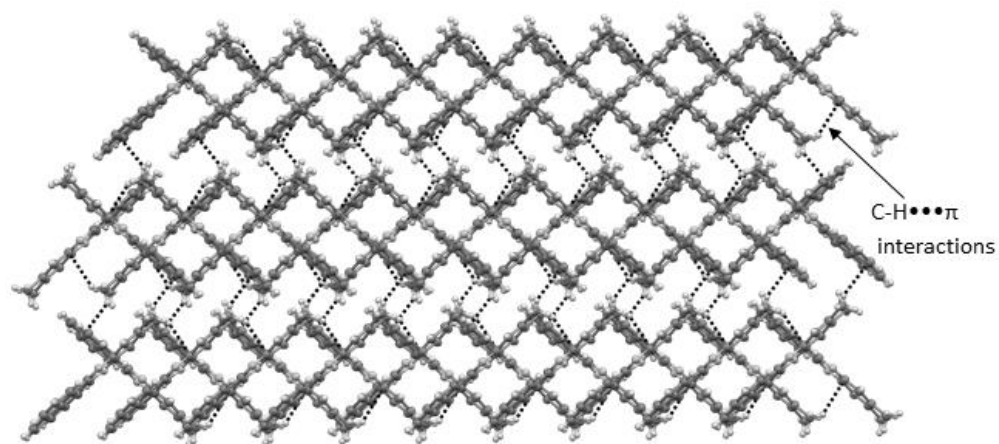


Figure 4.9. Section of crystal packing of **3ac** to show herring bond pattern, viewed along the *a*-axis.

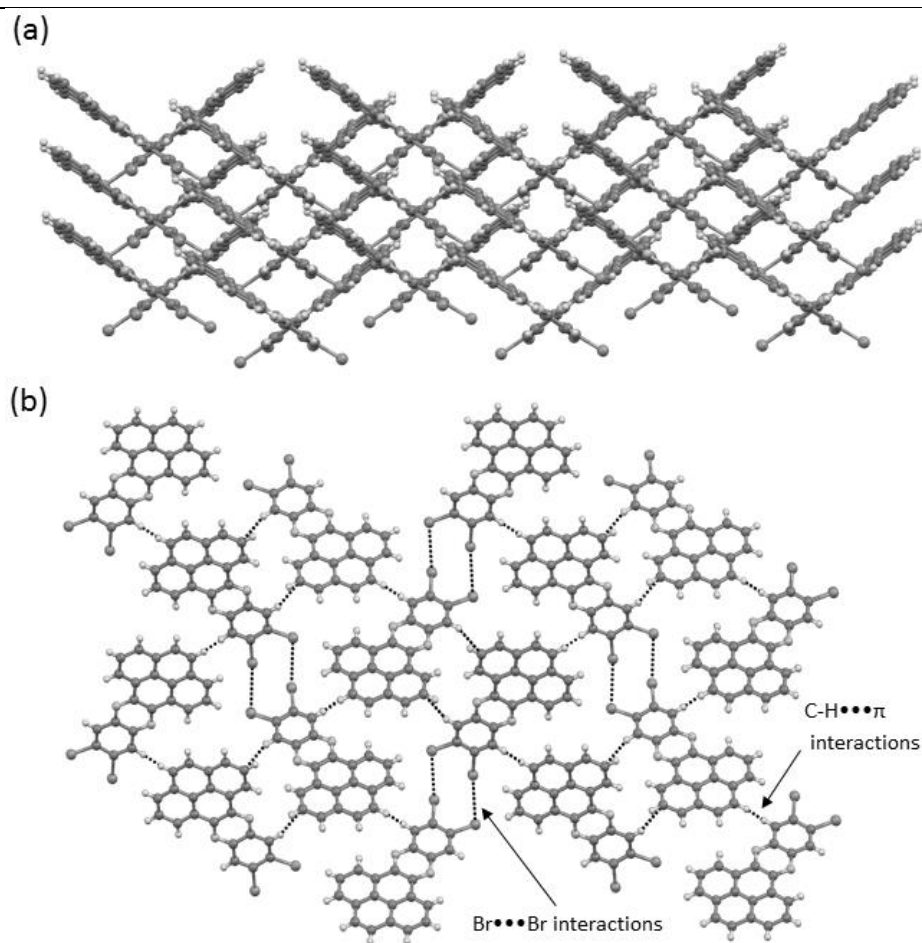


Figure 4.10. (a) Section of crystal packing of **3ae** to show herring bond pattern, viewed along the *a*-axis.

(b) Crystal packing viewed along the *a*-axis to $\text{Br}\cdots\text{Br}$ and $\text{C-H}\cdots\pi$ interactions.

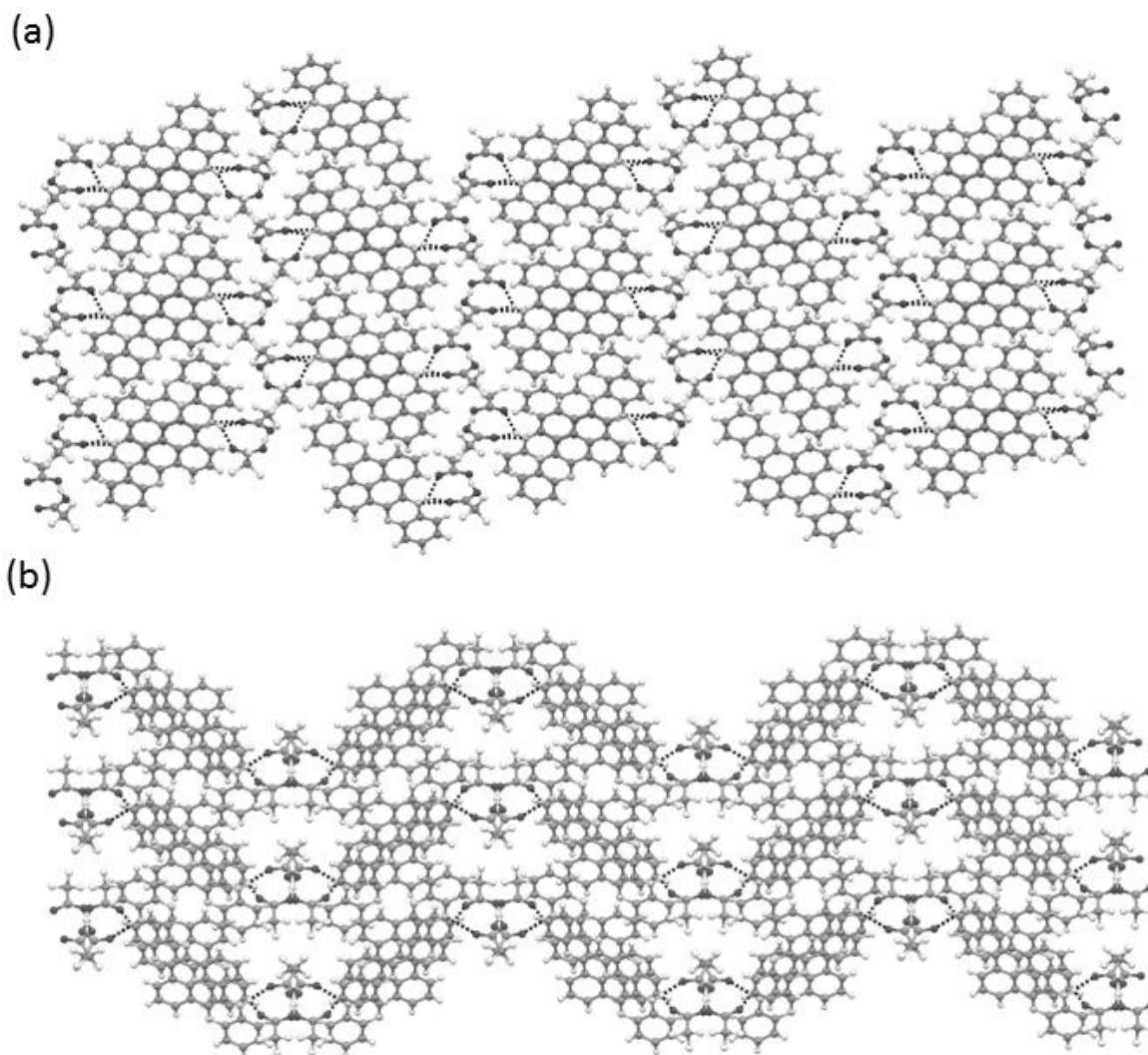


Figure 4.11. (a) Section of crystal packing of **3ba** to show herring bond pattern, viewed along the a -axis.
(b) Crystal packing viewed along the c -axis to display sinusoidal wave solid-state organization.

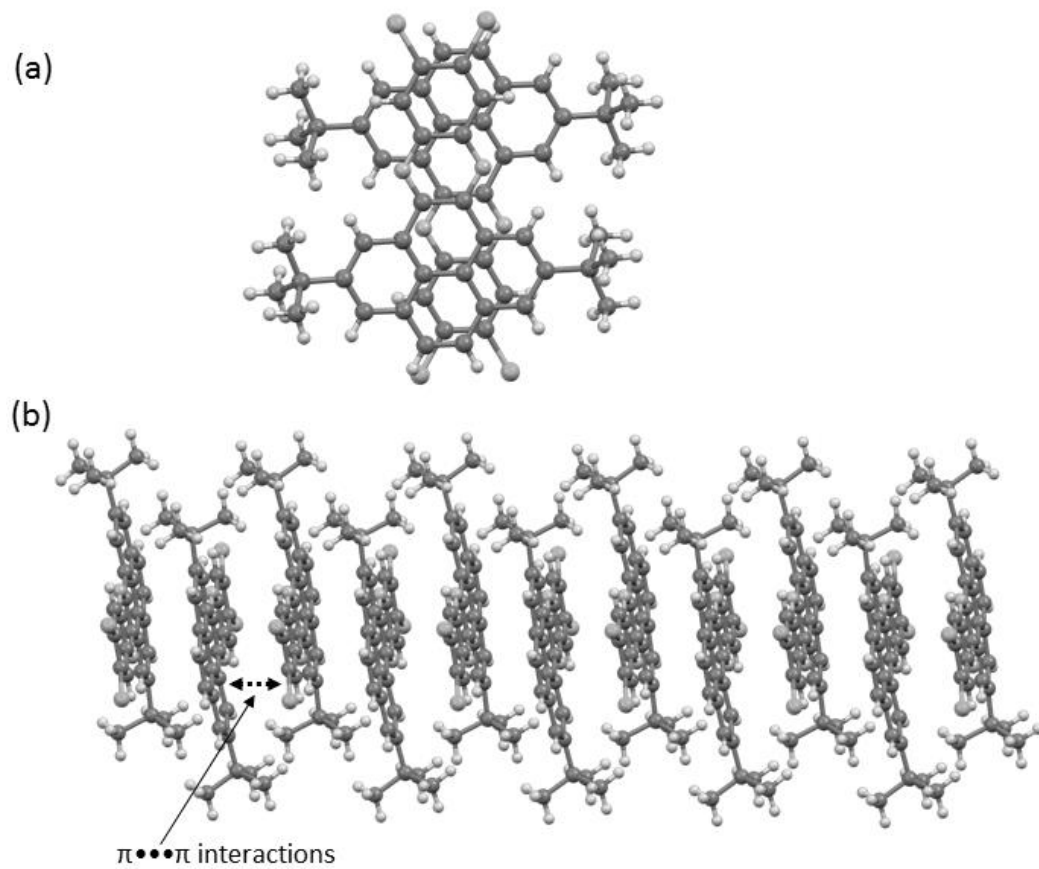
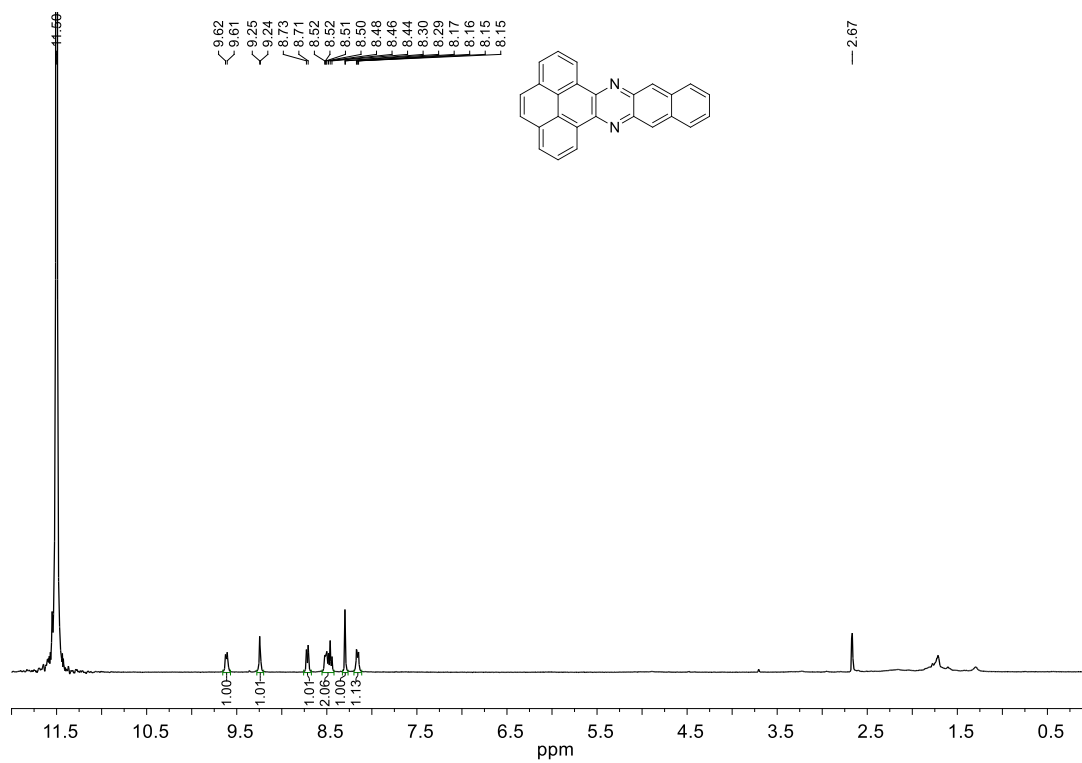
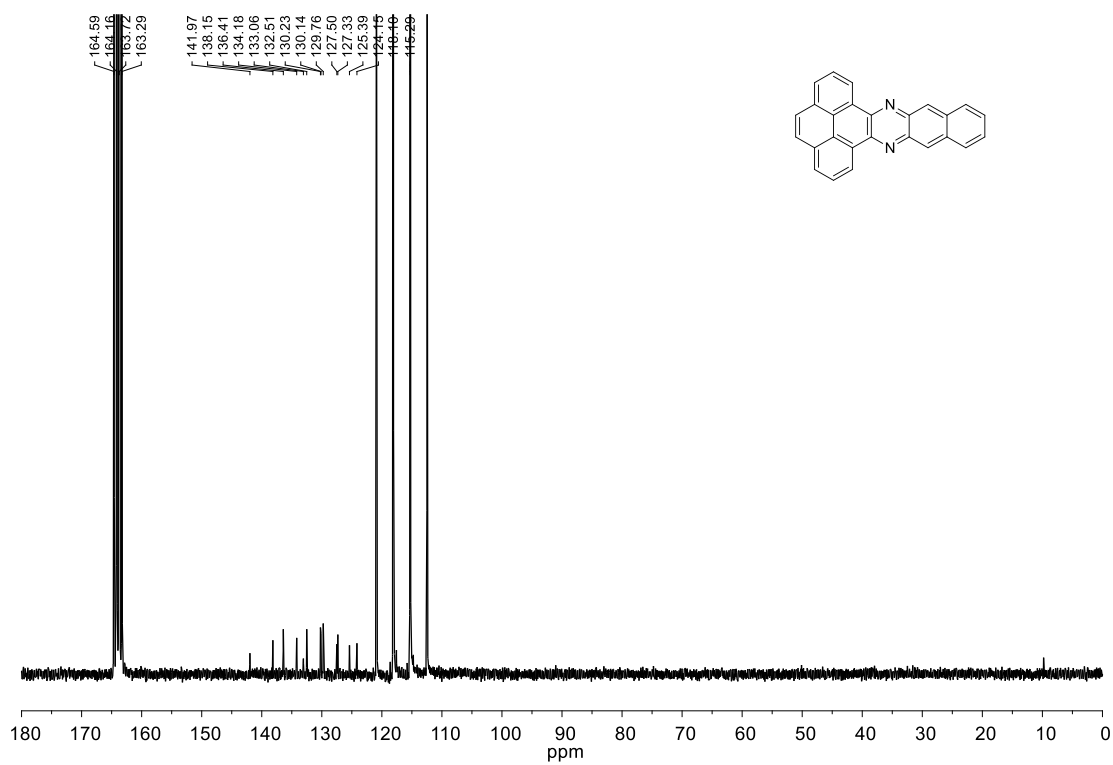


Figure 4.12. (a) Section of crystal packing of **3cf** viewed along the *a*-axis. (b) Crystal packing viewed along the *b*-axis to show $\pi \cdots \pi$ interactions between **3cf** molecules.

Figure 4.15. ¹H NMR spectrum of (**3ab**).Figure 4.16. ¹³C NMR spectrum of (**3ab**).

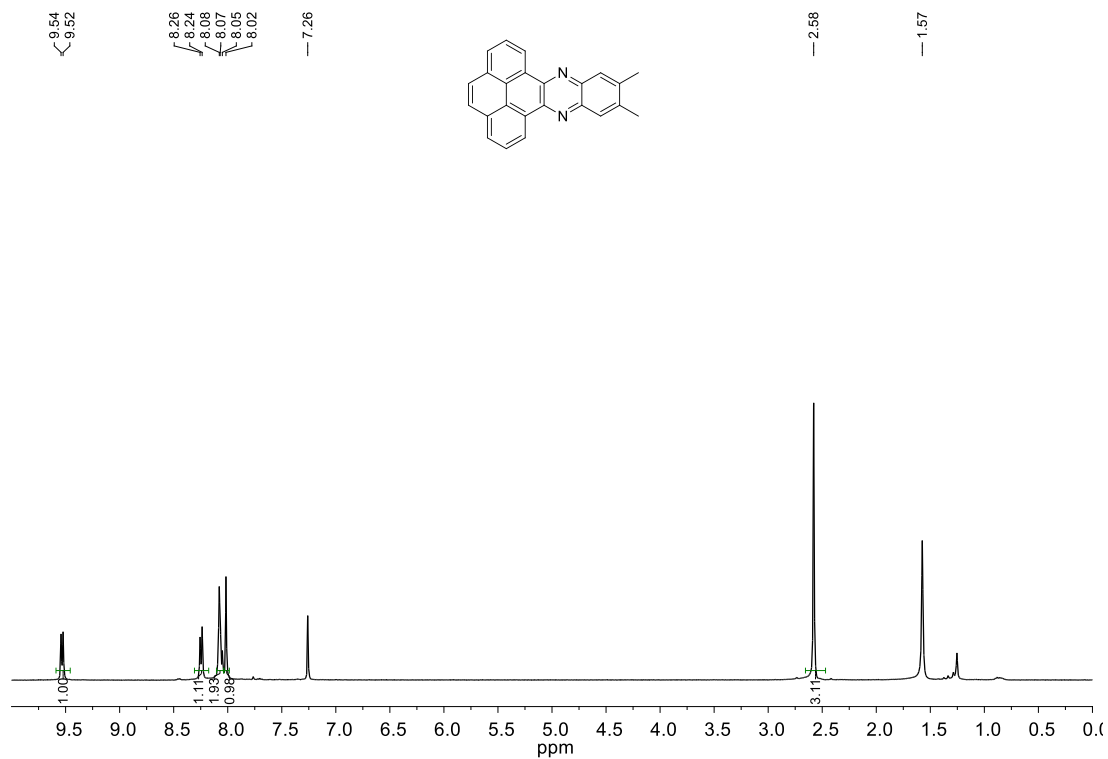


Figure 4.17. ¹H NMR spectrum of (**3ac**).

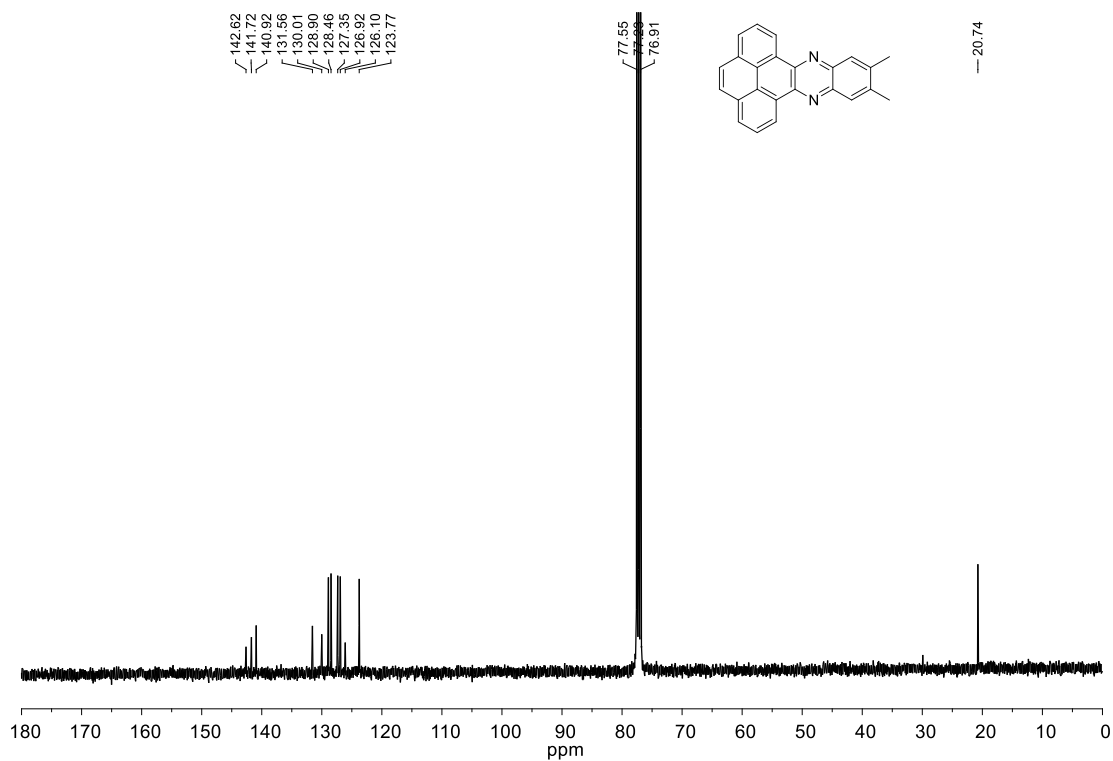


Figure 4.18. ¹³C NMR spectrum of (**3ac**).

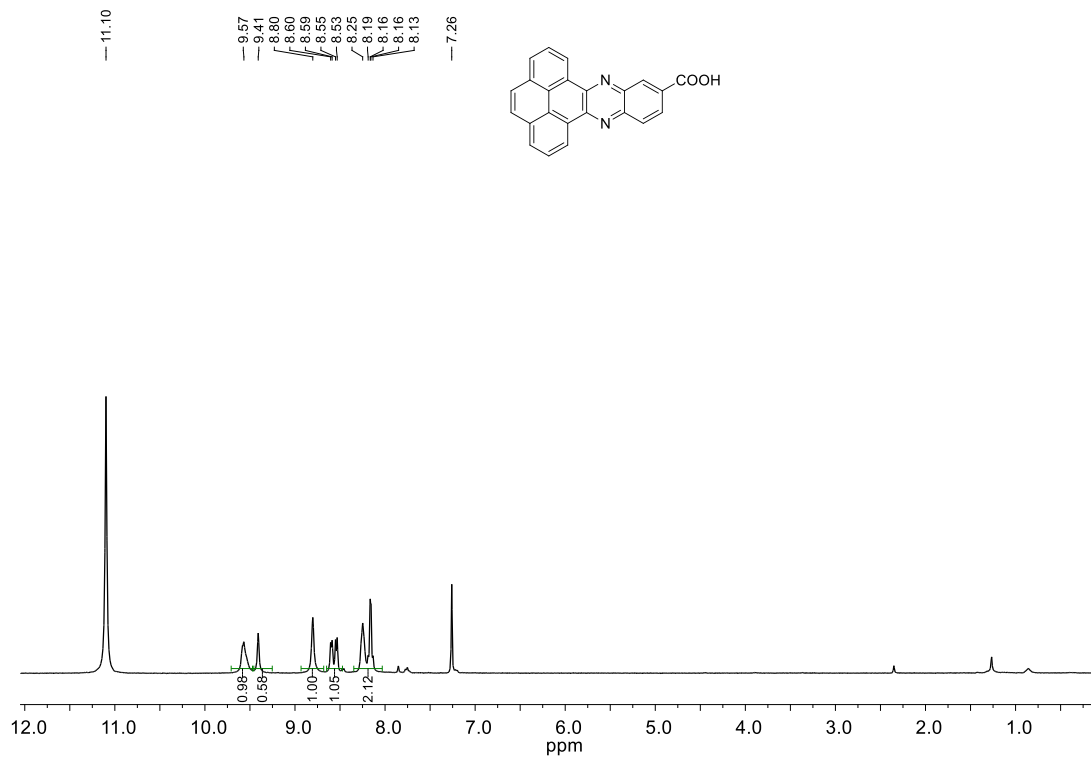


Figure 4.19. ^1H NMR spectrum of (**3ad**).

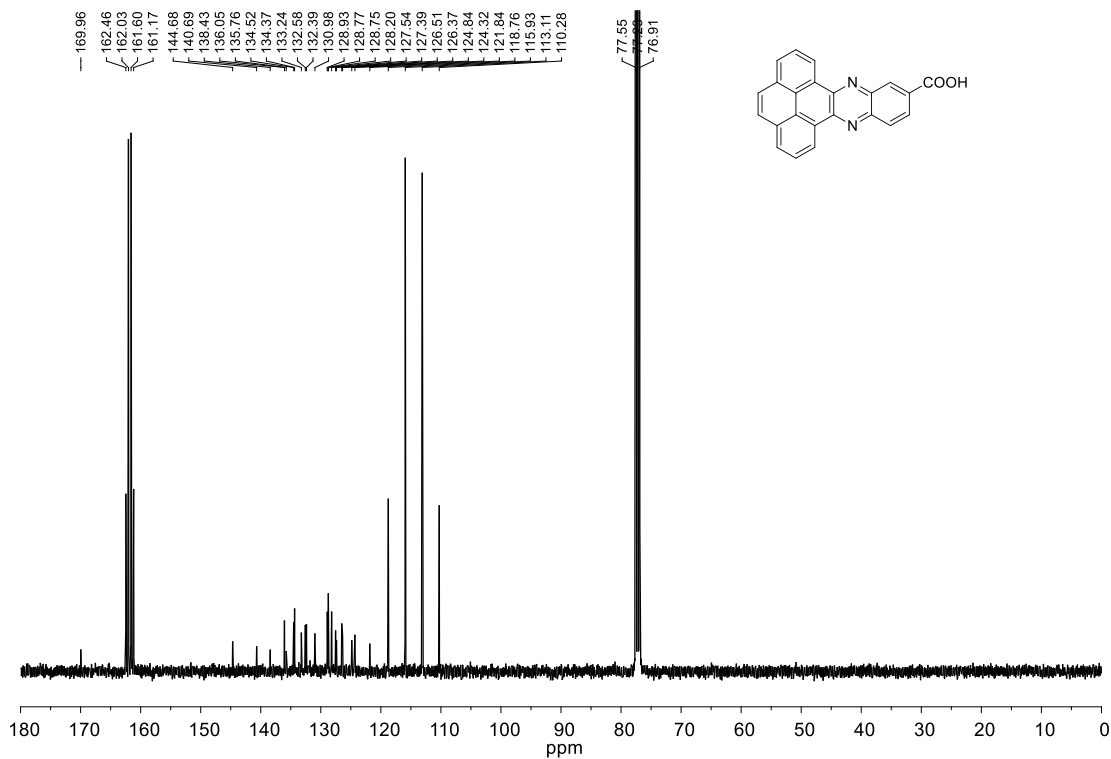


Figure 4.20. ^{13}C NMR spectrum of (**3ad**).

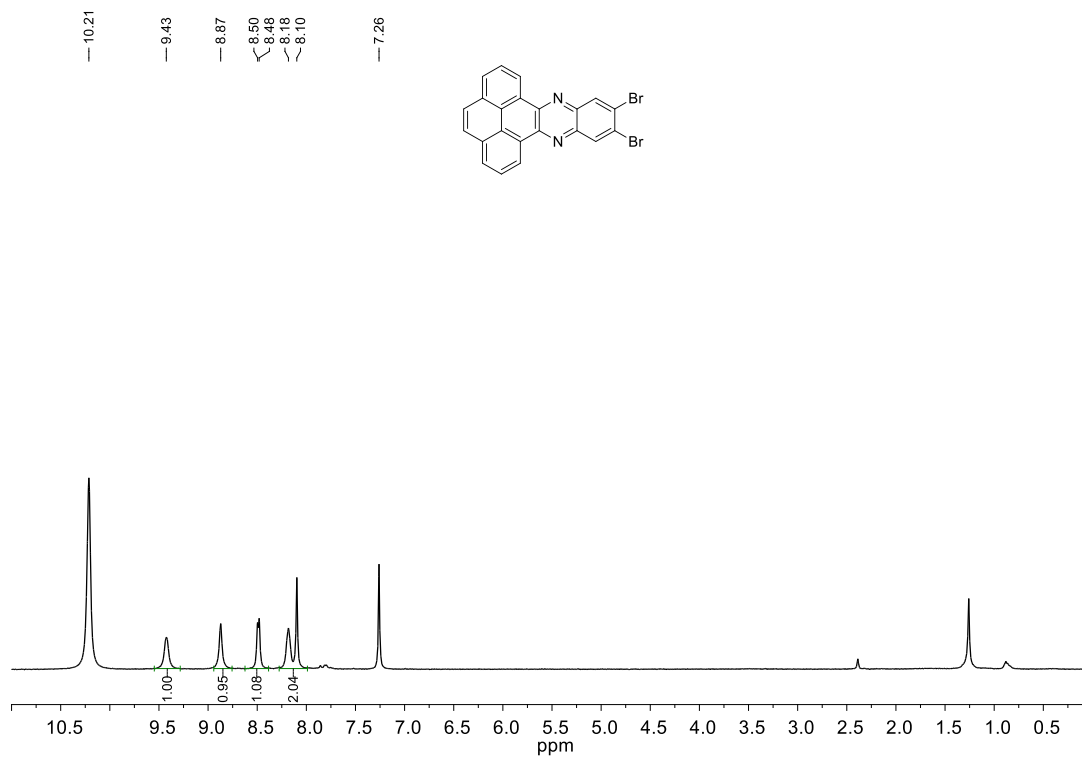


Figure 4.21. ¹H NMR spectrum of (**3ae**).

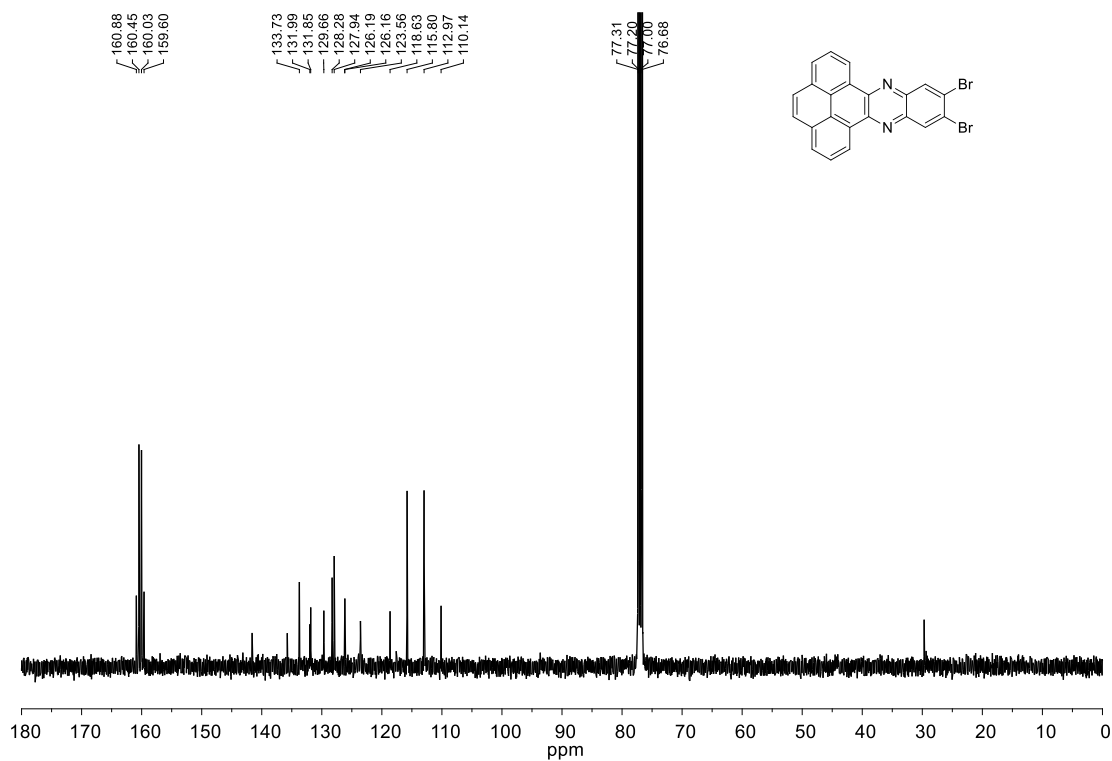


Figure 4.22. ¹³C NMR spectrum of (**3ae**).

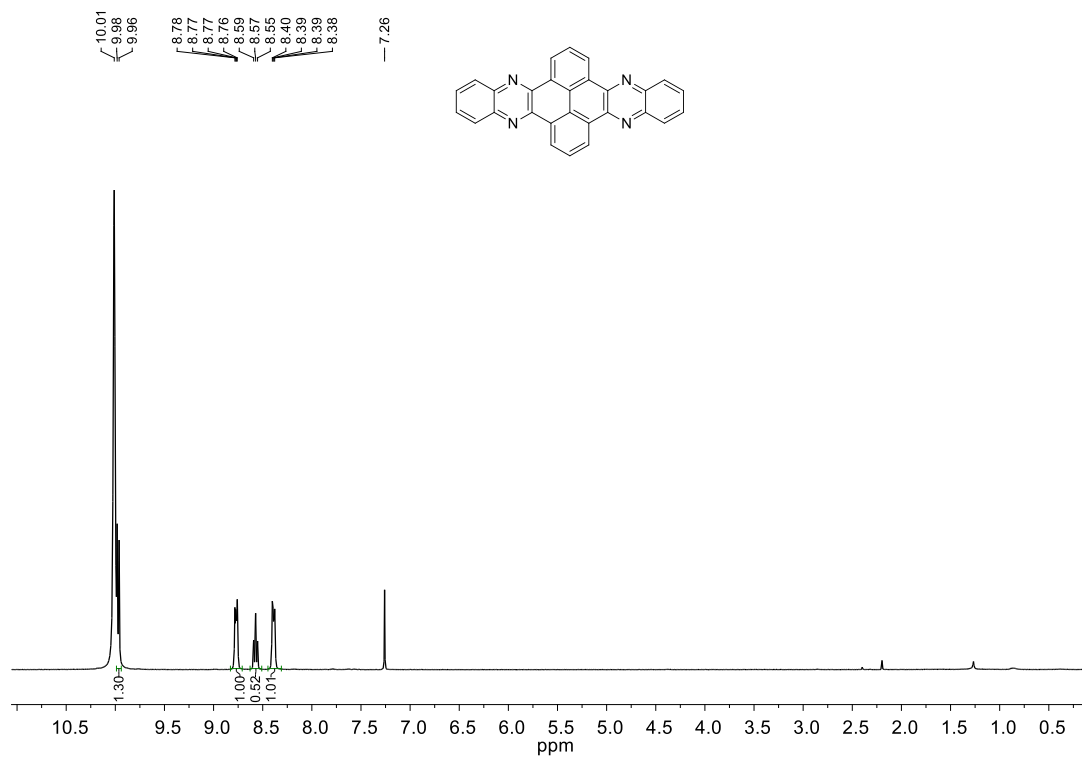


Figure 4.23. ^1H NMR spectrum of (3ba).

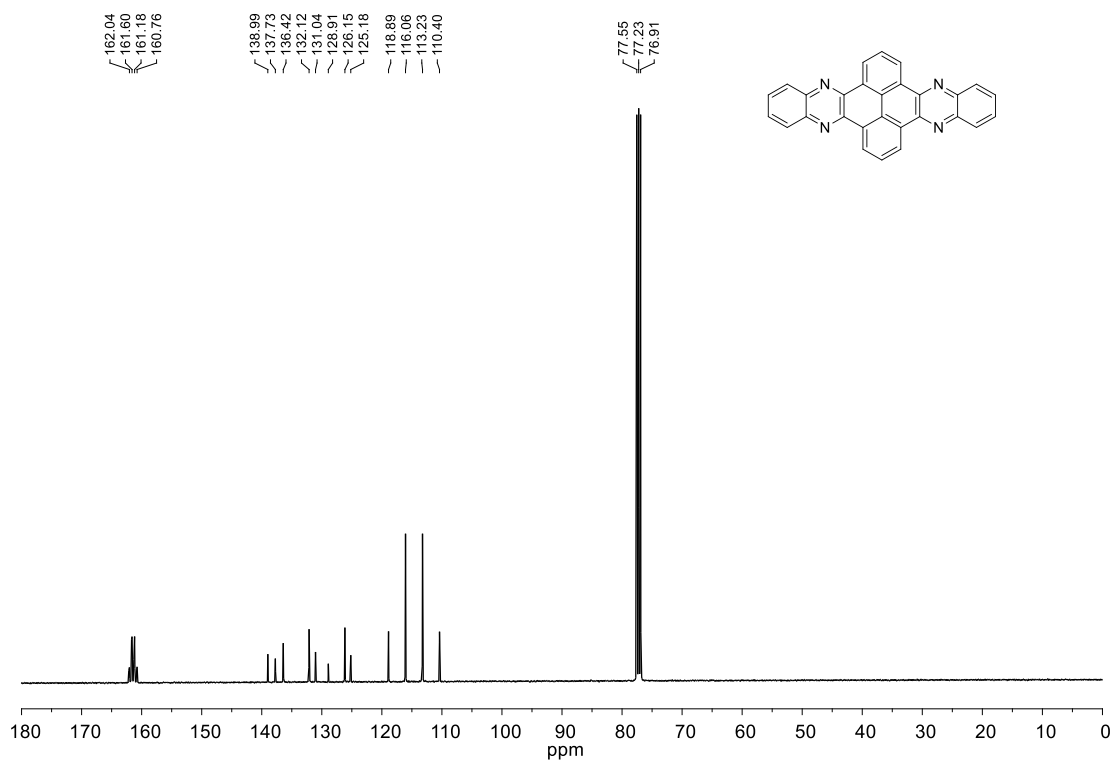


Figure 4.24. ^{13}C NMR spectrum of (3ba).

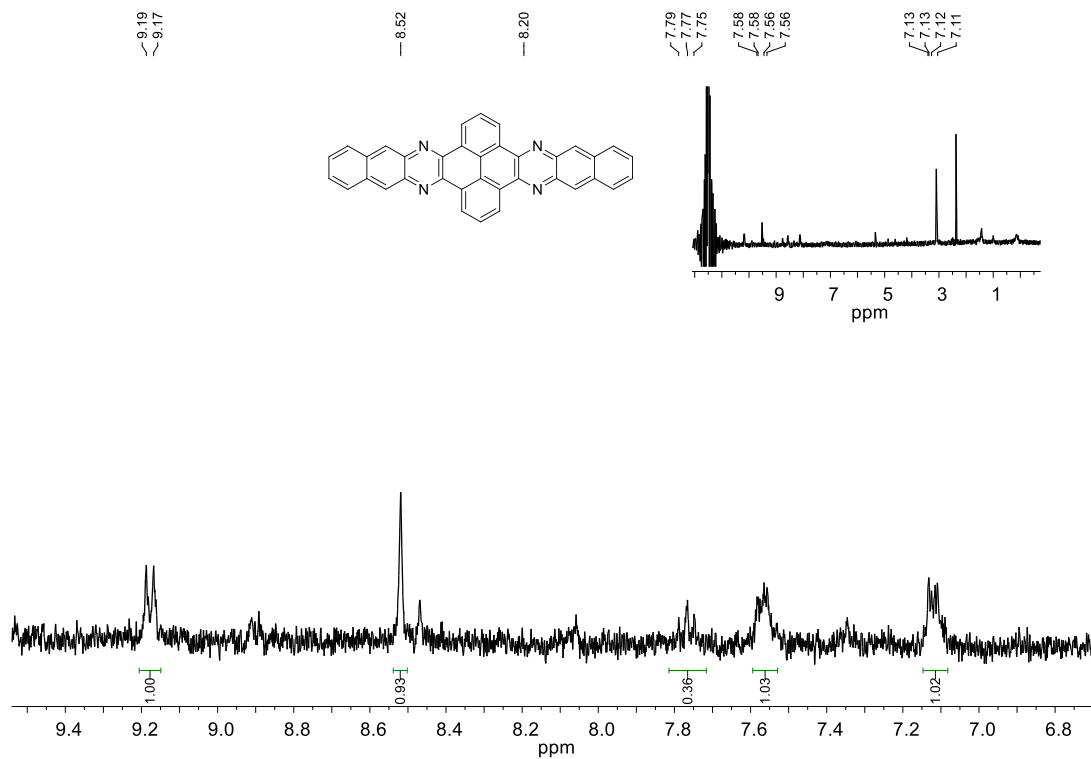


Figure 4.25. ^1H NMR spectrum of **(3bb)**.

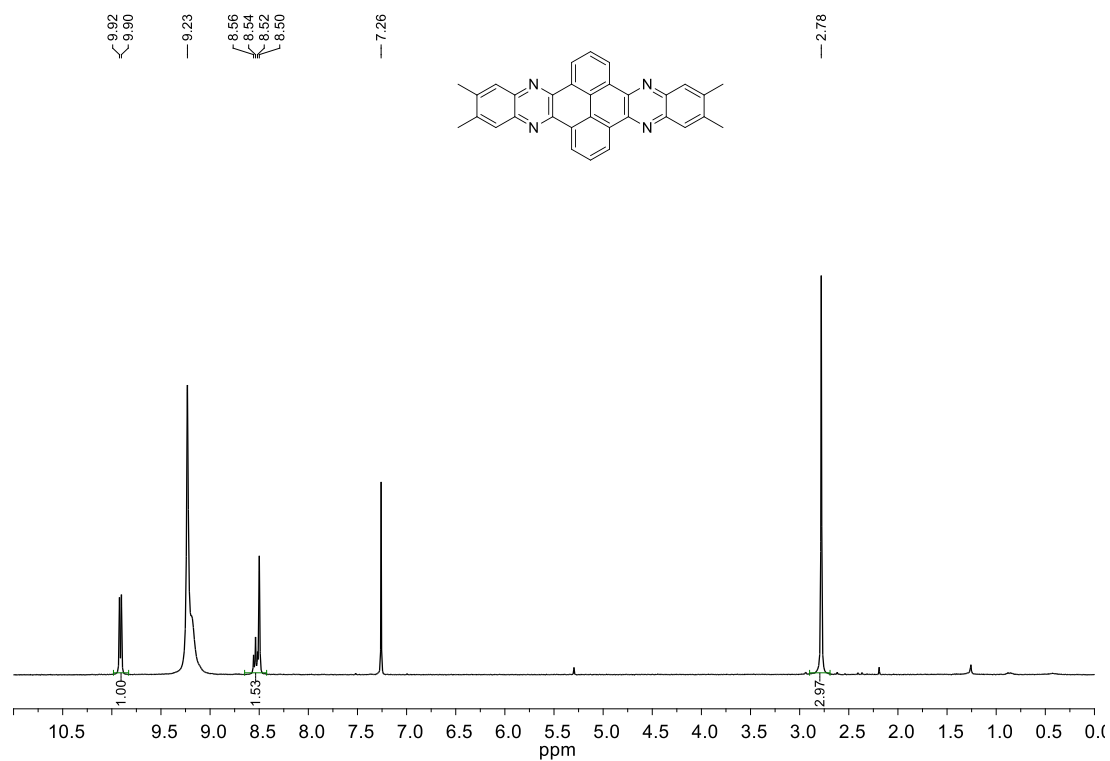


Figure 4.26. ^1H NMR spectrum of **(3bc)**.

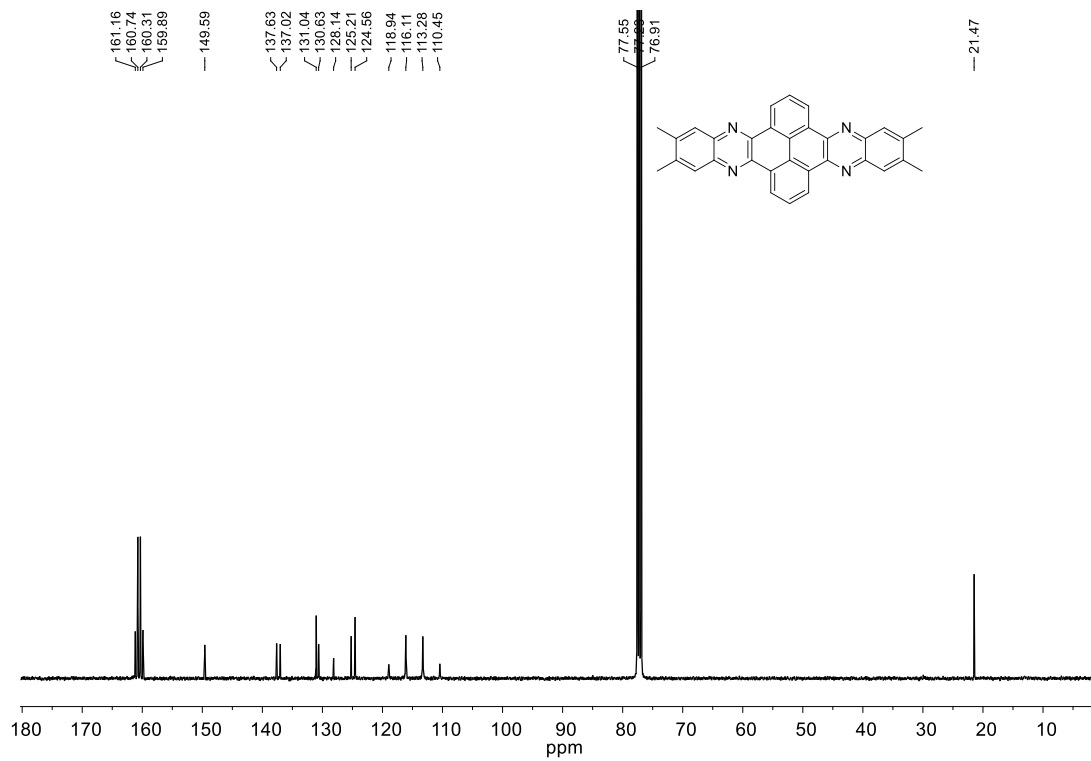


Figure 4.27. ^{13}C NMR spectrum of **(3bc)**.

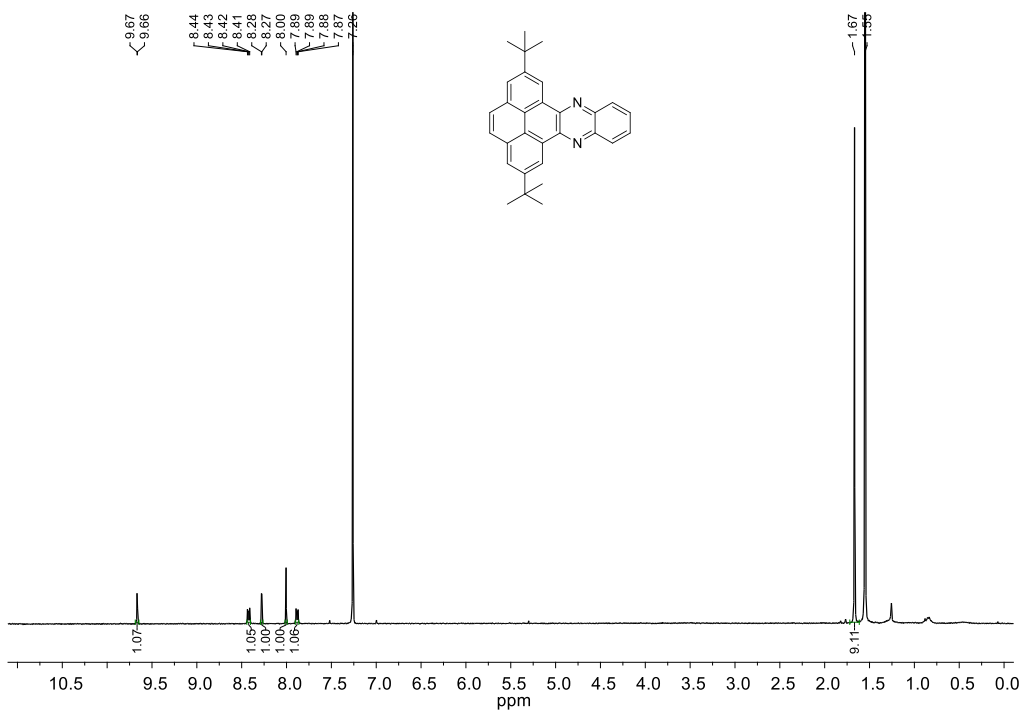


Figure 4.28. ^1H NMR spectrum of **(3ca)**.

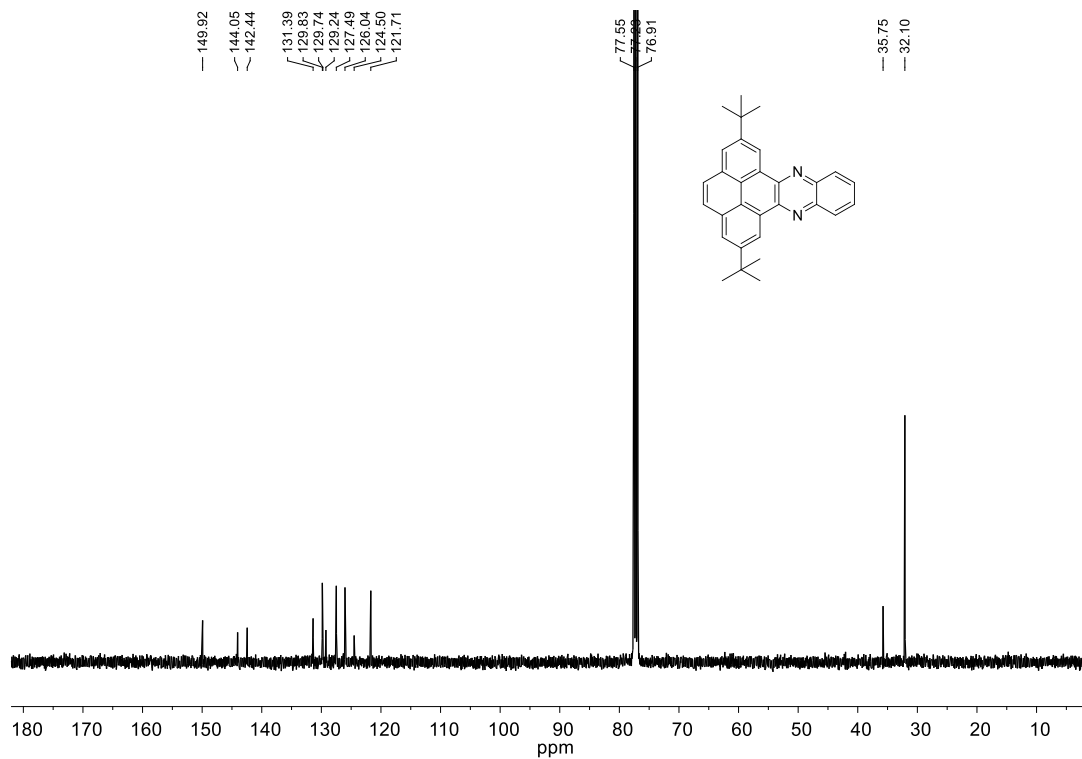


Figure 4.29. ^{13}C NMR spectrum of (**3ca**).

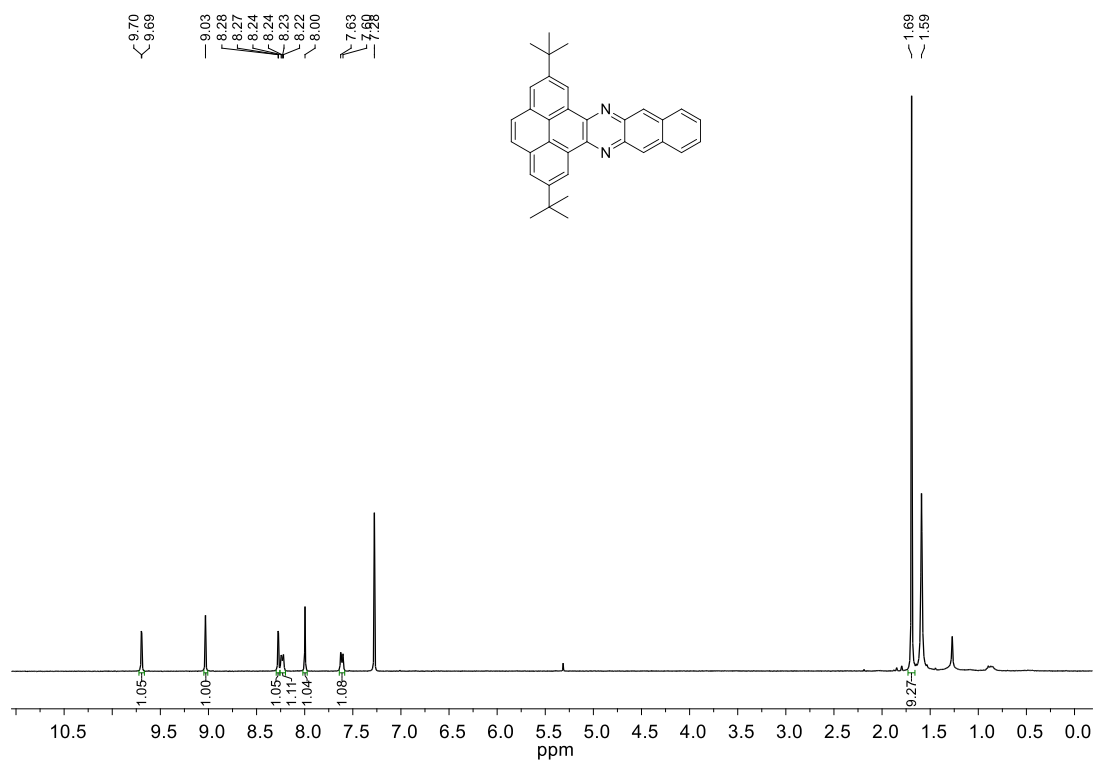


Figure 4.30. ^1H NMR spectrum of (**3cb**).

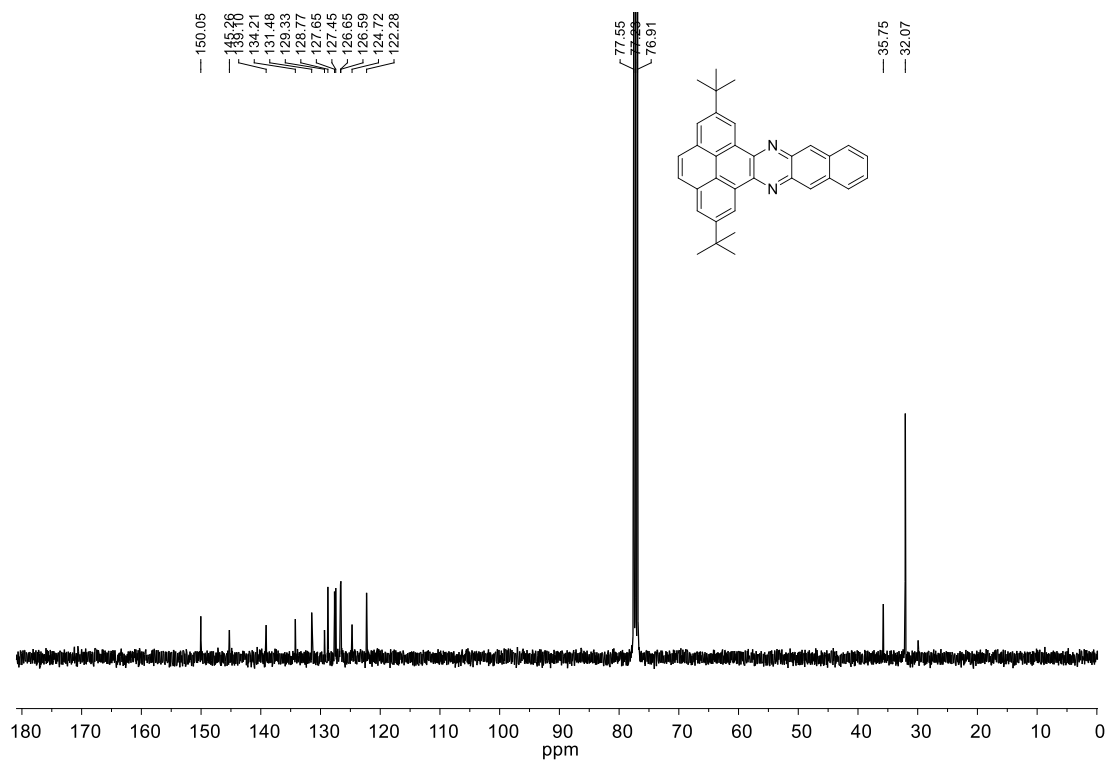


Figure 4.31. ^{13}C NMR spectrum of **(3cb)**.

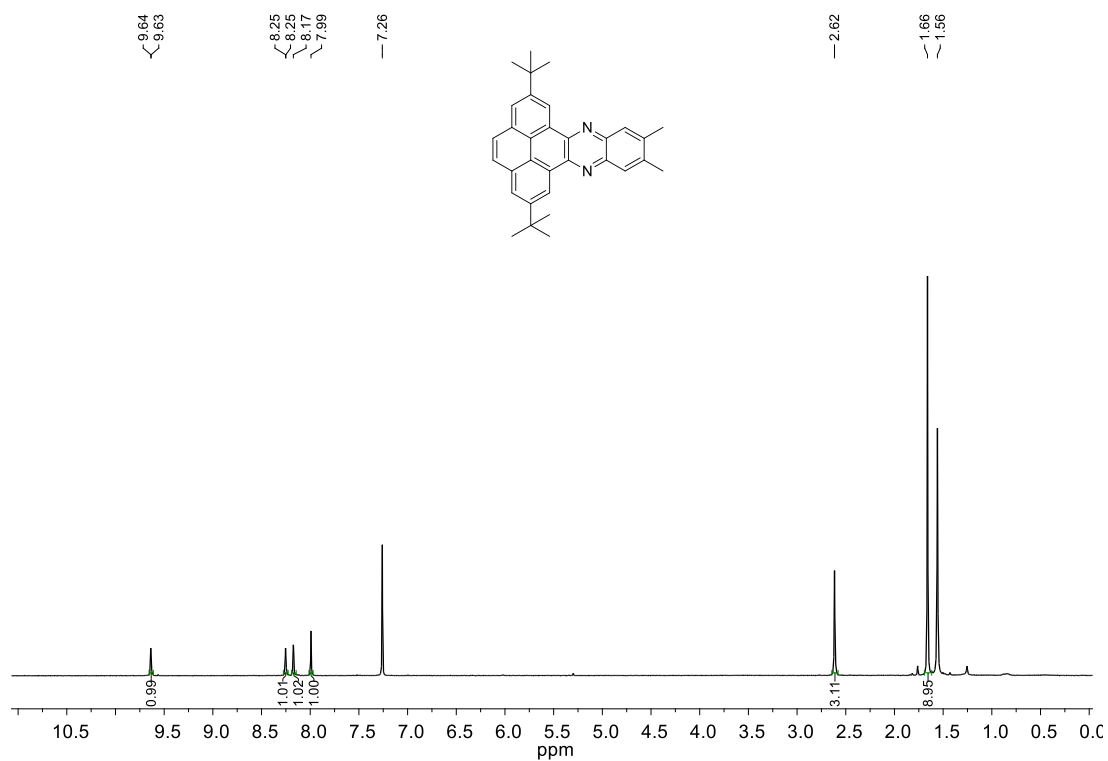


Figure 4.32. ^1H NMR spectrum of **(3cc)**.

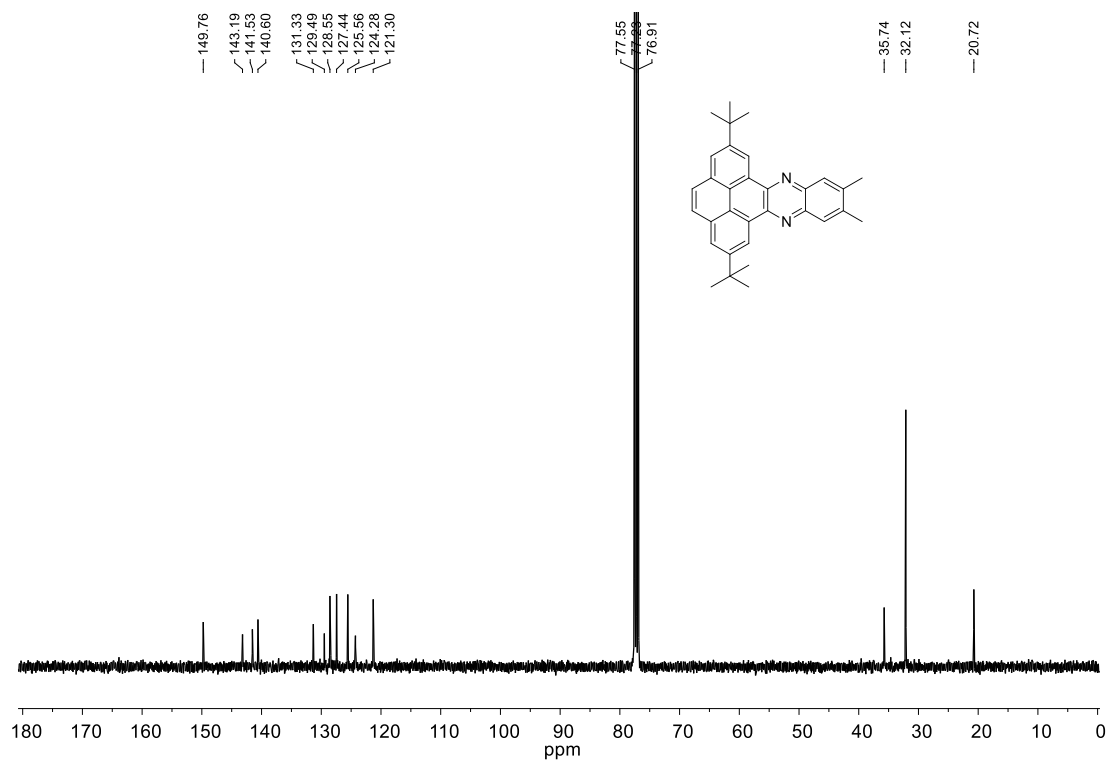


Figure 4.33. ^{13}C NMR spectrum of (**3cc**).

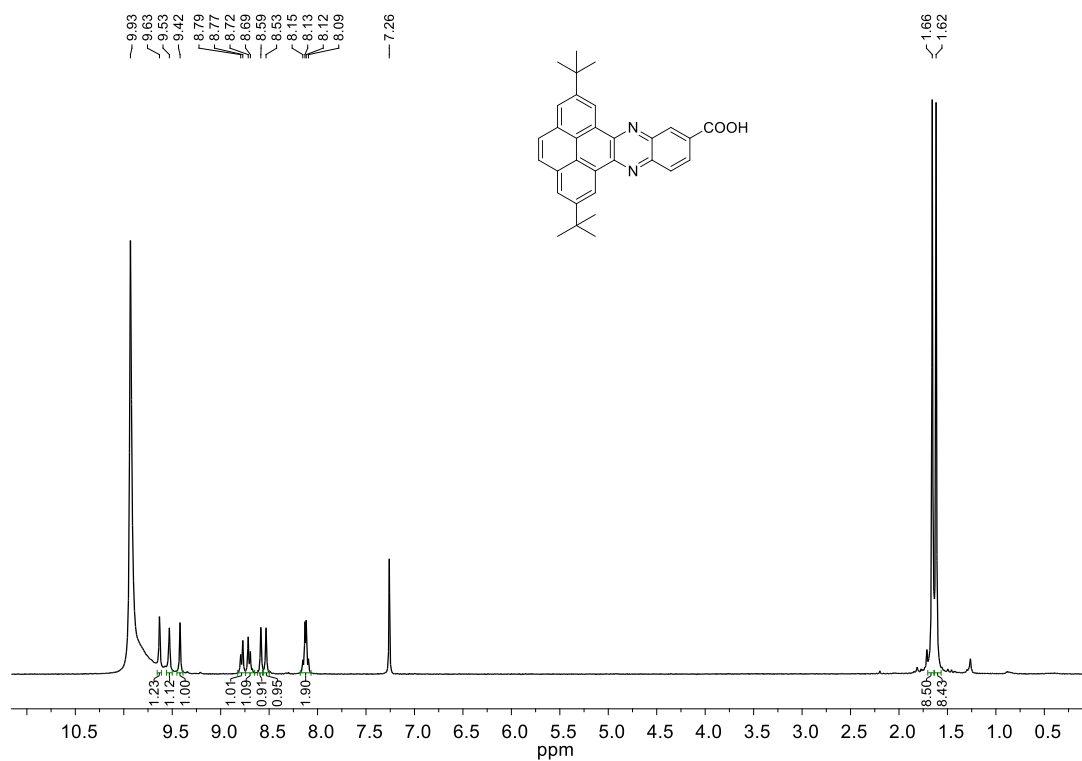
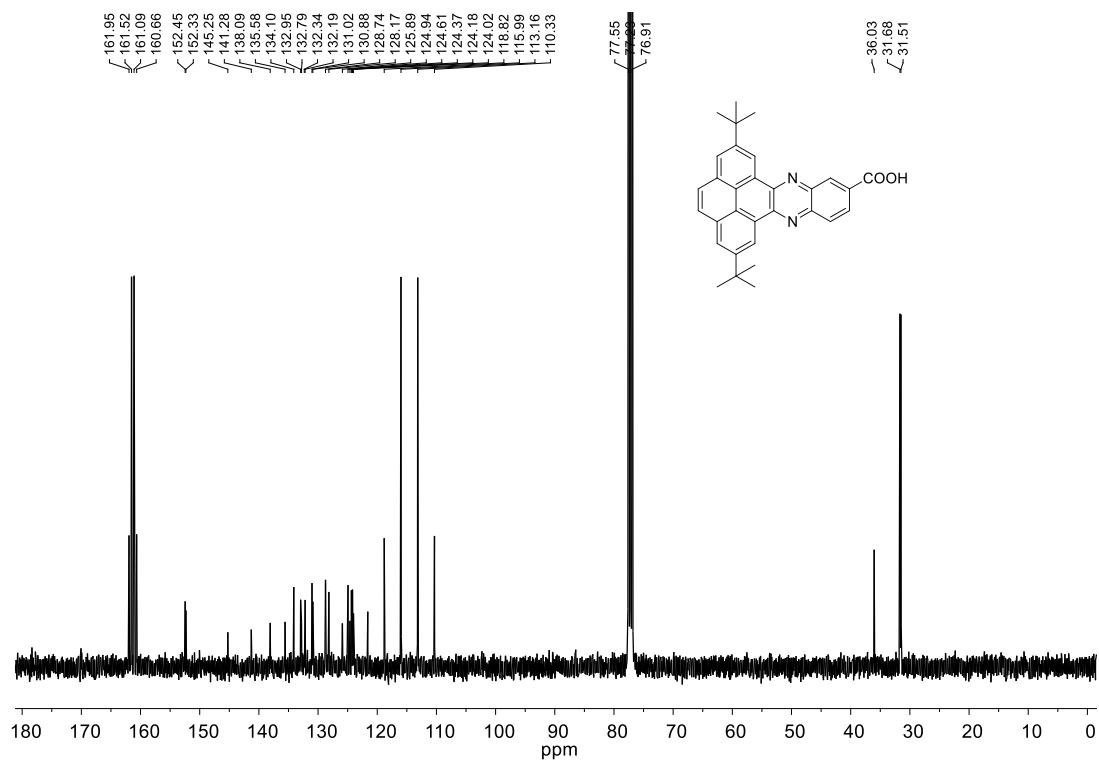
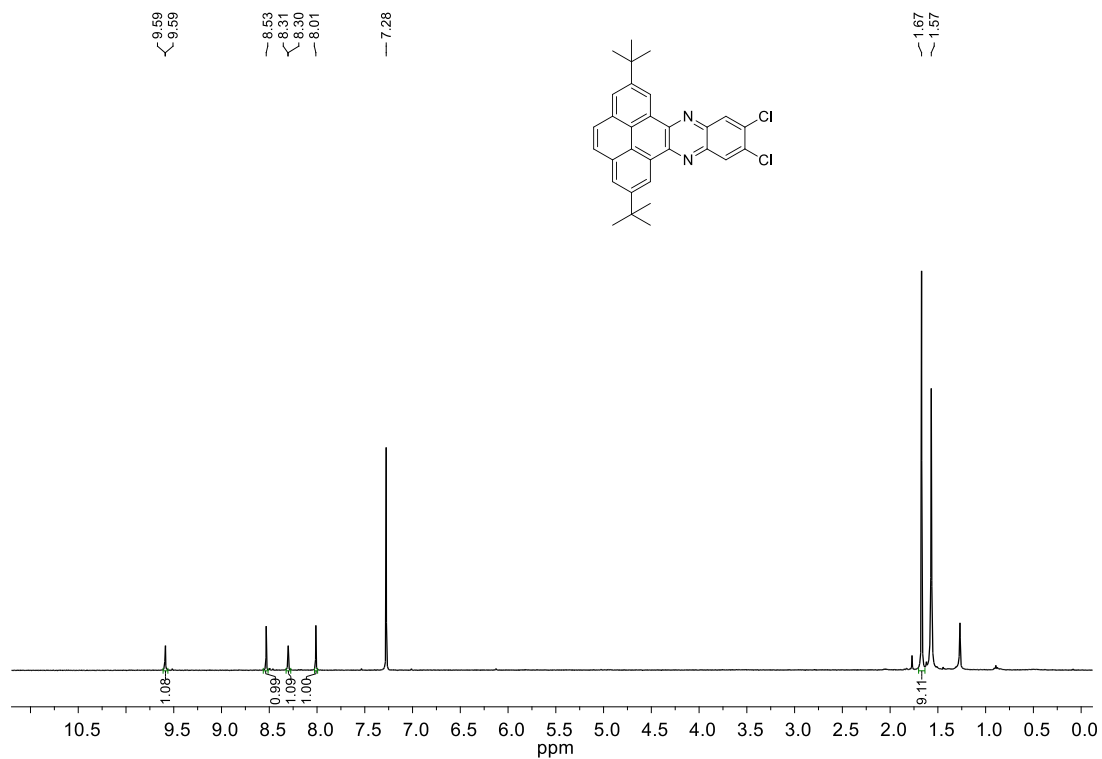


Figure 4.34. ^1H NMR spectrum of (**3cd**).

Figure 4.35. ^{13}C NMR spectrum of (**3cd**).Figure 4.36. ^1H NMR spectrum of (**3cf**).

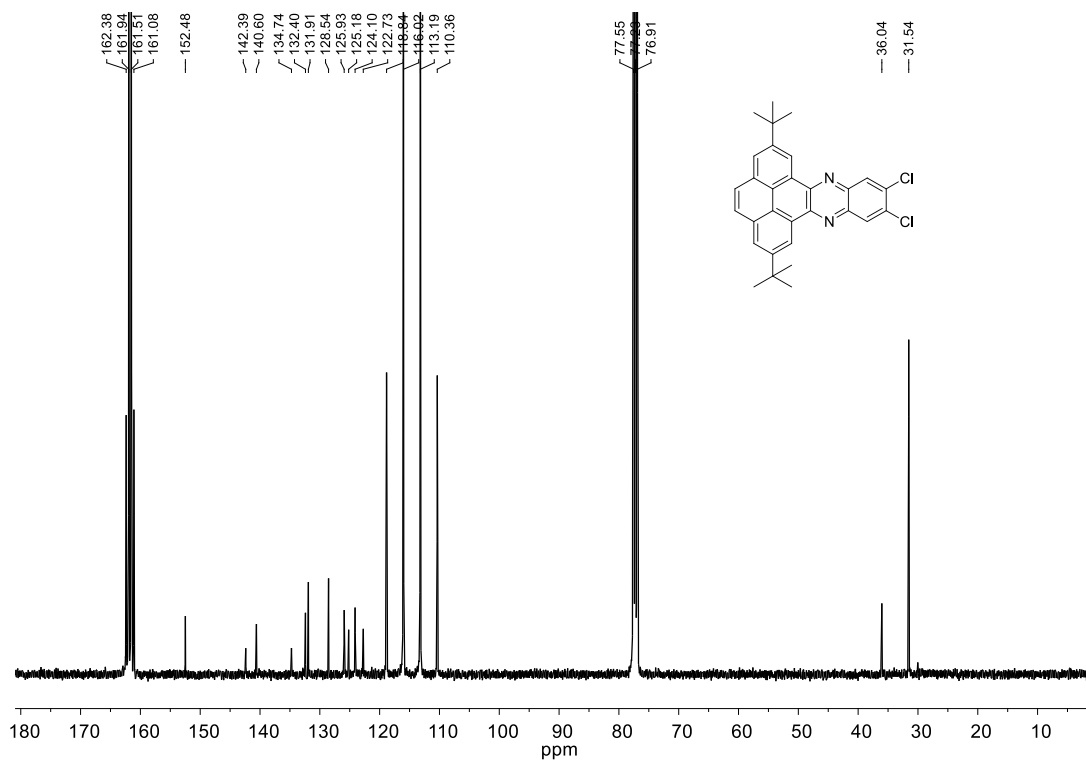


Figure 4.37. ^{13}C NMR spectrum of (**3cf**).

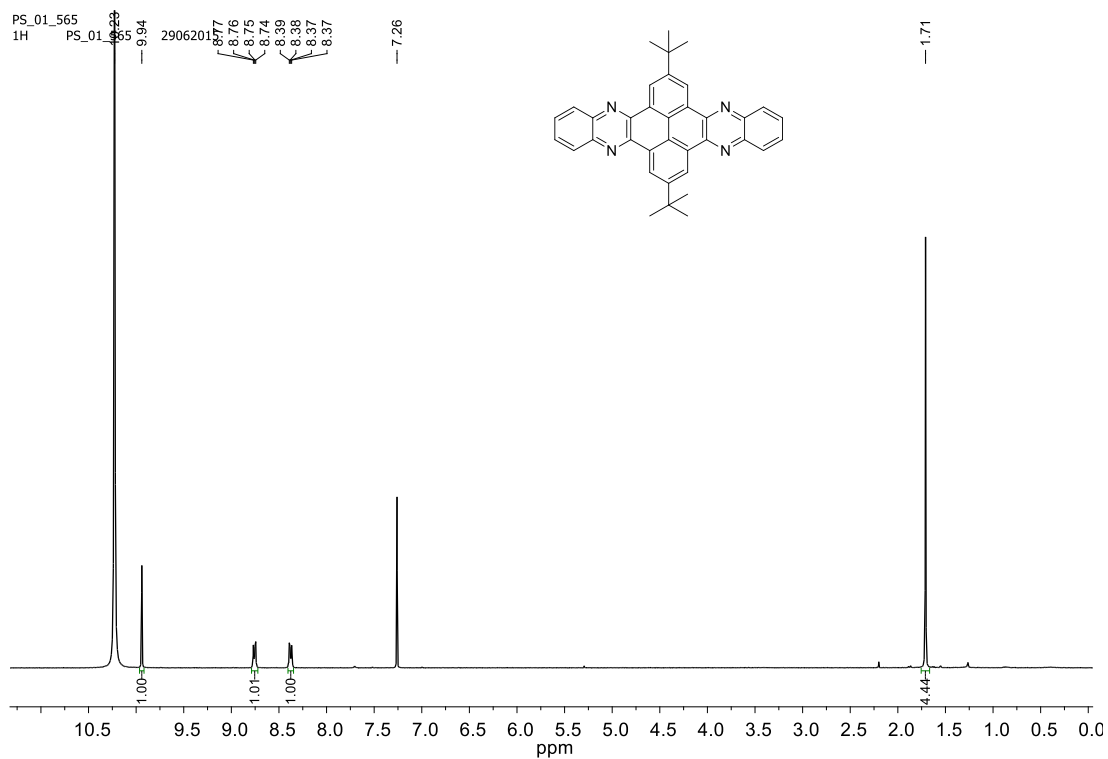


Figure 4.38. ^1H NMR spectrum of (**3da**).

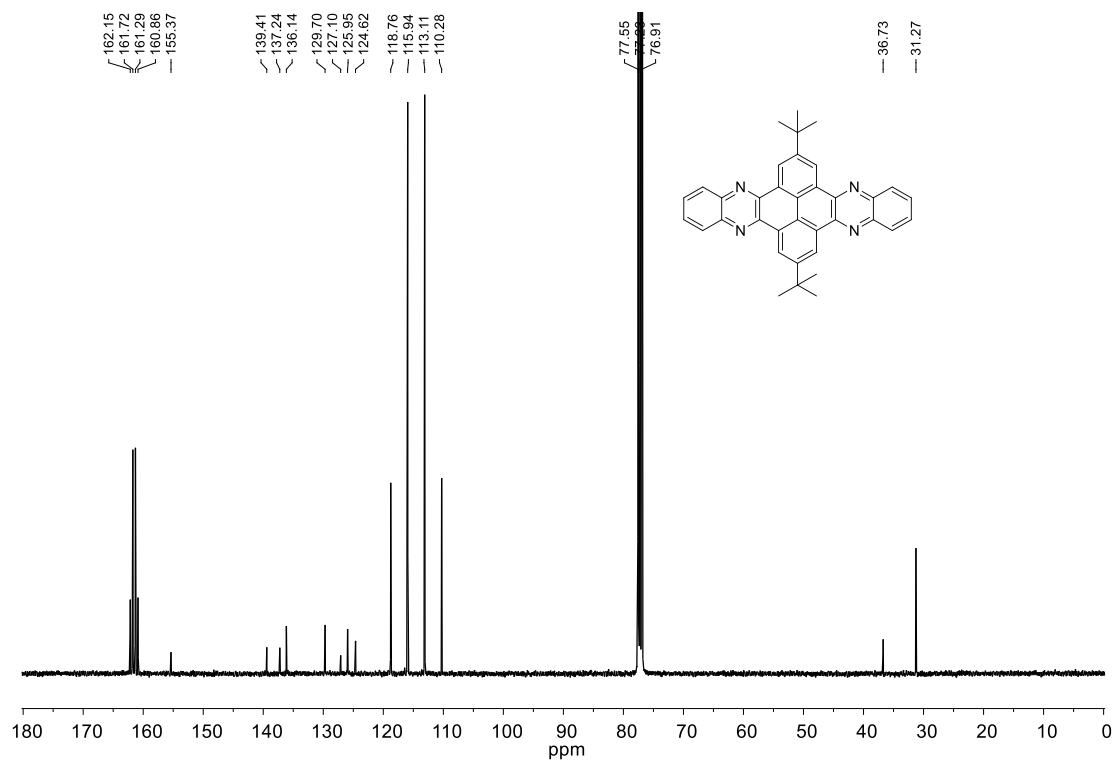


Figure 4.39. ^{13}C NMR spectrum of (**3da**).

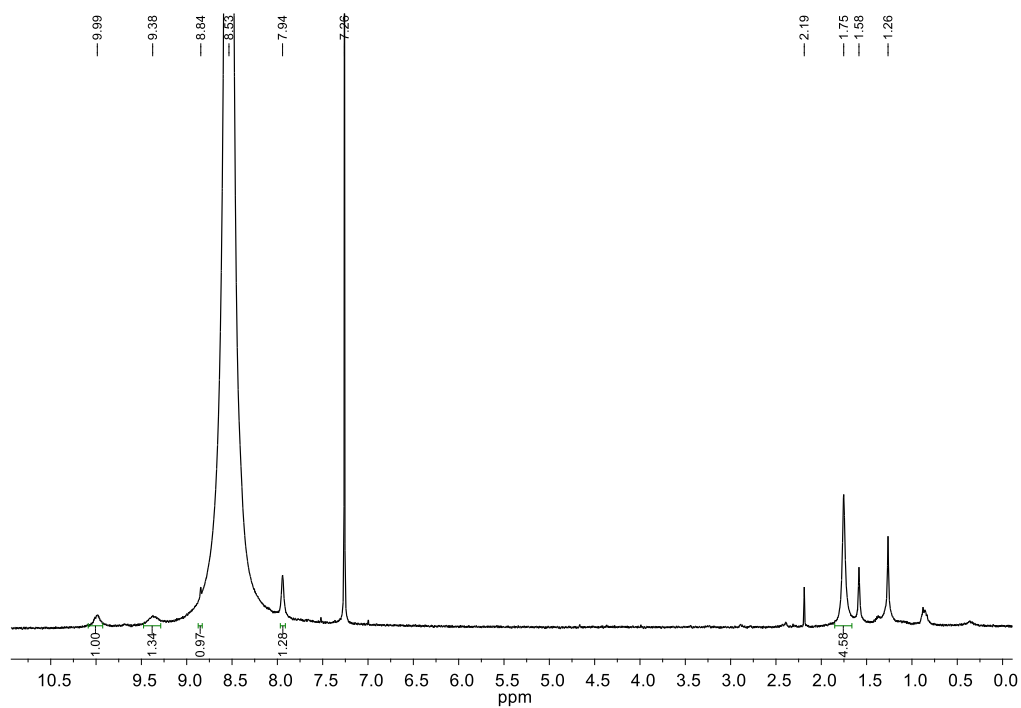


Figure 4.40. ^1H NMR spectrum of (**3db**).

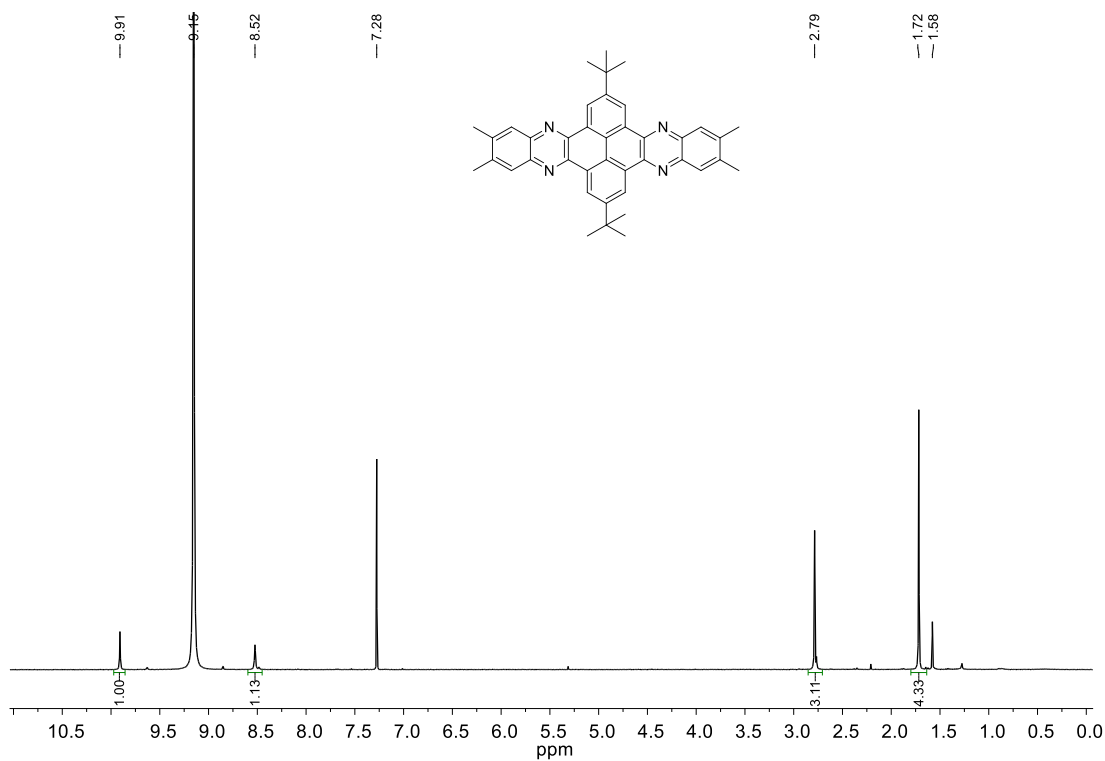


Figure 4.41. ^1H NMR spectrum of (**3dc**).

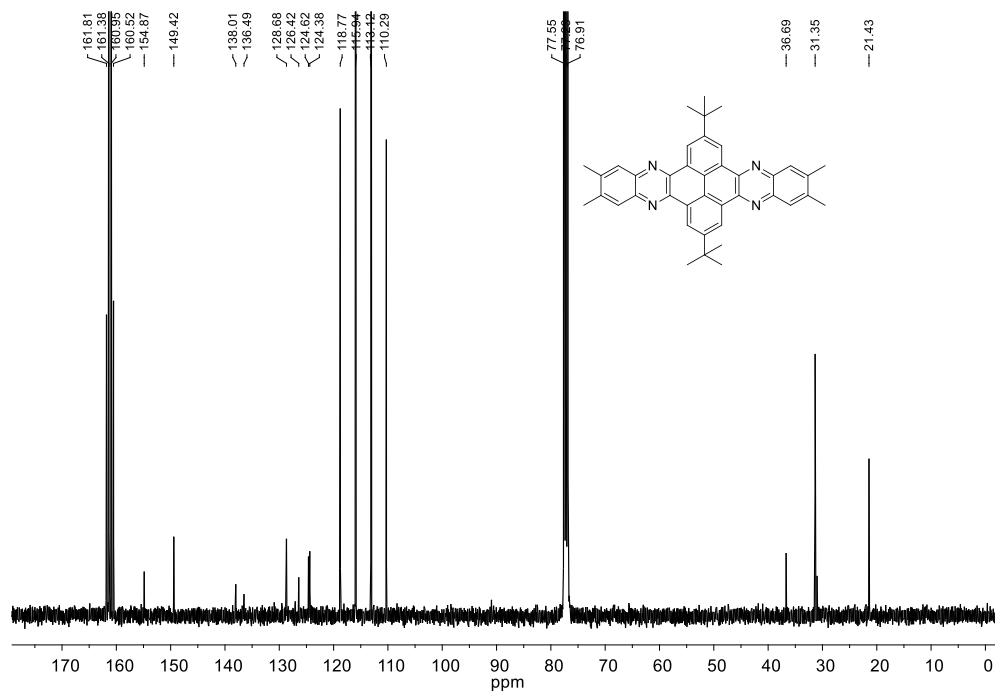
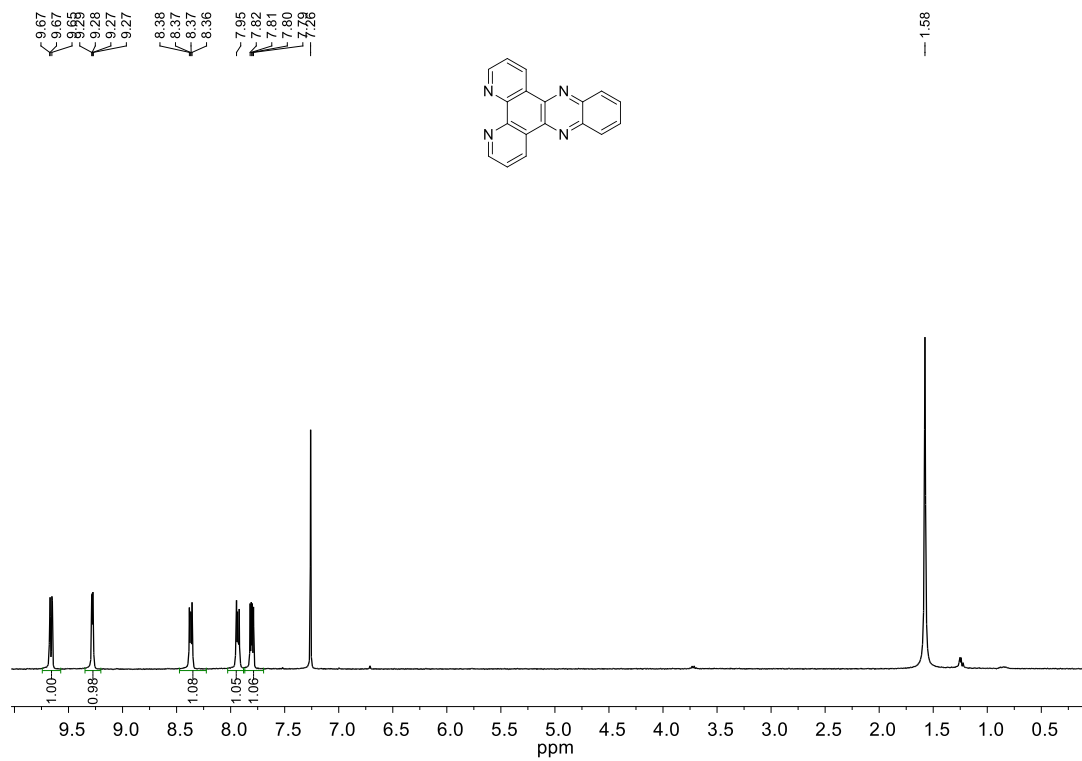
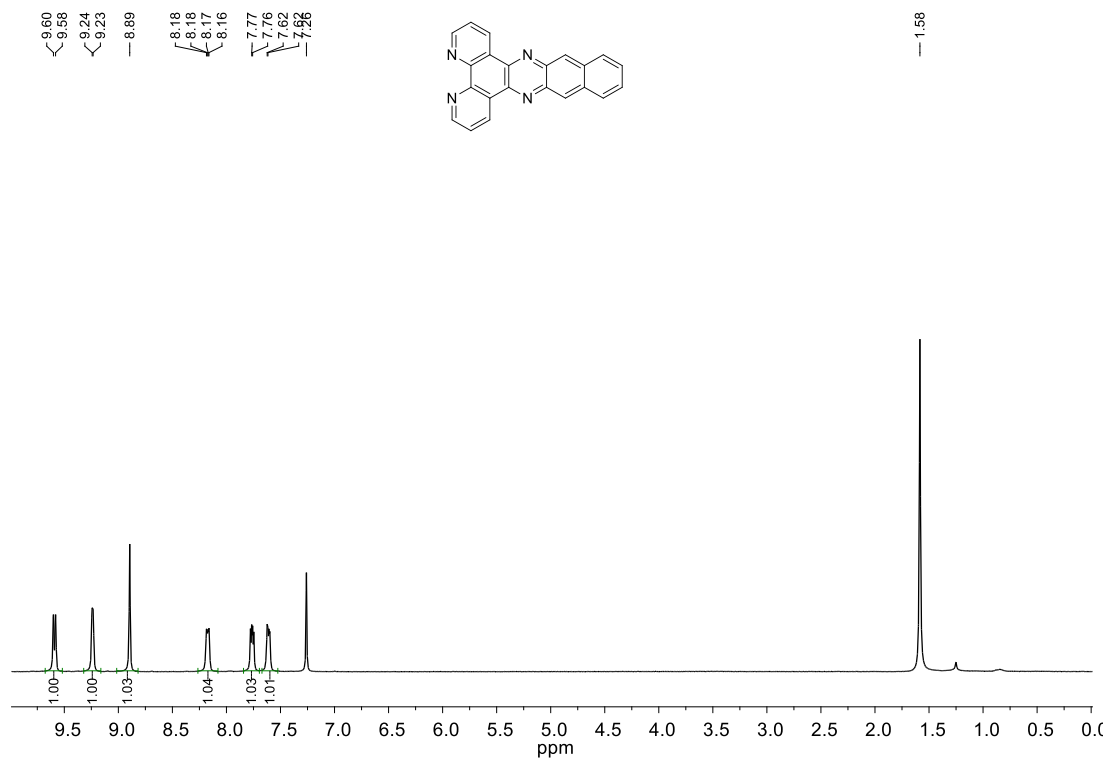


Figure 4.42. ^{13}C NMR spectrum of (**3dc**).

Figure 4.43. ¹H NMR spectrum of **(3ea)**.Figure 4.44. ¹H NMR spectrum of **(3eb)**.

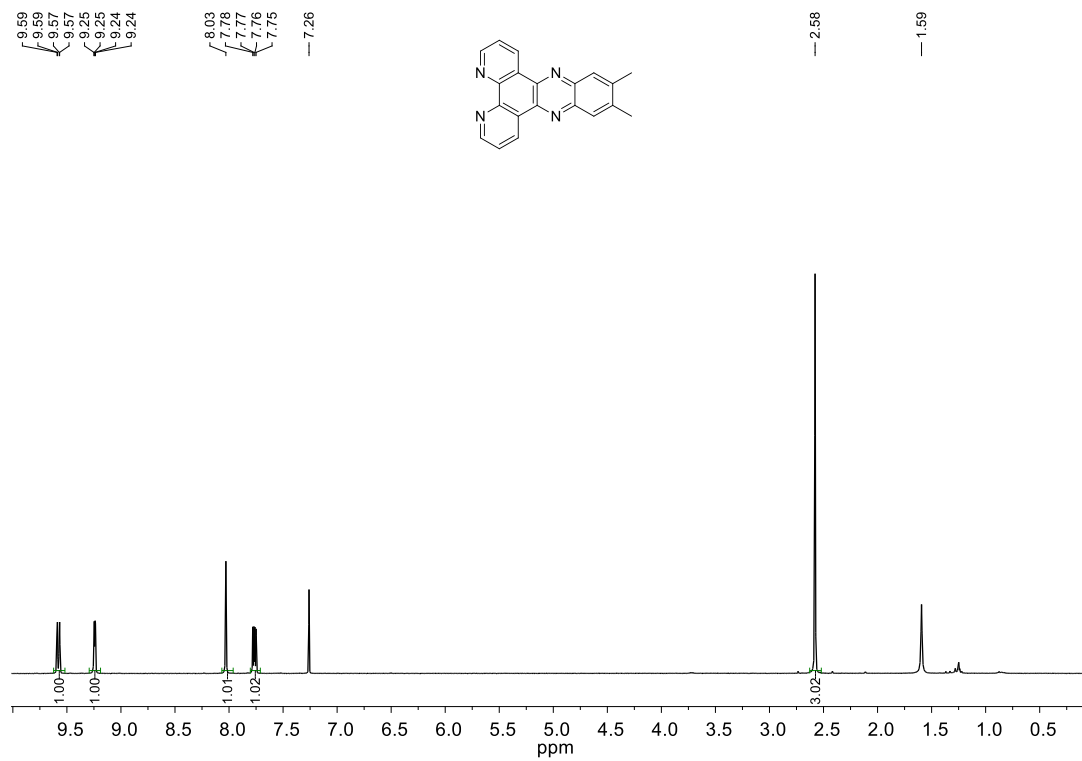


Figure 4.45. ^1H NMR spectrum of (**3ec**).

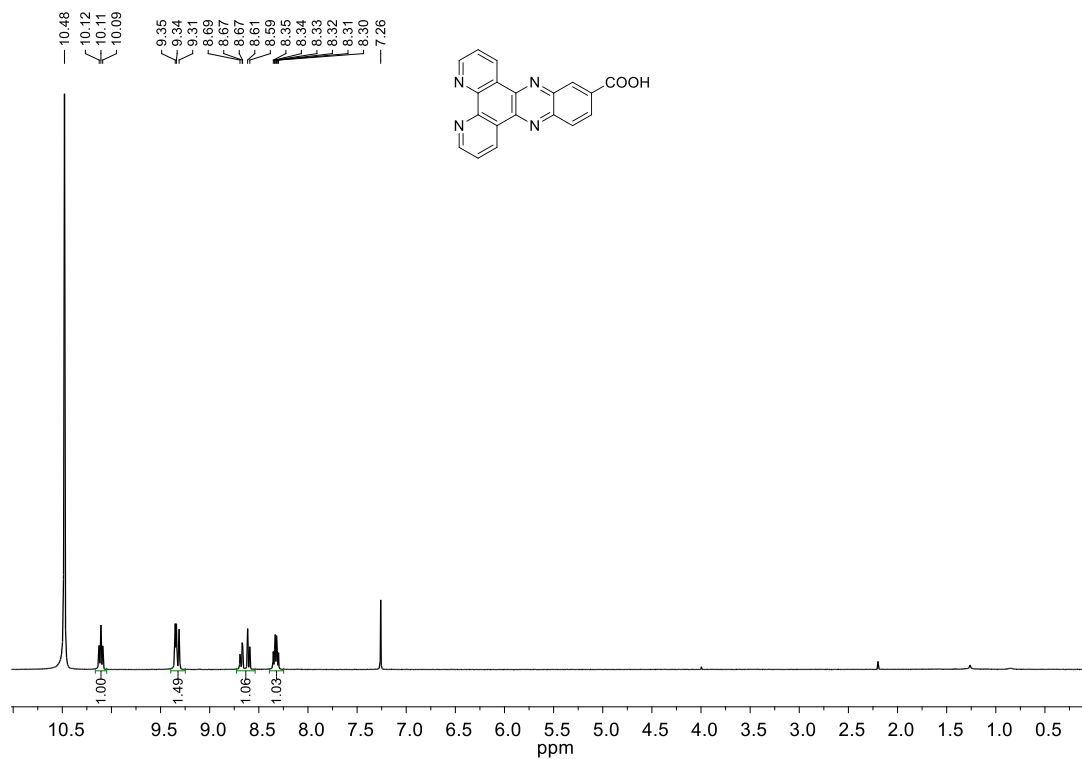
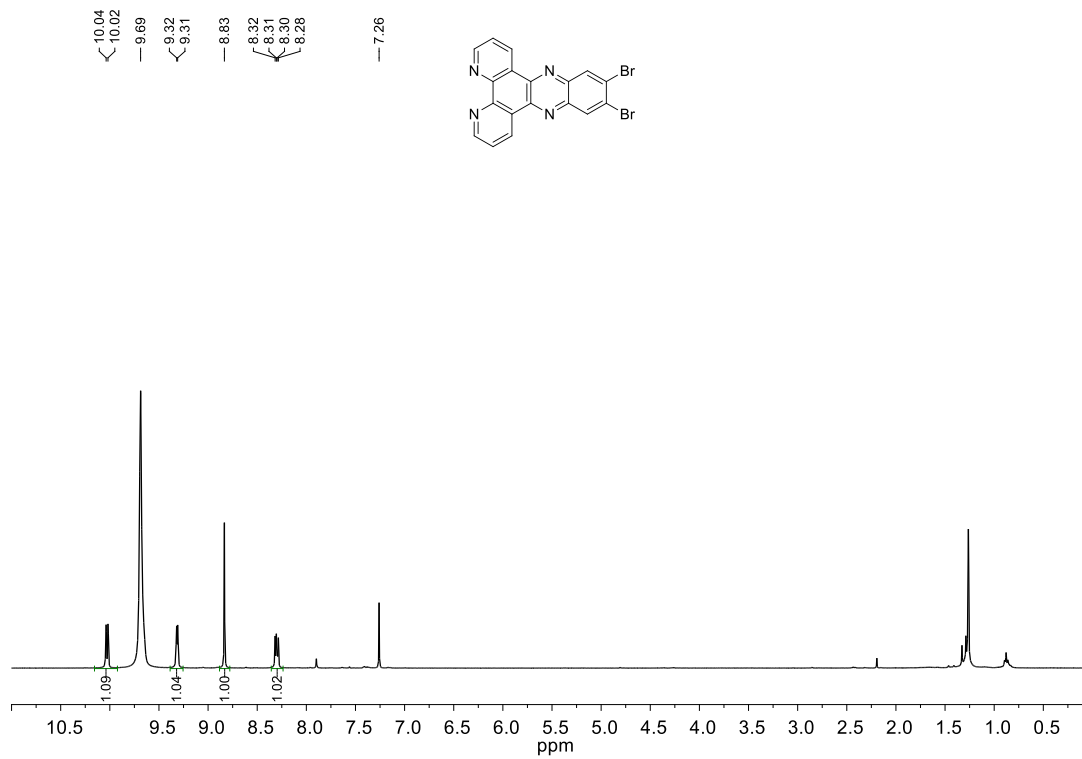
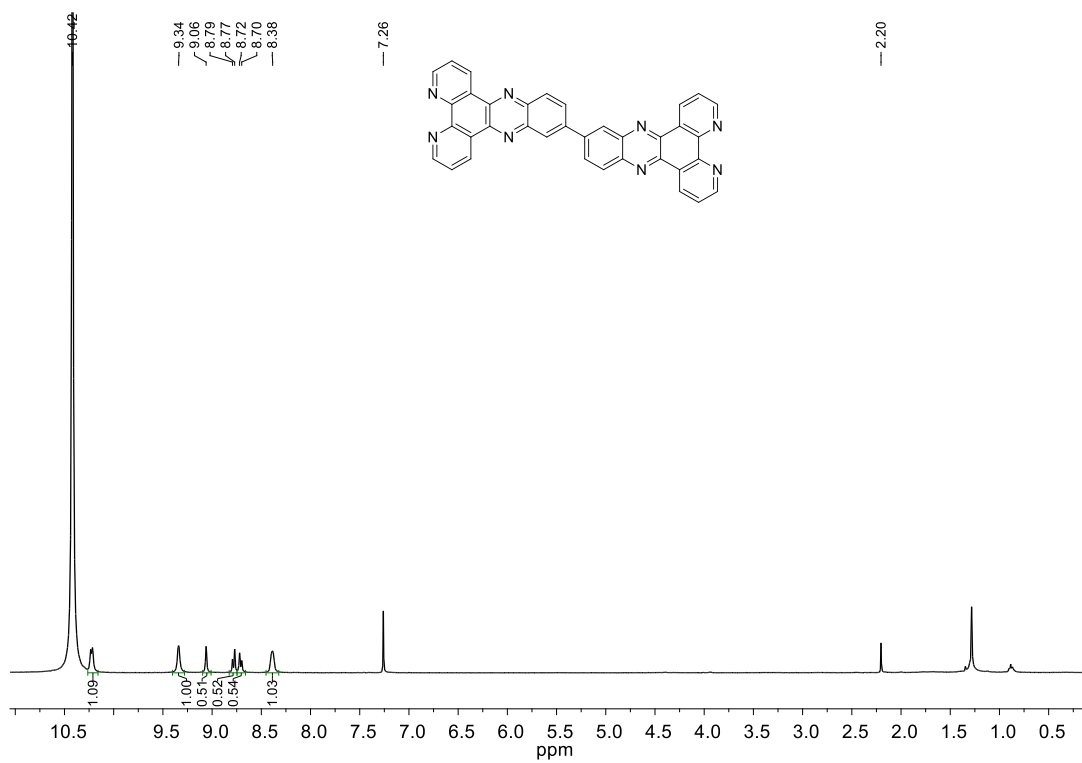


Figure 4.46. ^1H NMR spectrum of (**3ed**).

Figure 4.47. ¹H NMR spectrum of (**3ee**).Figure 4.48. ¹H NMR spectrum of (**3eg**).

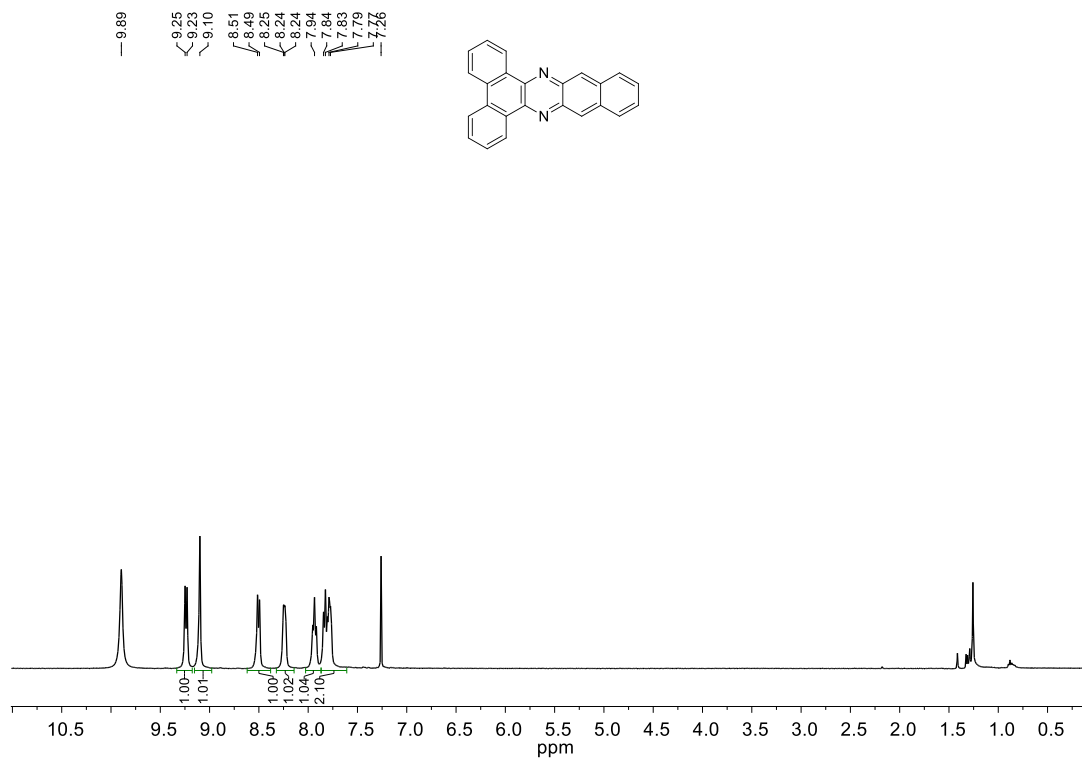


Figure 4.49. ^1H NMR spectrum of **(3fb)**.

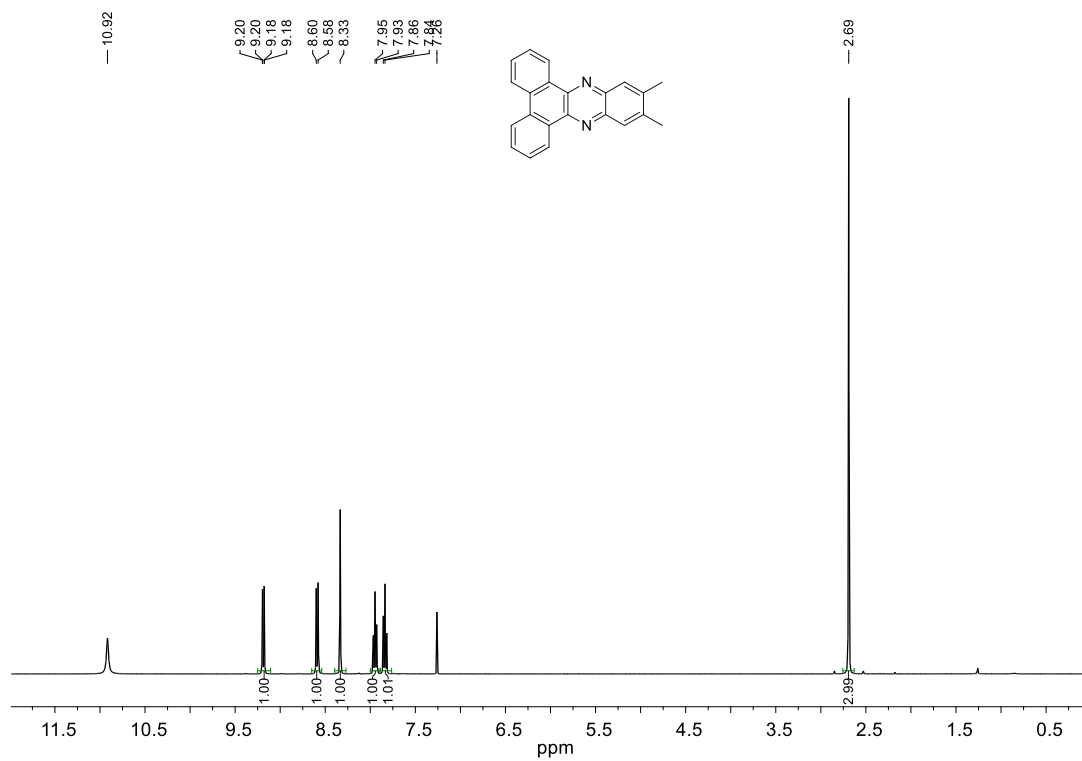


Figure 4.50. ^1H NMR spectrum of **(3fc)**.

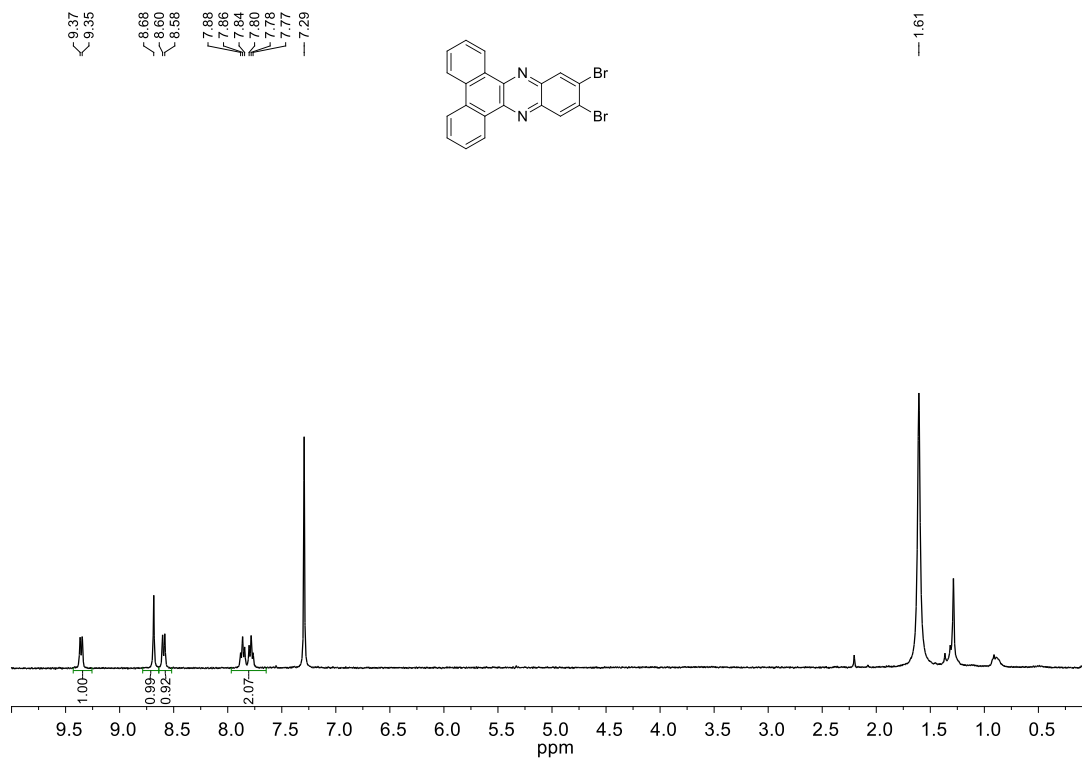


Figure 4.51. ¹H NMR spectrum of (**3fe**).

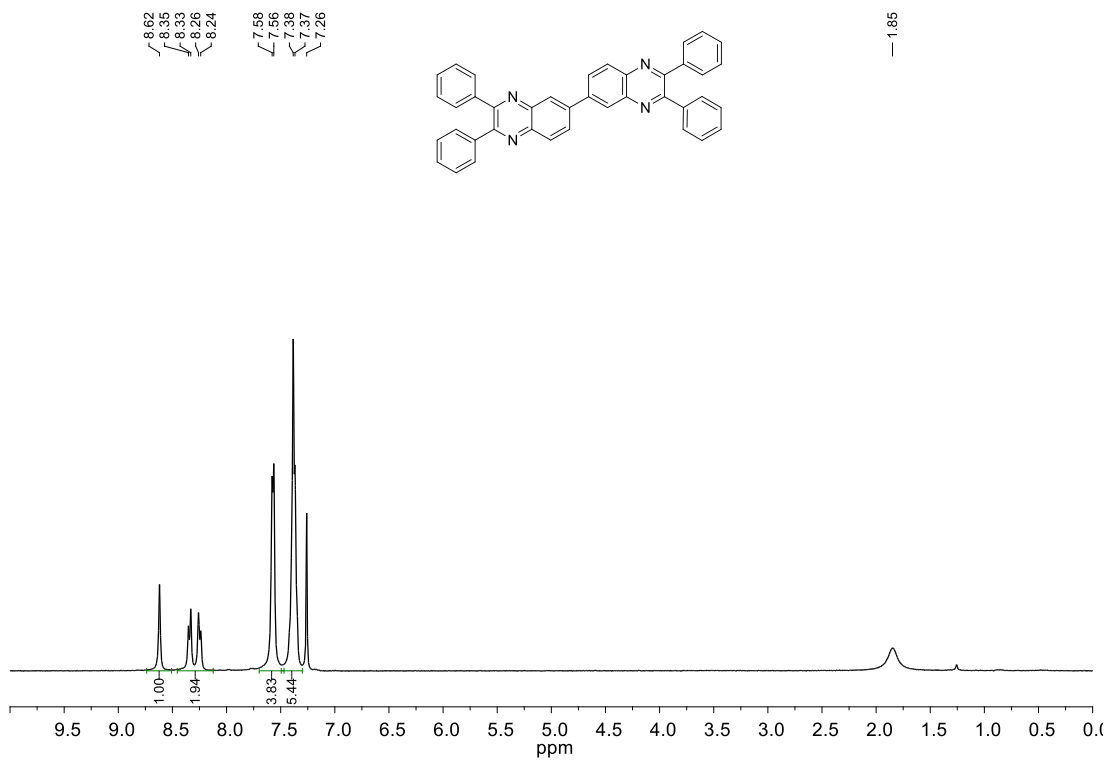


Figure 4.52. ¹H NMR spectrum of (**3gg**).

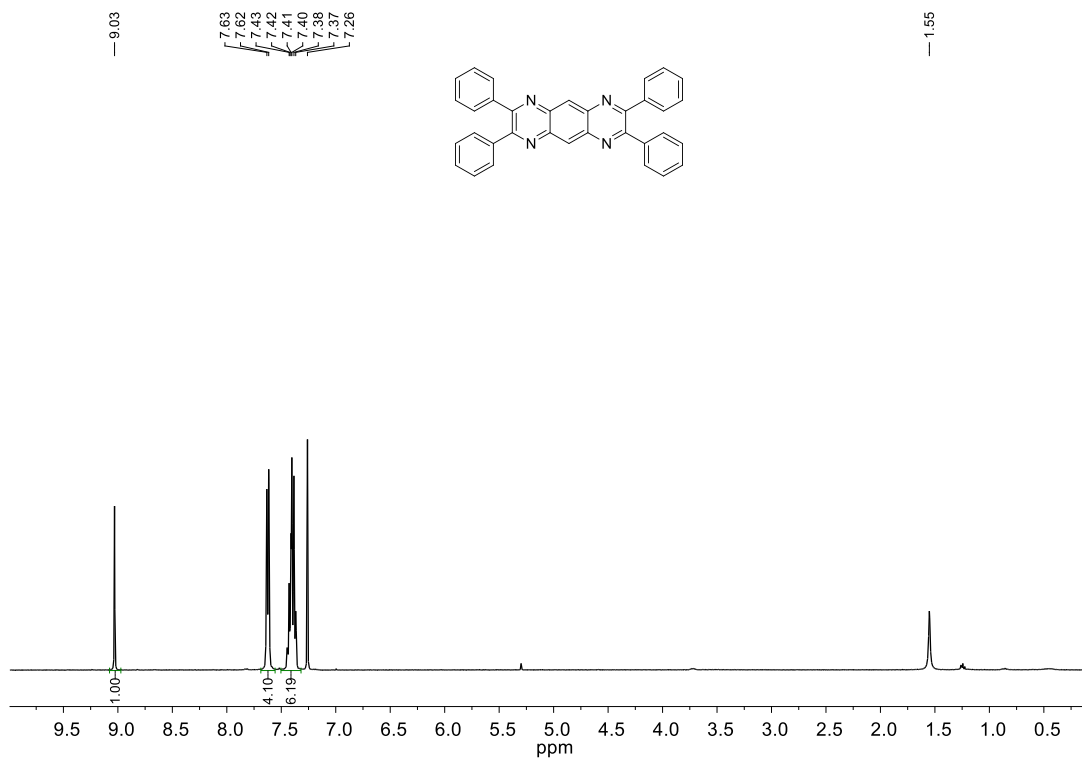


Figure 4.53. ^1H NMR spectrum of **(3gh)**.

4.6 NOTES AND REFERENCES

1. M. Randić, *Chem. Rev.*, 2003, **103**, 3449-3606.
2. Y. Ruiz-Morales, *J. Phys. Chem. A*, 2002, **106**, 11283-11308.
3. P. S. Vankar, R. Shanker, D. Mahanta and S. C. Tiwari, *Dyes Pigments*, 2008, **76**, 207-212.
4. A. Mateo-Alonso, N. Kulisic, G. Valenti, M. Marcaccio, F. Paolucci and M. Prato, *Chem. Asian. J.*, 2010, **5**, 482-485.
5. M. Winkler and K. N. Houk, *J. Am. Chem. Soc.*, 2007, **129**, 1805-1815.
6. J. E. Anthony, *Angew. Chem., Int. Ed.*, 2008, **47**, 452-483.
7. G.-W. Wang, *Chem. Soc. Rev.*, 2013, **42**, 7668-7700.
8. P. Balaz, M. Achimovicova, M. Balaz, P. Billik, Z. Cherkezova-Zheleva, J. M. Criado, F. Delogu, E. Dutkova, E. Gaffet, F. J. Gotor, R. Kumar, I. Mitov, T. Rojac, M. Senna, A. Streletskii and K. Wieczorek-Ciurowa, *Chem. Soc. Rev.*, 2013, **42**, 7571-7637.
9. T. Frišćić, I. Halasz, P. J. Beldon, A. M. Belenguer, F. Adams, S. A. J. Kimber, V. Honkimäki and R. E. Dinnebier, *Nature Chem.*, 2013, **5**, 66-73.
10. S. Ley, M. O'Brien and R. Denton, *Synthesis*, 2011, 1157-1192.
11. J.-L. Do, C. Mottillo, D. Tan, V. Štrukil and T. Frišćić, *J. Am. Chem. Soc.*, 2015, **137**, 2476-2479.
12. S. L. James, C. J. Adams, C. Bolm, D. Braga, P. Collier, T. Friscic, F. Grepioni, K. D. M. Harris, G. Hyett, W. Jones, A. Krebs, J. Mack, L. Maini, A. G. Orpen, I. P. Parkin, W. C. Shearouse, J. W. Steed and D. C. Waddell, *Chem. Soc. Rev.*, 2012, **41**, 413-447.
13. C. Giri, P. K. Sahoo, R. Puttreddy, K. Rissanen and P. Mal, *Chem. Eur. J.*, 2015, **21**, 6390-6393.

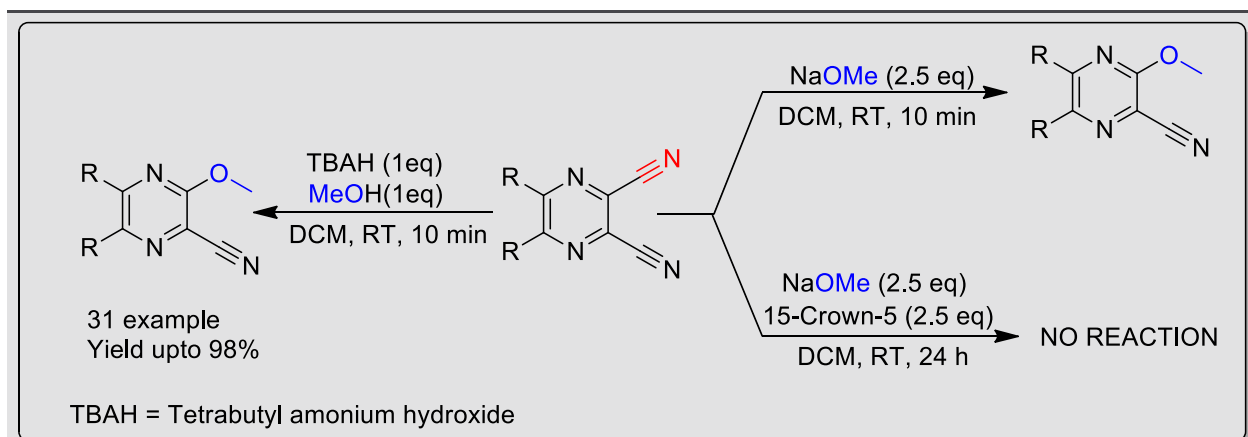
14. J. G. Hernandez, I. S. Butler and T. Friscic, *Chem. Sci.*, 2014, **5**, 3576-3582.
15. A. Stolle, T. Szuppa, S. E. S. Leonhardt and B. Ondruschka, *Chem. Soc. Rev.*, 2011, **40**, 2317-2329.
16. L. Takacs, *Chem. Soc. Rev.*, 2013.
17. N. Kulisic, S. More and A. Mateo-Alonso, *Chem. Commun.*, 2011, **47**, 514-516.
18. B. Kohl, F. Rominger and M. Mastalerz, *Org. Lett.*, 2014, **16**, 704-707.
19. A. Mateo-Alonso, C. Ehli, K. H. Chen, D. M. Guldi and M. Prato, *J. Phys. Chem. A*, 2007, **111**, 12669-12673.
20. A. Mateo-Alonso, N. Kulisic, G. Valenti, M. Marcaccio, F. Paolucci and M. Prato, *Chem. Asian J.*, 2010, **5**, 482-485.
21. J. Fleischhauer, S. Zahn, R. Beckert, U.-W. Grummt, E. Birckner and H. Görls, *Chem. Eur. J.*, 2012, **18**, 4549-4557.
22. Y. Wu, Z. Yin, J. Xiao, Y. Liu, F. Wei, K. J. Tan, C. Kloc, L. Huang, Q. Yan, F. Hu, H. Zhang and Q. Zhang, *ACS Appl. Mater. Interfaces*, 2012, **4**, 1883-1886.
23. U. H. F. Bunz, *Chem. Eur. J.*, 2009, **15**, 6780-6789.
24. F. G. Oberender and J. A. Dixon, *J. Org. Chem.*, 1959, **24**, 1226-1229.
25. B. Wex, A. a. O. El-Ballouli, A. Vanvooren, U. Zschieschang, H. Klauk, J. A. Krause, J. Cornil and B. R. Kaafarani, *J. Mol. Struct.*, 2015, **1093**, 144-149.
26. T. Yamato, M. Fujimoto, A. Miyazawa and K. Matsuo, *J. Chem. Soc., Perkin Trans. 1*, 1997, 1201-1208.
27. F. Ferretti, E. Gallo and F. Ragaini, *J. Organomet. Chem.*, 2014, **771**, 59-67.
28. W. Guo, B. J. Engelman, T. L. Haywood, N. B. Blok, D. S. Beaudoin and S. O. Obare, *Talanta*, 2011, **87**, 276-283.

29. A. Kleineweischede and J. Mattay, *Eur. J. Org. Chem.*, 2006, 947-957.
30. A. J. McConnell, M. H. Lim, E. D. Olmon, H. Song, E. E. Dervan and J. K. Barton, *Inorg. Chem.*, 2012, **51**, 12511-12520.
31. B. Schafer, H. Gorls, M. Presselt, M. Schmitt, J. Popp, W. Henry, J. G. Vos and S. Rau, *Dalton Trans.*, 2006, 2225-2231.
32. A. K. Bilakhiya, B. Tyagi, P. Paul and P. Natarajan, *Inorg. Chem.*, 2002, **41**, 3830-3842.
33. S. M. Baghbanian, *Chin. Chem. Lett.*, 2015, **26**, 1113-1116.
34. A. Putta, J. D. Mottishaw, Z. Wang and H. Sun, *Cryst. Growth Des.*, 2014, **14**, 350-356.
35. M. Lian, Q. Li, Y. Zhu, G. Yin and A. Wu, *Tetrahedron*, 2012, **68**, 9598-9605.
36. H. Takeshita, A. Mori, T. Nagao and T. Nagamura, *Chem. Lett.*, 1989, **18**, 1719-1722.
37. in *Principles of Fluorescence Spectroscopy*, ed. J. Lakowicz, Springer US, 2006, ch. 2, pp. 27-61.
38. R. Blessing, *J. Appl. Crystallogr.*, 1997, **30**, 421-426.
39. CrysAlisPro 2012, Agilent Technologies. Version 1.171.36.35.
40. G. Sheldrick, *Acta Crystallogr. Sect. A*, 2008, **64**, 112-122.
41. O. V. Dolomanov, L. J. Bourhis, R. J. Gildea, J. A. K. Howard and H. Puschmann, *J. Appl. Crystallogr.*, 2009, **42**, 339-341.

CHAPTER 5

Cation- π Induced C-C Activation on N-Acenes

5.1 ABSTRACT



Herein, we demonstrate how cation- π interaction can play a major role to activate the 1,2-disubstituted arenes for aromatic nucleophilic (S_NAr) ipso substitution with aliphatic alcohols for the synthesis of aryl ethers. The cations ${}^n\text{Bu}_4\text{N}^+$ or Na^+ were used as activator of the aromatic groups. However, the nucleophilic substitution reactions were failed in absence of cations led to confirmation for the participation of cation- π interaction for C-CN activation towards nucleophilic substitution reaction.

5.2 INTRODUCTION

Carbon-heteroatom bonds formation methodology draws significant interest during last couple of years.¹⁻⁴ Among the C-heteroatom bond formation reactions,⁵ C-O bond formation reactions have also been reported significantly. Alkyl aryl ethers (C-O bond) are of having most important in synthetic chemistry as it is used as solvent and key structural motifs in numerous natural

products, pharmaceuticals and are often use as a phenol precursors in fragrances and cosmetics.⁶⁻

¹⁰ Traditional Williamson ether synthesis¹¹ has been employed widely but have limited industrial applications due to requirement of activated aryl halides, large quantity of alkoxides, high reaction temperature, etc. Similarly scope of the classical copper-mediated Ullman ether synthesis is also unpopular due to involvement of harsh reaction conditions, requirement of strong bases such as alkoxides or sodium hydride and stoichiometric amount of copper salts.¹² Consequently, there are many metal catalyzed routes have been emerged with high yielding ethers, but usually suffers from the need of expensive catalysts, ligands and high reaction temperatures along with prolonged reaction times. Transition metal free intermolecular addition of alkoxy (-OR) group to olefins is a popular subject of interest for the synthesis of fine chemicals, agrochemicals, pharmaceuticals, materials, etc.⁶⁻¹⁰ In addition, Mitsunobu type reactions¹³ and base mediated arylation of phenols with diaryliodonium salts,¹⁴ etc. are well known as metal-free synthetic protocols for alkyl aryl ethers synthesis.¹⁵

On the other hand ipso-substitution reactions¹⁶ are also widely used in selective synthesis of alkyl aryl ethers where an Ar-O bond is formed in the expense of an Ar-X (X = halogen, carboxylate ester, sulfonate, N₂⁺, CN, etc.).¹⁷⁻²¹ Activation and cleavage of the thermodynamically stable C-CN bond (ca. 133 kcal mol⁻¹ for PhCN²²) can be achieved either photochemically or by the suitable metal catalyzed pathway (Figure **5.1A-B**).²³⁻²⁸ With properly engineered substitutions and conditions, the activation barrier of C-CN bond could trim down to make the reactions thermodynamically feasible.^{29, 30}

A. Photoinduced Carbon-Cyanide Bond Activation



B. Metal Mediated Carbon-Cyanide Bond Activation

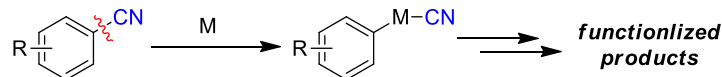
C. This Work: Transition Metal-free Cation- π Induced

Figure 5.1. Strategies for C–CN bond activation reaction.

As part of research activities on concerning cation- π mediated reactions, Mal and co-worker have demonstrated iodoetherification on unactivated olefins using trideuteriomethanol (CD_3OD), 2,2,2-trifluoroethanol ($\text{CF}_3\text{CH}_2\text{OH}$), etc.³¹

It has been well documented that supramolecular environments, such as cyclodextrins,^{32, 33} zeolites,³⁴ micelles¹⁹ and self-assembled cages^{35, 36} directs the regio- and stereoselectivities of a chemical reaction.^{37, 38} Similarly, cation- π interaction³⁹ acts as a conformation-controlling tools in large molecules (enzymes and proteins) as well as in small molecules due to its stronger interaction forces. Strong cation- π interactions facilitates regio- and stereoselective photochemical reactions,^{40, 41} such as [2 + 2] and [4 + 2] cycloaddition reactions,^{41, 42} synthesis of chiral dihydropyridines, enantioselective cyclopropanation and regioselective Schmidt rearrangements.^{43, 44} In literature thermodynamically stable C–CN activation is a well-known concept using transition metal catalyst.^{27, 29, 45-50} Best of our knowledge, transition metal-free C–CN bond activation through non-covalent interactions under mild reaction conditions is not

studied in details.^{18, 20, 21} Herein, transition metal-free selectively synthesis of alkyl aryl ethers through the cleavage of C–CN bond²⁵ of pyrazene derivatives *via* cation– π interactions is performed. Presumably, addition of nucleophiles during S_NAr reaction becomes more favorable by exploiting cation– π interaction resulting in decrease of electron density in pyrazene systems.⁵¹

5.3 RESULTS AND DISCUSSIONS

To investigate cation– π assisted alkyl aryl ether synthesis, 5,6-diphenylpyrazine-2,3-dicarbonitrile (**1a**) was employed as a model substrate. After treating 5,6-diphenylpyrazine-2,3-dicarbonitrile (**1a**) with NaOMe for 24 h in dichloromethane at room temperature, 3-methoxy-5,6-diphenylpyrazine-2-carbonitrile (**2aa**) was isolated in 80% yield. We considered, NaOMe delivers both cation (Na⁺) and ethereal counterpart (OMe). Faster reaction was observed when the amount of NaOMe was increased 2.5 fold and **2aa** obtained within 10 min, in excellent yield. Contrastingly, AgBF₄-MeOH (1:1.1), resulted a sluggish reaction with the moderate yield of **2aa** in 24 h. Similarly, NH₄OH was not delivered the desired ether with MeOH. However, tetrabutylammonium hydroxide (TBAH) and tetramethylammonium hydroxide (TMAH) were found to be efficient to produce ether **2aa** within 10 min in excellent yield. On the other hand, 0.5 equivalent of TBAH (with respect to **1a**), only 48% of **2aa** was isolated. It clearly indicates the need of quantitative amount of cationic part to facilitate the C–CN bond activation. Here, TBAH plays a dual role, anionic part OH[–] acts as a base to abstract proton from alcohol as well as the tetrabutyl ammonium cation interact with the pyrazene moiety through cation– π interaction towards activation of C–CN bond.

Table 5.1 Optimizations for the reaction conditions^a

Entry	Additives	Nucleophiles (1.1 equiv)	Time	Conversion (%) ^b
1	NaOMe (1 eq)	---	24 h	80
2	NaOMe (2.5 eq)	---	10 min	100
3	AgBF ₄ (1 eq)	MeOH	24 h	52
4	NH ₄ OH(1 eq)	MeOH	24 h	0
5	NH ₄ OH (2 eq)	MeOH	24 h	0
6	TBAH(1 eq)	MeOH	10 min	100
7	TMAH(1 eq)	MeOH	10 min	100
8	TBAH(0.5 eq)	MeOH	10 min	48

^a1 equiv of **1a** was treated with additives and 1.1 equiv of nucleophiles at room temperature in dichloromethane;

^b isolated yields; TBAH – Tetrabutylammonium hydroxide; TMAH – Tetramethylammonium hydroxide

After finding the optimized reaction condition, substrates scope was examined with TBAH (1 equiv) and 1.1 equivalent of different alcohols at room temperature. The ethers were synthesized in excellent yields at optimized condition. Alkyl aryl ethers from four different types of carbonitrile substrates *e.g.* 5,6-diphenylpyrazine-2,3-dicarbonitrile (**1a**) 5,6-di(thiophen-2-yl)pyrazine-2,3-dicarbonitrile (**1b**) pyrazino[2,3-*f*][1,10]phenanthroline-2,3-dicarbonitrile (**1c**) and dibenzo[*f,h*]quinoxaline-2,3-dicarbonitrile (**1d**), were isolated in very good to excellent yields. Similarly, various alcohols like methanol (**a**), ethanol (**b**), hexanol (**e**), propargyl alcohol (**g**), (4-chlorophenyl)methanol (**c**), (4-bromophenyl)methanol (**f**), benzo[*d*][1,3]dioxol-5-ylmethanol (**d**), deuterated methanol (**h**) and 2-(2-(2-hydroxyethoxy)ethoxy)ethyl 4-methylbenzenesulfonate (**i**) also facilitated excellent yields of the alkyl aryl ethers.

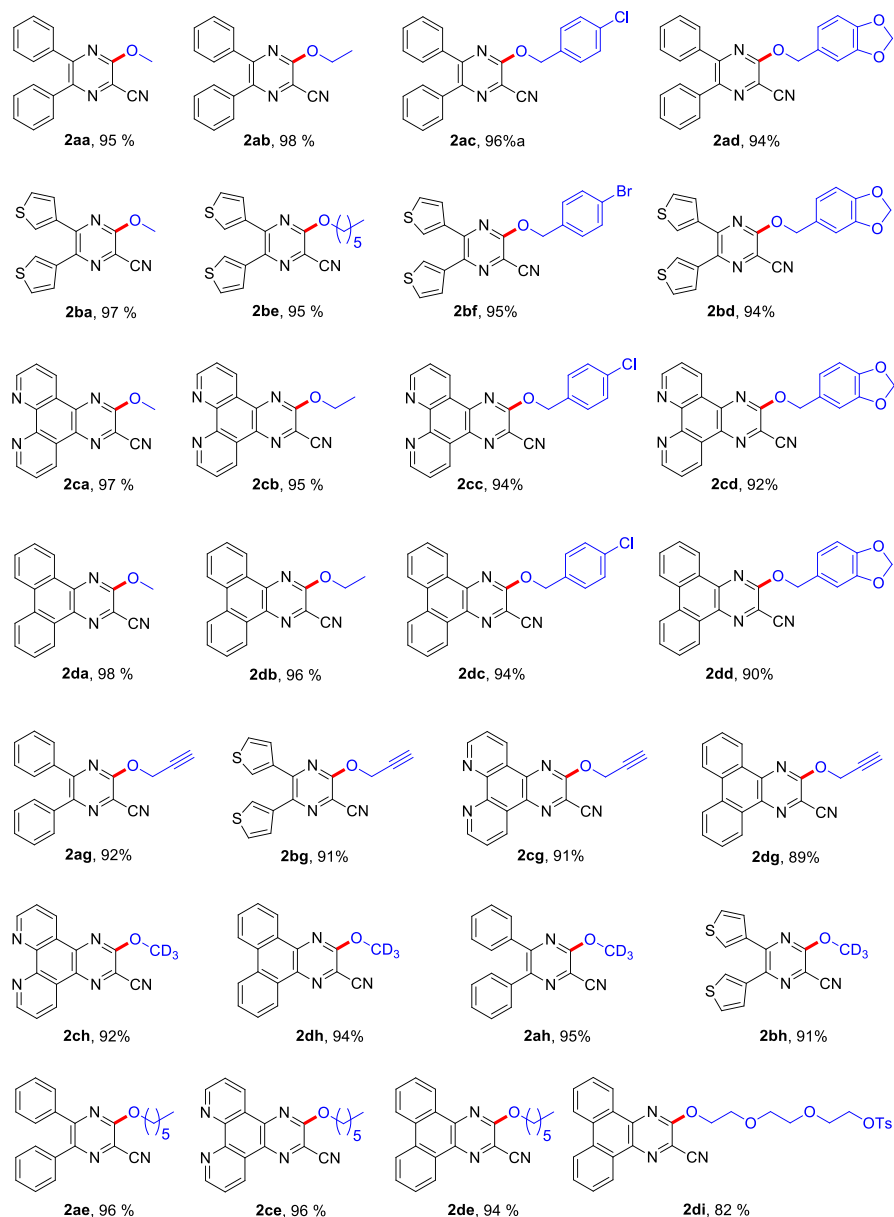


Figure 5.2. Synthesis of alkyl aryl ethers under optimized conditions.

To understand the mechanistic pathway of the reactions, we performed some controlled experiments (Fig. 5.3). 2.5 equivalent of NaOMe was efficiently transformed pyrazino[2,3-*f*][1,10]phenanthroline-2,3-dicarbonitrile (**1c**) to 3-methoxypyrazino[2,3-*f*][1,10]phenanthroline-2-carbonitrile (**2ca**) in 10 min with 95% yield. When same amount of 15-Crown-5 was used with

NaOMe, no ether (**2ca**) was obtained. As 15-Crown-5 is suitable for complexing with Na^+ ion *via* ion – dipole interaction, we expect Na^+ ion could not participate for cation- π interactions and resulting in no reactions. This was further established upon isolation of 93% of **2ca** when 15-Crown-5 was used in smaller quantities compared to NaOMe (Fig. 5.3).

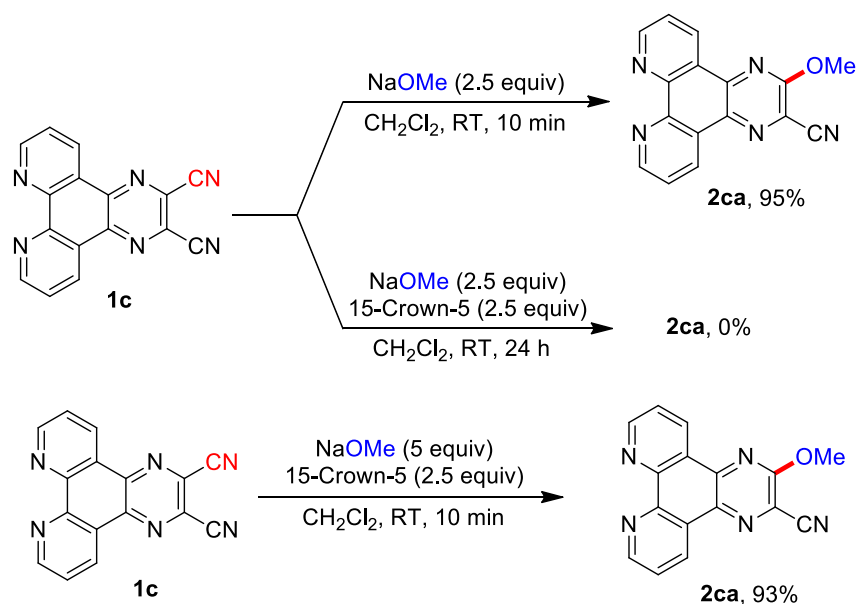


Figure 5.3. Controlled Experiments to establish the mechanism of cation- π participation.

Based on controlled experiments, we anticipated that cation (Na^+) plays an important role to $\text{S}_{\text{N}}\text{Ar}$ reactions by exploiting cation- π interactions which is well known to lead to decrease electron deficiency in aromatic systems.^{39, 43, 52} All the substrates used in this study are 1,2-dicyano derivatives, but after complete reactions only mono-substituted products were isolated. To understand this, we have proposed plausible mechanistic pathway in Fig. 5.4. The high selectivity of the mono-substitution reaction could be attributed to the unstable nature of σ – complex **2A**. Whereas after addition of first nucleophile, σ – complex **1A** was stabilized with the

adjacent nitrile group and facilitates selective mono-substitution by following the elimination step.

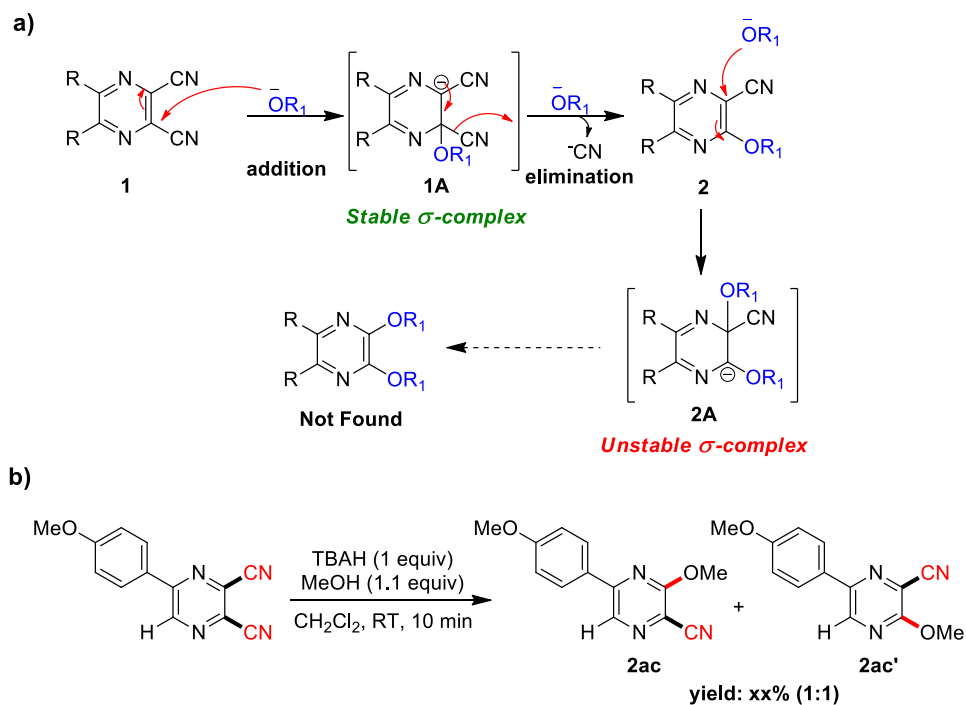


Figure 5.4. Mechanism of the proposed $\text{S}_{\text{N}}\text{Ar}$ reactions. a) Plausible reaction pathway. b) Limitation to selective alkyl aryl ether synthesis

5.4 CONCLUSIONS

In summary, we have developed a mild, efficient and transition metal-free synthetic approach towards alkyl aryl ether synthesis. Also we have successfully proposed that cations ($\text{n-Bu}_4\text{N}^+$ and Na^+) serve as templates to activate the thermodynamically stable C–CN bond through cation- π interactions. A series of alkyl aryl ethers containing pyrazene moiety have been synthesized within a very less time (ca. 10 min) and with excellent yields. This operationally simple technique will certainly be of interest not only to the synthetic organic chemist but also to

the supramolecular and material scientists looking for better methodology for synthesis of molecules containing donor and acceptor groups.

5.5 EXPERIMENTAL SECTION

General Methods. Experiments were carried out under open atmosphere and ball milling experiments were done in Retsch MM 200 high speed vibration milling instrument except stated otherwise. Crude compounds were purified by column chromatography technique using silica-gel (mesh 100-200) and dichloromethane as an eluent. All reported yields correspond to isolated compounds unless indicated otherwise. NMR spectra were recorded on Bruker AV 400 MHz instrument at 25 °C. NMR are reported in parts per million (ppm) with respect to residual chloroform (7.26 ppm for ^1H and 77.16 for ^{13}C) in the deuterated solvent and coupling constant (J) in Hz, unless otherwise stated. High-resolution mass spectra (HRMS) were recorded on a Bruker micrOTOF-Q II, ESI TOF (time of flight) mass spectrometer. Infrared spectra were recorded on PerkinElmer (Model: SPECTRUM RX1) and reported in wave number (cm^{-1}). Uncorrected melting points of the compounds were determined by using a digital melting point apparatus.

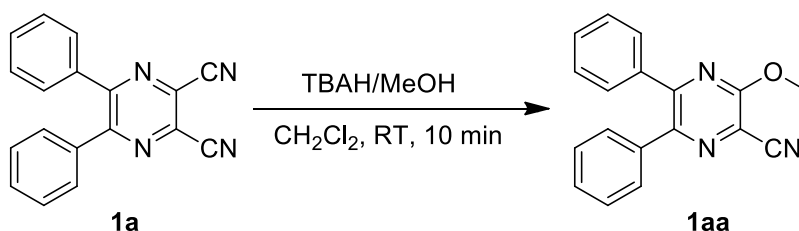
Representative procedure for the preparation of 2,3-dicarbonitrile derivatives



In a representative experimental procedure, benzil (0.5 mmol) and dicyanodiamine (0.5 mmol) were transferred to a 10 mL stainless steel jar equipped with grinding ball (15 mm

diameter, stainless steel) with 0.05 mmol of PTSA. The milling jar was kept for milling for 90 min. The progress of the reaction was monitored by thin layer chromatography (TLC). After completion of reactions, the crude mixture was washed with ethanol to isolate the desired product.

Representative procedure for the synthesis of alkyl aryl ethers



In a typical procedure, 50 mg (0.17 mmol) of 5,6-diphenylpyrazine-2,3-dicarbonitrile (**1a**) and 141 mg (0.17 mmol) of Tetrabutylammonium hydroxide (TBAH) were transferred to a 5 mL reactions vial equipped with magnetic stirring bar and the mixture was dissolved in 1 mL dichloromethane. Then 6 μ L (1.9 mmol) of MeOH was added to the solution and stirred for 10 min at room temperature. After completion of the reactions (confirmed by TLC) the solvent was removed under reduced pressure and the crude compound was purified through short pad silica column. *NMR data*

Compound Characterization Data

3-methoxy-5,6-diphenylpyrazine-2-carbonitrile (2aa): white solid; yield 95% (48 mg); mp 170 – 172 °C (lit. 165 – 167 °C); ¹H NMR (400 MHz, CDCl₃) δ 7.52 – 7.46 (m, 2H), 7.42 – 7.36 (m, 3H), 7.36 – 7.27 (m, 5H), 4.19 (s, 3H); ¹³C NMR (100 MHz, CDCl₃) δ 159.5, 152.8, 146.4, 137.1, 137.0, 130.1, 129.6, 128.9, 128.6, 128.5, 115.9, 114.6, 54.9; IR (KBr) $\tilde{\nu}$ 2894 (s), 2949 (s), 2924 (s), 2234 (s), 1542 (m), 1389 (m), 1196 (m), 1010 (s), 700 (m) cm⁻¹;

3-ethoxy-5,6-diphenylpyrazine-2-carbonitrile (2ab): off white solid; yield 98% (52 mg); mp 152 -154 °C (lit. 148 – 150 °C); ^1H NMR (400 MHz, CDCl_3) δ 7.50 – 7.44 (m, 2H), 7.38 (ddd, J = 7.2, 4.3, 2.5 Hz, 3H), 7.35 – 7.27 (m, 5H), 4.64 (q, J = 7.1 Hz, 2H), 1.55 – 1.51 (m, 3H); ^{13}C NMR (100 MHz, CDCl_3) δ 159.3, 152.7, 146.2, 137.2, 137.1, 130.0, 130.0, 129.6, 128.8, 128.5, 128.4, 115.9, 114.7, 64.1, 14.5; IR (KBr) $\tilde{\nu}$ 2982 (s), 2956 (s), 2926 (m), 2712 (s), 2230 (s), 1537 (m), 1450 (m), 1425 (m), 1398 (m), 1380 (m), 1187 (m), 1023 (m), 890 (s), 773 (s), 700 (m) cm^{-1} ;

3-((4-chlorobenzyl)oxy)-5,6-diphenylpyrazine-2-carbonitrile (2ac): white solid; yield 96% (67 mg); mp 190 – 192 °C; ^1H NMR (400 MHz, CDCl_3) δ 7.49 – 7.41 (m, 2H), 7.41 – 7.27 (m, 5H), 5.58 (s, 1H); ^{13}C NMR (100 MHz, CDCl_3) δ 158.7, 152.7, 146.8, 137.0, 136.9, 134.5, 134.1, 130.1, 130.0, 129.7, 129.6, 129.0, 128.6, 128.5, 116.0, 114.4, 68.5; IR (KBr) $\tilde{\nu}$ 2930 (s), 2854 (s), 2230 (s), 1536 (m), 1426 (m), 1392 (m), 1333 (m), 1189 (m), 1176 (m), 1008 (m), 811 (s), 703 (m) cm^{-1} ;

3-(benzo[d][1,3]dioxol-5-ylmethoxy)-5,6-diphenylpyrazine-2-carbonitrile (2ad): off white solid; yield 94% (68 mg); mp 154 – 156 °C; ^1H NMR (400 MHz, CDCl_3) δ 7.53 – 7.24 (m, 21H), 7.01 (d, J = 9.0 Hz, 4H), 6.83 (d, J = 7.3 Hz, 2H), 5.98 (s, 4H), 5.52 (s, 4H); ^{13}C NMR (100 MHz, CDCl_3) δ 158.9, 152.7, 148.0, 148.0, 146.6, 137.1, 137.0, 130.0, 129.6, 129.2, 128.9, 128.5, 128.5, 122.6, 116.1, 114.5, 109.2, 108.4, 101.3, 69.4; IR (KBr) $\tilde{\nu}$ 3057 (s), 2998 (s), 2956 (s), 2910 (s), 2226 (s), 1610 (s), 1536 (m), 1502 (m), 1490 (m), 1426 (m), 1396 (m), 1251 (m), 1200 (m), 1101 (m), 1038 (m), 962 (m), 917 (m), 860 (m), 808 (m), 776 (m), 698 (m) cm^{-1} ;

3-methoxy-5,6-di(thiophen-3-yl)pyrazine-2-carbonitrile (2ba): yellow solid; yield 97% (49 mg); mp 185 – 186 °C; ^1H NMR (400 MHz, CDCl_3) δ 7.61 (dd, $J = 2.9, 1.0$ Hz, 1H), 7.49 (dd, $J = 2.9, 1.0$ Hz, 1H), 7.33 (dd, $J = 5.0, 3.0$ Hz, 1H), 7.29 (dd, $J = 5.1, 3.0$ Hz, 1H), 7.21 (dd, $J = 5.1, 1.0$ Hz, 1H), 7.10 (dd, $J = 5.0, 1.0$ Hz, 1H), 4.17 (s, 3H); ^{13}C NMR (100 MHz, CDCl_3) δ 159.3, 147.6, 141.6, 138.3, 138.1, 129.3, 128.3, 128.1, 126.4, 126.2, 125.9, 115.2, 114.5, 54.8; IR (KBr) $\tilde{\nu}$ 2919 (m), 2851 (s), 2226 (m), 1633 (m), 1542 (m), 1513 (m), 1463 (m), 1430 (m), 1414 (m), 1386 (m), 1299 (s), 1179 (m), 805 (s), 784 (s), 702 (m) cm^{-1} ;

3-(hexyloxy)-5,6-di(thiophen-3-yl)pyrazine-2-carbonitrile (2be): yellowish brown solid; yield 95% (51 mg); mp 89 – 92 °C; ^1H NMR (400 MHz, CDCl_3) δ 7.58 (dd, $J = 3.0, 1.2$ Hz, 1H), 7.48 (dd, $J = 3.0, 1.1$ Hz, 1H), 7.33 (dd, $J = 5.0, 3.0$ Hz, 1H), 7.28 (dd, $J = 5.1, 3.0$ Hz, 1H), 7.19 (dd, $J = 5.1, 1.1$ Hz, 1H), 7.09 (dd, $J = 5.0, 1.1$ Hz, 1H), 4.53 (t, $J = 6.6$ Hz, 2H), 1.87 (dd, $J = 14.8, 6.9$ Hz, 2H), 1.50 (dd, $J = 14.9, 6.9$ Hz, 2H), 1.39 – 1.33 (m, 4H), 0.92 (t, $J = 7.0$ Hz, 3H); ^{13}C NMR (100 MHz, CDCl_3) δ 159.1, 147.5, 141.2, 138.3, 138.2, 129.2, 128.3, 128.1, 126.2, 126.1, 125.8, 115.1, 114.5, 68.1, 31.5, 28.7, 25.6, 22.6, 14.1; IR (KBr) $\tilde{\nu}$ 3076 (s), 2922 (s), 2850 (s), 2226 (s), 1512 (s), 1359 (m), 1299 (s), 1236 (s), 1179 (m), 1008 (s), 805 (s), 702 (m) cm^{-1} ;

3-((4-bromobenzyl)oxy)-5,6-di(thiophen-3-yl)pyrazine-2-carbonitrile (2bf): brown solid; yield 95% (73 mg); mp 144 – 147 °C; ^1H NMR (400 MHz, CDCl_3) δ 7.57 – 7.51 (m, 3H), 7.48 (dd, $J = 2.9, 1.2$ Hz, 1H), 7.39 (d, $J = 8.3$ Hz, 2H), 7.31 (ddd, $J = 10.8, 5.0, 3.0$ Hz, 2H), 7.17 (dd, $J = 5.1, 1.1$ Hz, 1H), 7.08 (dd, $J = 5.0, 1.1$ Hz, 1H), 5.54 (s, 2H); ^{13}C NMR (100 MHz, CDCl_3) δ 158.4, 147.5, 142.0, 138.2, 138.0, 134.6, 132.0, 129.8, 129.3, 128.2, 128.1, 126.5, 126.2, 126.1, 122.6, 115.3, 114.3, 68.4; IR (KBr) $\tilde{\nu}$ 3079 (s), 2925 (s), 2226 (s), 1638 (m), 1517

(s), 1441 (m), 1341 (m), 1302 (s), 1183 (m), 1068 (s), 963 (s), 858 (s), 794 (s), 784 (s), 704 (s) cm^{-1} ;

3-(benzo[d][1,3]dioxol-5-ylmethoxy)-5,6-di(thiophen-3-yl)pyrazine-2-carbonitrile (2bd):

yellowish brown solid; yield 94% (67 mg); mp 198 – 201 °C; ^1H NMR (400 MHz, CDCl_3) δ 7.58 (dd, $J = 3.0, 1.2$ Hz, 1H), 7.48 (dd, $J = 3.0, 1.2$ Hz, 1H), 7.31 (ddd, $J = 9.3, 5.0, 3.0$ Hz, 2H), 7.19 (dd, $J = 5.1, 1.2$ Hz, 1H), 7.08 (dd, $J = 5.0, 1.2$ Hz, 1H), 7.02 – 6.96 (m, 2H), 6.82 (d, $J = 7.8$ Hz, 1H), 5.98 (s, 2H), 5.49 (s, 2H); ^{13}C NMR (100 MHz, CDCl_3) δ 158.6, 148.1, 148.0, 147.5, 141.8, 138.3, 138.1, 129.3, 128.3, 128.1, 126.4, 126.2, 126.0, 122.5, 115.3, 114.4, 109.1, 108.4, 101.4, 69.3; IR (KBr) $\tilde{\nu}$ 2929 (s), 2885 (s), 2785 (s), 2231 (s), 1535 (s), 1508 (s), 1497 (s), 1446 (m), 1431 (m), 1369 (m), 1345 (m), 1256 (m), 1183 (m), 1036 (m), 1008 (s), 794 (m) 701 (s) cm^{-1} ;

3-methoxypyrazino[2,3-*f*][1,10]phenanthroline-2-carbonitrile (2ca): yellow solid; yield 97%

(49 mg); mp 268 – 270 °C; ^1H NMR (400 MHz, CDCl_3) δ 9.41 – 9.21 (m, 4H), 7.81 (dd, $J = 7.1, 3.4$ Hz, 2H), 4.37 (s, 3H); ^{13}C NMR (100 MHz, CDCl_3) δ 159.6, 153.6, 152.1, 148.6, 146.1, 140.1, 134.7, 134.2, 132.9, 126.2, 125.6, 124.6, 124.2, 120.2, 114.3, 55.4; IR (KBr) $\tilde{\nu}$ 3092 (s), 2949 (s), 2926 (s), 2854 (s), 2235 (s), 1552 (m), 1469 (m), 1390 (m), 1376 (m), 1222 (m), 995 (m), 743 (m) cm^{-1} ;

3-ethoxypyrazino[2,3-*f*][1,10]phenanthroline-2-carbonitrile (2cb): off white solid; yield 95%

(58 mg); mp 274 – 276 °C; ^1H NMR (400 MHz, CDCl_3) δ 9.38 – 9.31 (m, 3H), 9.27 (dd, $J = 4.4, 1.7$ Hz, 1H), 7.85 – 7.77 (m, 2H), 4.84 (q, $J = 7.1$ Hz, 2H), 1.65 (t, $J = 7.1$ Hz, 3H); ^{13}C NMR (100 MHz, CDCl_3) δ 159.2, 153.4, 151.8, 148.4, 145.8, 139.8, 134.3, 134.0, 132.7, 126.1, 125.5,

124.5, 124.1, 120.1, 114.3, 64.7, 14.3; IR (KBr) $\tilde{\nu}$ 2921 (s), 2894 (s), 2238 (s), 1637 (m), 1547 (m), 1410 (s), 1393 (s), 1367 (m), 1265 (m), 1226 (m), 1184 (m), 1021 (m), 820 (s), 743 (s) cm^{-1} ;

3-((4-chlorobenzyl)oxy)pyrazino[2,3-*f*][1,10]phenanthroline-2-carbonitrile (2cc): pale yellow solid; yield 94% (66 mg); mp 224 – 226 °C; ^1H NMR (400 MHz, CDCl_3) δ 9.34 (d, $J = 3.1$ Hz, 1H), 9.28 (dd, $J = 8.5, 4.3$ Hz, 3H), 7.87 – 7.75 (m, 2H), 7.55 (d, $J = 8.3$ Hz, 2H), 7.41 (d, $J = 8.4$ Hz, 2H), 5.77 (s, 2H); ^{13}C NMR (100 MHz, CDCl_3) δ 158.7, 153.7, 152.2, 148.8, 146.2, 139.8, 135.0, 134.8, 133.9, 133.5, 132.8, 129.5, 129.2, 126.0, 125.5, 124.6, 124.2, 120.2, 114.1, 69.1; IR (KBr) $\tilde{\nu}$ 3032 (s), 2924 (s), 2232 (s), 1633 (m), 1543 (m), 1492 (s), 1423 (s), 1395 (m), 1357 (m), 1219 (m), 1182 (m), 1080 (s), 991 (m), 814 (m), 800 (m), 743 (s) cm^{-1} ;

3-(benzo[*d*][1,3]dioxol-5-ylmethoxy)pyrazino[2,3-*f*][1,10]phenanthroline-2-carbonitrile (2cd): yellow solid; yield 92% (66 mg); mp 269 – 272 °C ; ^1H NMR (400 MHz, CDCl_3) δ 9.37 – 9.22 (m, 4H), 7.87 – 7.75 (m, 2H), 7.09 (d, $J = 6.0$ Hz, 2H), 6.85 (d, $J = 8.1$ Hz, 1H), 5.98 (s, 2H), 5.71 (s, 2H); ^{13}C NMR (100 MHz, CDCl_3) δ 158.9, 153.6, 152.1, 148.8, 148.2, 148.2, 146.2, 139.9, 134.8, 134.0, 132.9, 128.7, 126.1, 125.6, 124.6, 124.2, 122.5, 120.3, 114.2, 109.1, 108.6, 101.5, 70.0; IR (KBr) $\tilde{\nu}$ 2906 (s), 2879 (s), 2233 (s), 1546 (m), 1372 (m), 1342 (m), 1255 (m), 1039 (m), 969 (m), 933 (m), 814 (m), 798 (s), 743 (s) cm^{-1} ;

3-methoxydibenzo[*f,h*]quinoxaline-2-carbonitrile (2da): pale yellow solid; yield 98% (50 mg); mp 277 – 279 °C; ^1H NMR (400 MHz, CDCl_3) δ 9.07 – 8.91 (m, 2H), 8.58 (dd, $J = 14.7, 8.0$ Hz, 2H), 7.84 (t, $J = 7.7$ Hz, 1H), 7.75 (dd, $J = 16.0, 7.5$ Hz, 3H), 4.31 (s, 3H); ^{13}C NMR (100 MHz, CDCl_3) δ 159.0, 140.8, 136.0, 133.2, 131.2, 130.2, 129.3, 128.8, 128.3, 127.8, 126.5,

125.1, 123.1, 122.8, 118.4, 114.9, 54.9; IR (KBr) $\tilde{\nu}$ 2891 (s), 2956 (s), 2232 (s), 1551 (m), 1450 (m), 1394 (m), 1356 (s), 1214 (s), 1194 (s), 1164 (s), 1001 (s), 767 (m), 726 (s) cm^{-1} ;

3-ethoxydibenzo[*f,h*]quinoxaline-2-carbonitrile (2db): yellow solid; yield 96% (52 mg); mp 245 – 247 °C; ^1H NMR (400 MHz, CDCl_3) δ 8.77 (t, $J = 7.2$ Hz, 2H), 8.44 (dd, $J = 13.9, 8.1$ Hz, 2H), 7.76 (t, $J = 7.6$ Hz, 1H), 7.72 – 7.57 (m, 3H), 4.64 (q, $J = 7.1$ Hz, 2H), 1.59 (t, $J = 7.1$ Hz, 3H). ^{13}C NMR (100 MHz, CDCl_3) δ 158.4, 140.5, 135.5, 132.9, 130.9, 129.9, 129.1, 128.6, 128.2, 127.6, 126.3, 124.8, 122.9, 122.6, 118.3, 114.9, 64.0, 14.4; IR (KBr) $\tilde{\nu}$ 2982 (s), 2929 (s), 2904 (s), 2863 (s), 2230 (s), 1609 (s), 1542 (m), 1436 (m), 1380 (m), 1279 (s), 1208 (m), 1024 (m), 958 (s), 895 (s), 766 (s), 724 (s) cm^{-1} ;

3-((4-chlorobenzyl)oxy)dibenzo[*f,h*]quinoxaline-2-carbonitrile (2dc): pale yellow solid; yield 94% (67 mg); mp 263 – 265 °C; ^1H NMR (400 MHz, CDCl_3) δ 8.93 (d, $J = 7.8$ Hz, 2H), 8.55 (dd, $J = 17.9, 8.1$ Hz, 2H), 7.83 (t, $J = 7.4$ Hz, 1H), 7.79 – 7.66 (m, 3H), 7.55 (d, $J = 8.3$ Hz, 2H), 7.41 (d, $J = 8.4$ Hz, 2H), 5.69 (s, 2H); ^{13}C NMR (100 MHz, CDCl_3) δ 158.1, 140.7, 136.3, 134.5, 134.1, 133.3, 131.3, 130.3, 129.5, 129.4, 129.1, 128.7, 128.4, 128.3, 127.9, 126.4, 125.1, 123.2, 122.8, 118.5, 114.8, 68.5; IR (KBr) $\tilde{\nu}$ 3065 (s), 2922 (s), 2852 (s), 2229 (s), 1550 (m), 1393 (m), 1361 (m), 1275 (m), 1204 (s), 1005 (m), 806 (s), 764 (s) cm^{-1} ;

3-(benzo[*d*][1,3]dioxol-5-ylmethoxy)dibenzo[*f,h*]quinoxaline-2-carbonitrile (2dd): yellow solid; yield 90% (65 mg); mp 256 – 258 °C; ^1H NMR (400 MHz, CDCl_3) δ 9.09 – 8.97 (m, 2H), 8.60 (dd, $J = 18.1, 7.9$ Hz, 2H), 7.85 (dd, $J = 11.2, 4.1$ Hz, 1H), 7.81 – 7.70 (m, 3H), 7.10 (dd, $J = 4.0, 2.5$ Hz, 2H), 6.85 (d, $J = 8.3$ Hz, 1H), 5.98 (s, 2H), 5.68 (s, 2H); ^{13}C NMR (100 MHz,

CDCl₃) δ 158.4, 148.1, 148.1, 140.7, 136.2, 133.3, 131.2, 130.2, 129.3, 129.3, 128.8, 128.4, 128.4, 127.9, 126.5, 125.1, 123.2, 122.8, 122.5, 118.6, 114.8, 109.1, 108.5, 101.3, 69.4; IR (KBr) $\tilde{\nu}$ 2964 (s), 2910 (s), 2853 (s), 2229 (s), 1542 (m), 1449 (m), 1444 (s), 1391 (m), 1241 (m), 1175 (s), 1037 (s), 964 (s), 766 (m), 726 (s) cm⁻¹;

5,6-diphenyl-3-(prop-2-yn-1-yloxy)pyrazine-2-carbonitrile (2ag): white solid; yield 92% (51 mg); mp 160 – 161 °C; ¹H NMR (400 MHz, CDCl₃) δ 7.53 – 7.48 (m, 2H), 7.43 – 7.38 (m, 3H), 7.37 – 7.27 (m, 5H), 5.20 (d, J = 2.3 Hz, 2H), 2.58 (t, J = 2.3 Hz, 1H); ¹³C NMR (100 MHz, CDCl₃) δ 157.8, 152.5, 147.2, 136.9, 136.6, 130.2, 130.1, 129.6, 129.1, 128.6, 128.5, 115.8, 114.2, 77.5, 76.0, 55.1; IR (KBr) $\tilde{\nu}$ 2938 (s), 2880 (s), 2234 (s), 2134 (s), 1536 (m), 1419 (m), 1396 (s), 1351 (m), 1325 (m), 1184 (m), 1173 (m), 996 (m), 946 (s), 774 (s), 700 (m) cm⁻¹;

3-(prop-2-yn-1-yloxy)-5,6-di(thiophen-3-yl)pyrazine-2-carbonitrile (2bg): brown solid; yield 91% (50 mg); mp 163 – 165 °C; ¹H NMR (400 MHz, CDCl₃) δ 7.64 (dd, J = 3.0, 1.3 Hz, 1H), 7.52 (dd, J = 3.0, 1.3 Hz, 1H), 7.35 (dd, J = 5.0, 3.0 Hz, 1H), 7.29 (dd, J = 5.1, 3.0 Hz, 1H), 7.23 (dd, J = 5.1, 1.3 Hz, 1H), 7.11 (dd, J = 5.0, 1.3 Hz, 1H), 5.16 (d, J = 2.4 Hz, 2H), 2.56 (t, J = 2.4 Hz, 1H); ¹³C NMR (100 MHz, CDCl₃) δ 157.6, 147.4, 142.3, 138.0, 137.9, 129.7, 128.3, 128.1, 126.6, 126.3, 126.0, 115.1, 114.2, 76.0, 55.1, 31.1; IR (KBr) $\tilde{\nu}$ 2952 (s), 2922 (s), 2227 (s), 1536 (s), 1450 (s), 1428 (m), 1361 (m), 1299 (s), 1189 (m), 1015 (s), 972 (s), 848 (s), 800 (s), 750 (s), 695 (m) cm⁻¹;

3-(prop-2-yn-1-yloxy)pyrazino[2,3-*f*][1,10]phenanthroline-2-carbonitrile (2cg): pale yellow solid; yield 91% (52 mg); mp 261 – 265 °C; ¹H NMR (400 MHz, CDCl₃) δ 9.39 – 9.32 (m, 3H), 9.29 (dd, J = 4.4, 1.7 Hz, 1H), 7.87 – 7.79 (m, 2H), 5.38 (d, J = 2.4 Hz, 2H), 2.60 (t, J = 2.4 Hz,

1H); ^{13}C NMR (100 MHz, CDCl_3) δ 158.0, 153.7, 152.2, 148.5, 146.1, 139.8, 135.3, 134.3, 133.2, 126.1, 125.6, 124.7, 124.4, 120.1, 113.9, 76.5, 55.7; IR (KBr) $\tilde{\nu}$ 2948 (s), 2945 (s), 2237 (s), 2115 (s), 1547 (m), 1403 (m), 1346 (m), 1263 (s), 1223 (s), 1180 (m), 994 (m), 915 (s), 817 (s), 741 (m) cm^{-1} ;

3-(prop-2-yn-1-yloxy)dibenzo[*f,h*]quinoxaline-2-carbonitrile (2dg): yellow solid; yield 89% (50 mg); mp 247 – 250 °C; ^1H NMR (400 MHz, CDCl_3) δ 8.94 (td, $J = 8.2, 1.2$ Hz, 2H), 8.55 (dd, $J = 15.3, 8.1$ Hz, 2H), 7.88 – 7.80 (m, 1H), 7.80 – 7.67 (m, 3H), 5.28 (d, $J = 2.4$ Hz, 2H), 2.59 (t, $J = 2.4$ Hz, 1H); ^{13}C NMR (100 MHz, CDCl_3) δ 157.2, 140.4, 136.5, 133.2, 131.3, 130.3, 129.5, 128.5, 128.4, 128.1, 127.9, 126.6, 125.1, 123.1, 122.7, 118.1, 114.6, 76.0, 55.2; IR (KBr) $\tilde{\nu}$ 2923 (s), 2856 (s), 2237 (s), 1544 (s), 1396 (m), 1358 (m), 1279 (s), 1212 (m), 1185 (m), 1002 (m), 769 (s), 725 (s) cm^{-1} ;

3-methoxy- d_3 -pyrazino[2,3-*f*][1,10]phenanthroline-2-carbonitrile (2ch): pale yellow solid; yield 92% (47 mg); mp 279 – 282 °C; ^1H NMR (400 MHz, CDCl_3) δ 9.40 – 9.24 (m, 2H), 7.82 (dd, $J = 8.0, 4.1$ Hz, 1H); ^{13}C NMR (100 MHz, CDCl_3) δ 159.6, 153.6, 152.1, 148.7, 146.2, 140.0, 134.7, 134.1, 132.8, 126.1, 125.6, 124.6, 124.2, 120.1, 114.3; IR (KBr) $\tilde{\nu}$ 2923 (s), 2856 (s), 2235 (s), 1547 (m), 1424 (m), 1408 (m), 1379 (m), 1263 (s), 1224 (m), 1086 (m), 984 (s), 742 (s) cm^{-1} ;

3-methoxy- d_3 -dibenzo[*f,h*]quinoxaline-2-carbonitrile (2dh): pale yellow solid; yield 94% (49 mg); mp 269 – 271 °C; ^1H NMR (400 MHz, CDCl_3) δ 9.08 – 8.92 (m, 2H), 8.58 (dd, $J = 14.5, 8.0$ Hz, 2H), 7.84 (t, $J = 7.1$ Hz, 1H), 7.80 – 7.65 (m, 3H); ^{13}C NMR (100 MHz, CDCl_3) δ 159.02, 133.26, 131.18, 130.22, 129.33, 128.85, 128.38, 127.82, 126.55, 125.06, 123.17, 122.82,

114.99; IR (KBr) $\tilde{\nu}$ 3067 (s), 2925 (s), 2233 (s), 1547 (m), 1433 (m), 1392 (m), 1212 (m), 1189 (s), 1086 (m), 985 (m), 767 (s), 725 (s) cm^{-1} ;

3-methoxy- d_3 -5,6-diphenylpyrazine-2-carbonitrile (2ah): white solid; yield 95% (49 mg); mp 180 – 182 °C; ^1H NMR (400 MHz, CDCl_3) δ 7.52 – 7.46 (m, 2H), 7.43 – 7.36 (m, 3H), 7.32 (ddd, $J = 9.1, 5.1, 2.3$ Hz, 5H); ^{13}C NMR (100 MHz, CDCl_3) δ 159.5, 152.8, 146.4, 137.1, 137.0, 130.0, 129.6, 128.9, 128.5, 128.4, 115.8, 114.6; IR (KBr) $\tilde{\nu}$ 3057 (s), 2935 (s), 2234 (s), 1535 (m), 1393 (m), 1340 (m), 1231 (m), 1180 (s), 1096 (m), 924 (m), 774 (s), 700 (s) cm^{-1} ;

3-methoxy- d_3 -5,6-di(thiophen-3-yl)pyrazine-2-carbonitrile (2dh): pale yellow solid; yield 91% (47 mg); mp 214 – 216 °C; ^1H NMR (400 MHz, CDCl_3) δ 7.61 (dd, $J = 2.8, 1.0$ Hz, 1H), 7.49 (dd, $J = 2.8, 1.0$ Hz, 1H), 7.33 (dd, $J = 5.0, 3.0$ Hz, 1H), 7.29 (dd, $J = 5.0, 3.0$ Hz, 1H), 7.21 (dd, $J = 5.1, 1.0$ Hz, 1H), 7.10 (dd, $J = 5.0, 1.0$ Hz, 1H); ^{13}C NMR (100 MHz, CDCl_3) δ 159.31, 147.66, 141.57, 138.30, 138.15, 129.33, 128.32, 128.12, 126.38, 126.22, 125.97, 115.14, 114.55; IR (KBr) $\tilde{\nu}$ 3096 (s), 2973 (s), 2225 (s), 1514 (m), 1505 (m), 1428 (m), 1360 (m), 1302 (m), 1199 (m), 1083 (m), 955 (m), 804 (s), 787 (s), 700 (s) cm^{-1} ;

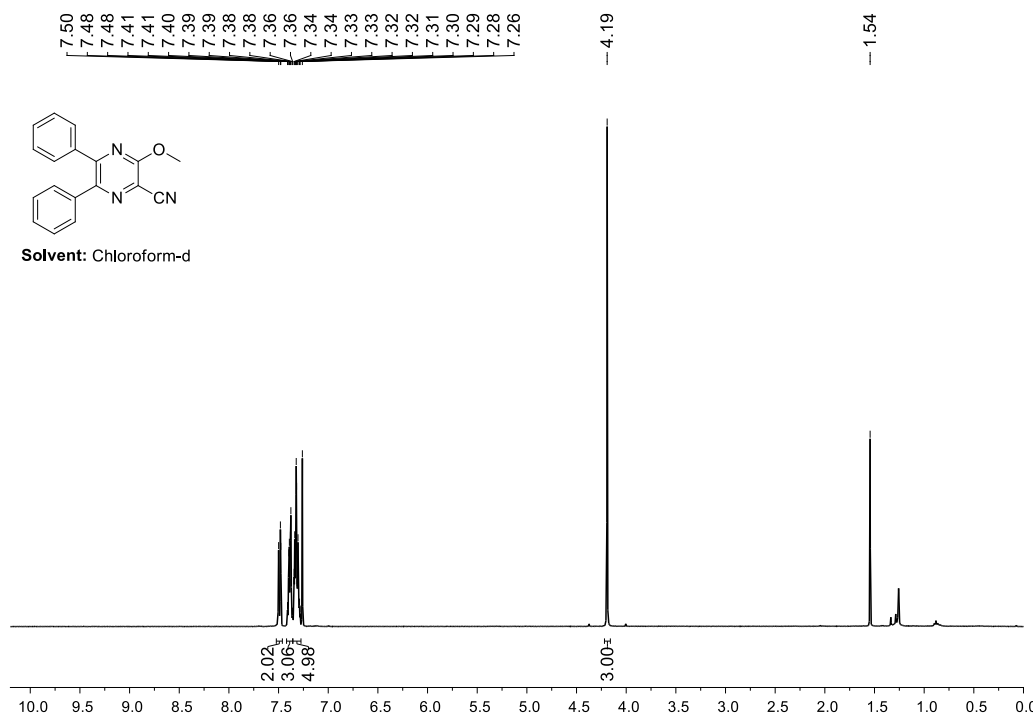
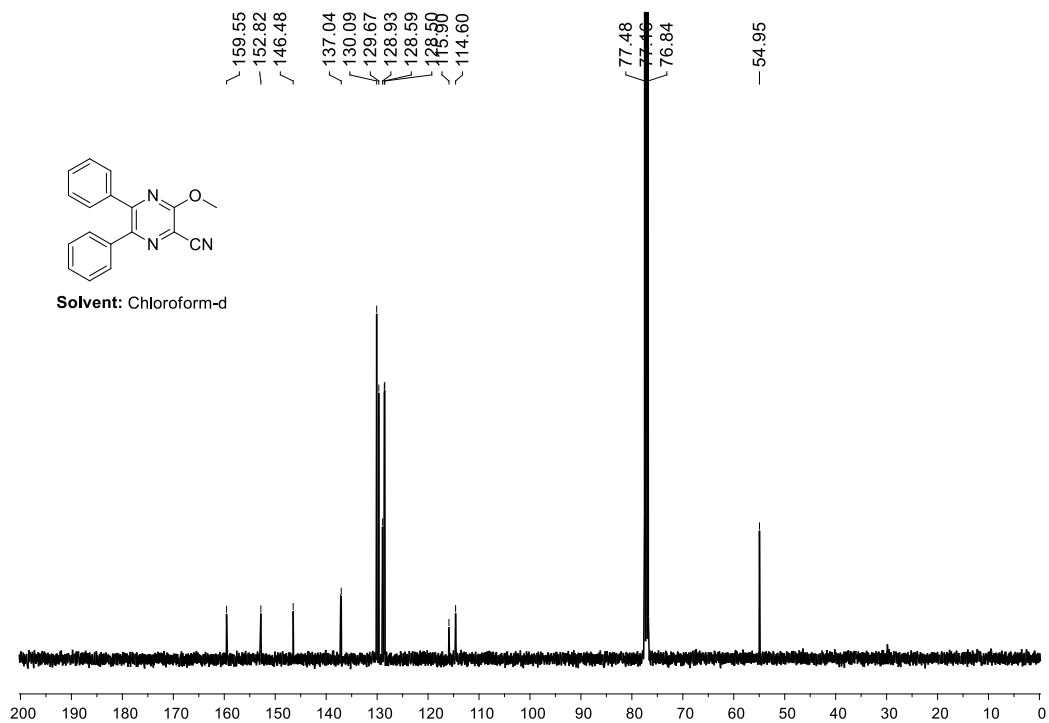
3-(hexyloxy)-5,6-diphenylpyrazine-2-carbonitrile (2ae): white solid; yield 96% (51 mg); mp 53 – 55 °C; ^1H NMR (400 MHz, CDCl_3) δ 7.50 – 7.45 (m, 2H), 7.39 (ddd, $J = 7.1, 4.4, 2.6$ Hz, 3H), 7.35 – 7.27 (m, 5H), 4.57 (t, $J = 6.7$ Hz, 2H), 1.96 – 1.84 (m, 2H), 1.57 – 1.45 (m, 2H), 1.44 – 1.31 (m, 4H), 0.99 – 0.86 (m, 3H); ^{13}C NMR (100 MHz, CDCl_3) δ 159.4, 152.7, 146.1, 137.2, 137.1, 130.0, 129.9, 129.6, 128.8, 128.5, 128.4, 115.8, 114.6, 68.2, 31.5, 28.7, 25.6, 22.6, 14.1; IR (KBr) $\tilde{\nu}$ 2960 (m), 2921 (m), 2858 (s), 2230 (s), 1542 (m), 1535 (m), 1427 (m), 1360 (m), 1190 (m), 1173 (m), 987 (m), 939 (s), 701 (m) cm^{-1} ;

3-(hexyloxy)pyrazino[2,3-*f*][1,10]phenanthroline-2-carbonitrile (2ce): yellowish brown solid; yield 96% (51 mg); mp 159 – 161 °C; ^1H NMR (400 MHz, CDCl_3) δ 9.37 – 9.21 (m, 12H), 7.86 – 7.74 (m, 6H), 4.74 (t, $J = 6.6$ Hz, 6H), 2.06 – 1.95 (m, 6H), 1.91 (s, 4H), 1.66 – 1.53 (m, 6H), 1.42 (dq, $J = 9.1, 6.2$ Hz, 11H), 0.94 (t, $J = 6.9$ Hz, 9H); ^{13}C NMR (100 MHz, CDCl_3) δ 159.4, 153.5, 151.9, 148.5, 145.9, 140.0, 134.4, 134.1, 132.9, 126.2, 125.7, 124.6, 124.2, 120.3, 114.3, 68.9, 31.6, 28.6, 25.7, 22.6, 14.1; IR (KBr) $\tilde{\nu}$ 2955 (s), 2932 (m), 2871 (s), 2861 (s), 2232 (s), 1548 (m), 1415 (m), 1391 (m), 1347 (m), 1224 (m), 1186 (s), 978 (m), 813 (s), 741 (s) cm^{-1} ;

3-(hexyloxy)dibenzo[*f,h*]quinoxaline-2-carbonitrile (2de): yellow solid; yield 94% (50 mg); mp 155 – 157 °C; ^1H NMR (400 MHz, CDCl_3) δ 8.88 – 8.80 (m, 2H), 8.48 (dd, $J = 14.7, 8.0$ Hz, 2H), 7.82 – 7.75 (m, 1H), 7.69 (ddt, $J = 14.3, 11.9, 4.3$ Hz, 3H), 4.60 (t, $J = 6.7$ Hz, 2H), 2.03 – 1.88 (m, 2H), 1.63 – 1.54 (m, 2H), 1.49 – 1.35 (m, 4H), 0.96 (t, $J = 7.0$ Hz, 3H); ^{13}C NMR (100 MHz, CDCl_3) δ 158.6, 140.5, 135.5, 132.9, 130.9, 129.9, 129.1, 128.7, 128.2, 128.2, 127.6, 126.3, 124.8, 122.9, 122.6, 118.3, 114.9, 68.2, 31.7, 28.7, 25.8, 22.7, 14.2; IR (KBr) $\tilde{\nu}$ 2961 (s), 2924 (s), 2869 (m), 2856 (s), 2229 (s), 1563 (m), 1438 (m), 1402 (m), 1370 (m), 1363 (m), 1277 (m), 1207 (m), 1117 (s), 981 (m), 768 (m), 725 (s), 617 (s) cm^{-1} ;

2-(2-(2-((3-cyanopyrazino[2,3-*f*][1,10]phenanthroline-2-yl)oxy)ethoxy)ethoxy)ethyl 4-methylbenzenesulfonate (2di): yellow solid; yield 82% (82 mg); mp 115 – 117 °C; ^1H NMR (400 MHz, CDCl_3) δ 9.00 – 8.87 (m, 2H), 8.55 (dd, $J = 13.6, 7.9$ Hz, 2H), 7.87 – 7.64 (m, 6H), 7.31 (d, $J = 8.1$ Hz, 2H), 4.81 (dd, $J = 5.5, 4.2$ Hz, 2H), 4.21 – 4.14 (m, 2H), 4.02 (dd, $J = 5.4, 4.2$ Hz, 2H), 3.80 – 3.69 (m, 4H), 3.66 (dd, $J = 5.6, 3.5$ Hz, 2H), 2.41 (s, 3H); ^{13}C NMR (100 MHz, CDCl_3) δ 158.4, 144.9, 140.6, 136.0, 133.2, 133.1, 131.2, 130.2, 129.9, 129.3, 128.7, 128.3, 128.2, 128.1, 127.8, 126.4, 125.0, 123.1, 122.8, 118.3, 114.9, 71.1, 70.9, 69.4, 69.1, 68.9,

67.3, 21.7; IR (KBr) $\tilde{\nu}$ 2920 (s), 2894 (s), 2230 (s), 1756 (w), 1546 (m), 1432 (m), 1363 (m), 1355 (m), 1334 (m), 1189 (m), 1109 (m), 1011 (s), 907 (m), 768 (m);

^1H and ^{13}C NMR Spectra**Figure 5.5.** ^1H NMR of 3-methoxy-5,6-diphenylpyrazine-2-carbonitrile (2aa)**Figure 5.6.** ^{13}C NMR of 3-methoxy-5,6-diphenylpyrazine-2-carbonitrile (2aa)

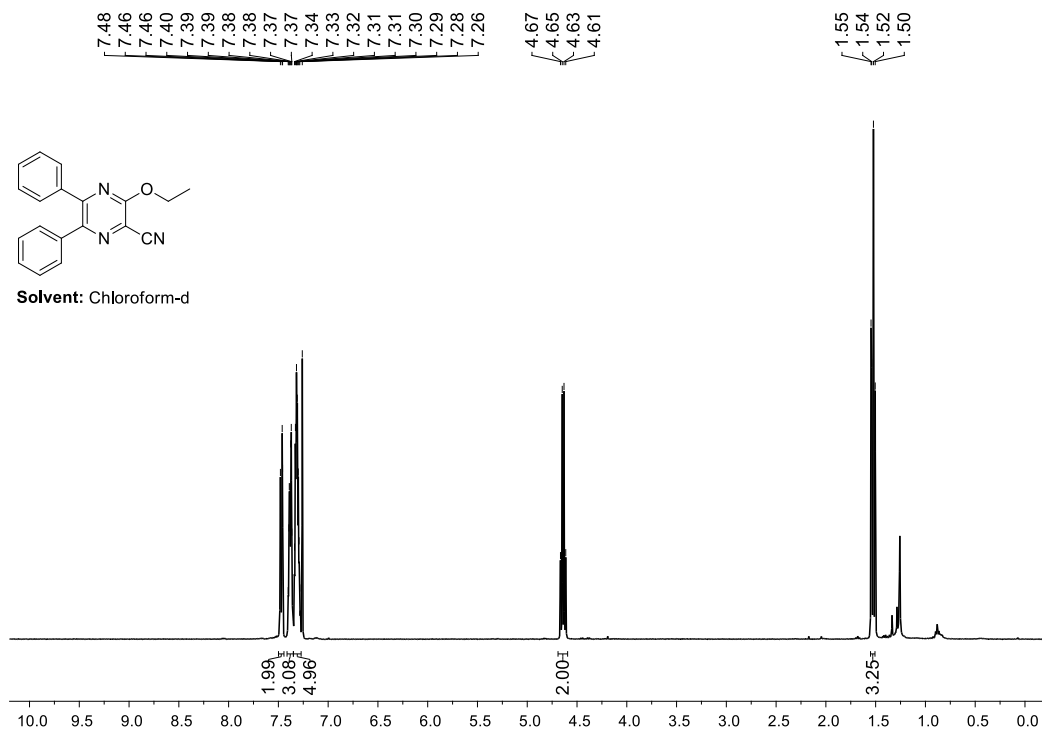


Figure 5.7. ¹H NMR of 3-ethoxy-5,6-diphenylpyrazine-2-carbonitrile (2ab)

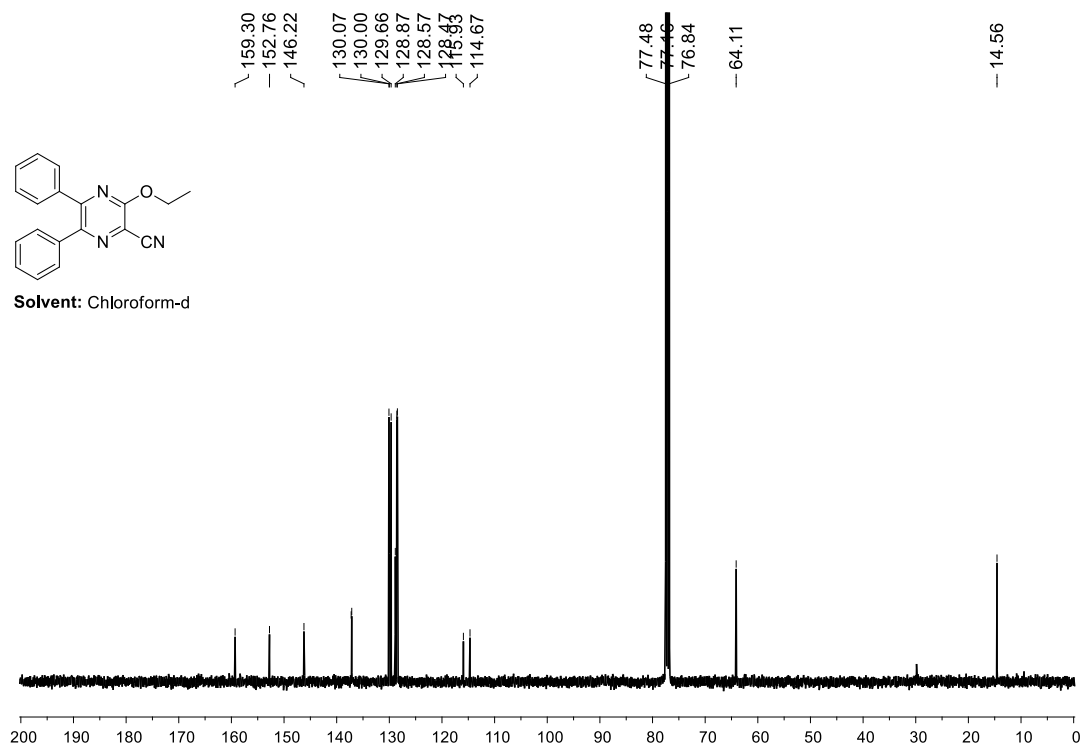


Figure 5.8. ¹³C NMR of 3-ethoxy-5,6-diphenylpyrazine-2-carbonitrile (2ab)

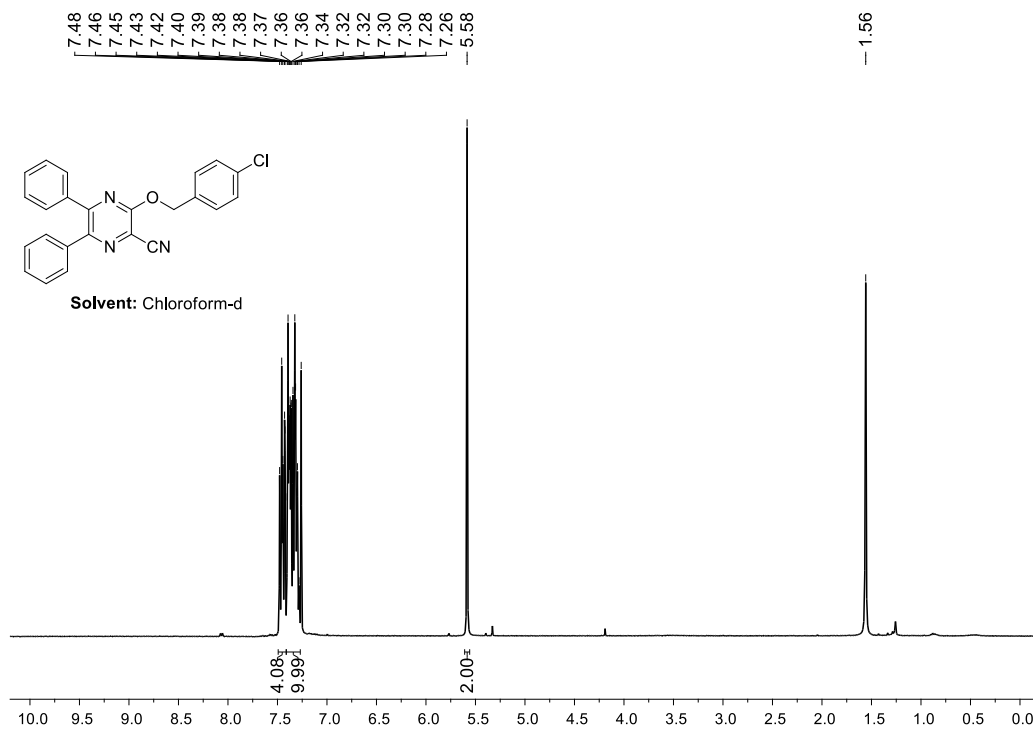


Figure 5.9. ^1H NMR of 3-((4-chlorobenzyl)oxy)-5,6-diphenylpyrazine-2-carbonitrile (**2ac**)

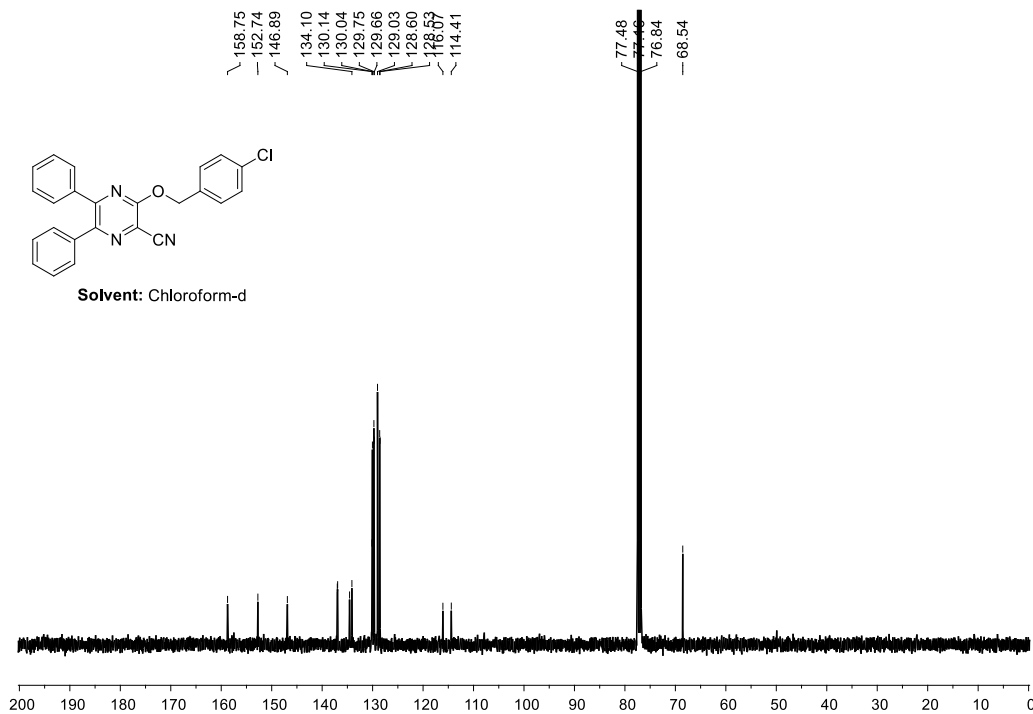


Figure 5.10. ^{13}C NMR of 3-((4-chlorobenzyl)oxy)-5,6-diphenylpyrazine-2-carbonitrile (**2ac**)

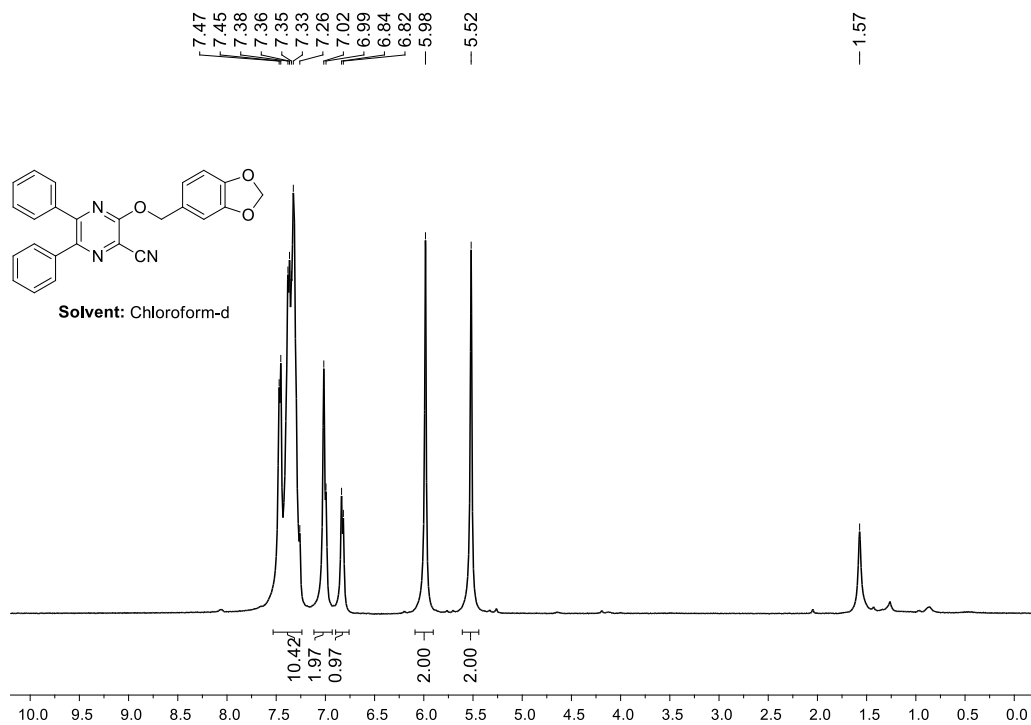


Figure 5.11. ¹H NMR spectrum of 3-(benzo[d][1,3]dioxol-5-ylmethoxy)-5,6-diphenylpyrazine-2-carbonitrile (**2ad**)

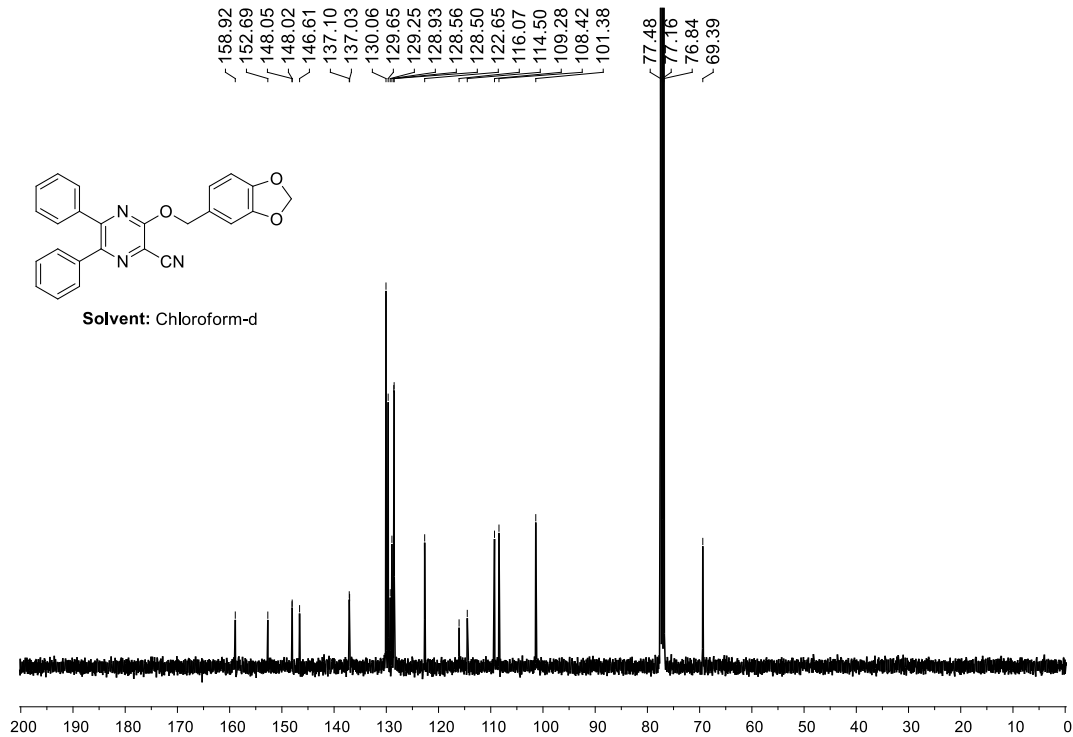


Figure 5.12. ¹³C NMR spectrum of 3-(benzo[d][1,3]dioxol-5-ylmethoxy)-5,6-diphenylpyrazine-2-carbonitrile (**2ad**)

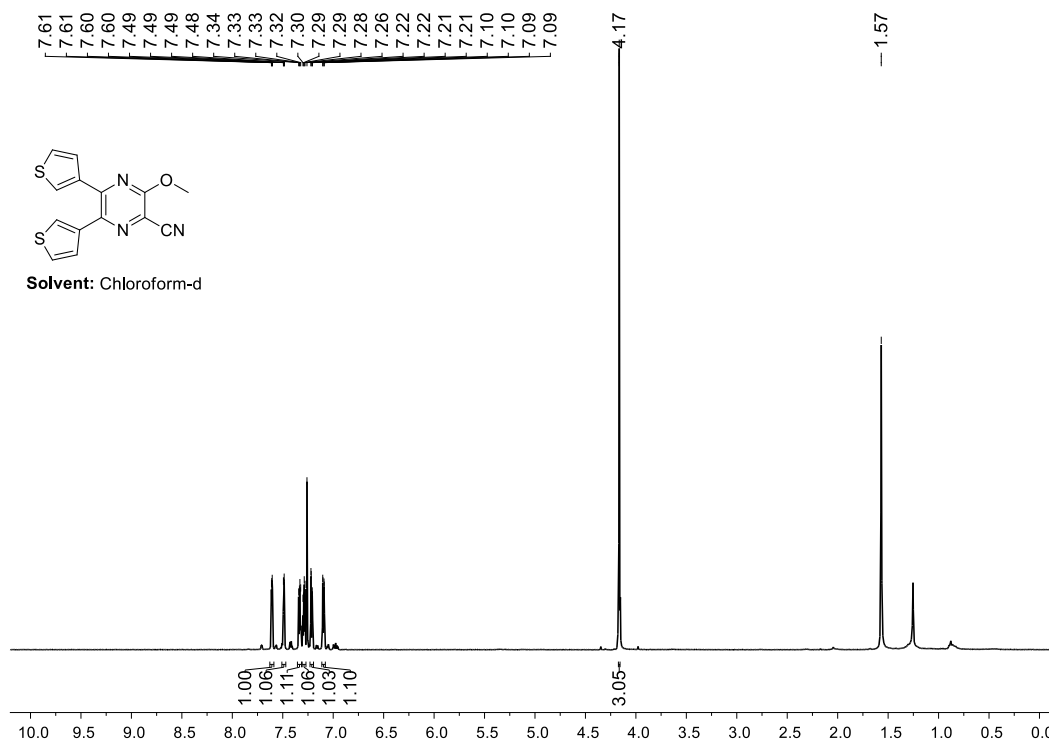


Figure 5.13. ¹H NMR spectrum of 3-methoxy-5,6-di(thiophen-3-yl)pyrazine-2-carbonitrile (**2ba**)

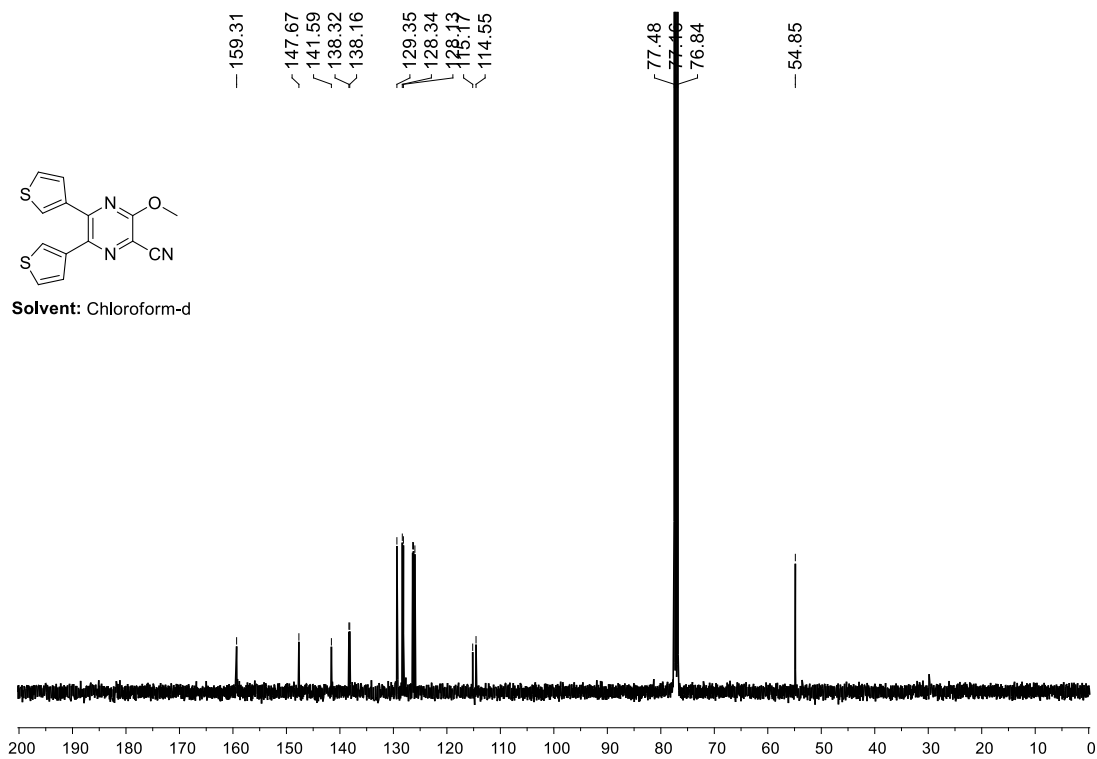


Figure 5.14. ¹³C NMR spectrum of 3-methoxy-5,6-di(thiophen-3-yl)pyrazine-2-carbonitrile (**2ba**)

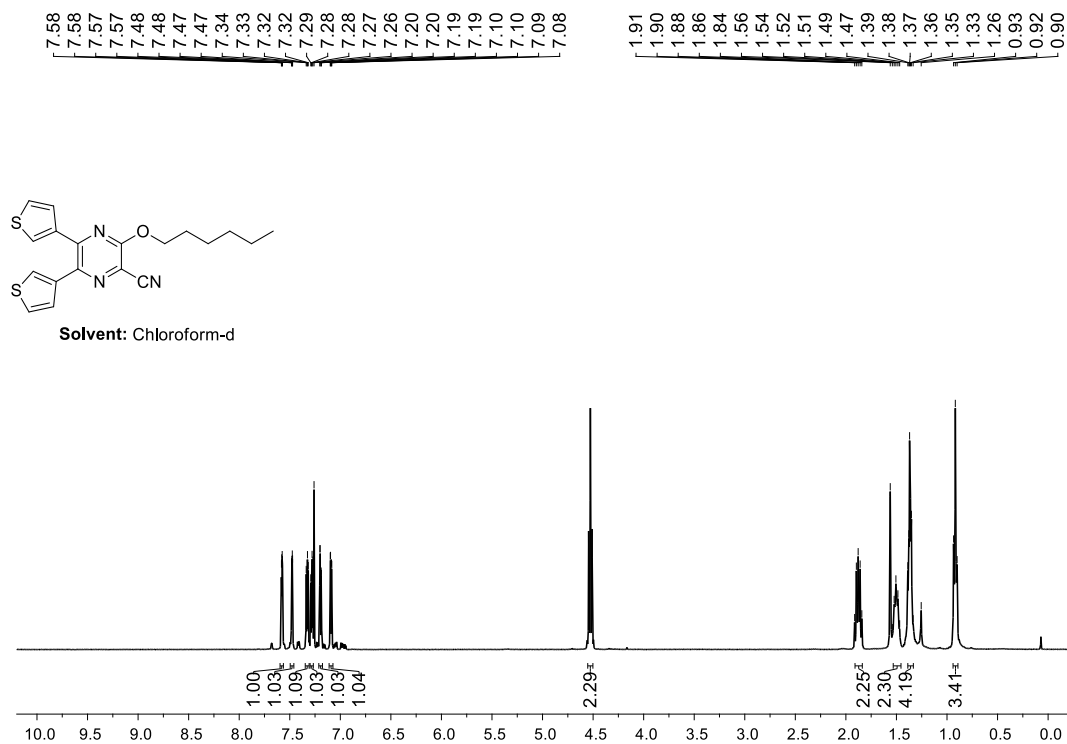


Figure 5.15. ¹H NMR spectrum of 3-(hexyloxy)-5,6-di(thiophen-3-yl)pyrazine-2-carbonitrile (2be)

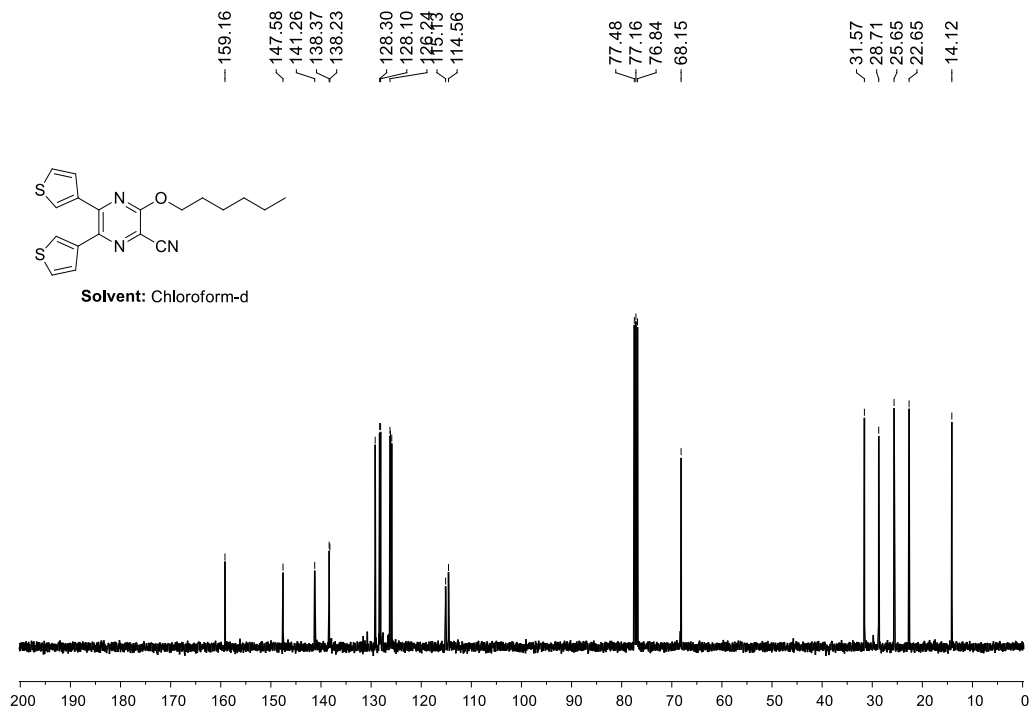


Figure 5.16.: ¹³C NMR spectrum of 3-(hexyloxy)-5,6-di(thiophen-3-yl)pyrazine-2-carbonitrile (2be)

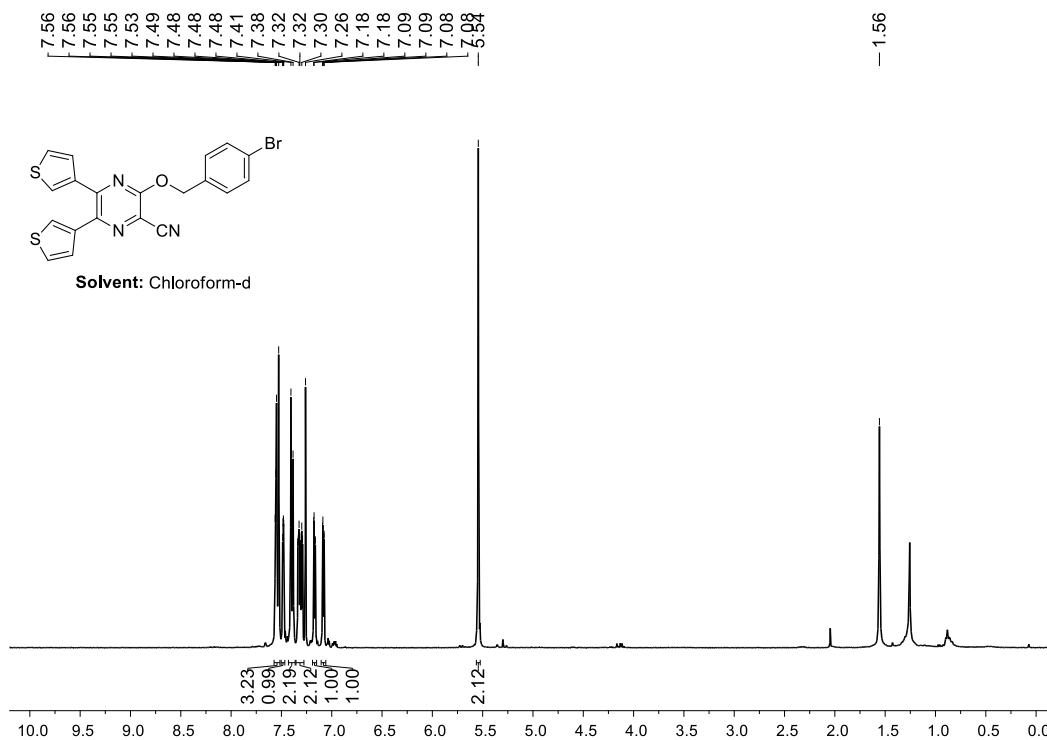


Figure 5.17. ¹H NMR spectrum of 3-((4-bromobenzyl)oxy)-5,6-di(thiophen-3-yl)pyrazine-2-carbonitrile (2bf)

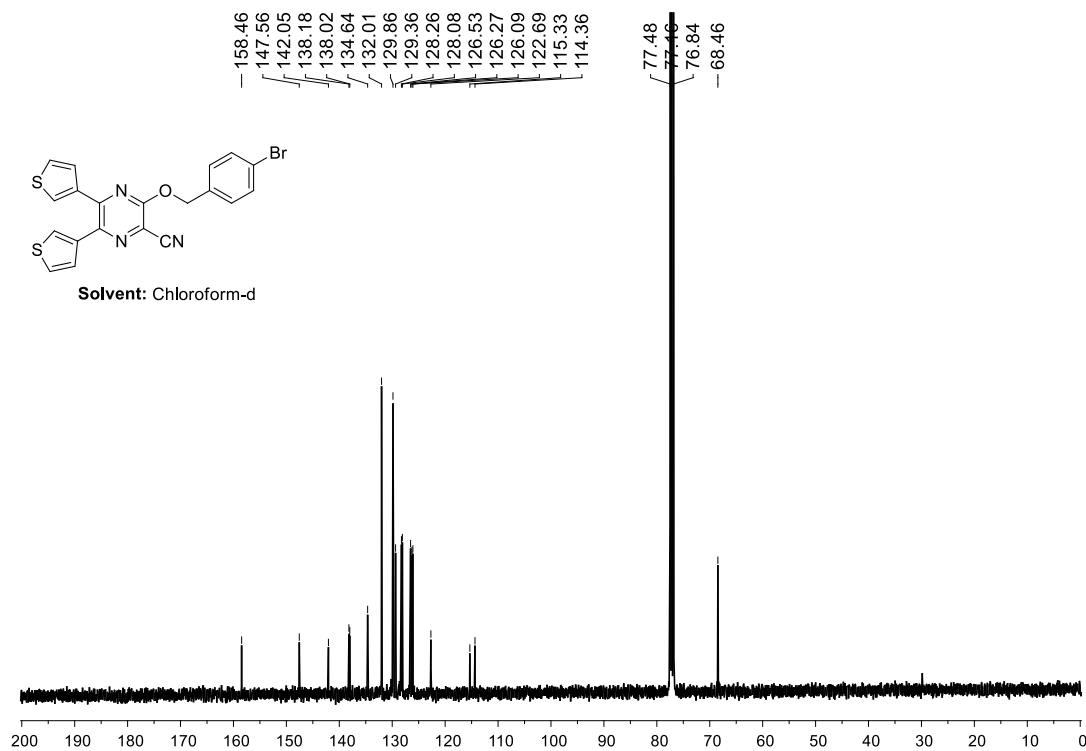


Figure 5.18. ¹³C NMR spectrum of 3-((4-bromobenzyl)oxy)-5,6-di(thiophen-3-yl)pyrazine-2-carbonitrile (2bf)

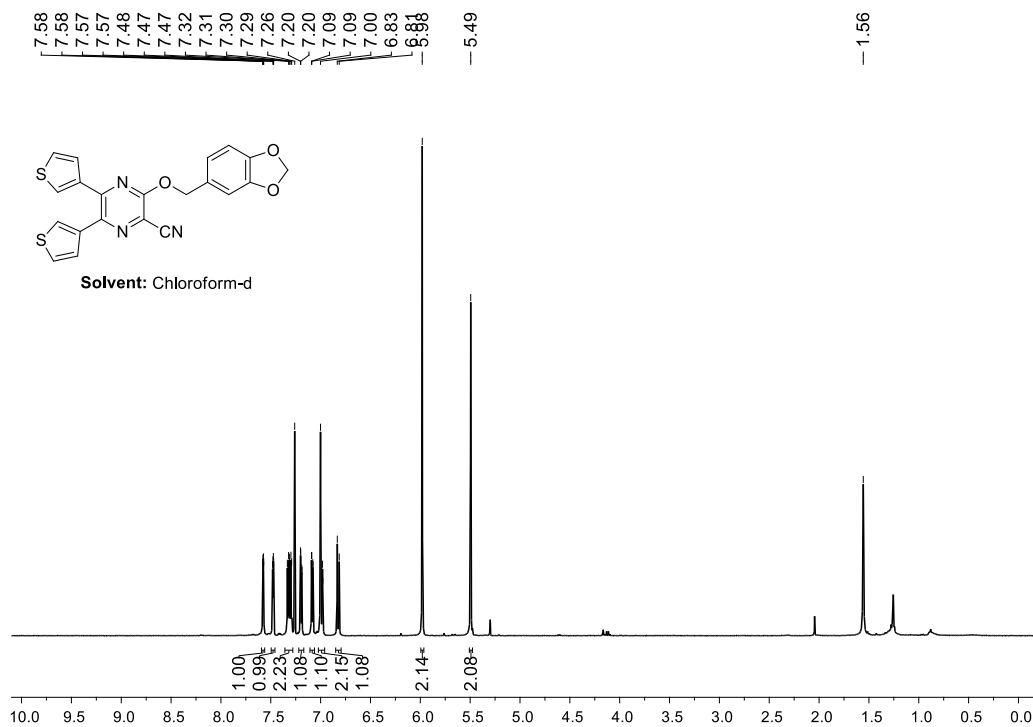


Figure 5.19. ¹H NMR spectrum of 3-(benzo[d][1,3]dioxol-5-ylmethoxy)-5,6-di(thiophen-3-yl)pyrazine-2-carbonitrile (**2bd**)

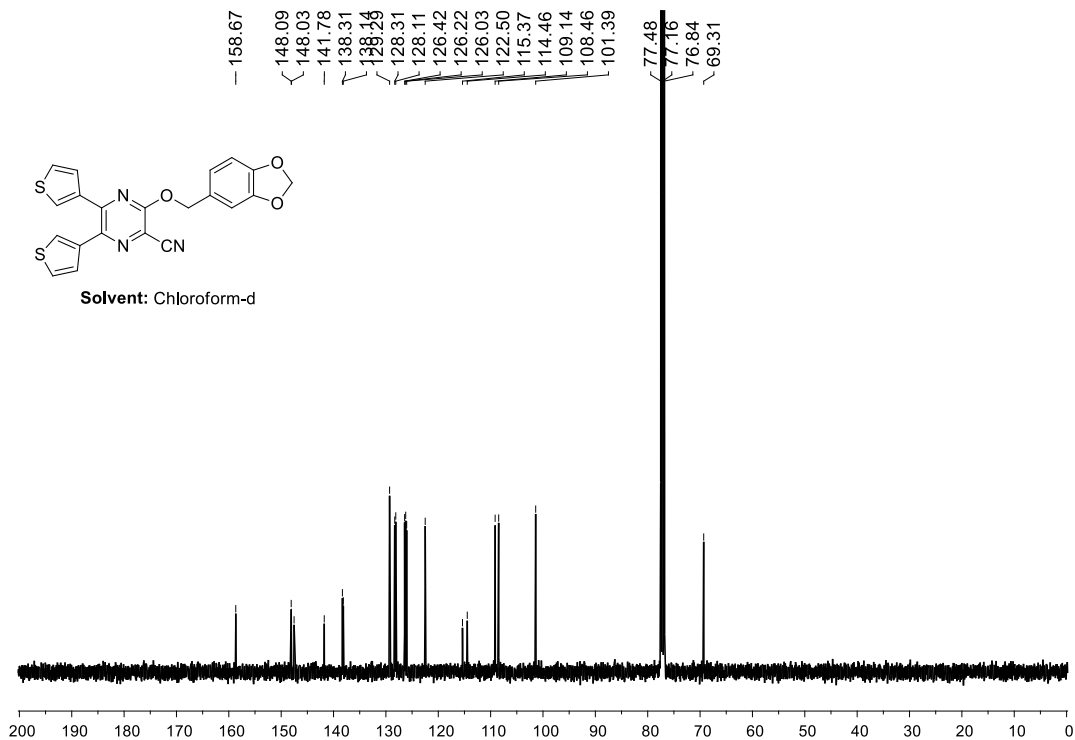


Figure 5.20. ¹³C NMR spectrum of 3-(benzo[d][1,3]dioxol-5-ylmethoxy)-5,6-di(thiophen-3-yl)pyrazine-2-carbonitrile (**2bd**)

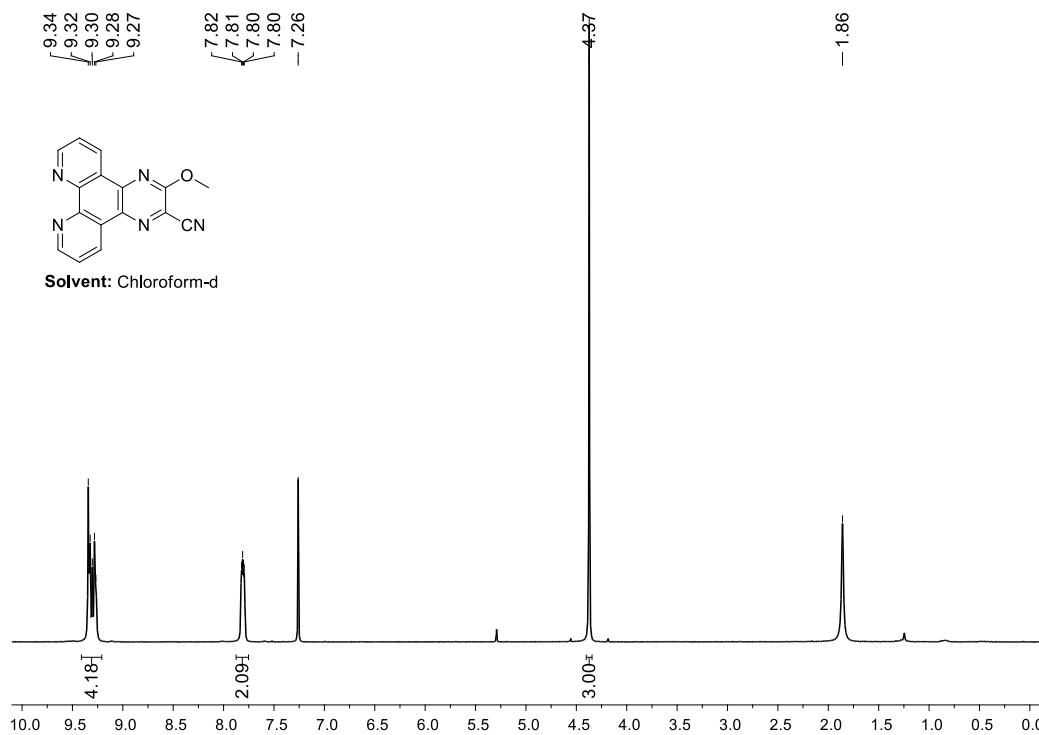


Figure 5.21. ¹H NMR spectrum of 3-methoxypyrazino[2,3-f][1,10]phenanthroline-2-carbonitrile (2ca)

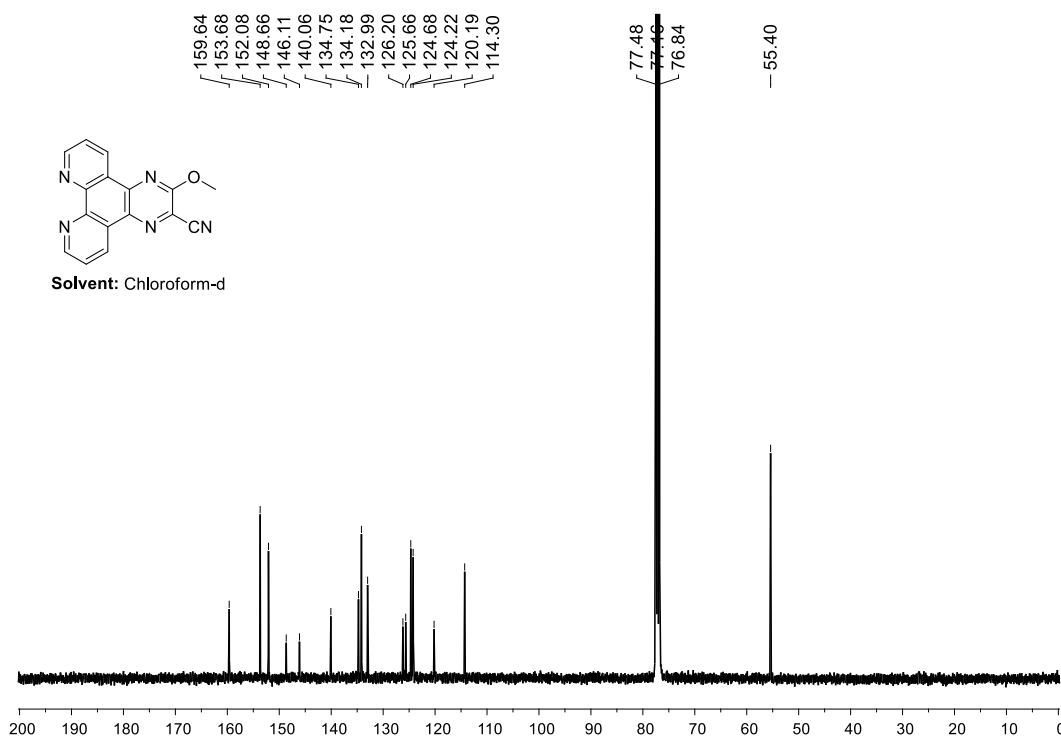


Figure 5.22. ¹³C NMR spectrum of 3-methoxypyrazino[2,3-f][1,10]phenanthroline-2-carbonitrile (2ca)

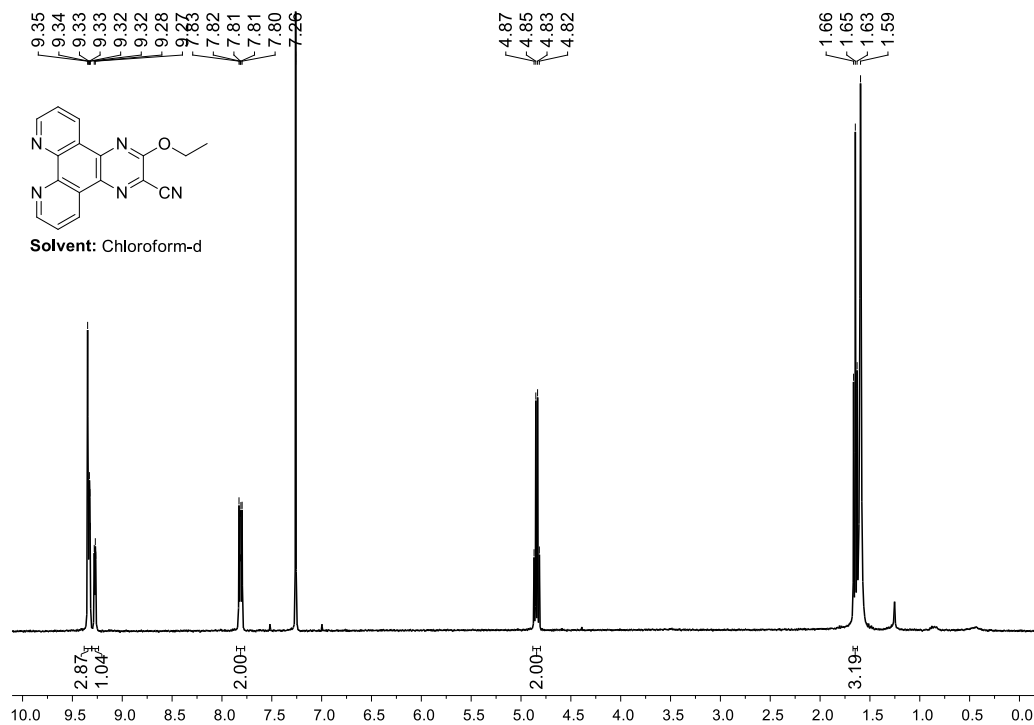


Figure 5.23. ^1H NMR spectrum of 3-ethoxypyrazino[2,3-*f*][1,10]phenanthroline-2-carbonitrile (**2cb**)

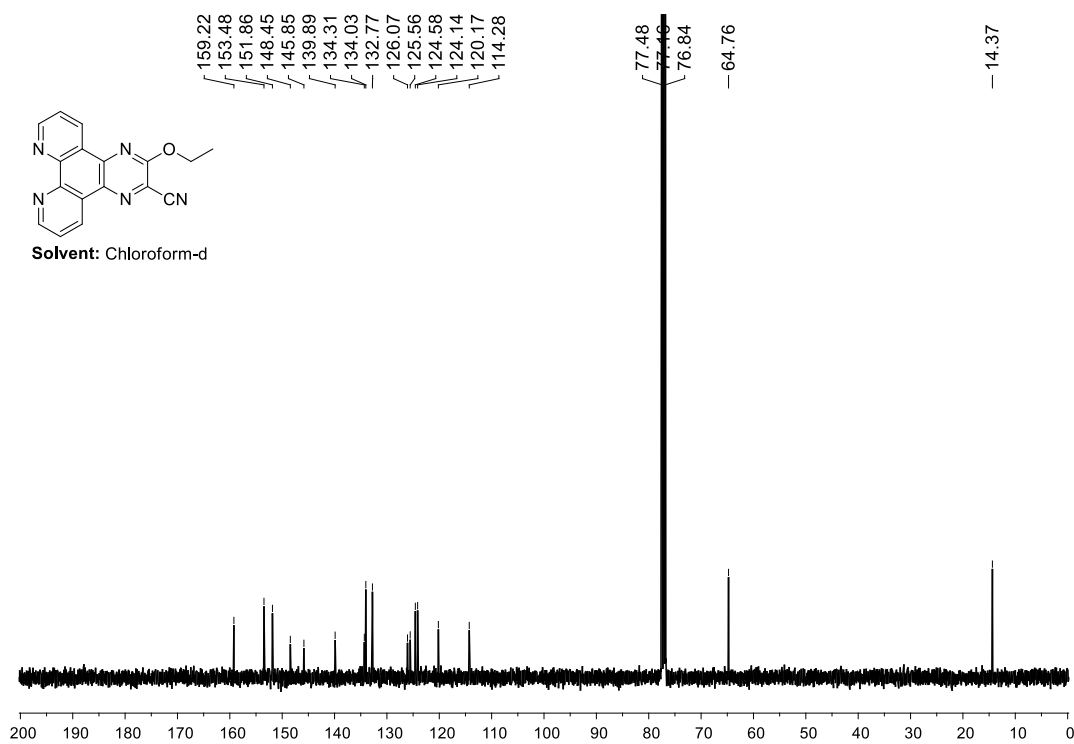


Figure 5.24. ^{13}C NMR spectrum of 3-ethoxypyrazino[2,3-*f*][1,10]phenanthroline-2-carbonitrile (**2cb**)

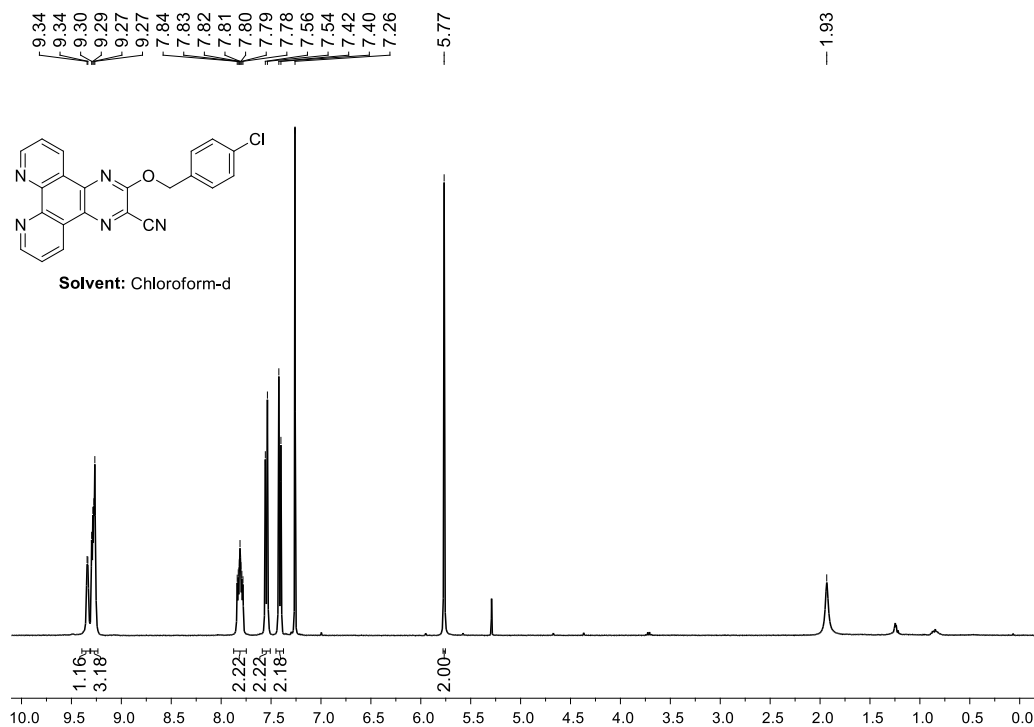


Figure 5.25. ^1H NMR spectrum of 3-((4-chlorobenzyl)oxy)pyrazino[2,3-f][1,10]phenanthroline-2-carbonitrile (**2cc**)

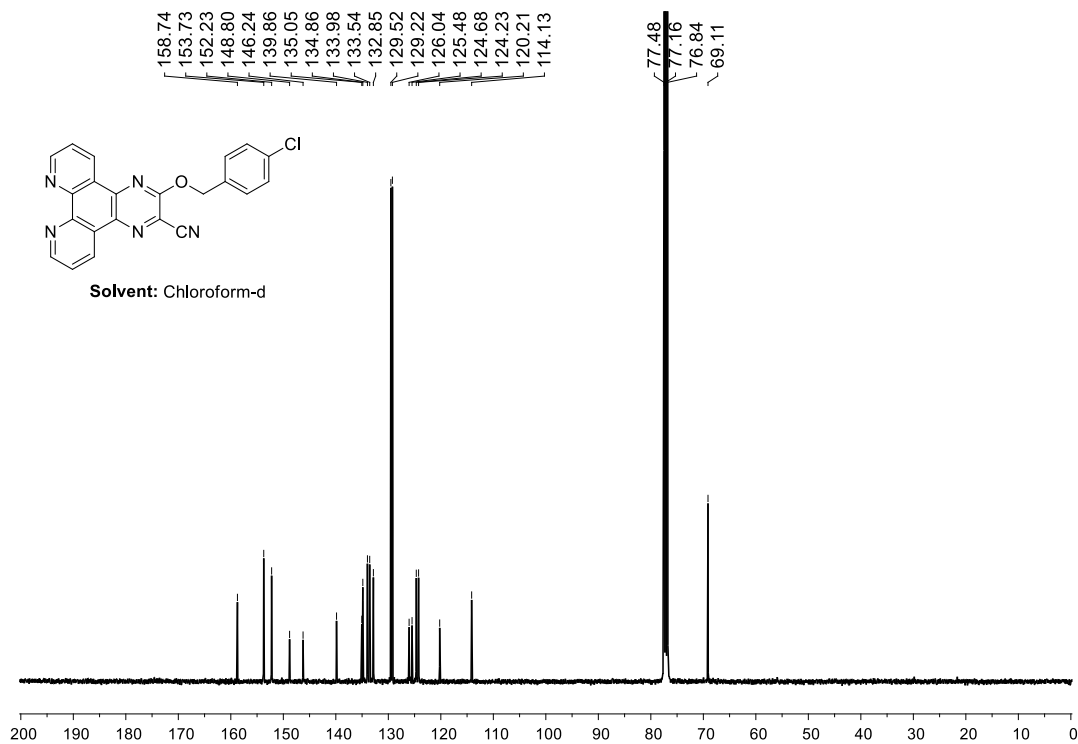


Figure 5.26. ^{13}C NMR spectrum of 3-((4-chlorobenzyl)oxy)pyrazino[2,3-f][1,10]phenanthroline-2-carbonitrile (**2cc**)

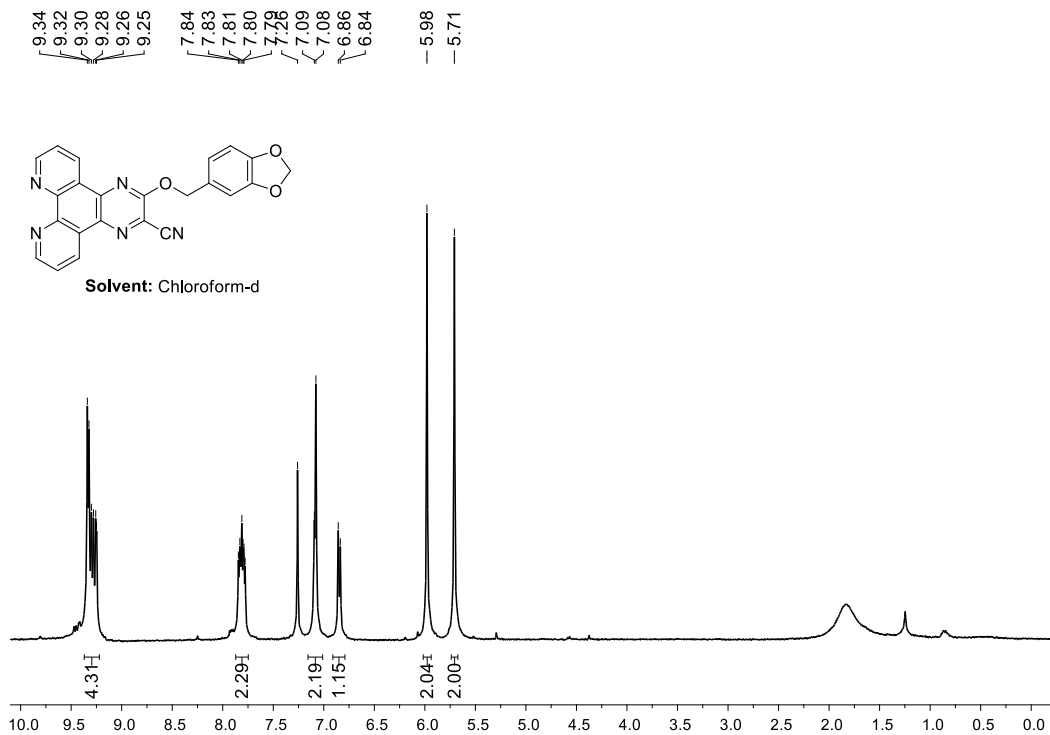


Figure 5.27. ¹H NMR spectrum of 3-(benzo[d][1,3]dioxol-5-ylmethoxy)pyrazino[2,3-f][1,10]phenanthroline-2-carbonitrile (**2cd**)

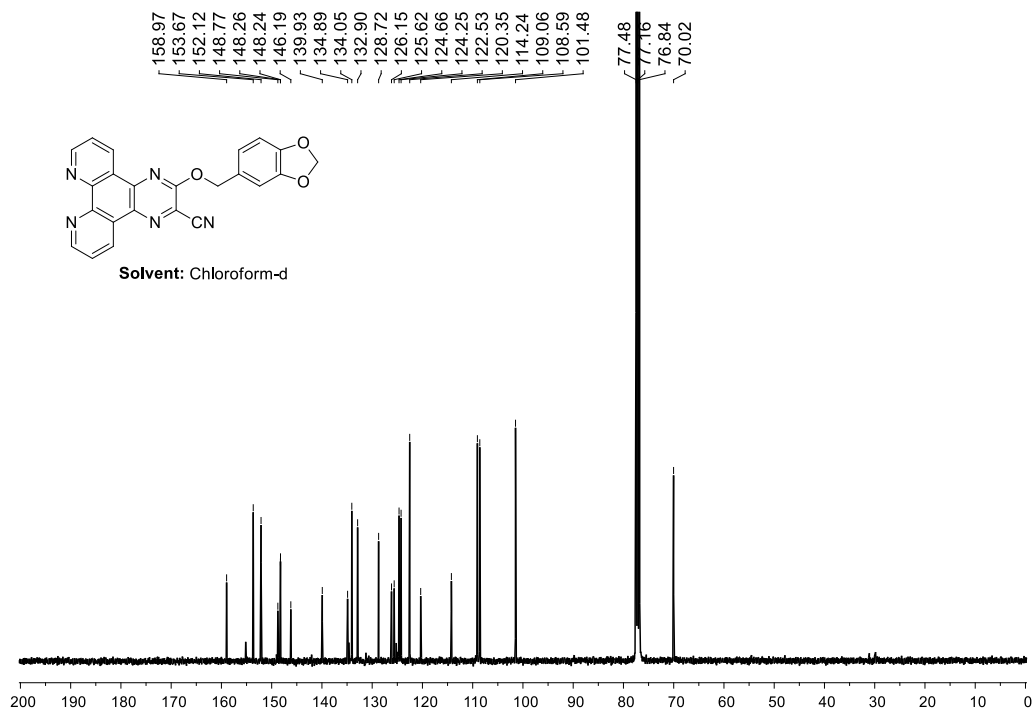


Figure 5.28. ¹³C NMR spectrum of 3-(benzo[d][1,3]dioxol-5-ylmethoxy)pyrazino[2,3-f][1,10]phenanthroline-2-carbonitrile (**2cd**)

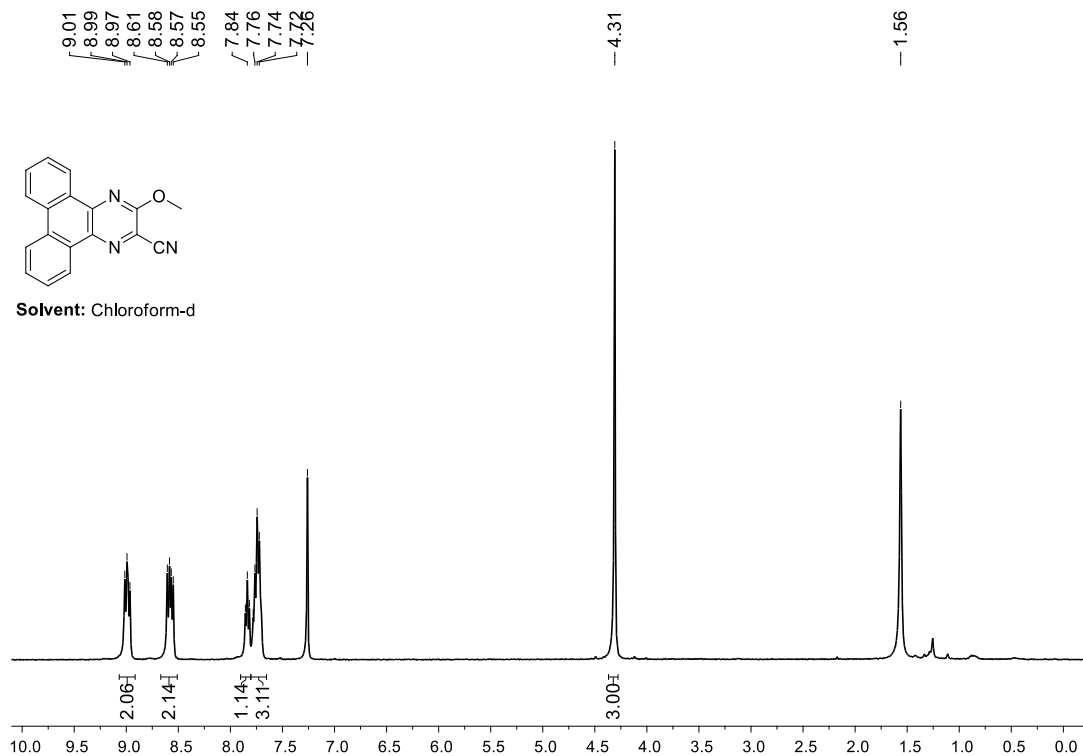


Figure 5.29. ¹H NMR spectrum of 3-methoxydibenzo[*f,h*]quinoxaline-2-carbonitrile (2da)

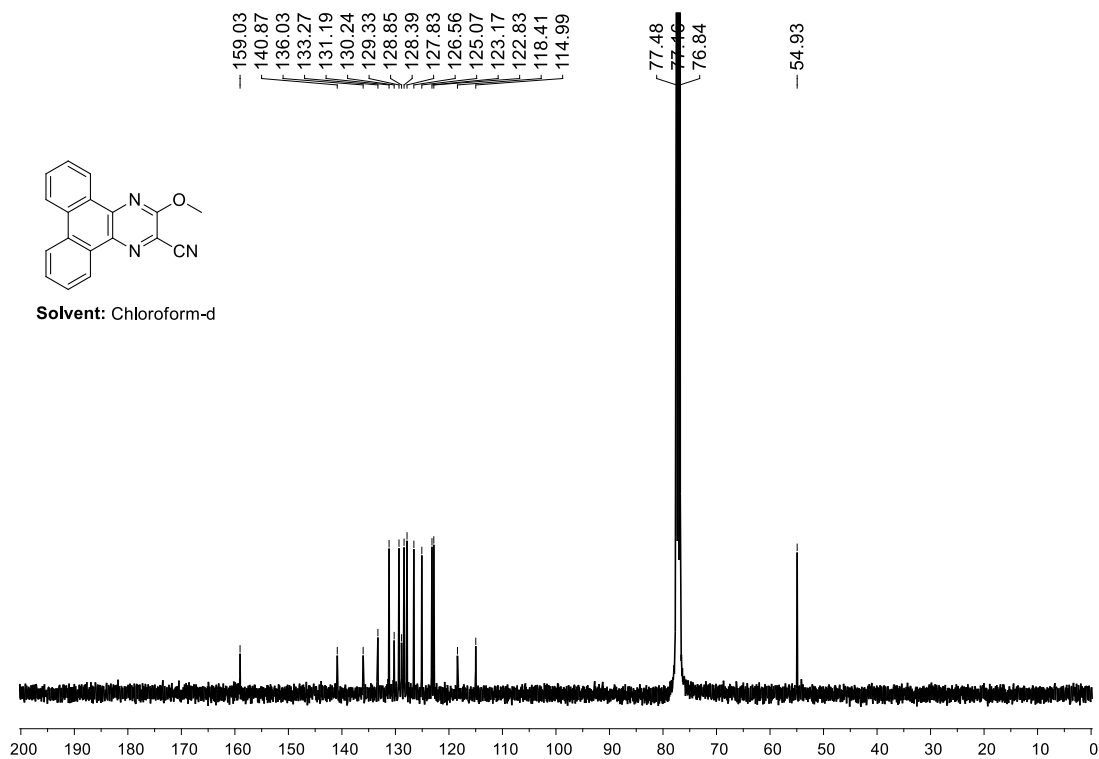


Figure 5.30. ¹³C NMR spectrum of 3-methoxydibenzo[*f,h*]quinoxaline-2-carbonitrile (2da)

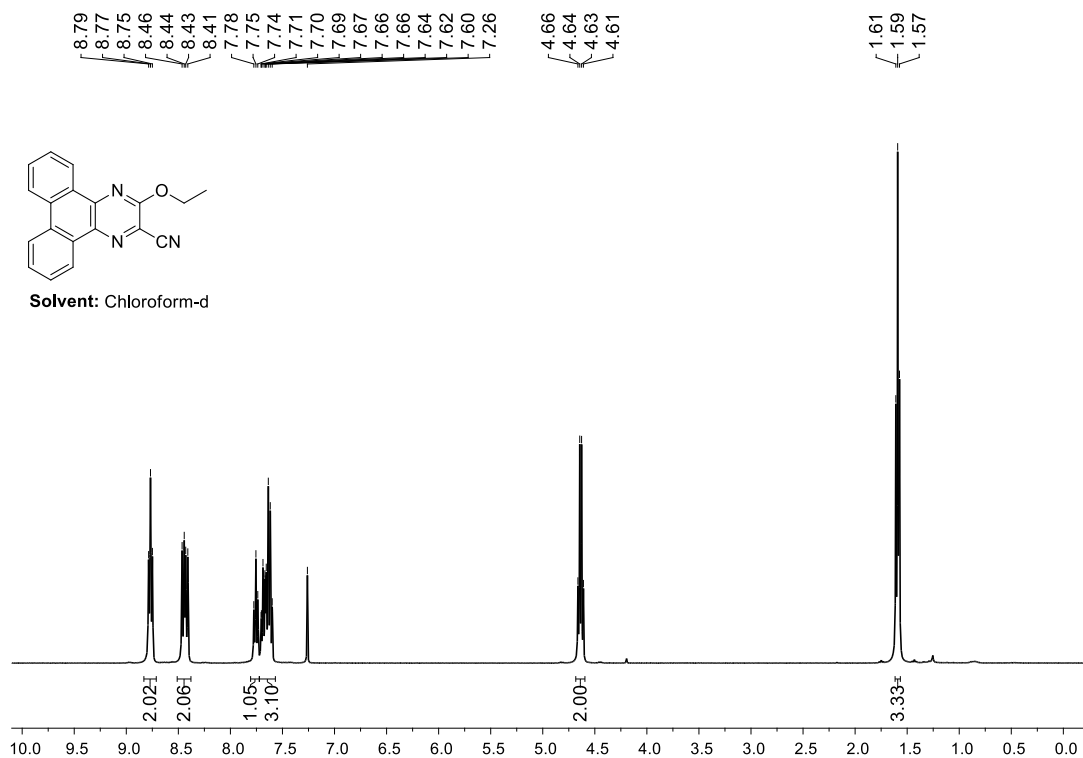


Figure 5.31. ¹H NMR spectrum of 3-ethoxydibenzo[*f,h*]quinoxaline-2-carbonitrile (2db)

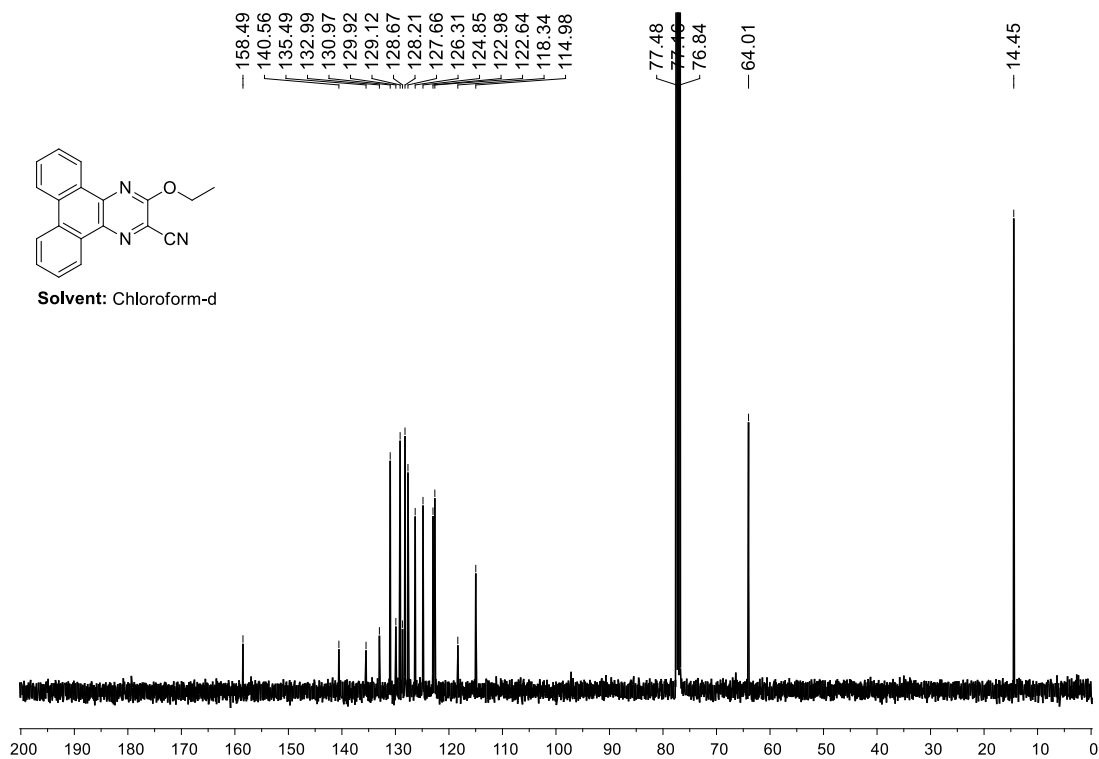


Figure 5.32. ¹³C NMR spectrum of 3-ethoxydibenzo[*f,h*]quinoxaline-2-carbonitrile (2db)

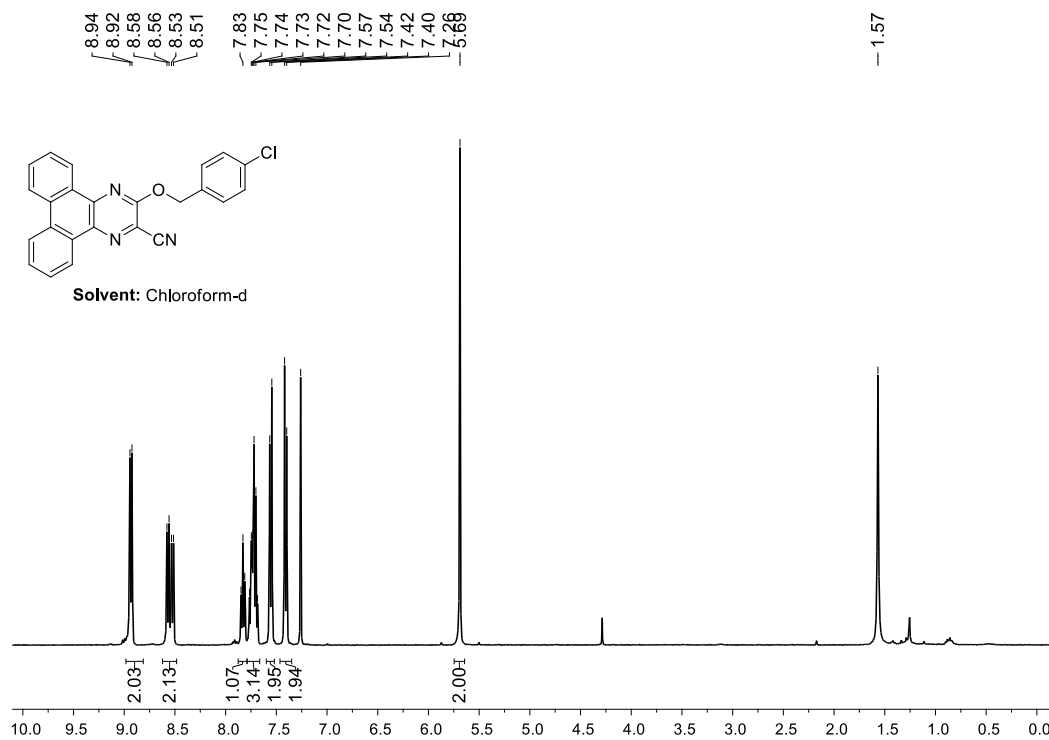


Figure 5.33. ¹H NMR spectrum of 3-((4-chlorobenzyl)oxy)dibenzo[*f,h*]quinoxaline-2-carbonitrile (2dc)

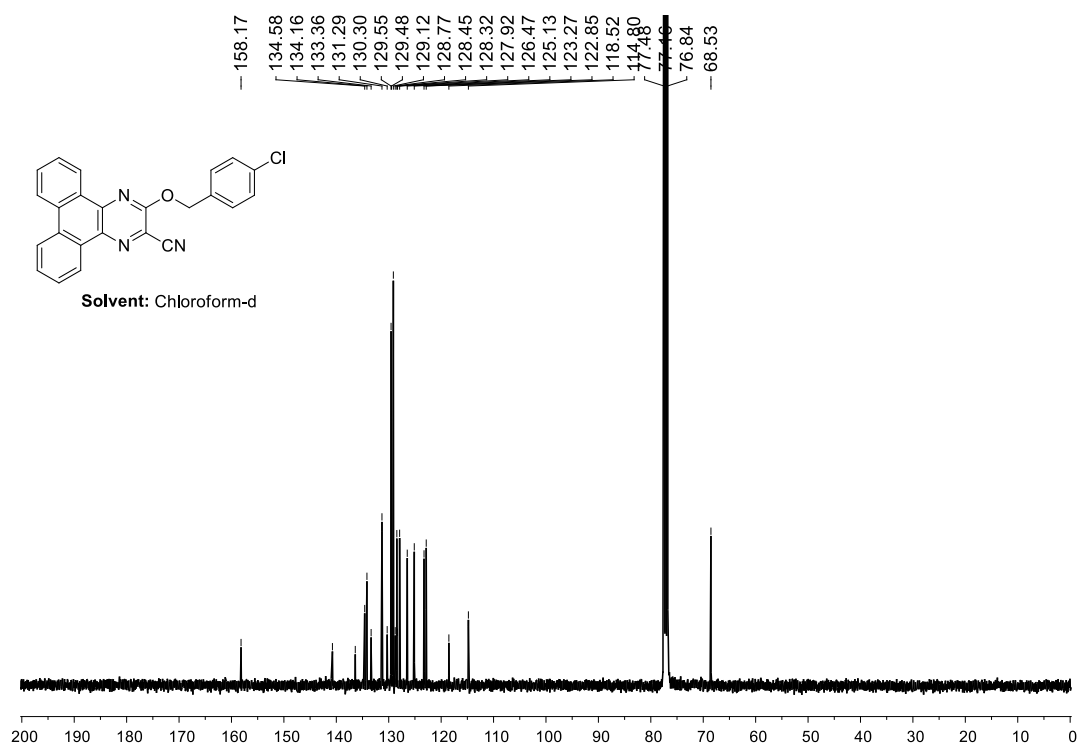


Figure 5.34. ¹³C NMR spectrum of 3-((4-chlorobenzyl)oxy)dibenzo[*f,h*]quinoxaline-2-carbonitrile (2dc)

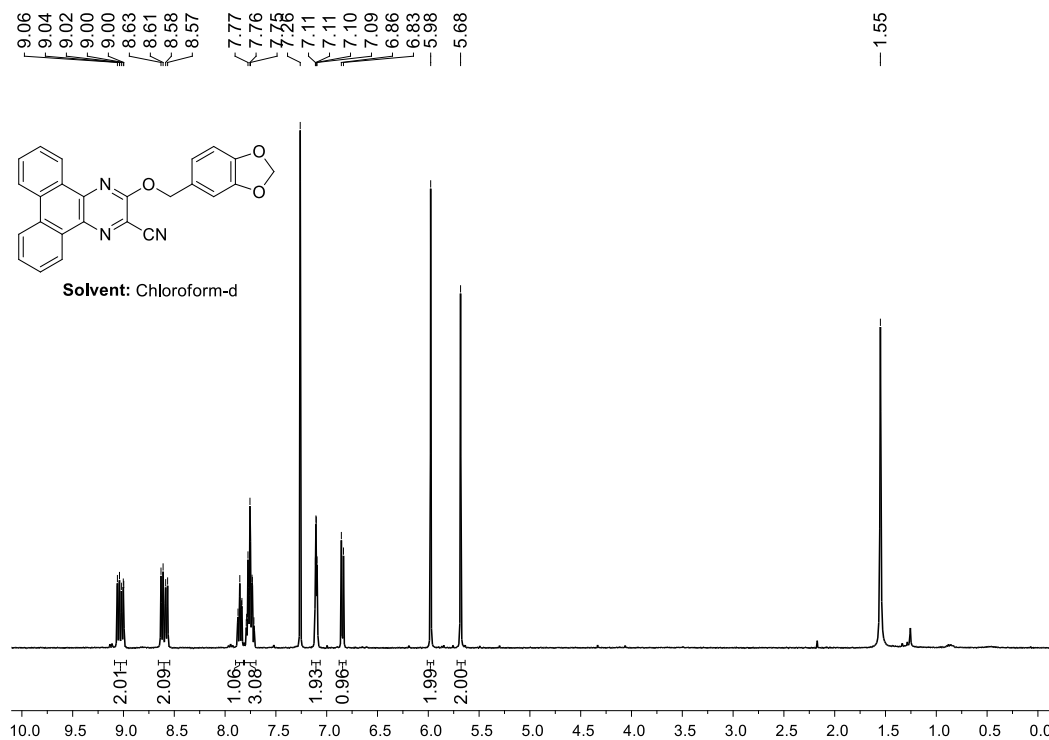


Figure 5.35. ¹H NMR spectrum of 3-(benzo[d][1,3]dioxol-5-ylmethoxy)dibenzo[f,h]quinoxaline-2-carbonitrile (**2dd**)

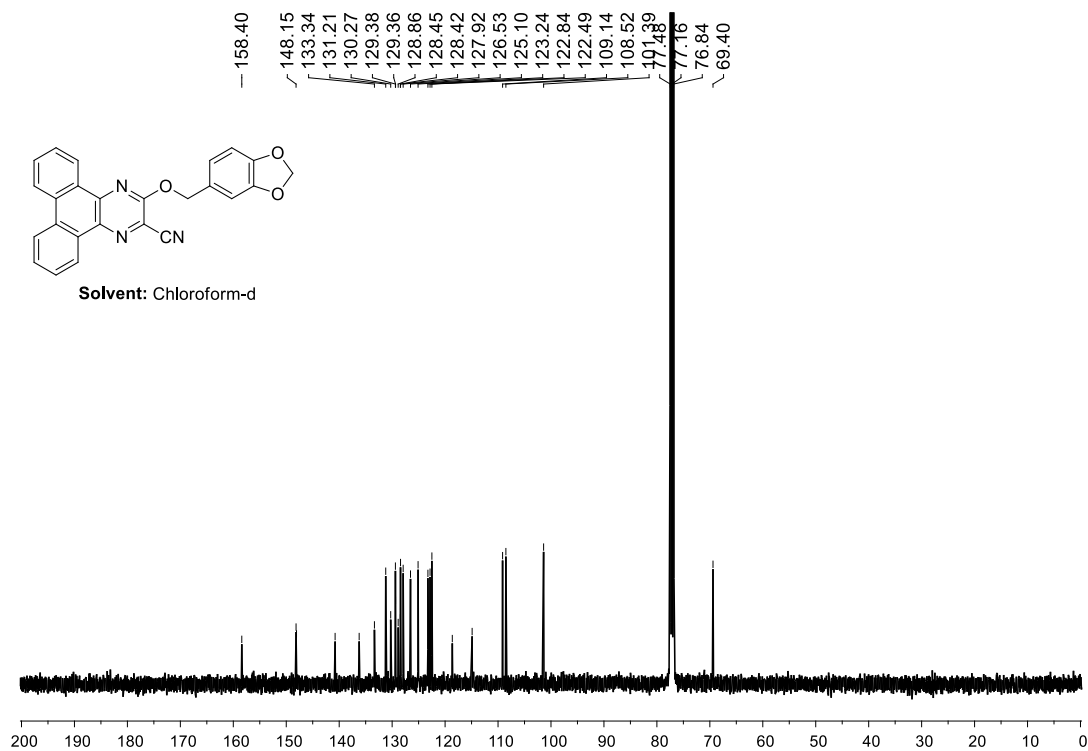


Figure 5.36. ¹³C NMR spectrum of 3-(benzo[d][1,3]dioxol-5-ylmethoxy)dibenzo[f,h]quinoxaline-2-carbonitrile (**2dd**)

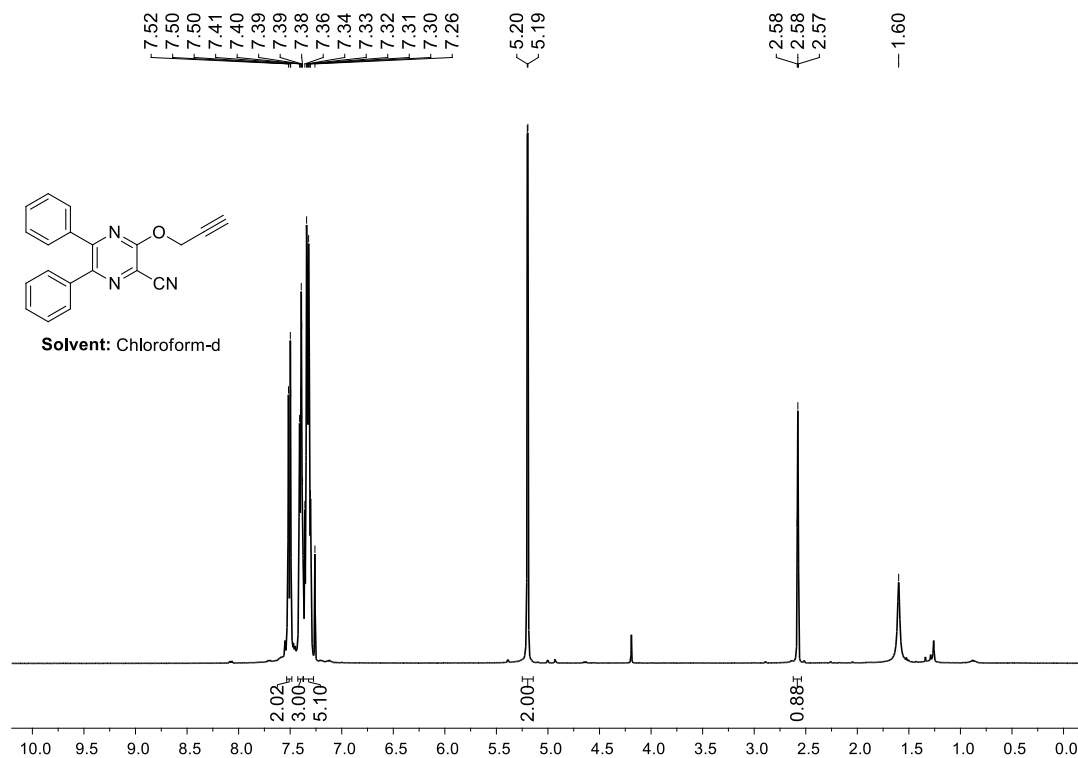


Figure 5.37. ^1H NMR spectrum of 5,6-diphenyl-3-(prop-2-yn-1-yloxy)pyrazine-2-carbonitrile (**2ag**)

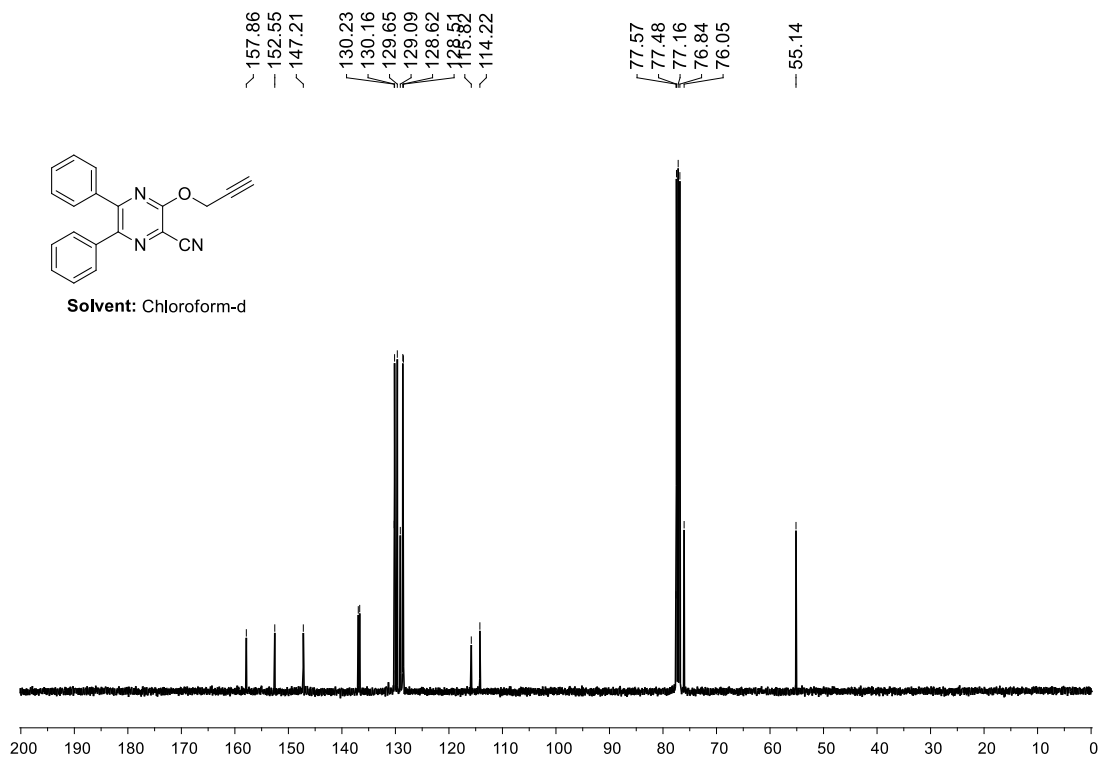


Figure 5.38. ^{13}C NMR spectrum of 5,6-diphenyl-3-(prop-2-yn-1-yloxy)pyrazine-2-carbonitrile (**2ag**)

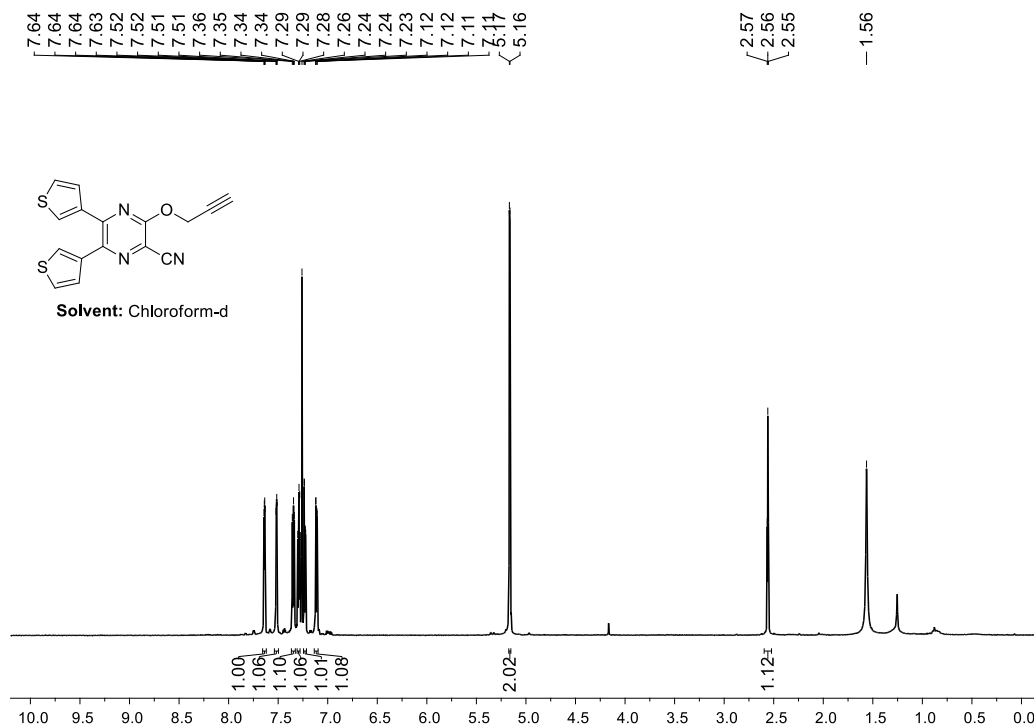


Figure 5.39. ^1H NMR spectrum of 3-(prop-2-yn-1-yloxy)-5,6-di(thiophen-3-yl)pyrazine-2-carbonitrile (2bg)

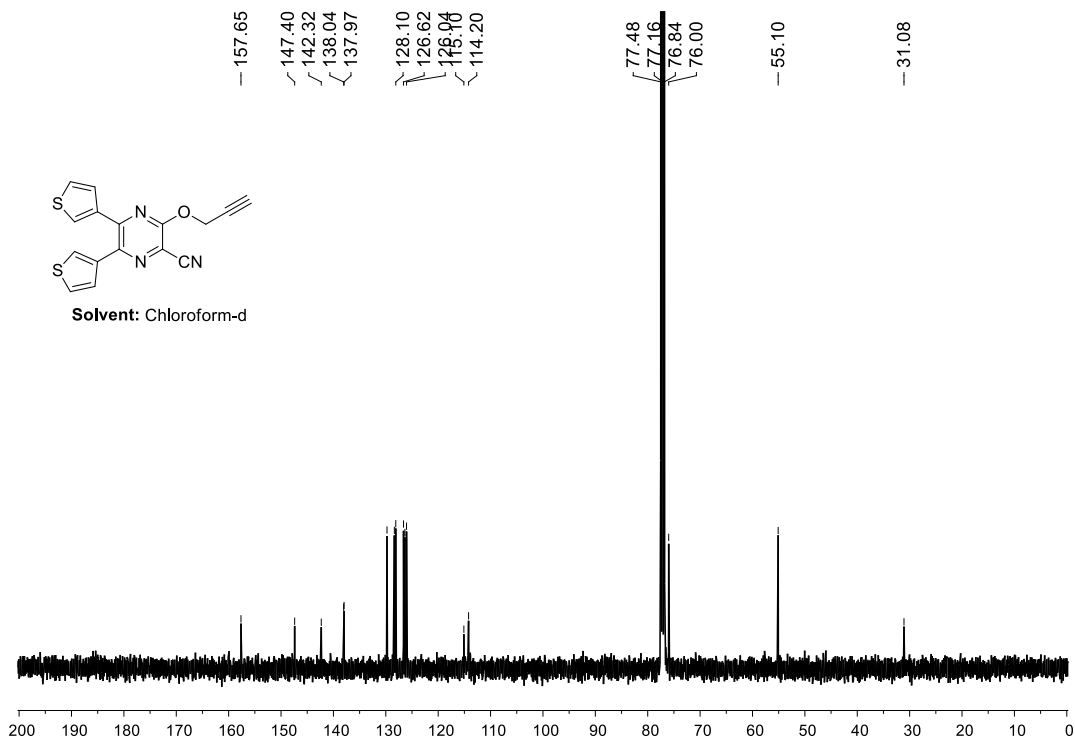


Figure 5.40. ^{13}C NMR spectrum of 3-(prop-2-yn-1-yloxy)-5,6-di(thiophen-3-yl)pyrazine-2-carbonitrile (2bg)

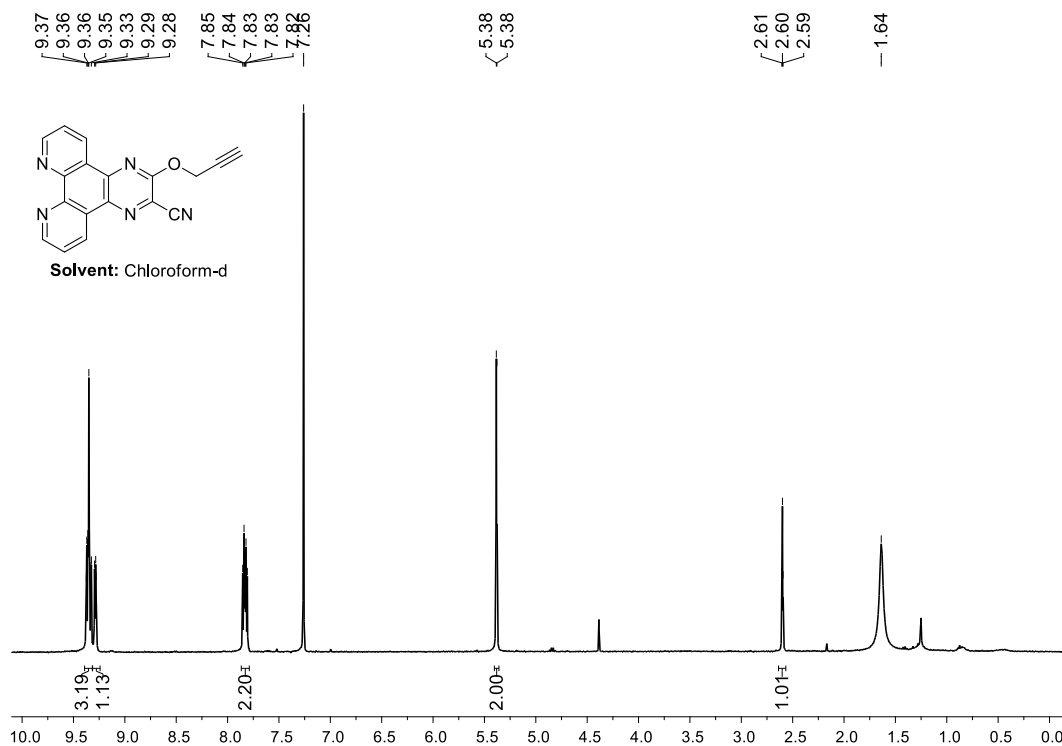


Figure 5.41. ^1H NMR spectrum of 3-(prop-2-yn-1-yloxy)pyrazino[2,3-*f*][1,10]phenanthroline-2-carbonitrile (**2cg**)

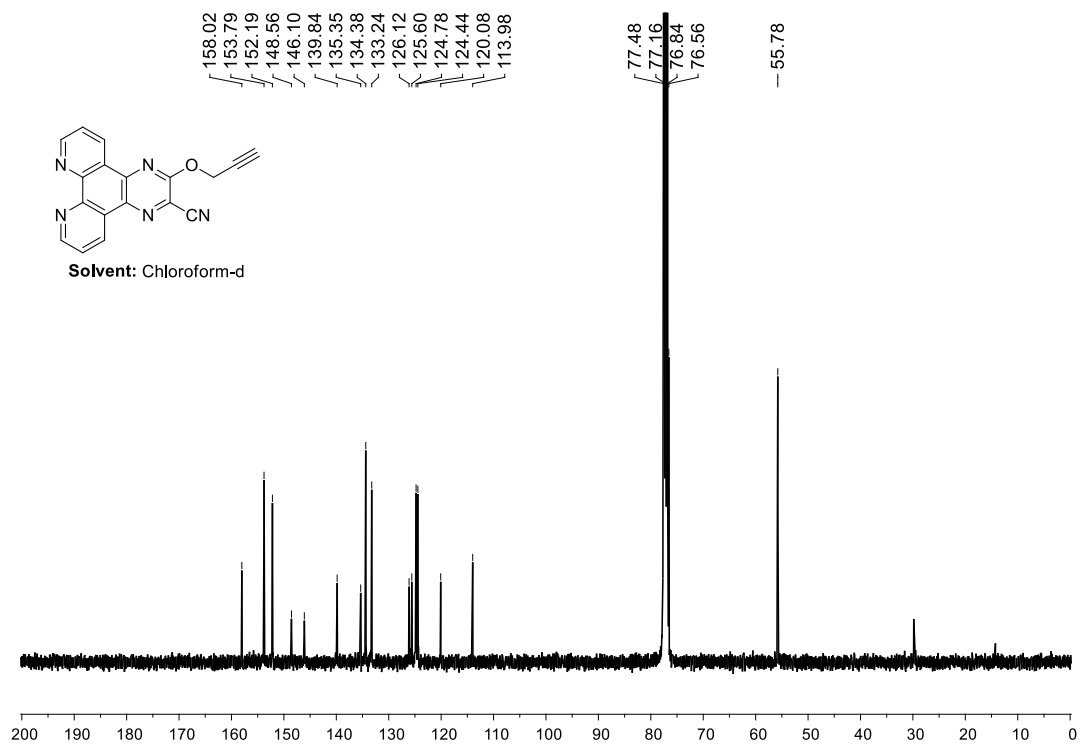


Figure 5.42. ^{13}C NMR spectrum of 3-(prop-2-yn-1-yloxy)pyrazino[2,3-*f*][1,10]phenanthroline-2-carbonitrile (**2cg**)

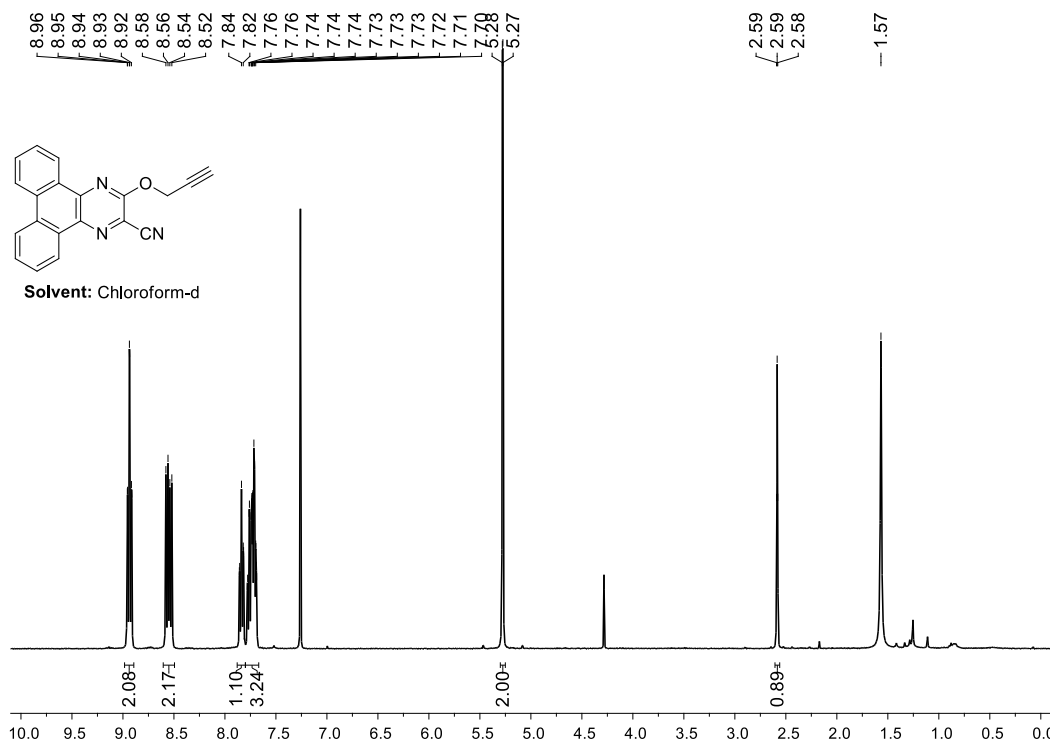


Figure 5.43. ¹H NMR spectrum of 3-(prop-2-yn-1-yloxy)dibenzo[f,h]quinoxaline-2-carbonitrile (**2dg**)

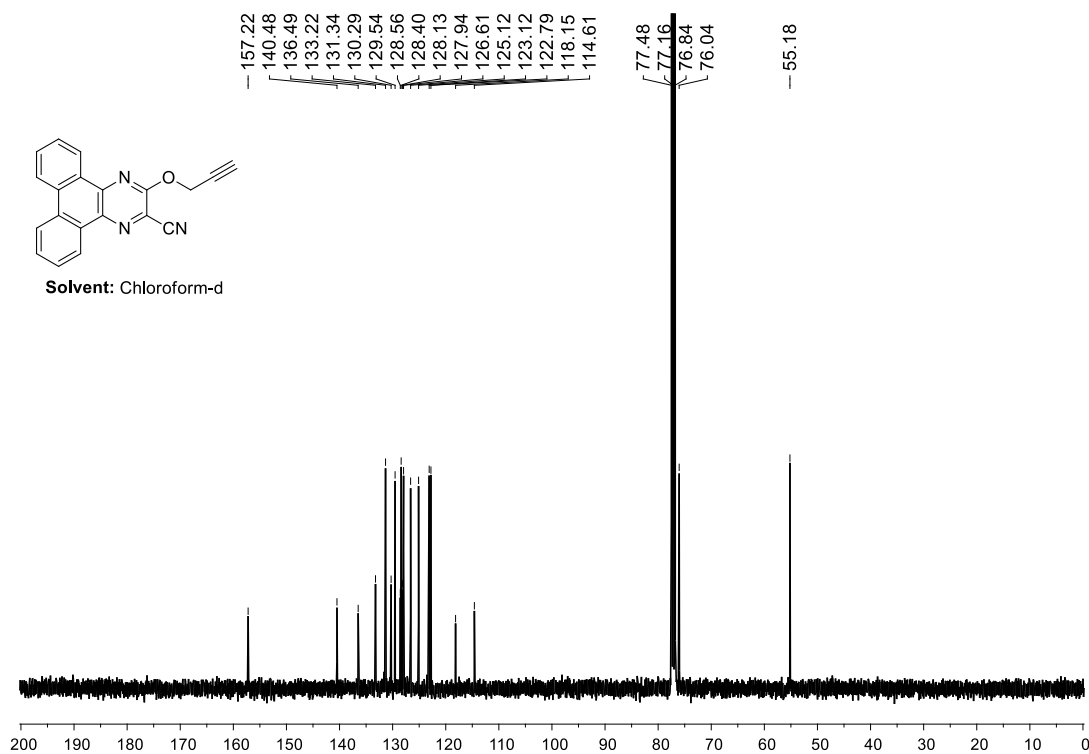


Figure 5.44. ¹³C NMR spectrum of 3-(prop-2-yn-1-yloxy)dibenzo[f,h]quinoxaline-2-carbonitrile (**2dg**)

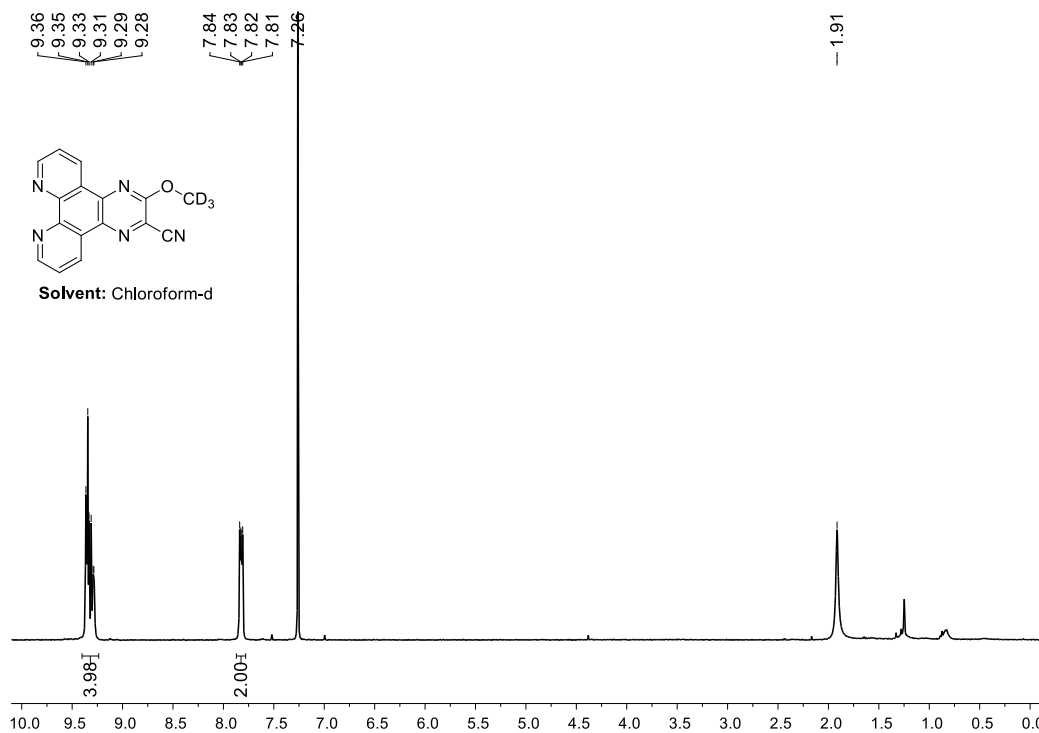


Figure 5.45. ^1H NMR spectrum of 3-methoxy- d_3 -pyrazino[2,3-*f*][1,10]phenanthroline-2-carbonitrile (**2ch**)

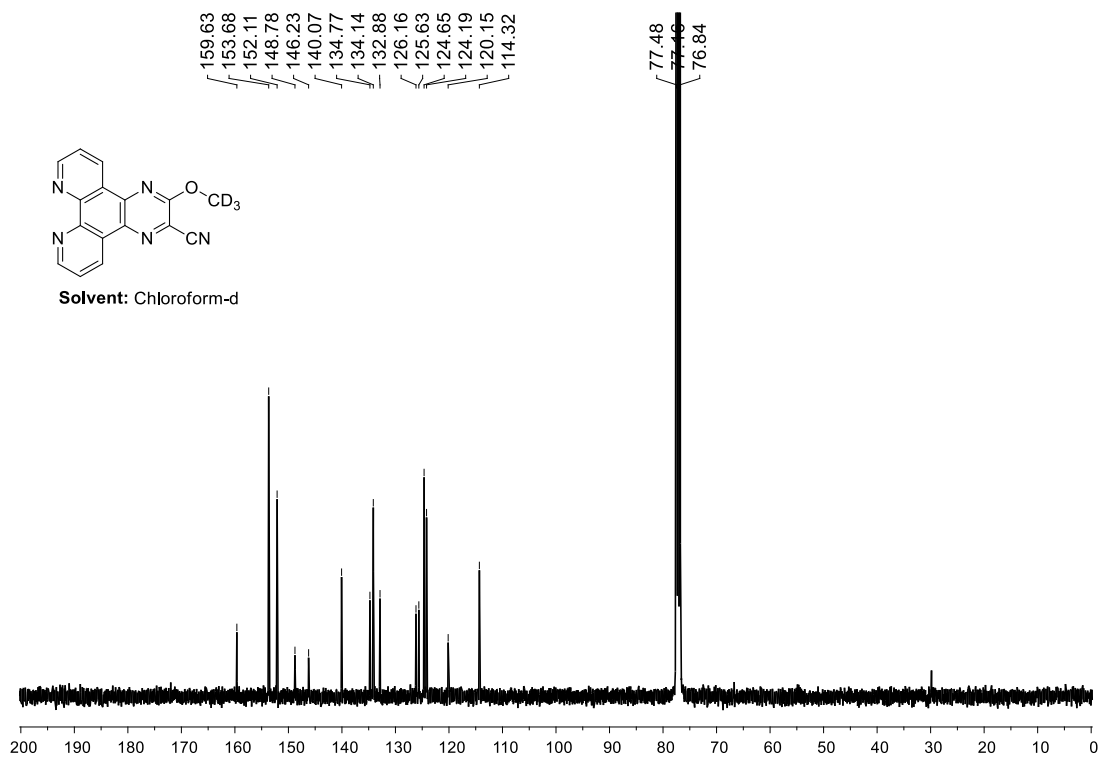


Figure 5.46. ^{13}C NMR spectrum of 3-methoxy- d_3 -pyrazino[2,3-*f*][1,10]phenanthroline-2-carbonitrile (**2ch**)

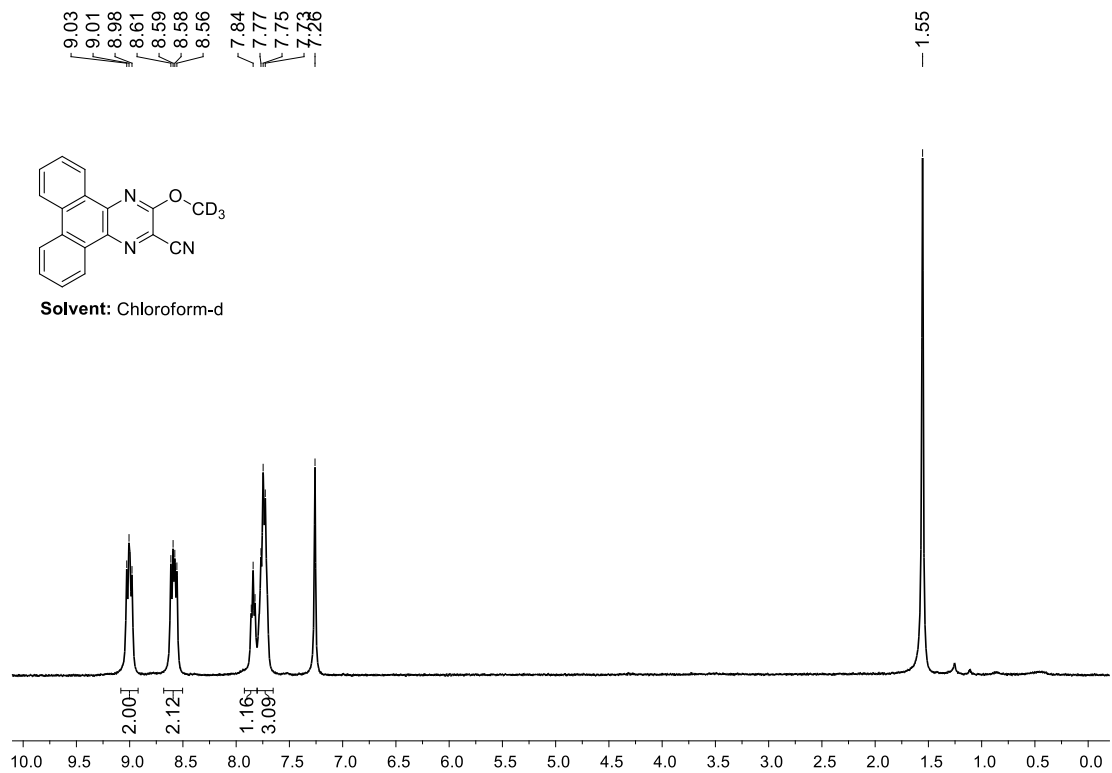


Figure 5.47. ¹H NMR spectrum of 3-methoxy-*d*₃-dibenzo[*f,h*]quinoxaline-2-carbonitrile (**2dh**)

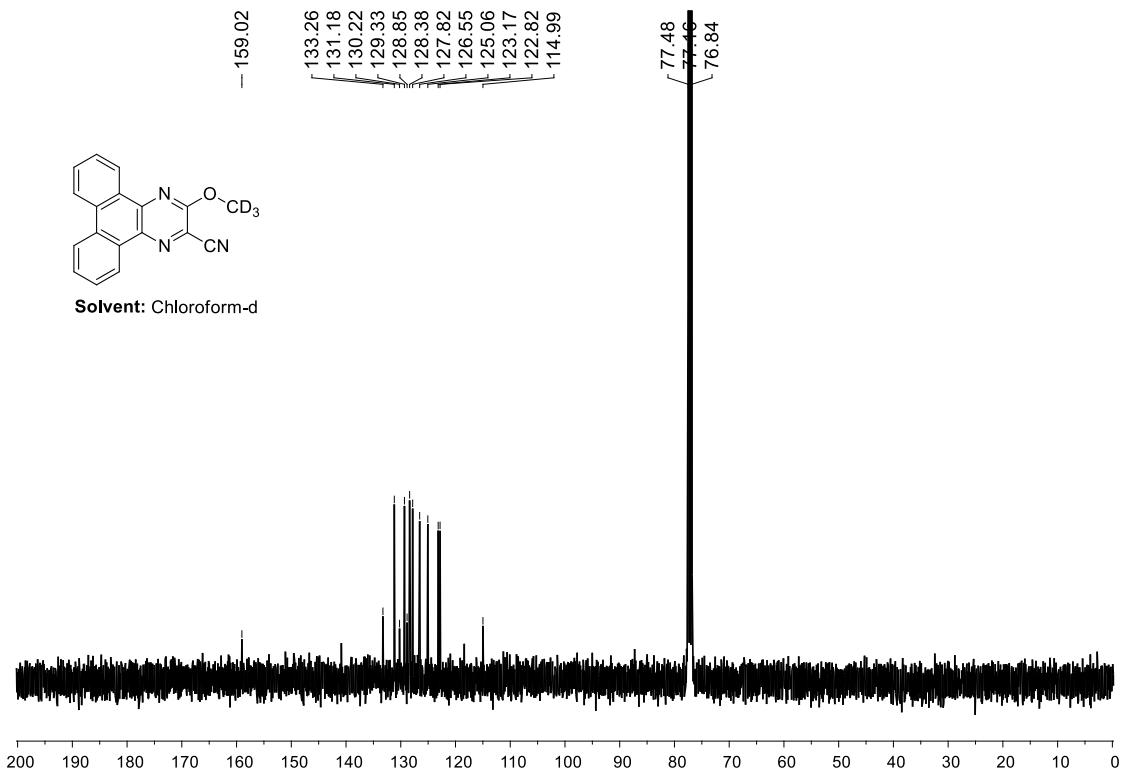


Figure 5.48. ¹³C NMR spectrum of 3-methoxy-*d*₃-dibenzo[*f,h*]quinoxaline-2-carbonitrile (**2dh**)

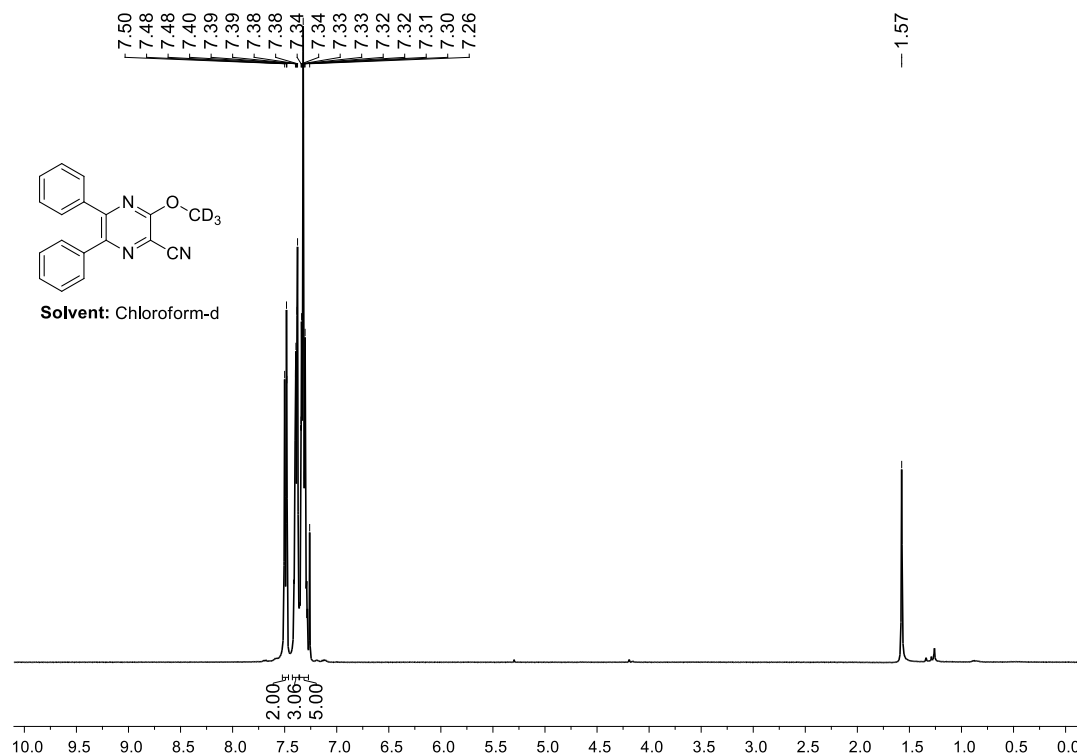


Figure 5.49. ^1H NMR spectrum of 3-methoxy- d_3 -5,6-diphenylpyrazine-2-carbonitrile (**2ah**)

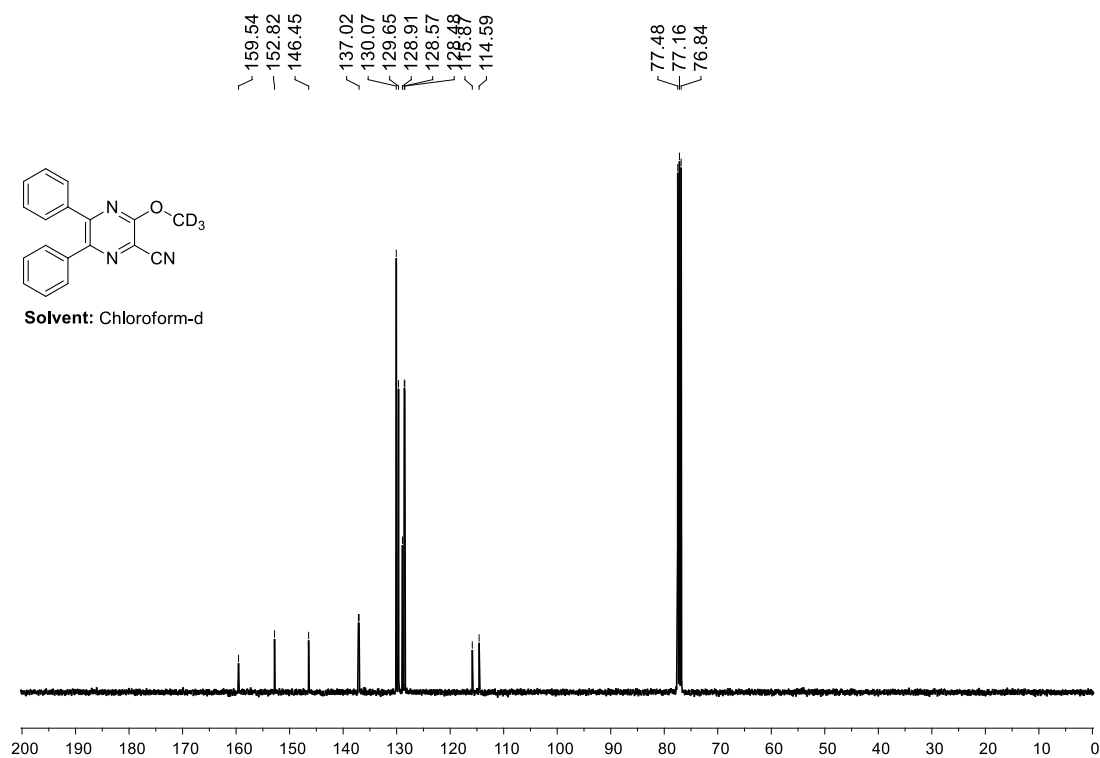


Figure 5.50. ^{13}C NMR spectrum of 3-methoxy- d_3 -5,6-diphenylpyrazine-2-carbonitrile (**2ah**)

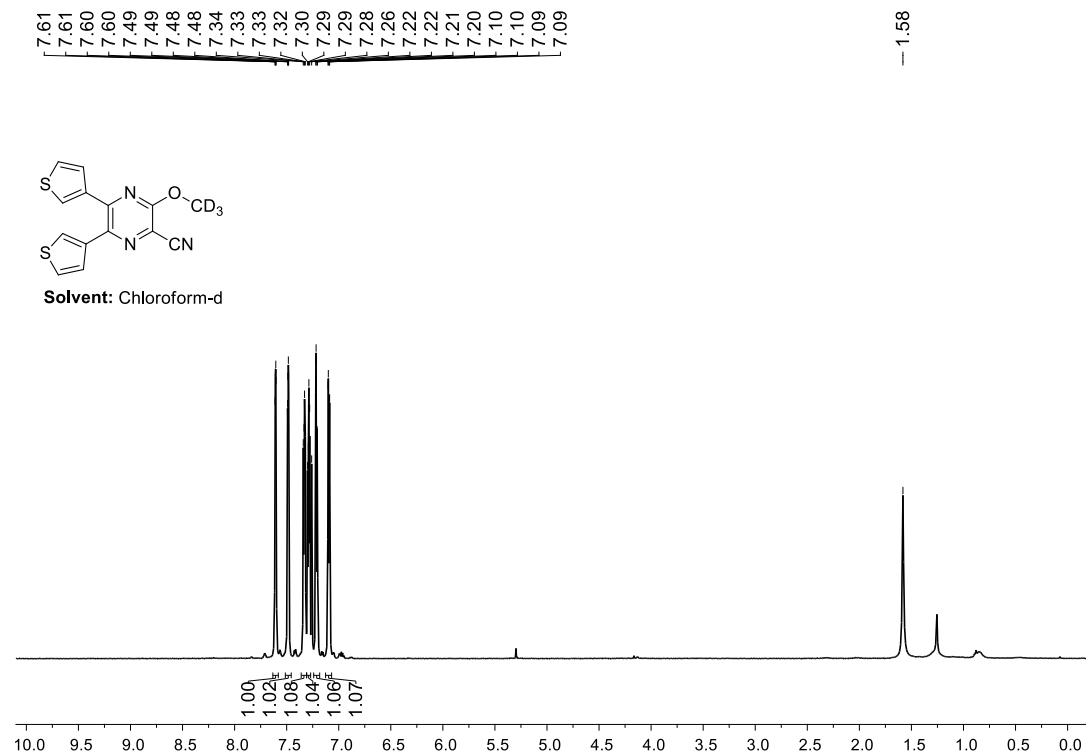


Figure 5.51. ¹H NMR spectrum of 3-methoxy-d₃-5,6-di(thiophen-3-yl)pyrazine-2-carbonitrile (**2dh**)

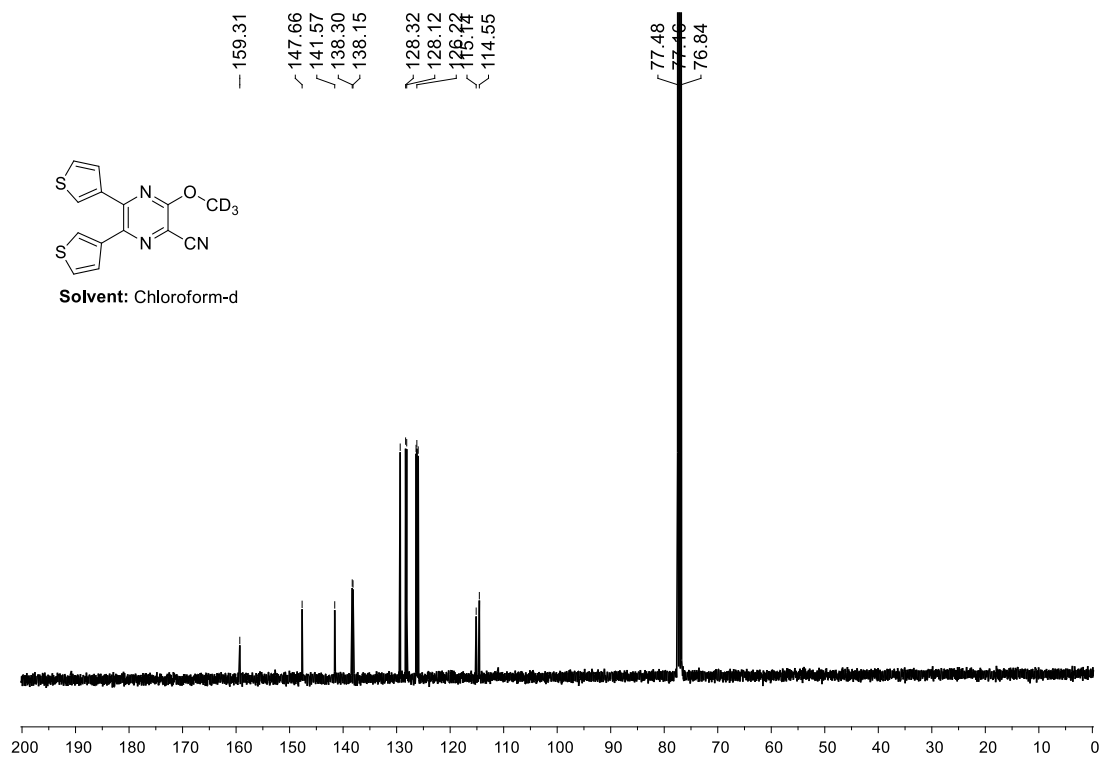


Figure 5.52. ¹³C NMR spectrum of 3-methoxy-d₃-5,6-di(thiophen-3-yl)pyrazine-2-carbonitrile (**2dh**)

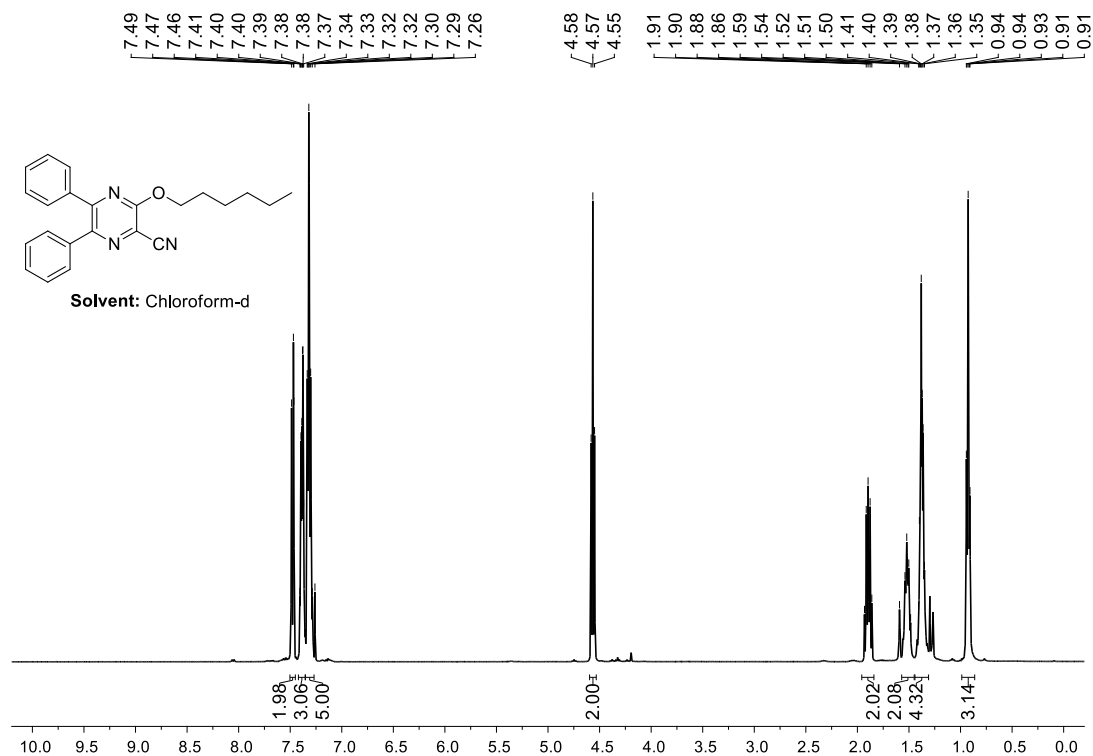


Figure 5.53. ^1H NMR spectrum of 3-(hexyloxy)-5,6-diphenylpyrazine-2-carbonitrile (**2ae**)

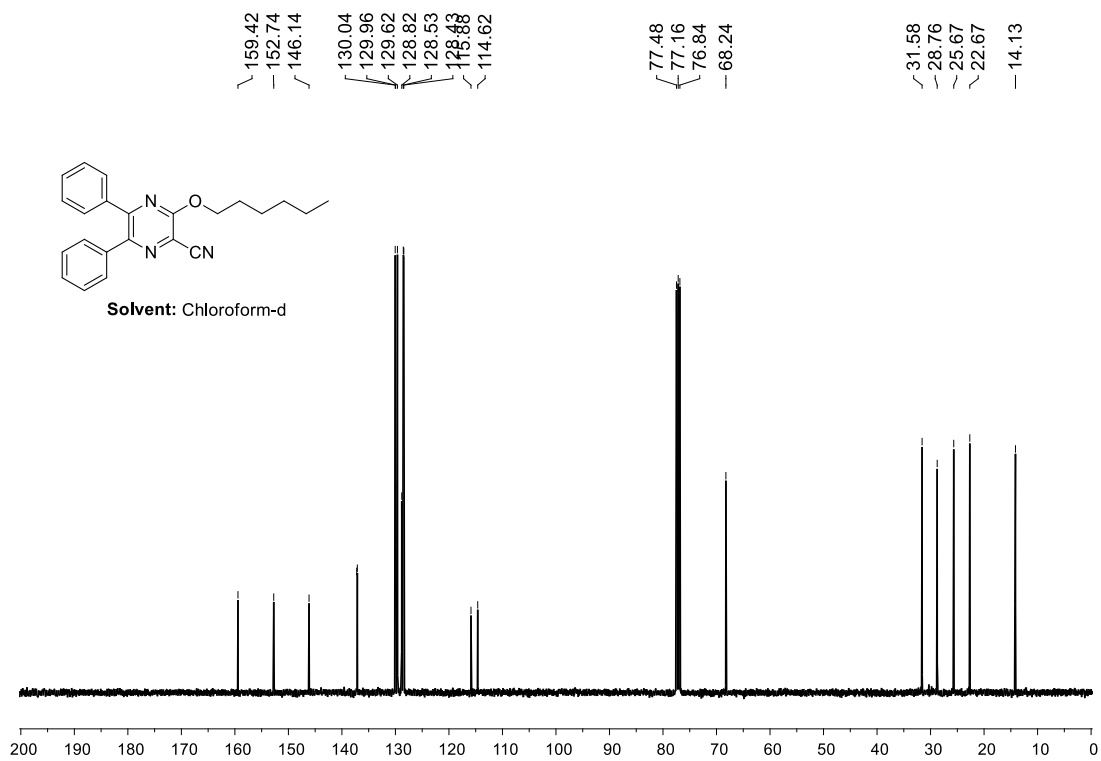


Figure 5.54. ^{13}C NMR spectrum of 3-(hexyloxy)-5,6-diphenylpyrazine-2-carbonitrile (**2ae**)

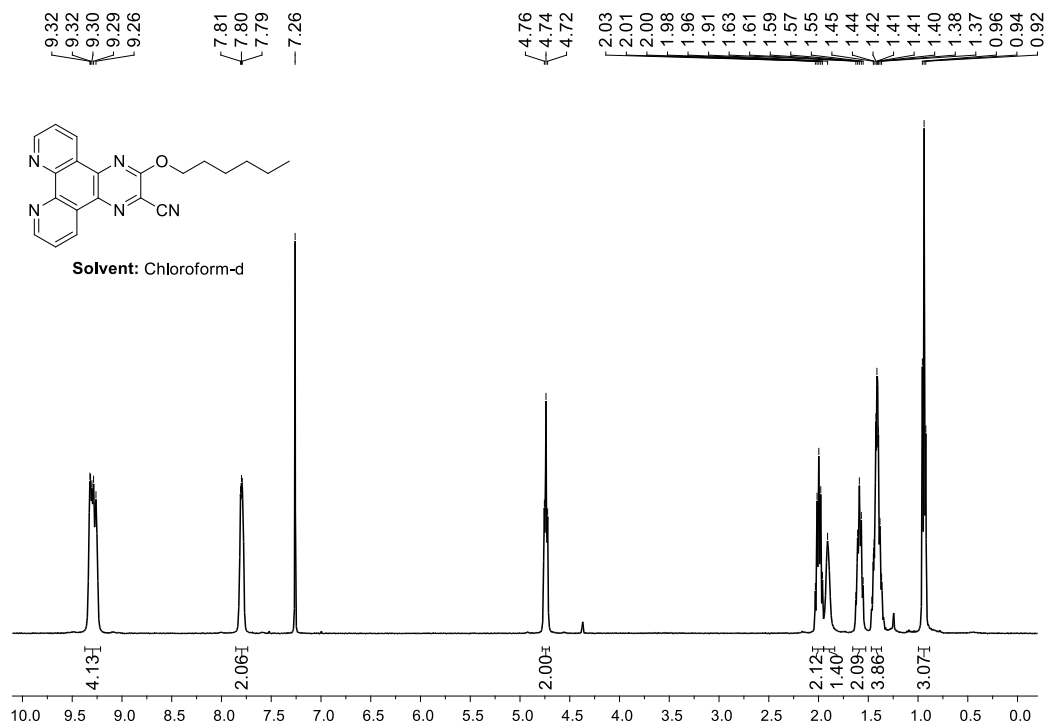


Figure 5.55. ^1H NMR spectrum of 3-(hexyloxy)pyrazino[2,3-*f*][1,10]phenanthroline-2-carbonitrile (**2ce**)

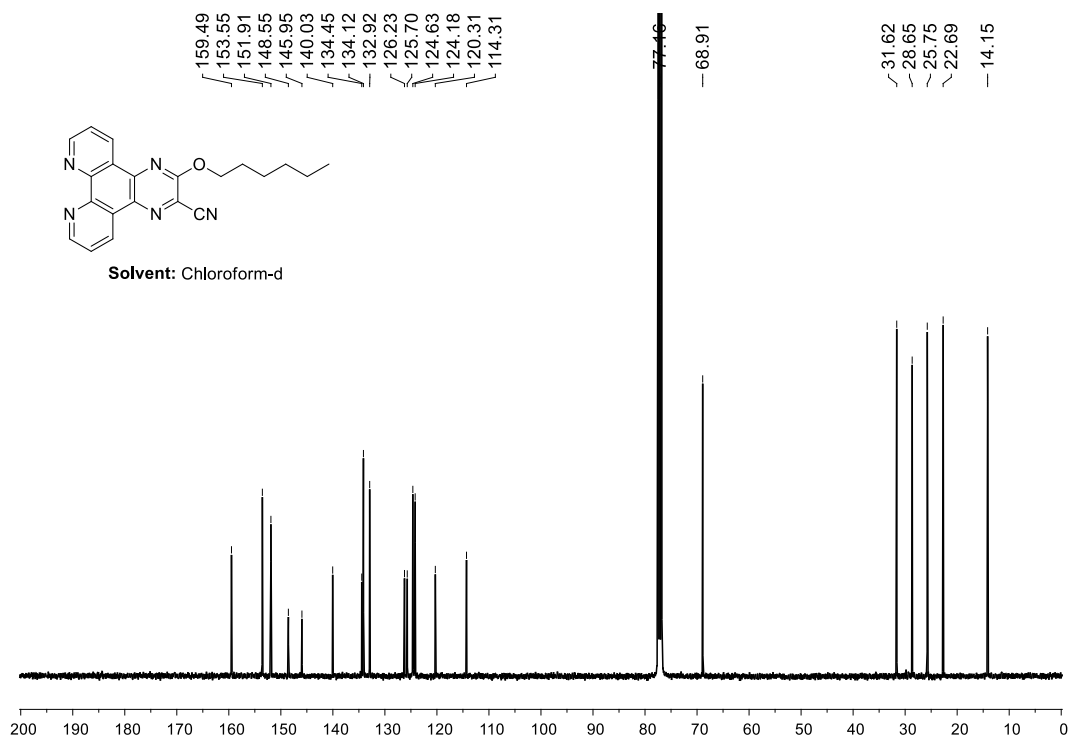


Figure 5.56. ^{13}C NMR spectrum of 3-(hexyloxy)pyrazino[2,3-*f*][1,10]phenanthroline-2-carbonitrile (**2ce**)

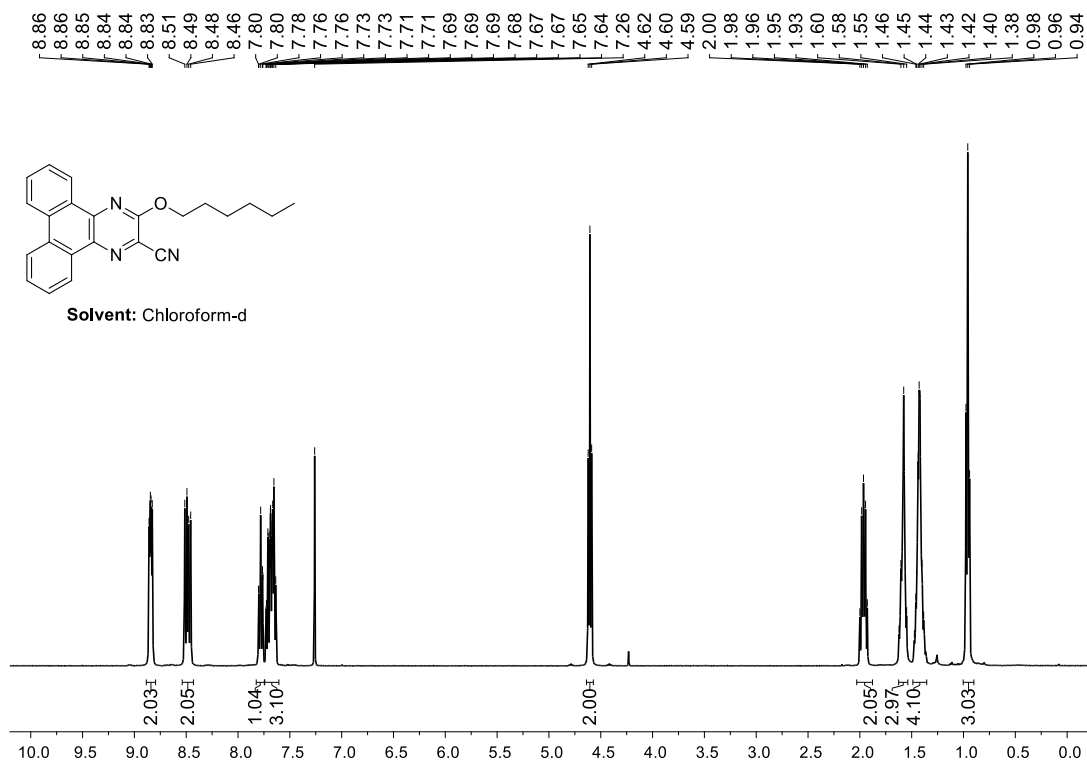


Figure 5.57. ^1H NMR spectrum of 3-(hexyloxy)dibenzo[*f,h*]quinoxaline-2-carbonitrile (**2de**)

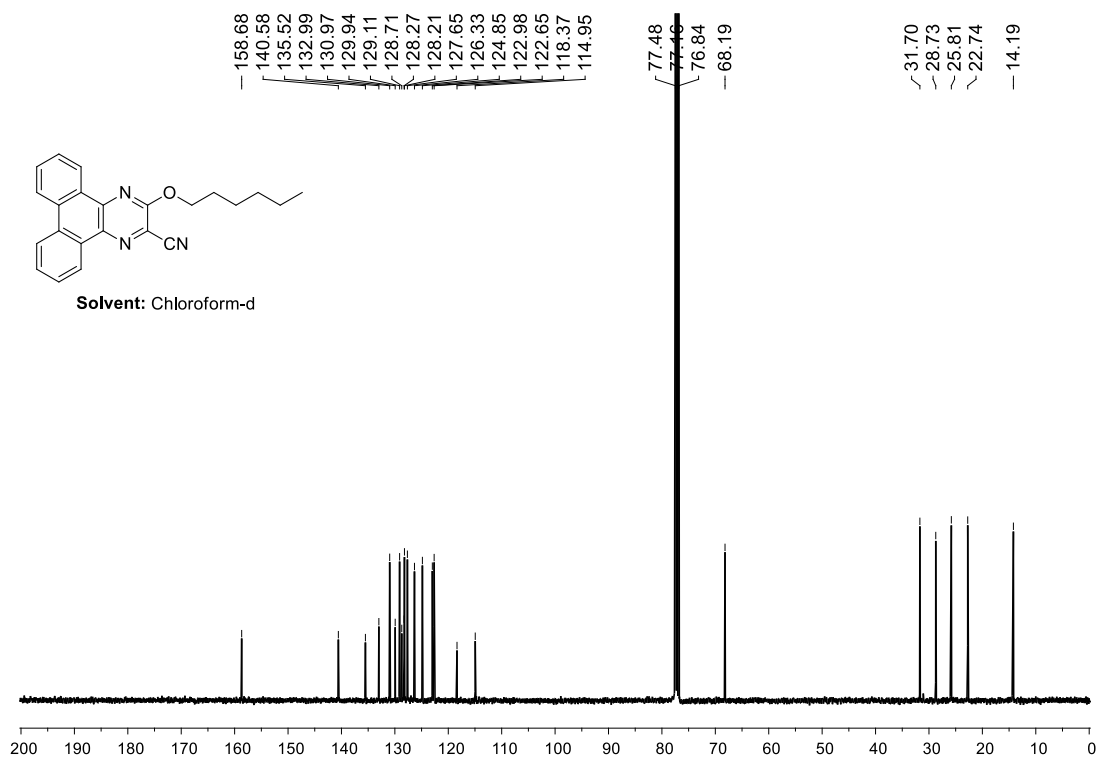


Figure 5.58. ^{13}C NMR spectrum of 3-(hexyloxy)dibenzo[*f,h*]quinoxaline-2-carbonitrile (**2de**)

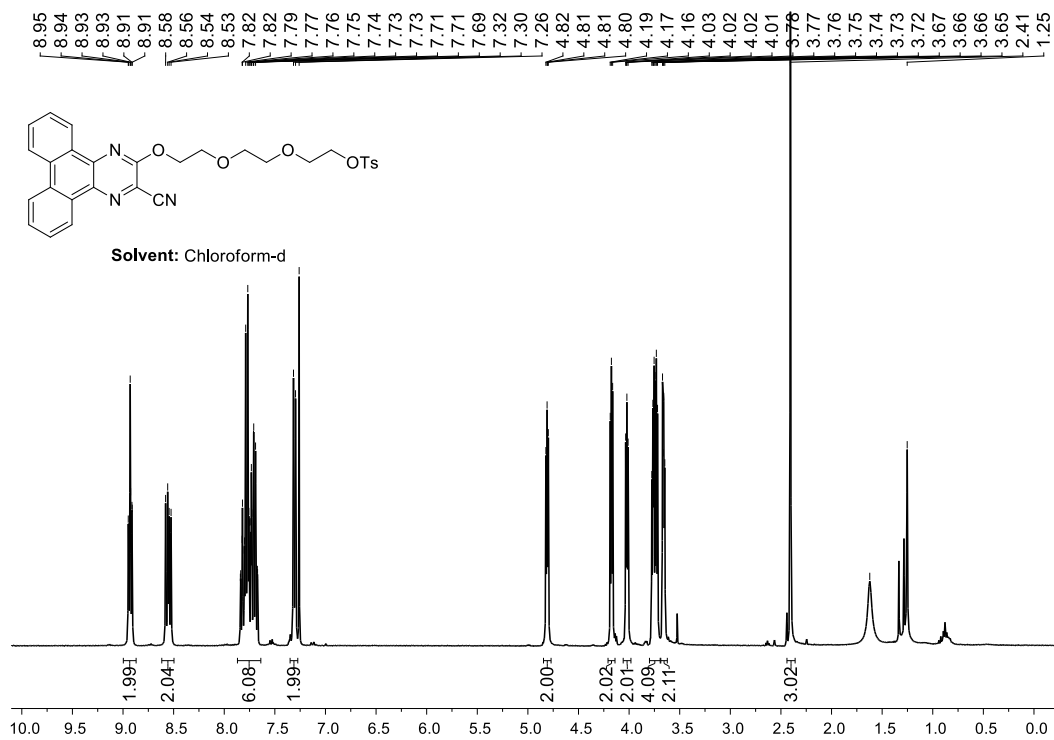


Figure 5.59. ^1H NMR spectrum of 2-(2-(2-((3-cyanodibenzo[*f,h*]quinoxalin-2-yl)oxy)ethoxy)ethoxy)ethyl 4-methylbenzenesulfonate (**2di**)

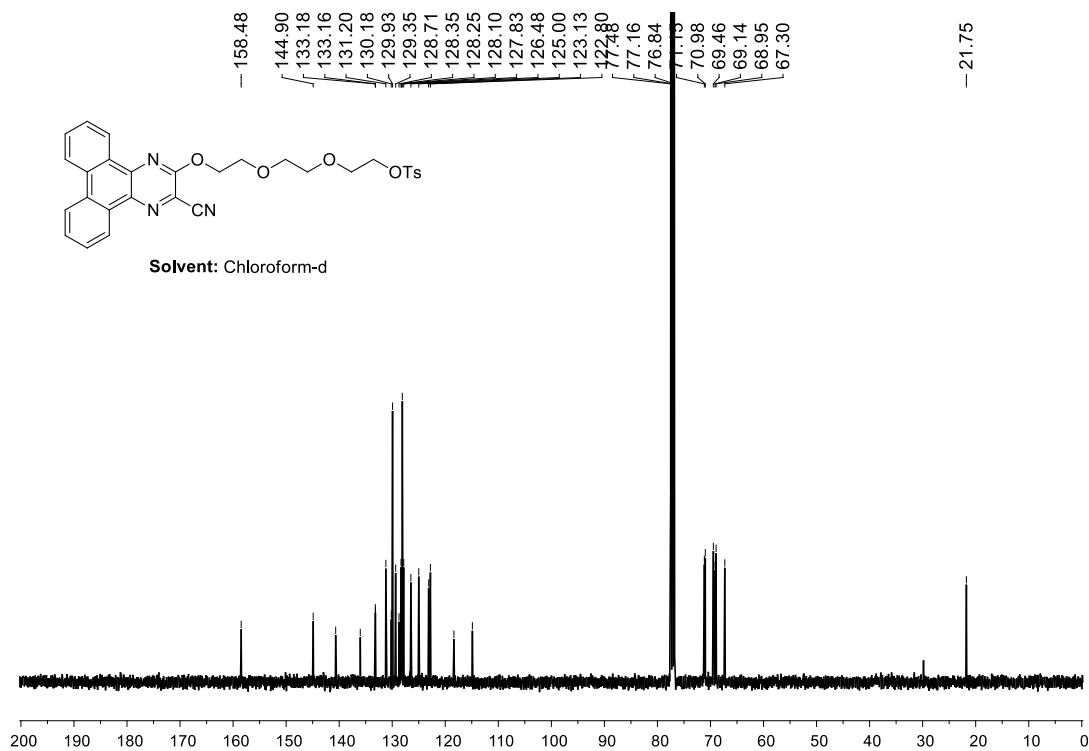


Figure 5.60. ^{13}C NMR spectrum of 2-(2-(2-((3-cyanodibenzo[*f,h*]quinoxalin-2-yl)oxy)ethoxy)ethoxy)ethyl 4-methylbenzenesulfonate (**2di**)

5.6 NOTES AND REFERENCES

1. C.-J. Li, *Acc. Chem. Res.*, 2009, **42**, 335-344.
2. C. S. Yeung and V. M. Dong, *Chem. Rev.*, 2011, **111**, 1215-1292.
3. M.-L. Louillat and F. W. Patureau, *Chem. Soc. Rev.*, 2014, **43**, 901-910.
4. A. Studer and D. P. Curran, *Nature Chem.*, 2014, **6**, 765-773.
5. W.-J. Yoo and C.-J. Li, *Top. Curr. Chem.*, 2010, **292**, 281-302.
6. F. Theil, *Angew. Chem. Int. Ed.*, 1999, **38**, 2345-2347.
7. J. F. Burnett and R. E. Zahler, *Chem. Rev.*, 1951, **49**, 273-412.
8. J. Zhu, *Synlett*, 1997, **1997**, 133-144.
9. E. N. Pitsinos, V. P. Vidali and E. A. Couladouros, *Eur. J. Org. Chem.*, 2011, 1207-1222.
10. J. Scott Sawyer, *Tetrahedron*, 2000, **56**, 5045-5065.
11. A. W. Williamson, *Q. J. Chem. Soc.*, 1852, **4**, 229-239.
12. F. Monnier and M. Taillefer, *Angew. Chem. Int. Ed.*, 2009, **48**, 6954-6971.
13. T. Shintou and T. Mukaiyama, *J. Am. Chem. Soc.*, 2004, **126**, 7359-7367.
14. L. Chan, A. McNally, Q. Y. Toh, A. Mendoza and M. J. Gaunt, *Chem. Sci.*, 2015, **6**, 1277-1281.
15. J. Malmgren, S. Santoro, N. Jalalian, F. Himo and B. Olofsson, *Chem. Eur. J.*, 2013, **19**, 10334-10342.
16. S. M. Bonesi and M. Fagnoni, *Chem. Eur. J.*, 2010, **16**, 13572-13589.
17. H. Hirano, R. Lee and M. Tada, *J. Heterocycl. Chem.*, 1982, **19**, 1409-1413.
18. K. Tsuzuki and M. Tada, *J. Heterocycl. Chem.*, 1985, **22**, 1365-1368.
19. K. Takagi, B. R. Suddaby, S. L. Vadas and C. A. Backer, *J. Am. Chem. Soc.*, 1986, **108**, 7865-7867.

20. S. Masaoka, D. Tanaka, H. Kitahata, S. Araki, R. Matsuda, K. Yoshikawa, K. Kato, M. Takata and S. Kitagawa, *J. Am. Chem. Soc.*, 2006, **128**, 15799-15808.
21. D. Tanaka, S. Masaoka, S. Horike, S. Furukawa, M. Mizuno, K. Endo and S. Kitagawa, *Angew. Chem., Int. Ed.*, 2006, **45**, 4628-4631.
22. A. A. Zavitsas, *J. Phys. Chem. A*, 2003, **107**, 897-898.
23. M. Sun, H.-Y. Zhang, Q. Han, K. Yang and S.-D. Yang, *Chem. Eur. J.*, 2011, **17**, 9566-9570.
24. T. Tanabe, M. E. Evans, W. W. Brennessel and W. D. Jones, *Organometallics*, 2011, **30**, 834-843.
25. Y. Nakao, *Top. Curr. Chem.*, 2014, **346**, 33-58.
26. R. Wang and J. R. Falck, *Catal. Rev.: Sci. Eng.*, 2014, **56**, 288-331.
27. R. Wang and J. R. Falck, *RSC Adv.*, 2014, **4**, 1062-1066.
28. Q. Wen, P. Lu and Y. Wang, *RSC Adv.*, 2014, **4**, 47806-47826.
29. T. A. Atesin, T. Li, S. Lachaize, W. W. Brennessel, J. J. Garcia and W. D. Jones, *J. Am. Chem. Soc.*, 2007, **129**, 7562-7569.
30. T. A. Ateşin, T. Li, S. Lachaize, W. W. Brennessel, J. J. García and W. D. Jones, *J. Am. Chem. Soc.*, 2007, **129**, 7562-7569.
31. T. K. Achar, S. Maiti and P. Mal, *Org. Biomol. Chem.*, 2016, **14**, 4654-4663.
32. N. A. Liberto, S. de Paiva Silva, Â. de Fátima and S. A. Fernandes, *Tetrahedron*, 2013, **69**, 8245-8249.
33. J. W. Steed, *Nature Chem.*, 2011, **3**, 9-10.
34. V. Ramamurthy, J. Shailaja, L. S. Kaanumalle, R. B. Sunoj and J. Chandrasekhar, *Chem. Commun.*, 2003, 1987-1999.

35. Y. Inokuma, M. Kawano and M. Fujita, *Nat Chem*, 2011, **3**, 349-358.
36. S. Karthikeyan and V. Ramamurthy, *J. Org. Chem.*, 2007, **72**, 452-458.
37. D. Fujita and M. Fujita, *ACS Central Science*, 2015, **1**, 352-353.
38. B. M. Schmidt, T. Osuga, T. Sawada, M. Hoshino and M. Fujita, *Angew. Chem. Int. Ed.*, 2016, **55**, 1561-1564.
39. D. A. Dougherty, *Acc. Chem. Res.*, 2013, **46**, 885-893.
40. S. Yamada, N. Uematsu and K. Yamashita, *J. Am. Chem. Soc.*, 2007, **129**, 12100-12101.
41. S. Yamada and Y. Tokugawa, *J. Am. Chem. Soc.*, 2009, **131**, 2098-2099.
42. S. Yamada and C. Kawamura, *Org. Lett.*, 2012, **14**, 1572-1575.
43. A. S. Mahadevi and G. N. Sastry, *Chem. Rev.*, 2013, **113**, 2100-2138.
44. L. Yao and J. Aubé, *J. Am. Chem. Soc.*, 2007, **129**, 2766-2767.
45. J. A. Miller, J. W. Dankwardt and J. M. Penney, *Synthesis*, 2003, 1643-1648.
46. F. L. Taw, P. S. White, R. G. Bergman and M. Brookhart, *J. Am. Chem. Soc.*, 2002, **124**, 4192-4193.
47. J. A. Miller and J. W. Dankwardt, *Tetrahedron Lett.*, 2003, **44**, 1907-1910.
48. S. Mukhopadhyay, J. Lasri, M. F. C. Guedes da Silva, M. A. Januario Charmier and A. J. L. Pombeiro, *Polyhedron*, 2008, **27**, 2883-2888.
49. T. A. Atesin, T. Li, S. Lachaize, J. J. Garcia and W. D. Jones, *Organometallics*, 2008, **27**, 3811-3817.
50. N. Liu and Z.-X. Wang, *Adv. Synth. Catal.*, 2012, **354**, 1641-1645.
51. S. Tsuzuki, M. Mikami and S. Yamada, *J. Am. Chem. Soc.*, 2007, **129**, 8656-8662.
52. C. L. Sun, H. Li, D. G. Yu, M. Yu, X. Zhou, X. Y. Lu, K. Huang, S. F. Zheng, B. J. Li and Z. J. Shi, *Nature Chem.*, 2010, **2**, 1044-1049.